Max Planck Institute

for

Dynamics and Self-Organization

RESEARCH REPORT

2019

Directors

Prof. Dr. Dr. h.c. Eberhard Bodenschatz (Managing Director)
Prof. Dr. Ramin Golestanian
Prof. Dr. Stephan Herminghaus

Scientific Advisory Board

Prof. Dr. Bruno Eckhardt, Philipps-Universität Marburg, Germany
Prof. Dr. Leon M. Glass, McGill University, Montreal, Canada
Prof. Dr. Steve Granick, Ulsan Nat. Inst. of Sci. & Technol., Rep. of Korea
Prof. Dr. Elisabeth Guazzelli, Polytech Marseille, France
Prof. Dr. Andrea Liu, University of Pennsylvania, Philadelphia, USA
Prof. Dr. Charles Meneveau, Johns Hopkins University, Baltimore, USA
Prof. Dr. Elisha Moses, Weizmann Institute of Science, Rehovot, Israel
Prof. Dr. Haim Sompolinsky, The Hebrew University Jerusalem, Israel
Prof. Dr. Ph.D. Cécile Sykes, Institut Curie Paris, France
Prof. Dr. Wim van Saarloos, Universiteit Leiden, The Netherlands

No matter how well we understand how a single droplet of water is formed in the laboratory, we cannot predict how countless droplets form clouds that substantially affect the Earth's climate. And although we can accurately characterize a single neuron's impulse, we do not yet understand how billions of them form a single thought. In such systems, animate or inanimate, processes of self-organization are at work: Many interacting parts organize themselves independently, without external control, into a complex whole. At our institute we explore the mechanisms underlying these processes in order to gain a detailed understanding of complex systems. Also the major challenges of the 21st century, from climate change and economic crises to problems in energy supply and transport, are closely linked to these scientific questions. Without a deep understanding of dynamics and self-organization in complex and highly networked systems we cannot face these challenges. With our basic research not only do we want to deepen our understanding of nature, but also want to contribute to a sustainable existence on this planet.

The three directors of the MPIDS (from left): Eberhard Bodenschatz, Stephan Herminghaus and Ramin Golestanian (Göttingen, February 2019).

CONTENTS

Research

Support

INTRODUCTION

1

The Max Planck Institute for Dynamics and Self-Organization (MPIDS) is engaged in a wide variety of research activities on a diverse set of systems; from endeavouring to make synthetic forms of lifelike organelles to understanding how the brain works; from uncovering how slime moulds evolve, sense, and decide to deciphering the inner workings of the adaptive immune system; from probing the interplay between electro-physiology and nonlinear mechanics in the heart to understanding turbulence. And, the list goes on. The plethora of physical problems, however, can be formally viewed within a common conceptual framework, in which the aim is to understand the collective behaviour of complex systems with many interacting degrees of freedom. This pursuit is built on solid theoretical framework within the context of nonequilibrium statistical physics, nonlinear dynamics, condensed matter physics, and fluid physics, and makes use of a broad range of theoretical, computational, and experimental tools and techniques. The commonality of the underlying principles behind the diverse research programmes naturally provides MPIDS researchers with a common language, and enables them to achieve synergistic interactions by crossing traditional disciplinary boundaries. The unique environment allows them to take ideas and techniques from one field to another and open up new horizons of research.

In the last three years, MPIDS has had a remarkable period with many ongoing initiatives that have been vigorously pursued and expanded, new initiatives that have started and some previous research activities that have been concluded. Moreover, the institute went through a substantial change with the retirement of Professor Theo Geisel, who is now helping MPIDS as an emeritus director while still pursuing active research, and the appointment of a new director as his replacement, Professor Ramin Golestanian from Oxford University, who has established the Department of Living Matter Physics. The vision behind the new department (that started from 1st March 2018) is to study living systems as self-organized active soft matter that are away from equilibrium "just the right way". The researchers in the department aim to theoretically understand the complex dynamics of living matter well enough to be able to make it from the bottom-up; i.e. from molecules to systems. Their research topics cover chemical and mechanical nonequilibrium activity in living matter across the scales, broadly speaking, and connects seamlessly with the experimental activities in the other two departments of MPIDS.

The synergistic interactions across MPIDS have resulted in a number of major initiatives. There are many projects that aim to take ideas and techniques from physics in a research direction that can ultimately lead to novel and revolutionizing medical applications. A number of MPIDS research directions will clearly have the potential for major impact on sustainability of life on earth; these include implementation of new models of shared transportation, understanding the dynamics of clouds, and the physics of wind farms. Many researchers in MPIDS are passionate about making the transition from matter to life. While the institute has been extensively involved with the Max Planck Society initiative MaxSynBio and it maintains a key role in the society-wide graduate school Matter-to-Life, the establishment of the new department of Living Matter Physics has boosted these MPIDS-wide activities. These institute-wide initiatives have brought in additional opportunities for scientists across MPIDS to collaborate with each other, as well as reaching out to other institutions in the Göttingen Campus and across Germany.

We have broadly categorized the research across MPIDS during the last three years, which has been reported here in the form of 94 contributions, under the following headings: (i) spatio-temporal complexity and order in driven systems, (ii) active matter, and (iii) dynamics, geometry and information. These contributions highlight the strengths of individual groups and showcase the common underlying principles behind all the different projects. The report also contains information about the facilities and the infrastructure of the institute, which are widely shared and communally developed, as well as our vibrant and multifaceted outreach activities.

As our institute continues to evolve and take on new scientific challenges, it strives to preserve its current dynamic and diverse environment and helps to empower its members to successfully progress through their careers at every stage.

This yearbook 2019 summarizes the developments of our institute over the past 3 years. Next to presenting the senior personnel and the institute structure, it gives an in-depth look at the individual research projects and also at the insitute-wide research initiatives. These are Physics to Sustainability, Physics to Life, and Physics to Medicine.

INITIATIVES

2

Contents

2.1 PHYSICS TO SUSTAINABILITY

Arguably one of the most important questions of our time is whether (and how) humankind can devise a sustainable management of its ecological niche on planet Earth. If we do not come up with satisfactory answers to this question swiftly, humankind will quarrel over land and sea use. Rising sea levels will lead to major migrations of people, threatening the social and economic stability of human society. In order to mitigate the consequences of climate change and to organize a stable and sustainable Anthropocene, it is an urgent matter to better understand the earth and climate system, to lay the foundations of sustainable supply systems for energy and nutrition, and to devise viable concepts for transport and mobility systems. Central to all of these is a deep understanding of complex systems in general, and, in particular, of the collective phenomena which emerge when very many active agents are coupled to a complex whole – a topic at the very core of the scientific research at the MPIDS. Quite a number of large-scale projects are devoted to this field of problems.

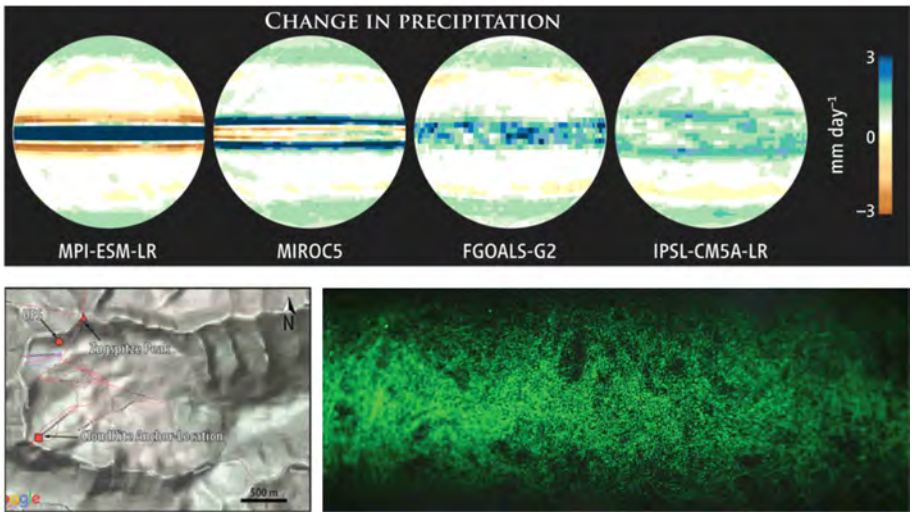

Figure 2.1: *Top panel:* Current uncertainties in climate model predictions, illustrated with respect to a homogeneous global warming by 4 degrees, by comparing the predictions of four common climate models in a all water world [1]. The changes in precipitation are well predicted in the boreal and polar regions, but very poorly in the tropic and equatorial regions. In some parts of the latter, predictions even of the sign of the change vary from model to model. *Bottom left:* Top view model of the mountain range of the Zugspitze, highest mountain in Germany and location of the Schneefernerhaus environmental laboratory where the MPIDS has a laboratory *Bottom right:* Laser sheet illumination view into a live cloud on the Zugspitze. The height of the image corresponds to 50 cm. The 'holes' in the droplet distribution are clearly visible.

The poor understanding of cloud micro physics, such as droplet size and spatial distribution, is the main source of substantial uncertainties in climate models. One reason lies in the turbulent transport and mixing of cloud particles, moisture, and temperature. As wet clouds determine the albedo in the equatorial regions of Earth, the uncertain

parametrization in climate models leads to large uncertainties in the predicted temperature evolution. This is best illustrated by comparing several common climate models for a simplified situation of an all ocean earth in their predicted temperature evolution, as shown in the top panel of Fig. 2.1. Clearly, there are strongly conflicting predictions for the tropical zones. It is therefore imperative to study the micro-physics both under idealized conditions in the laboratory and also in the field. Experiments on moist convection, droplet nucleation, and and the impact of turbulence are being carried out in the Max Planck Turbulence Facility. In the field we investigate the cloud micro physics experiments on the Environmental Research Station Schneefernerhaus on Zugspitze, the highest mountain in Germany (bottom left of Fig. 2.1). The bottom right panel shows the interior of a Zugspitze cloud in the light of a Nd:YAG laser sheet, making visible its structure. Clearly visible are turbulence-induced 'holes' in the droplet distribution. Such micro-scale measurements therefore yield unprecedented insight into the cloud microstructure and help to better understand the role of turbulence.

Access to clouds from the ground surface is provided by a combination of a kite with a buoyant balloon carrying a data acquisition setup (CloudKite) into clouds up to 1km height above ground. The main objective of the Cloudkite research platform is the investigation of the impact of turbulence on the initiation of rain. In addition the CloudKite laboratory will be used in a Fraunhofer-MPG collaboration (TWISTER: Turbulent Weather In Structured TERrain) where a new 3D Lidar system is to be developed by the Fraunhofer Institute for Physical Measurement Techniques in Freiburg and used to compare with numerical simulations by the Wilczek group.

Figure 2.2: Artistic rendering of a simulation of turbulent flow through a wind farm. Turbulent wind fluctuations generate significant power-output fluctuations, which have a detrimental impact on the power-grid stability. Simulations help to better understand the spatio-temporal structure of wind fluctuations, and may help to design improved layouts of wind farms and power grids.

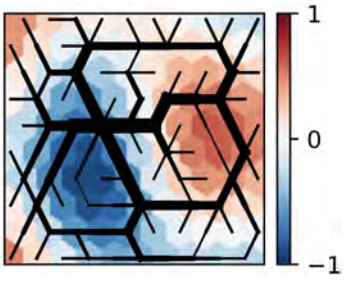

Figure 2.3: Example of a network topology, which optimally cancels out correlated input noise [4]. One realization of the noise is shown color-coded in the background.

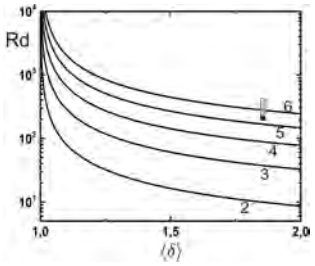

Figure 2.4: Contour curves of the average number of passengers per vehicle, in the plane spanned by the dimensionless request frequency (Rd) and the average tortuosity, δ, of the vehicle routes. The error bar applies to all curves and is partly due to the unknown Riemann curvature of the traffic network (grey) and partly due to the unknown distribution of travel distances (black).

Other research activities are furthermore concerned with possibilities for sustainable energy supply, in particular wind energy. Throughout the last years, the wind energy capacity installed worldwide has continued to grow. The transition to renewable energies, however, comes with a range of challenges: for example, turbulence imposes significant structural fatigue loads on wind turbines which can lead to failure. Integrating wind energy – a fluctuating resource – into a decentralized power grid poses further challenges with respect to power grid stability due to the presence of strong fluctuations. The understanding of turbulence and its interaction with wind energy systems has therefore become an urgent matter with an immediate societal impact, which motivated a number of research projects at our institute.

In order to quantify the impact of turbulence on wind energy systems, it is important to characterize the spatio-temporal structure wind velocity fluctuations in the atmospheric boundary layer as well as in wind farms. We found that for typical wind farm configurations, turbulence between subsequent rows is strongly correlated (see Fig. 2.2). As a result, power fluctuations from the individual turbines will not simply average out across the wind farm. Statistical models [3], however, can be employed to characterize these fluctuations and may help to mitigate their detrimental impact.

As we cannot control the fluctuations of atmospheric turbulence, these findings motivated the question of whether power output fluctuations can be reduced by optimizing the underlying wind farm design and, on a larger level, the power grid. Using tools from network theory, we devised general design rules for *optimal noise-canceling networks*, which reduce output fluctuations changing the wiring diagram only [4]. In the future this may help to design more stable and resilient power grids.

Finally, there is a strongly growing activity towards the development of transport systems which minimize fuel consumption at an affordable price for the customer. As a first step, we have investigated the statistical physics of ride pooling systems. Through an analytical mean field approach [2], we found general characteristics governing the performance of such systems as shown in Fig. 2.4. Important parameters are the dimensionless demand frequency (from the customers), Rd, and the average tortuosity, δ, which would be accepted by the customers. The figure allows to predict what average occupancy (labels of the curves) one can expect. This number is an important economic indicator for the system which decides under what circumstances the system can be maintained economically.

It was furthermore found that such systems exhibit a first-order-type phase transition between a niche market and market dominance if interacting with already established business (like, e.g., the private car). In Fig. 2.5 the region where this phase transition exists is denote by **I**, while in the region denoted **II** there is only the niche market. One of the main goals of the project is to find ways to establish the latter phase under realistic conditions. Under the label '*EcoBus*', we are therefore conducting pilot projects in several areas not too far from Göttingen. In these projects, data are collected which hopefully will allow to devise

cooperative public transport systems for future mobility in both rural and urban settings.

In Fig. 2.6, the occupancy of one of our vehicles (image of the vehicle see top right) is plotted as a function of time over the course of a full day. Operation starts at 6 a.m. and stops very late at night, at 2 a.m.. As one can see, there is already considerable pooling of customer requests, with up to four passengers in the vehicle at the same time. So far our system is well within region **II** of Fig. 2.5 due to the limited number of customers. With about 30 new registrations every day, however, we hope to improve these figures soon.

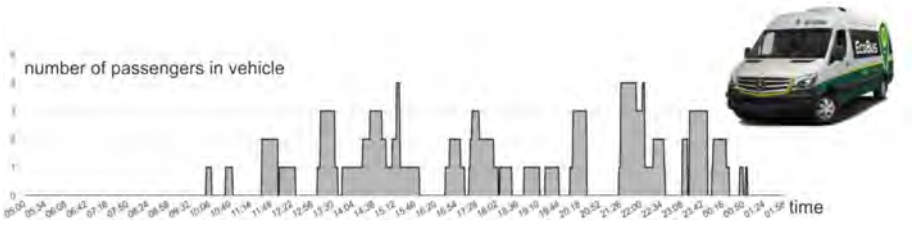

Figure 2.6: Example of occupation of a single vehicle (see top right image) in the course of a day during the pilot project in the Harz mountains. Significant pooling is obviously achieved.

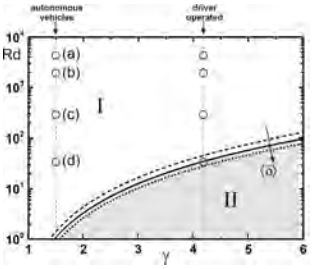

Figure 2.5: If γ is the ratio of the costs for running a minibus (including driver salary) divided by the costs for running a private car, the white area (I) indicates parameters for which the system can be run economically if there are enpugh customers. Open circles correspond to parameters if existing scenarios. (a) New York City; (b) Hamburg; (c) Göttingen; (d) Eichsfeld (rural area near Göttingen).

[1] B. Stevens, S. Bony, *What are climate models missing?*, Science **340**, 1053 (2013)

[2] S. Herminghaus, *Mean field theory of demand responsive ride pooling systems*, Transportation Research A **119**, 15-28 (2018).

[3] L. Lukassen, R. Stevens, C. Meneveau, M. Wilczek. *Wind Energy* **21**, 474 (2018).

[4] H. Ronellenfitsch, J. Dunkel, M. Wilczek. *Phys. Rev. Lett.* **121**, 208301 (2018).

2.2 PHYSICS TO LIFE

Figure 2.7: Matter-to-Life is one of the three graduate schools that have been recently established across the Max Planck Society. The school is a collaboration of the Max Planck Society with the three universities Göttingen, Heidelberg and TU Munich. As national network of Master's/PhD education, the Max Planck Schools provide a direct track PhD in an excellence program initially funded by the Federal Ministry of Education and Research (BMBF) and the Max Planck Society for a period of five years. Per year 30 graduate students are competitively selected and will be educated by the 50 fellows of the school. At Göttingen, all MPIDS Directors, Fred Wolf and Helmut Grubmüller and Stefan Hell from the MPIBPC are part of the school as well as 6 colleagues from the University of Göttingen.

In recent years biology, biochemistry, and biophysics have revolutionized our understanding of living systems from single cells to complex organisms, and even collections thereof. This has been made possible by the rapid advances in molecular biology paired with advanced experimental capabilities and unprecedented computational power for quantitative analysis. Theoretical advances in physical theories of self-organization in complex systems begin to provide a quantitative understanding of the complexity of life-like processes. Research at the center of these developments that aims to bring 'Matter to Life' was part of the agenda of the Max Planck Institute for Dynamics and Self-Organization since its foundation in 2004. Moreover, the newly established department of Living Matter Physics will bring in the experience of its director who has been actively involved in this line of research for many years. To highlight the leadership role of MPIDS in this field at the global scale, we can mention the organization of the American Physical Society's "Physics Next" workshop on *Physics of Living Matter* (April 2018, Long Island NY), and the central role at the organization of the Max Planck Synthetic Biology Initiative (MaxSynBio) and the new national Max Planck School Matter-to-Life (www.maxplanckschools.de/en/matter-to-life; see Fig. 2.7), as well as the UK national Engineering and Physical Sciences Research Council (EPSRC) *NetworkPlus* "Physics of Life".

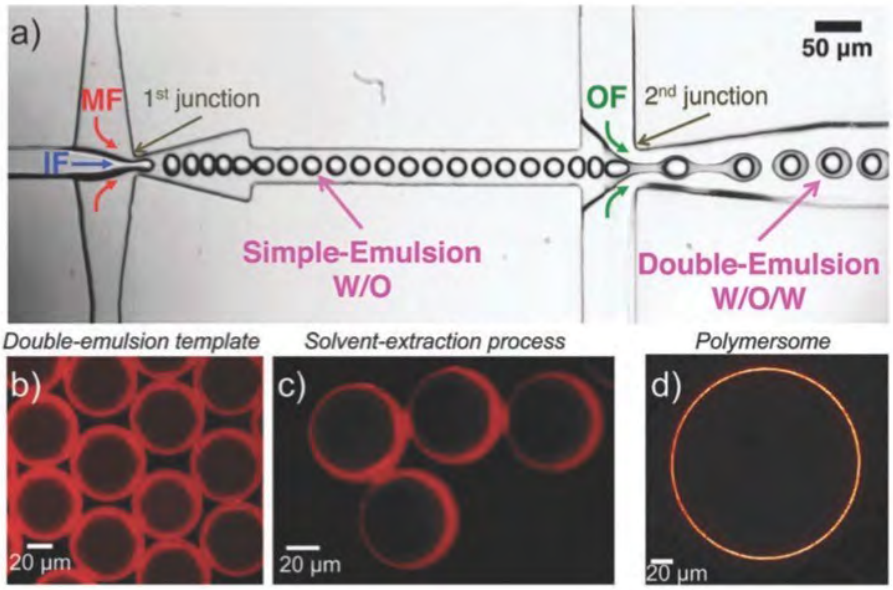

Figure 2.8: (a) Picture of the lab on a chip. IF is the aqueous inner fluid consisting of a mixture of water and surfactant, MF is the middle oil fluid in which the polymer was dissolved and the OF (outer fluid) consisting of an aqueous mixture of water, surfactant, salts and ethanol. (b) Fluorescently labeled compartments at the exit of the microfluidic chip. (c) Compartments after solvent extraction in the aqueous OF. (d) Final compartment after completed solvent extraction (Figure from [2]).

In order to achieve progress in understanding living systems, one can study strongly reduced life-like systems which function under controllable boundary conditions and environment. Concurrently with the huge advances in biochemistry, the micro-fabrication of microfluidic systems has reached a level of maturity that allows for high throughput production under well-controlled conditions. An example can be found in a recent work [1] where a group of scientists from MaxSynBio were able to sequentially assemble functional protocells from the bottom-up; see Fig. 2.8.

The mechanisms and processes that lead to mechanical activity, which is manifested in motility, transport, and conformational changes, has been studied using a variety of simple theoretical and experimental models. These include simple models of micro-swimmers like the three-sphere model and its molecular/stochastic extension that applies to enzymes [3], and the notion of using localized catalytic activity to induce self-propulsion; an idea that is now widely used, even in applications in drug delivery across the blood-brain barrier.

In the design of protocells, active emulsions can provide mechanisms for propulsion, compartment design, or interaction with interfaces [4]. Due to their sensing and transport capabilities, tunability and facility of microfluidic high throughput production at high monodispersity, active droplets are also applicable in the field of smart materials like sensors and microbots. For example, the slow dissolution of the oil droplet into a highly micellar surfactant solution can power oil droplets, which are sensitive to external surfactant gradients, as well as to trails of oil filled micelles left by themselves or other droplets; they have repulsive auto-chemotaxis (shown in Fig. 2.9).

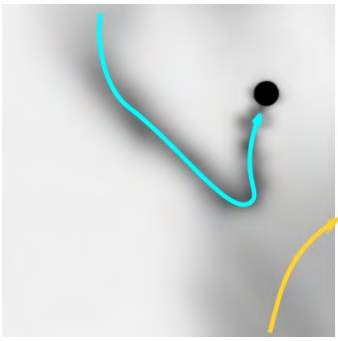

Figure 2.9: Trajectory of a chemotacting self-propelled droplet (blue path) that approaches the oil filled micelles (darker gray) left behind by a droplet that passed the area (yellow trajectory) [5].

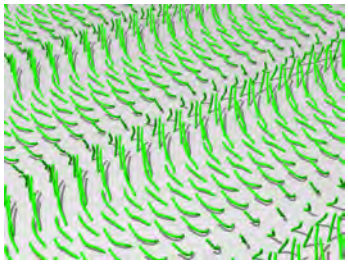

Figure 2.10: Cilia carpets are known to propel fluid in a directed way [6].

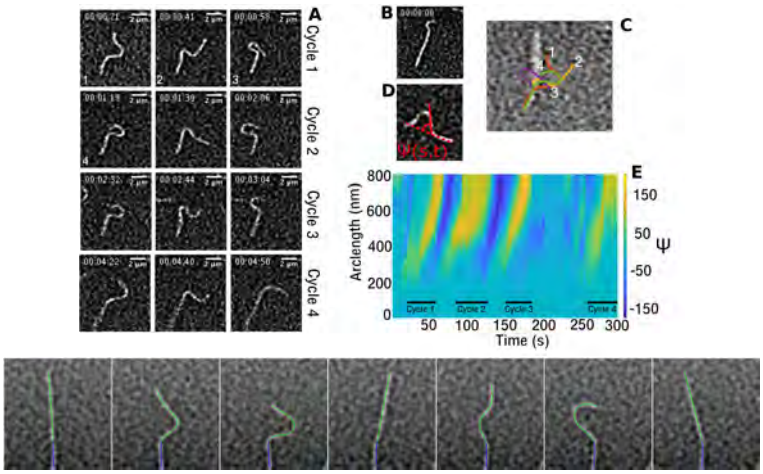

Figure 2.11: (a) Oscillation cycles of a single filament clamped on the surface over time starting at t= 0 from the configuration shown in (b). (b) Starting position of clamped filament. (c) Filament tracking shows the time evolution of the emergent oscillations. The numbers indicate the chronology of the oscillation as well as correspond to the filament positions shown in (a) (see numbers on the bottom left of the micrographs). (d) Tangent angle ψ(s,t) as a function of arc-length s along the flagellum. (e) Kymograph of the tangent angle over time along the filament. The oscillations and their duration of each cycle are pointed out in the figure. The lower panel shows overlapping theoretical and experimental conformations of the beating filament.

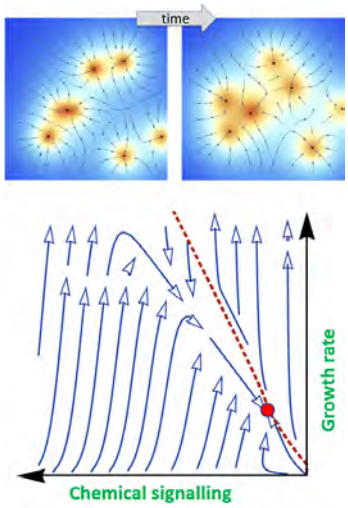

Figure 2.12: How can we predict stability of a tissue or an organism when their individual components are undergoing stochastic time evolution? We show the dynamical phase diagram for a population of diving and chemotactic cells from a dynamical Renormalization Group calculation for a stochastic field theory [7].

Cilia and flagella are self-organized proto-filaments that undergo regular oscillatory beat patterns, and coordinate to (see Fig. 2.10). We are building upon our expertise at MPIDS to design and characterize synthetic cilia and use them to make carpets for fluid transport. Using a bottom-up approach we focus our effort on building synthetic biomimetic beating structures that resemble the natural cilia and therefore allow us to get an insight into the mechanism that drives cilia to beat with a stroke and a recovery phase. These structures rely only on microtubules and the motor proteins for force generation. This approach has the advantage of reducing the complex structure of a cilium to a minimal system that we can study in terms of biopolymers and force generators both experimentally and theoretically; see Fig. 2.11. Further more, in collaboration with the Single Molecule Spectroscopy and Imaging for Biophysics and Complex Systems Group at Göttingen University we are using the novel multi-plane phase contrast imaging technique to record the three-dimensional beating pattern of isolated axonemes from *C. reinhardtii* that beat in the vicinity of a substrate and their collective behavior.

The question of how to understand life from the bottom-up has very important aspects when we move to the level of mesoscopic description and ask what happens when we couple a large number of agents with non-equilibrium life-like behavior. This forms an important next step for our research agenda in this theme. As an example, we mention that we have uncovered a mechanism by which cell proliferation and chemical signalling can lead to a homeostatic balance at the large scale, giving rise to a stable but constantly renewing state as in a normal tissue, which can undergo a dynamical phase transition to a state where proliferation is not regulated by chemical signalling and grows out of control, as is the case in cancer metastasis; see Fig. 2.12. This example suggests that significant and nontrivial *new physics* is waiting to be discovered when we push this research agenda further. This is a very exciting prospect for future research at MPIDS.

[1] M. Weiss et al., *Sequential bottom-up assembly of mechanically stabilized synthetic cells by microfluidics*, Nature Materials **17** (2018) 89-95, DOI:10.10.38/NMAT5005

[2] J. Petit et al., *Modular approach for multifunctional polymersomes with controlled adhesive properties*, Soft Matter **14** (2018), 894-900, DOI: 10.1039/c7sm01885a

[3] R. Golestanian and A. Ajdari, Mechanical Response of a Small Swimmer Driven by Conformational Transitions, Phys. Rev. Lett. **100**, 038101 (2008)

[4] Herminghaus, S. et al., *Interfacial Mechanisms in Active Emulsions*. Soft Matter **10**, 7008–7022 (2014)

[5] Jin, C. et al., *Chemotaxis and Autochemotaxis of Self-Propelling Droplet Swimmers*, Proc. Natl. Acad. Sci. U. S. A. **114** (2017) 5089–5094

[6] N. Osterman and A. Vilfan, Proc. Natl. Acad. Sci. USA **108**, 15727-15732 (2011)

[7] A. Gelimson and R. Golestanian, Collective Dynamics of Dividing Chemotactic Cells, Phys. Rev. Lett. **114**, 028101 (2015)

2.3 PHYSICS TO MEDICINE

Biological systems are open, dissipative, and nonlinear. Therefore, concepts from nonlinear dynamics may play a key role to understand physiological function. Physiological disorders are often characterized by sudden changes in the qualitative dynamics of a physiological control mechanism, which may lead to disease [1]. The term dynamical diseases has been coined, suggesting that a dynamical systems perspective may contribute to elucidate mechanisms underlying disease onset as well as progression and may open novel diagnostic and therapeutic approaches. Research areas at the MPIDS include the spatial-temporal dynamics of excitable biological media, such as heart and brain, and biological flows, including vascular flow, flow in the brain, and nasal airflow. The MPIDS carries out evidence-based, fundamental research in these areas, addressing relevant medical needs and opening paths for clinical applications.

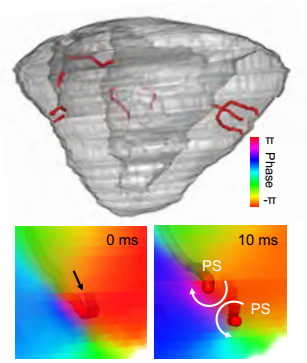

Figure 2.13: 3D Electromechanical phase singularities during ventricular fibrillation inside the ventricles. Breakthrough of the U-shaped intramural mechanical filament (red) on the left ventricular epicardial surface [2].

Cardiac arrhythmia is a prominent example of a dynamical disease. While it has been hypothesized that cardiac arrhythmias are driven by three-dimensional scroll waves, their visualization evaded experimental realization. Recently, researchers at the MPIDS have developed a novel ultrasound-based imaging technology to visualize three-dimensional electro-mechanical waves inside the heart muscle [2] (Figure 2.13). In collaboration with cardiologists at the University Medical Center Goettingen, we will translate this technology to clinical application.

The control of spatial-temporal dynamics in cardiac tissue during arrhythmias is a fundamental scientific challenge that also addresses a significant medical need. Researcher at the MPIDS focus on elucidating the mechanisms underlying the dynamics and control of vortices in cardiac tissue by theoretical and experimental means [3, 4]. Based on Low-Energy Anti-Fibrillation Pacing (LEAP), we continue to further develop and optimize this approach in preclinical experiments in porcine disease models (heart failure, myocardial infarction). Following the successful completion of these experiments, a first-in-man study will be conducted in collaboration with cardiologists at the University Medical Center Goettingen.

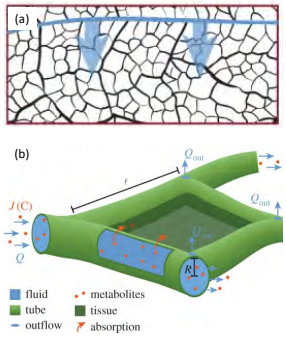

Figure 2.14: (a) The secondary vein (thick blue) supplies the tubular higher order vein network with metabolites and fluid. (b) Xylem vessel network modelled as network of tubes of varying radius and length [6].

Heart failure is a common and potentially fatal disease, in which progressive structural and functional remodeling of cardiac tissue results in loss of pump function and/or the onset of lethal cardiac arrhythmias. In the collaborative research center SFB 1002, researchers of the MPIDS and the University Medical Center Goettingen investigate the molecular mechanisms underlying the transitions to heart failure. In a related project, MPI researchers develop electromechanical models of the heart and study electrophysiology and mechanics of engineered heart muscle (EHM). EHM is obtained from induced pluripotent stem cells and may be applied for heart muscle repair, aiming for restoring its mechanical function. This innovative therapy concept is currently tested in silico and in vivo in preclinical experiments in non-human

primates (macaque monkeys) in collaboration with researchers at the University Medical Center.

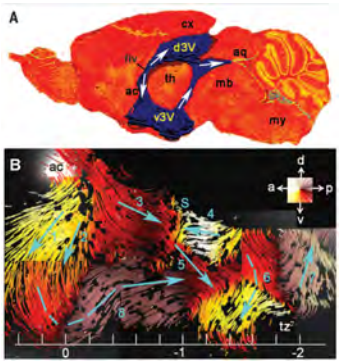

Figure 2.15: Anatomy of the third ventricle in the mouse and flow map of the v3V. (A) Sagittal section through the third ventricle (blue), consisting of a dorsal (d3V) and a ventral (v3V) part connected by two ducts. As indicated by white arrows, CSF enters the v3V through the foramen interventriculare and exits through the aqueduct. (B) The flow map of the v3V, generated by particle tracking, shows that near-wall flow is sub- divided into multiple flow domains. The associated eight major flow directions are indicated with turquoise arrows [5].

Life and functioning of higher organisms depend on the continuous supply of metabolites to tissues and organs. Fluid flow-based transport through a vascular network is the indispensable mean to supply nutrients, hormones, and metabolites to all cells in a tissue. For example, brain microvasculature needs to be set up to locally increase supply if required by neuronal activity, which is facilitated by vessel dilation. How can the local dilation of a single vessel result in a robust increase in supply within the globally coupled vascular network? With our theoretical framework we identify three regimes of supply dynamics of which the one with advection governed transport dominates real microvasculature [6] (Figure 2.14). We justify analytically why this specific regime allows for robust increase in supply following vessel dilation independent of network architecture. Our framework is instrumental to interpret fMRI data, predict drug delivery, design blood vessel architecture in organs in health and disease. For example, it has been hypothesized that impaired cardiac function results in impaired flow in glymphatic system, reduced liquor clearance in the brain, associated with an increased risk of neurodegenerative disorders.

To further elucidate the role of biological flow in the brain, researchers at the MPIDS and the MPI for Biophysical Chemistry showed that the cilia lining the ventral third ventricle (v3V) surface of the mammalian brain are oriented to create rather complex flow networks instead of a straight through flow of the cerebrospinal fluid [5] (Figure 2.15). The ventral third ventricle is located in close proximity of several brain nuclei, as for instance the Hypothalamus, and therefore may be directly connected to multiple body functions like the sleep/wake cycle. The current research efforts therefore focus on how the flow networks are formed and how those networks impact the transport of chemical transmitters, such as hormones. There is also increasing experimental evidence that impairment of the cilia-based flow network in the brain ventricles is associated with neurological dysfunction and disease.

Nasal airflow is another example of biological flow. Nasal obstruction is an enormous clinical problem, where structural malformations of the nasal airway often need to be treated with surgical techniques. However, currently there is no clinically useful standard for the objective measure of nasal obstruction, which has hampered efforts to perform large randomized treatment trials, and has created a dependence exclusively on patient reported outcomes measures (PROMs) to determine success. To overcome this lack of a quantitative approach, researchers at the MPIDS use a combination of 3d reconstructions of nasal geometries using CT scan data and computational fluid dynamics to determine airflow reliably [7]. The resulting resistances are correlated to PROMs in a series of patients undergoing surgical nasal airway correction. Defining the relationship between specific nasal deformities, predicted nasal airflow, resistance, and outcomes will provide the objective measure tool that is essential for future clinical trial design and implementation to reduce the rate of treatment failures.

[1] L. Glass and M.C. Mackey, *Ann. N.Y. Acad. Sci.* **316**, 214-235 (1979)
[2] J. Christoph et al., *Nature* **555**, 667-672 (2018)
[3] S. Luther, F.H. Fenton et al., *Nature* **475**, 235-239 (2011)
[4] V. Zykov et al., *PNAS* **114**, 1281-1286 (2017)
[5] R. Faubel et al. *Science* **353**, 176-178 (2016)
[6] F.J. Meigel, K. Alim, *J. R. Soc. Interface* **15**, 20180075 (2018)
[7] D. Zwicker et al., *PNAS* **115**, 2936-2941 (2018)

PART I

ORGANIZATION

DEPARTMENTS

3

Contents

3.1 DEPARTMENT OF DYNAMICS OF COMPLEX FLUIDS

Prof. Dr. Stephan Herminghaus received a PhD in physics from the University of Mainz in 1989. After a postdoctoral stay at the IBM Research Center in San Jose (California, USA), he became a research associate at the University of Konstanz, where he received his habilitation in 1994 and a Heisenberg Fellowship in 1995. In 1996 he became head of an independent Max Planck Research Group at the MPI for Colloids and Interfaces in Berlin. In 1998, he received calls on full professorships at the Universities of Fribourg (Switzerland) and Ulm, and decided for heading the department of Applied Physics in Ulm. Since 2003 he has been Director at the MPIDS, and since 2005 is an adjunct professor at the University of Göttingen. He was appointed as Professeur Invité to the Université Paris VI (2006/7) and Université Paris Sud (2013). He is member of the Scientific Advisory Council of the National IOR Centre Norway and Scientific Advisor to the ESA (Chair of Physical Sciences).

A complex fluid consists of (a large number of) similar mobile entities which are complex enough by themselves to preclude a straightforward prediction of the collective behaviour of the whole. Our research aims at understanding phenomena of self-organization, such as pattern formation and self-assembly, in complex fluids. We hope to identify suitable model systems which yield insight into overarching principles of self-organization in systems as diverse as aggregation of planetesimals in primordial clouds, swarming in bacterial colonies, or patterns in traffic flow. One challenging question is: are there general common 'principles' behind the various instances of symmetry breaking, structure formation, and emergence in open systems? Either finding such principles or proving their non-existence would be equally rewarding.

On the fundamental side, we consider general descriptions of systems far from equilibrium, such as Master equations and the Fokker-Planck equation. It is known that when a system is classified not according to its macrostates, but according to closed cycles in the space of macrostates, the corresponding Master equation fulfills detailed balance in general. We explore the possibilities to exploit this fact in the continuum (Fokker-Planck) picture, trying to find analytical expressions for the relative weights of non-equilibrium steady states.

On the complex side, biological matter provides the most intricate systems we are studying, but we try to concentrate on those which are still simple enough to be described by physical and physicochemical principles. The swarming behaviour of Chlamydomonas reinhardtii compares well with our observations in active emulsions, although there are bio-specific ramifications which are complex (e.g., light switchable) and by no means understood.

The project with by far the closest connection to everyday life concerns collective behaviour in public transportation systems. After having studied the mean-field behaviour of ride pooling systems analytically and by simulations, we are performing real-world experiments (pilot projects) in order to test and develop a demand-driven system which may become comfortable and cheap enough eventually outcompete the private car on our roads.

During the last two years there have been substantial fluctuations in our personnel. Lucas Goehring and Marco Mazza have received (and accepted) offers of professor positions at Universities abroad, while Stefan Karpitschka, who joined us through our Max-Planck-UTwente Center, has set up his research group on interfaces of complex fluids.

Dr. Corinna Maaß studied Physics at the University of Konstanz, Germany. She was a fellow with the International Research Training Group "Soft Condensed Matter Physics of Model Systems" and received her PhD in 2009 from the University of Konstanz for research on levitated granular gases. From 2010-2013 Corinna worked as a postdoc in DNA nanotechnology at New York University, USA, from 2010-2011 as a fellow of the German Academic Exchange Service. She joined our institute in 2014 as leader of the working group 'Active Soft Matter'. Her current research focuses on droplet swimmers in complex geometries as well as collective interactions in large scale swimmer systems under variable dimensional confinement.

Dr. Oliver Bäumchen studied physics and mathematics at Saarland University (Germany) and graduated in physics in 2006. In 2010 he received his PhD in soft matter physics from Saarland University. He worked as a lecturer at the University of Applied Sciences (Saarbrücken) from 2007 to 2008. In 2011 he was awarded a DFG research fellowship and joined the McMaster University, Canada, as a PostDoc. Since August 2013 he has been a group leader at our institute. Aside from instabilities of complex liquids, he is interested in biological systems at interfaces. In 2015 he was awarded a 'Joliot Chair' and joined the ESPCI Paris as a visiting faculty.

Dr. Stefan Karpitschka received his Diploma in Physics with distinction in 2007. As a PhD student he joined the Max Planck Institute of Colloids and Interfaces in Potsdam, Germany, where he also completed his first PostDoc position in 2013. Then he went to the University of Twente in Enschede, The Netherlands and to the Stanford University, USA for other PostDoc projects. Since 2017 he is a Research Group Leader in our department and in the Max Planck - University of Twente Center for Complex Fluid Dynmamics. This group investigates the behavior of complex fluids at their interfaces with solids and gases.

Dr. Christian Bahr studied chemistry at the TU Berlin and received his PhD in 1988. Research stays and postdoctoral work took place at the Raman Research Institute (Bangalore, India) and the Laboratoire de Physique des Solides of the Université Paris-Sud (Orsay, France). After his habilitation for physical chemistry at the TU Berlin in 1992, he moved to the University Marburg as a holder of a Heisenberg-Fellowship in 1996. From 2001 he worked as a software developer in industrial projects before he joined our institute in 2004. Research topics comprise experimental studies of soft matter, mainly thermotropic liquid crystals.

Dr. Kristian Hantke studied physics at the University of Manchester (B.Sc. 2000) and at the Philipps-University Marburg (Diploma 2002). In 2005 he received his PhD from the University of Marburg. After studying the optical injection of spin currents during a post-doctoral stay at the University of Marburg he joined the group of Prof. S. Herminghaus at our institute as a scientific staff member in 2007. Being the lab coordinator for the laser and microscopy setups, his work centers around the application of new experimental techniques based on nonlinear vibrational imaging and multi-photon laser scanning microscopy.

Associated Scientists

Dr. Lucas Goehring obtained his PhD at the University of Toronto in 2008 and has continued to study geophysical pattern formation through experimentally accessible analogues. In 2008 he was elected a research fellow of Wolfson College at the University of Cambridge and joined our institute in 2011. He became associate professor for physics and mathematics at Nottingham Trent University in 2018.

Dr. Marco G. Mazza received his PhD in 2009 at Boston University with H. Eugene Stanley. Between 2009 and 2012 he was a postdoc and lecturer at TU Berlin. In 2012 he joined the MPIDS as a group leader, performing research on nonequilibrium physics of granular, soft, and biological matter. He left in 2018 for a position as Lecturer in Applied Mathematics at Loughborough University.

Dr. Matthias Schröter obtained his PhD in physics in 2003 from Magdeburg University. After a postdoctoral stay with Harry Swinney at the Center for Nonlinear Dynamics at the U. of Austin he joined the MPIDS as a group leader in 2008. In May 2015 he left for a senior scientist position at the university of Erlangen, but is still doing joined research with the Department for Dynamics of Complex Fluids.

Prof. Dr. Ralf Seemann studied physics at the University of Konstanz and received his PhD in 2001 from the University of Ulm. After a postdoctoral stay at the University of California in Santa Barbara, he joined the MPIDS as a group leader in 2005. In 2007 he was appointed as professor at the Saarland Univ. but is still associated with the MPIDS in the framework of the GeoMorph project funded by BP.

Prof. Dr. Marc Timme received his PhD at the University of Göttingen. After a research stay at Cornell University, he became head of a research group on Network Dynamics at the MPIDS. In the Department for Dynamics of Complex Fluids, Marc was one of the driving forces in the EcoBus project. Since 2017, he holds the Chair for Network Dynamics at TU Dresden.

Technical Staff

Monika Teuteberg and Barbara Kutz (top left) take care the secretary offices and administrative issues of the department and of the MPRGs. Guido Schriever (top center) is our scientific assistant, which implies scientific reporting, maintenance of the web page and organization of visits and events. Diana Strüver and Markus Benderoth (top right) are responsible for our chemical and biological laboratories, which includes daily operation in all safety issues. Wolf Keiderling (bottom left) operates our mechanical workshop, and Thomas Eggers (bottom right) supports the desktop computers of the scientists, the computer clusters, the DCF network and the email accounts.

3.2 DEPARTMENT OF FLUID PHYSICS, PATTERN FORMATION AND BIOCOMPLEXITY

Our research is focusing on the physics of self-organization in fluidic and biological systems. The four research fields studied are *Synthetic Biology, Biodynamics and Biofluids, Cloud Micro Physics,* and *Turbulence/Convection.* Additionally, since 2006 the department supports financially with 1/3 of its funds the Max Planck Research Group Biomedical Physics led by Prof. Stefan Luther. The Department's Director is a full member of the faculty of physics at Göttingen University in the Physics Institute for Dynamics of Complex Systems. He is also the Co-Director of the Max Planck University of Twente Center for Complex Fluid Dynamics and Vize Chair of the Max Planck School Matter to Life. The department has 13 Group Leaders that individually conduct research within the four foci.

The aim of the department's research is focused on understanding the physics of complex systems. In that respect we define systems to be complex, when the physics emerges from coupled, nonlinear, and sometimes nonlocal interactions. In our approach we rely on methods from non-equilibrium statistical mechanics, pattern formation and nonlinear systems theory. Currently we are investigating turbulence in thermal convection; fundamentals of turbulence; inertial and tracer particle transport in fully developed turbulence with implications for fundamental theories, but also, for practical issues like turbulent mixing, particle aggregation and cloud micro-physics; the spatio-temporal dynamics in reaction diffusion systems; biofluid mechanics of the heart and brain; and the intra-cellular and self-organizing processes leading to eukaryotic cell motility, chemotaxis, electrotaxis, curvotaxis, and tissue development; and on the building of fluid transport systems with artificial cilia that we call synthonemes. We are also partner in the Max Planck Synthetic Biology Initiative. The laboratory provides a microscopy facility, a cell biology laboratory, and shares with the other groups a class 1000 clean room for micro-fabrication. It established the Max Planck Turbulence Facility, which consists of a set of experimental systems and a compressed gas facility to achieve ultra-high turbulence levels. For investigations of cloud micro-physics, we have an outpost at the Environmental Research Station Schneefernerhaus on the Zugspitze at 2650m, where we are also part of the Virtual Alpine Observatory. With our mobile cloud kite laboratory, we investigate cloud microphysics in real clouds.

Our research has been and will continue to be truly interdisciplinary from engineering, material science, physics, geophysics, and applied mathematics, to chemistry, biology, and medicine. We connect seamlessly to the other departments and research groups and are a member of the International Collaboration for Turbulence Research and the German Centre for Cardiovascular Research (DZHK). We collaborate with groups at the MPI for Biophysical Chemistry, the Physics Department, and the Medical Center at the University of Göttingen.

Prof. Dr. Dr. h.c. Eberhard Bodenschatz received his PhD in theoretical physics from U. Bayreuth in 1989. In 1991 he accepted a faculty position in experimental physics at Cornell and joined the faculty from 1992 until 2005. In 2003 he was appointed Director at the MPIDS. Since 2005 he is Adj. Prof. at Cornell in Physics and Engineering and since 2007 Prof. at U. Göttingen. Since 2016 he is Chair Prof. at Tsinghua and since 2017 oversea Expert at NWPU. He has a long history of important service to the scientific society. Among others, from 2012 to 2017 he was Vice Chair and Chair of the Chemistry, Physics and Technology Section of MPS (32 institutes). He served as Editor in Chief of NJP and on the editorial boards of Ann. Rev. Cond. Mat. Phys., EPJH, Physica D, Phys. Rev F. and SIAM JADS. Currently he is a Member of the Steering Committee of the MaxSynBio, on the Executive Board of the Max Planck School Matter to Life, Codirector of the Max Planck Twente Center on Complex Fluid Dynamics, site vice speaker for the German Center for Cardiovascular Research and on the presidential board of the German Physical Society. He is member in the Göttingen Academy of Sciences, carries a Honorary Doctorate from the ENS Lyon, and is Fellow of the APS, IOP, EPS, and EuroMech. He is a recipient of the Stanley Corrsin Award of the APS.

Dr. Gholamhossein (Mohsen) Bagheri studied mechanical engineering at the Perisan Gulf Univeristy (BA) and Shahid Bahonar University (MSc), Iran, before doing his PhD at the University of Geneva, Switzerland. During his PhD he carried out experimental and numerical investigations on dynamics of irregular particles in laminar and turbulent flows, for which he received his doctorate in 2015. Shortly after he was awarded an 18-months Swiss National Science Foundation scholarship to join the institute as a guest postdoc and now he is a group leader. His current research interests include experimental investigation of cloud microphysics and turbulence with the Cloudkite. He is also involved in the cloud measurements carried out at the research station Schneefernerhaus (UFS) near Zugspitze.

Prof. Dr. Carsten Beta studied Chemistry in Tübingen, Karlsruhe, and Paris. In 2001, he joined the the Fritz Haber Institute (Prof. G. Ertl) and graduated from the Free University Berlin in 2004. After working as a postdoctoral researcher at Cornell and UCSD, he became a senior scientist at the institute in 2005. In 2007 he was appointed Prof. of Biological Physics at U. Potsdam and stayed associated with the institute. His research focuses on biophysics (cell motility, chemotaxis, actin dynamics, single cell manipulation techniques) and on pattern formation in reaction-diffusion systems.

Dr. Azam Gholami studied physics at Sharif University (Iran) where she received her bachelor in 1999. After her master in physics from the Institute for Advanced Studies in Basic Sciences (Zanjan, Iran) in 2001, she continued her study in theoretical physics at the LMU, München and graduated in 2007. In 2008, she joined the institute to work on actin-based motility and flow-driven waves in *Dictyostelium discoideum*. Since 2012, she is a group leader. She is coordinating the MaxSynBio project and works on artificial cilia and cilia-driven motility.

Dr. Isabella Guido began her study in electrical engineering at the University of Bologna, Italy. In 2006 she joined the Fraunhofer IBMT in Potsdam and in 2010 received her doctorate in physical engineering from the TU Berlin. From 2010-12 she was postdoctoral researcher at Peking University (China) and from 2012-13 at U. Glasgow developing microsystems for single cells manipulation and characterizing cellular mechanical properties. In June 2013 she joined the institute as a postdoctoral researcher working on cell electrotaxis. Since August 2014 she is a group leader within the synthetic biology initiative *MaxSynBio* working on constituting artificial cilia.

Dr. Hyejeong Kim studied mechanical engineering at Pohang University of Science and Technology (POSTECH) where she received her bachelor in 2012. She received her Integrated PhD degree in August 2017 at POSTECH with thesis of "Development of Advanced Biomimetic Technologies Inspired by Leaf Transpiration." From August 2017 to May 2018 she was a postdoctoral research at POSTECH, and developed efficient water management technologies. She joined the institute in June 2018, and works on Living Foam project as a postdoctoral associate. She is interested in broad range of experimental approaches to microfluidics, soft materials, and their applications.

Dr. habil. Alexei Krekhov received his PhD in theoretical physics from the Perm State University (Russia) in 1990 studying defects in liquid crystals. During his Humboldt Research Fellowship at U. Bayreuth from 1994-96 he studied pattern formation in liquid crystals. Starting 1999 he was a researcher at U. Bayreuth working on pattern formation in complex fluids and soft matter theory. In 2010 he received the habilitation in theoretical physics from U. Bayreuth. He joined the institute in October 2013. His current research interests include nonlinear dynamics in excitable media, two phase convection and modeling of cell motility. He leads the theory group on pattern formation.

Dr. Rupamanjari Majumder received her PhD degree in Physics, from the Indian Institute of Science, Bangalore, in July 2014. From 2014-2017, she remained as a postdoctoral researcher in the Leiden University Medical Center, where, she was appointed as assistant professor in early 2017. She joined the institute in June 2018 as a postdoctoral researcher, specializing in numerical studies of wave dynamics and spatiotemporal chaos in anatomically realistic, electrophysiological models of mammalian cardiac tissue. Her current research interests as a postdoctoral associate include nonlinear dynamics in cardiac tissue, manipulation of spiral waves in anatomically and ionically realistic heart models, and cardiac optogenetics.

Dr. Jan Moláček studied mathematics at the University of Cambridge (UK), where he received his BA and MA degrees. He received his PhD in applied mathematics from the Massachusetts Institute of Technology (Cambridge, USA) in 2013 for his experimental and theoretical investigation of droplets bouncing and walking on a vibrating liquid bath. He joined the MPIDS in September 2013 as a postdoctoral researcher. He leads the experimental group on cloud microphysics investigation on Mount Zusgpitze. His research interests as a postdoctoral associate include experimental investigations of atmospheric turbulence, particles in turbulence and droplet dynamics in general.

Dr. habil. Holger Nobach received his doctorate in electrical engineering from the University of Rostock in 1997. During his postdoctoral research at Dantec Dynamics in Copenhagen (Denmark) and at the Technical University of Darmstadt, he developed measurement techniques for flow investigations. Since 2005 he has been a group leader at the institute with a research visit at Cornell University (NY, USA). In 2007, he received the habilitation in mechanical engineering from the Technical University of Darmstadt. He works on the experimental investigation of turbulent flows and thermal convection and is editor for ISRN Signal Processing. Since January 2018 he leads the Research Unit Electronics.

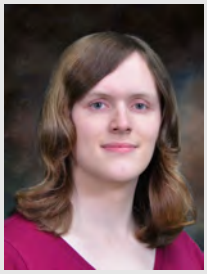

Dr. Freja Nordsiek studied Physics at Michigan Technological University (Houghton, USA) where she received her bachelor in 2010 and did research on the clustering of water droplets in air in the Cloud Physics Laboratory. She then received her doctorate in Physics in 2015 at the University of Maryland (College Park, USA) for research on transport in Taylor-Couette flow and granular electification. She joined the institute in December 2015 as a postdoctoral researcher to investigate turbulence in the laboratory and the atmosphere. She works primarily on the Cloudkite, a tethered lighter than air aerostat to measure cloud particles and turbulence *in situ* in clouds.

Dr. Oliver Schlenczek studied Meteorology in Mainz. In early 2018, he received his PhD in Meteorology from the University of Mainz where he developed a new airborne holographic system (called "HALOHolo") for investigating the microphysical composition of liquid, mixed-phase and ice clouds. He was involved in various airborne field campaigns which targeted mixed-phase clouds in the Arctic, cirrus clouds in the mid latitudes and convective clouds in the tropics and subtropics. In late 2017 he joined the institute as a postdoctoral associate with the Cloudkite being his main project. His research interests cover all aspects of experimental cloud physics.

PD Dr. Olga Shishkina studied mathematics at the Lomonosov Moscow State University (LMSU) until 1987. In 1990 she received her doctorate in scientific computing from the Moscow University for Telecommunication & Informatics. After being a senior lecturer at the Rybinsk Aviation Technological Academy until 1994, she worked as a researcher at the LMSU until 2002 and at the DLR Göttingen until 2014. In 2009 she habilitated in fluid mechanics at the TU Ilmenau and in 2014 also in mathematics at U. Göttingen. In 2014 she became Heisenberg fellow and joined the institute where she leads an independent group. As of April 2019 she leads the group theoretical study of thermally driven turbulence.

Dr. Marco Tarantola received his diploma at the Würzburg U. in 2005 - focusing on biotechnology - and his PhD in 2010 at the physical chemistry of the Mainz U. for the study of dynamics of epithelial monolayers. In 2010, he became coordinator of the CRC 937. He then joined the institute as a postdoctoral scientist until 2012 to work on D. discoideum (D.d.) actin oscillations, before leaving for a stay at the UC San Diego until 2013, where he focused on adhesion and cell polarization of D.d.. Since 2014, he is a group leader and currently studies quantitative biology of D.d. and cardiac fibrosis and comparable synthetic model systems.

Dr. Laura Turco received her master's degree in Biomedical Engineering from Politecnico di Milano and her PhD in Biophysics at the Max Planck Institute for Dynamics and Self-Organization. She studies cardiac contractile dynamics focusing on the mechano-electrical coupling, connectivity between cardiomyocytes and fibroblasts, and the influence of external stimuli on cellular functional and morphological changes. She is leading the MPIDS microfluidic facility and is also involved in the design and fabrication of microfluidic platforms for synthetic biology and biomedical applications within the MaxSynBio initiative.

Dr. Yong Wang studied Process Equipment & Controlling Engineering, and Applied Mathematics at Xi'an Jiaotong University (China). In 2010, received his PhD degree in Engineering Thermal Physics for his development of a lattice Boltzmann method as applied to thermoacoustics and PIV measurements for oscillatory flows. From 2011–15 he was a postdoctoral researcher at UC Irvine (USA), and investigated the turbulent flow in human upper airway with DNS. He then joined the institute as a group leader in March 2015. His research interests are in biofluidics and biomechanics, such as failing heart regeneration and cilia coordinated flow.

Dr. Stephan Weiß has received his diploma in physics from the University of Bayreuth in 2005 and a PhD in experimental physics from the Georg-August University Göttingen/MPIDS in 2009. He worked as a postdoc at the University of California Santa Barbara (DFG-Fellowship) on turbulent thermal convection and at the University of Michigan on spirals in oscillating chemical reactions. In August 2015 he joined the MPIDS as a group leader, where he leads the experimental research on thermal convection. Current topics include rotating turbulent thermal convection, convection under phase transition, and convection with strongly varying fluid properties.

Dr. Christian Westendorf studied biology at the U. Rostock (Germany). After finishing the Diploma thesis in microbiology in 2006 and a short research stay at the University's Institute of Technical Chemistry in 2007, he joined the department of Eberhard Bodenschatz as a Ph.D student. He graduated in physics at the U. Göttingen in 2012, with his thesis focusing on the biophysics of the actin cytoskeleton. From 2013–2015 he worked at the U. Graz (Austria) on plasmodial slime mold biology. He rejoined the institute in late 2015 to investigate the quantitative biology of different multicellular aggregates. Since 2016, he is also in charge of the department's microscope facility.

Dr. Vladimir S. Zykov studied physics at the Institute of Physics and Technology (Moscow, Russia). He graduated in 1973, received PhD in 1979, was habilitated in 1990 and occupied the position of leading scientific researcher at the Institute of Control Sciences (Moscow, Russia). In 1992 he joined the group of Prof. Mueller first at the MPI of Molecular Physiology and since 1996 at the Magdeburg University. Since 2001 he was a research scientist at the TU Berlin and in 2010 joined the institute. His research interests include pattern formation processes in nonlinear reaction-diffusion media and control methods of self-organization.

3.3 DEPARTMENT OF LIVING MATTER PHYSICS.

Prof. Dr. Ramin Golestanian obtained his PhD in 1998 from the Institute for Advanced Studies in Basic Sciences (IASBS) in Zanjan, under the remote supervision of Mehran Kardar from MIT. He was subsequently an independent postdoctoral research fellow at the Kavli Institute for Theoretical Physics at UCSB. He has held academic positions at IASBS, the University of Sheffield, and Oxford University, and risen through the ranks until he became a Full Professor in 2007. Golestanian is distinguished for his work on active matter, and in particular, for his role in developing microscopic swimmers and active colloids. He is elected Fellow of APS and IoP, and recipient of the Holweck Medal of the Société Française de Physique and the Institute of Physics, EPJE Pierre-Gilles de Gennes Lecture Prize, Martin Gutzwiller Fellowship of the MPI-PKS, Nakamura Lecturer Award of UCSB, and 50th-Anniversary Most Distinguished Alumni Award of Sharif University of Technology. He has held many visiting positions, including CNRS Visiting Professor, Visiting Professor at College de France (hosted by the late Nobel Laureate Pierre-Gilles de Gennes), Frederic Joliot Visiting Chair at ESPCI, and Visiting Scholar at MIT. He currently serves as Chair of IUPAP C6 Commission on Biological Physics, and Divisional Associate Editor (DAE) at Physical Review Letters (APS).

The conceptualization of "Dynamics and Self-Organization" by Immanuel Kant in his 1790 book *Critique of Judgment* was inspired by comparing man-made complex devices with nature. Interestingly, his description can be used today as an inspiration in our modern interpretation of the quest for physical understanding of living systems, which is undoubtedly one of the central themes of the 21st century science. Complexity in biological systems has been studied intensely in the past two decades, mostly in the context of the flow of information, such as the structure of signalling, metabolic, and transcription-regulatory networks, as well as evolution. However, the systemic view of cellular functional organization has so far included very little input from the physical aspects of the dynamical processes inside the cell, such as where and when they take place, and how they are organized and regulated in the physical sense, in terms of (physical not genetic) interactions, reaction, diffusion, transport, and self-assembly. The idea of thinking about biological systems as *Living Matter* can be traced back to Erwin Schrödinger's visionary 1944 book, *What is Life?*, where he writes on the 1st page of chapter 1: "The large and important and very much discussed question is: How can the events in space and time which take place within the spatial boundary of a living organism be accounted for by physics and chemistry?" We can put this question in context as follows: Suppose we know how to make a sack of chemicals that contains all the ingredients of a cell. Then, how could the chemicals in the sack organize themselves to form a Living Cell? Despite having been around for more than half a century, there has been relatively little progress along these lines, perhaps because the foundations needed for studying the statistical physics of the collective behaviour of nonequilibrium soft matter systems are only just beginning to be developed.

To help answer Schrödinger's question, we could invoke the most fundamental dynamical governing rule in biology, *i.e.* evolution. A glance at the empirical evidence that is available today about how life has started points to two incredibly fascinating observations: **(i)** all known forms of life seem to have descended from a *Universal Common Ancestor* (UCA) that existed around 3.5 billion years ago, and **(ii)** the first living cell was very similar to any other living cell (from a physicist's point of view) in terms of the basic structure. These observations strongly suggest the possibility that the occurrence of a UCA could be regarded as a singularity—drawing on an appealing analogy to cosmology—that could have resulted, or *emerged*, from the collective behaviour of many constituents, reminiscent of a phase transition. This possibility would have significant consequences. For example, this might mean that a search for *the origin of life* should not necessarily seek a smooth transition down to simpler and simpler forms of life. More importantly, it means that as condensed matter physicists we might be able to help significantly with the quest to find the origin of life, because of our extensive previous success in unraveling mysteries that had similar features (such as ferromagnetism and superconductivity) using concepts such as spontaneous symmetry breaking. To under-

stand *emergence*, we need to be able to study collective properties of microscopic elements that might not possess a discernible signature of the emergent property—that could reveal itself through sharp onsets, sensitive responses, or appearance of large-scale correlations—using minimal yet tractable models that include the essential ingredients. Since there is no systematic way to find out how such a minimal effective description could be constructed, carrying out such a study for complex systems could be far from straightforward (as the example of high-T_c superconductivity has revealed). Studying living matter using this approach will undoubtedly be a daunting challenge, but one that has potential for significant breakthrough.

The vision behind the newly established Department of Living Matter Physics is to study living systems as self-organized active soft matter that are away from equilibrium "just the right way". The aim is to understand the complex dynamics of living matter well enough to be able to make it from the bottom-up; i.e. from molecules to systems. The research topics cover, broadly speaking, chemical and mechanical nonequilibrium activity in Living Matter across the scales.

The growing Department of Living Matter Physics (from left to right): Yorck-Fabian Beensen, Asal Atakhani, Philip Bittihn, Saeed Mahdisoltani, Evelyn Tang, Suropriya Saha, Jaime Agudo Canalejo, Viktoryia Novak, Tunrayo Adeleke-Larodo, Yoav Pollack, Prathyusha Kokkoorakunnel Ramankutty, Andrej Vilfan, Ramin Golestanian, Fanlong Meng, Benoit Mahault, Babak Nasouri

Dr. Evelyn Tang studied physics at Yale University and the University of Cambridge (where she was a Gates scholar). She obtained her PhD in condensed matter theory at the Massachusetts Institute of Technology in 2015, focusing on topological phases in electronic systems. Subsequently she did postdoctoral research at the University of Pennsylvania in computational neuroscience, and was a research fellow at the Simons Institute for the Theory of Computing in the spring of 2018. From September 2018 she has been a group leader at the Department of Living Matter Physics at the MPIDS, working on problems at the intersection of active matter and neuroscience.

Dr. Andrej Vilfan studied physics and received his doctorate from the Technical University Munich in 2000. He worked as a postdoctoral researcher at Cambridge University (UK) and as a visiting scientist at the Max Planck Institute for the Physics of Complex Systems in Dresden. Before joining the MPIDS in June 2018, he worked as a senior research fellow at the J. Stefan Institute in Ljubljana (Slovenia). As a theoretical physicist, he has worked on molecular motors, auditory receptors, hydrodynamics of biological and artificial cilia, as well as other colloidal systems.

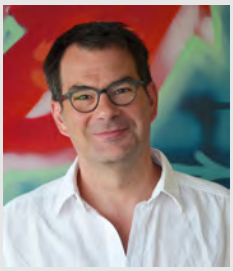

Yorck-Fabian Beensen studied physics at the Georg-August-University Göttingen and the University of Aarhus (Denmark). In 1997 he received his diploma from the faculty of geophysics for a work in the field of seismological data analysis which earned him a stipend from the Berliner-Ungewitter-Stiftung. He joined the institute in 2000 as an IT administrator in the former theory department. Since 2018 he has worked as an IT specialist in the department of Living Matter Physics.

Ayse Bolik is a European Business Assistant certified in English and French and has been administrative assistant in the department of Nonlinear Dynamics since 2010. Since March 2018, she is an administrative assistant to Prof. Golestanian in the department of Living Matter Physics. **Viktoryia Novak** studied foreign languages at the Gomel State University (Belarus) and international economics at the University of Göttingen (Germany). She joined the MPIDS in 2011, working as a department assistant, mainly supporting the director of the Bernstein Center for Computational Neuroscience, Prof. Fred Wolf, in administrative issues, coordination, and management of external funds. Since 2018 she has been working for the department of Living Matter Physics, and is responsible for the guest program of the department as well as an administrative assistance to Prof. Ramin Golestanian.

RESEARCH GROUPS

4

Contents

4.1 MAX PLANCK RESEARCH GROUP: BIOLOGICAL PHYSICS AND MORPHOGENESIS

Dr. Karen Alim studied physics in Karlsruhe, Manchester and Munich. She obtained an MSc in Theoretical Physics in 2004 from Manchester University, U.K., followed by a Diplom (MSc) in Physics and Biophysics at the LMU Munich. During her PhD at the LMU in Munich she investigated the form of biological materials like DNA or actin and patterning mechanism during leaf development. As a grad fellow at the KITP in Santa Barbara, United States, she investigated the mechanics of plant growth. From 2010 to 2015 she was a postdoctoral fellow at Harvard University, where she focused on the adaptation dynamics of the network-like forager *Physarum polycephalum*. Since 2015 she is as an independent group leader at the Max Planck Institute for Dynamics and Self-Organization. Karen is recipient of the John Birks Award of Manchester University, and held an appointment as lecturer in Applied Mathematics at Harvard University. She is a faculty member at the Institut for Nonlinear Dynamics and the Georg-August University School of Science (GAUSS) and a Fellow of the Schiemann Kolleg.

How can an organism grow to form a desired structure and pattern? Understanding the morphogenesis of an organism, the collective self-organization of cells that gives rise to a functional structure is at the heart of decoding life. Unveiling the physical mechanisms nature uses to control the dynamics of development also generates new concepts for bioengineering and synthetic implementations of biological processes in smart materials. We aim to identify the rules of development by studying the physical principles underlying the formation and adaptation of biological organisms. We combine insights from biological signals with knowledge of physical processes to discover how physical forces induce, transmit and respond to biological signals and thus control development and shape morphology.

The key physical players we focus on are mechanics and fluid flows. Mechanical forces propagate quickly over large spatial scales and are therefore crucial to coordinate cell dynamics within the rapidly developing organism. Here, we develop theoretical models studying the principles of how the feedback between mechanics and cell dynamics/biochemical signalling drives collective dynamics. Current work focuses on organ outgrowth in plants and cell rearrangements in the fruit fly embryo. Fluid flows propagate resources and signals through a vascular network and thereby shape surrounding tissue and the morphology of the vasculature itself. We aim to identify the self-organising principles of the feedback between flows and network morphology. Here, the challenge is that flows are globally coupled within a network. To overcome this challenge we combine theory of fluid flows within networks with quantitative experimental observations of flow network self-organisation observing the slime mould *Physarum polycephalum*. This integrative strategy shows that flows are an integral part of the self-organisation machinery of life itself. We work on translating physical principles in living systems to bio-mimetic applications by developing theoretical models of active porous media.

We collaborate nationally and internationally with physicists, biologists, mathematicians and material scientists. We are members of the research unit FOR 2581 on *Plant Morphodynamics*. In Göttingen we enjoy collaborations with the department *Dynamics of Complex Fluids*, other Max Planck Research Groups, the Medical Center and are members of the SFB 937 on *Collective Behaviour of Soft and Biological Matter*. Our group engages in service for the committee "Opportunities" by the Max Planck Society, the Dorothea Schlözer Mentoring program by the University of Göttingen and on the PhD student level as representatives of the International Max Planck Research School *Physics and Biology of Complex Systems*, the institute-wide and nation-wide PhDnet of the Max Planck Society even including the student representative on the Göttingen Graduate School for Neurosciences, Biophysics, and Molecular Biosciences Board among us.

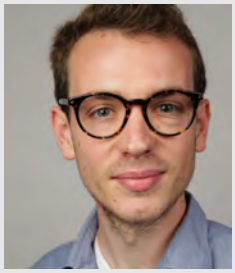

Dr. Philipp Fleig received his Masters degree in Physics at Imperial College London in 2010. He completed his Ph.D. at the MPI for Gravitational Physics in Potsdam in the field of High Energy Theoretical Physics. He went on to join the Institut des Hautes Études Scientifiques in Paris as a CARMIN Postdoctoral Fellow, where he continued his work on the intersection between String Theory and pure mathematics and co-authored a book, published in 2018 by Cambridge University Press. He joined the group in fall 2016 with the interest of understanding the emergence of large-scale behaviour in complex biological networks.

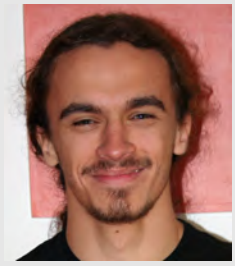

Dr. Jean-Daniel Julien received his Master's degree in physics at the École Normale Supérieure de Lyon (ENS Lyon, France) in 2012. As a PhD student, he worked on the mechanics and growth of plants morphogenesis, using computational approaches, in the Physics laboratory and the Plants Reproduction and Development laboratory of the ENS Lyon. In 2015 he was a graduate fellow in the Kavli Institute for Theoretical Physics (Santa Barbara, United States). His domains of interest are continuum mechanics, non-linear physics, statistical mechanics, and scientific programming. He joined the group in January 2016.

Associated Scientists

Dr. Natalie Andrew studied Physics and Cognitive Science at the University of Birmingham, UK. She completed her PhD studying cell motility and pseudopod formation patterns in *D. discoideum* in 2006. In 2007 she moved to Harvard Medical School's Systems Biology to investigate calcium signalling dynamics in mammalian cells. In 2013 she joined the department of Organismic and Evolutionary Biology at Harvard University and began research on flow dynamics and foraging behaviour in the slime mould *P. polycephalum*. Dr. Andrew has been an associate researcher with the group since 2016.

Dr. Sophie Marbach received her Master's degree in physics at the École Normale Supérieure de Paris (ENS Paris, France) in 2014. As a PhD student at ENS Paris, she worked on the transport of fluids at the nanoscale and designed innovative concepts for filtration, such as active filtration with fluctuating pores inspired by biological porins. Her domains of interest are continuum mechanics, out-of-equilibrium physics, statistical mechanics, and scientific programming. She has worked with the group since 2015, investigating mechanisms leading to spontaneous pruning.

Technical Staff

Anne Weber studied biotechnology at the Ernst-Abbe-University in Jena. After her Diploma in 2007 she worked shortly in industry before joining the MPI for Biophysical Chemistry. In those years she gained experience in molecular, micro-, and cell biology and biochemistry dealing with forensic DNA analytics, single-use bioreactors, plasmid design and protein expression, purification and characterisation, among many other methods. In September 2017 she joined the group to support the laboratory work and to investigate the genetic manipulation of *P. polycephalum*.

4.2 MAX PLANCK RESEARCH GROUP: TURBULENCE, COMPLEX FLOWS & ACTIVE MATTER

Dr. Michael Wilczek studied physics at the Westfälische Wilhelms-University Münster from which he received his diploma in 2007 and doctorate in 2011 under supervision of Prof. Rudolf Friedrich. During his postdoctoral time at the Institute of Theoretical Physics at the University of Münster and the Kavli Institute for Theoretical Physics at Santa Barbara he worked on fundamental aspects of turbulent flows. In 2013, he joined the group of Prof. Charles Meneveau at the Department of Mechanical Engineering at the Johns Hopkins University, Baltimore, extending his research portfolio to atmospheric turbulence and wind energy. Since summer 2015 he is heading his group dedicated to the investigation of turbulence, complex flows and active matter. Michael is a faculty member at the Institute for Dynamics of Complex Systems and the Georg-August University School of Science (GAUSS). He received the 2018 Fulbright-Cottrell Award in recognition of his efforts of combining research and innovative teaching.

From the fascinating self-organization of bacterial flows to large-scale flow patterns in the atmosphere – flowing matter gives rise to a wide range of intriguing phenomena. A common feature of these complex systems is the tight interplay of disorder, fluctuations and emergent order. The goal of our research is to gain a deeper understanding of open problems from the fields of turbulence, complex flows and active matter. Our research approach utilizes a broad spectrum of methods covering theory, simulations and, enabled through the collaborative environment at MPIDS, experiments.

Fully developed turbulence, one of our main fields of research, constitutes a paradigmatic problem of non-equilibrium statistical mechanics and, at the same time, plays a key role in many engineering applications ranging from mixing and combustion to wind energy conversion. From the viewpoint of fundamental research, we are witnessing an exciting era in which the latest experiments and state-of-the-art numerical simulations provide insights into turbulent flows at an unprecedented level of detail. In view of the rapid development of experimental and numerical techniques since the start of this century, the time is right to focus on novel theoretical concepts, which we develop in a simulation-assisted theoretical approach.

Our atmosphere and the oceans represent two prime examples where turbulence interacts with complex boundaries and additional physical phenomena. Such geometrically constrained settings give rise to entirely new dynamics, whose understanding is not only important from a fundamental point of view but also has significant implications, for example, for the field of renewable energies. The goal of our research in this area is to understand the interaction of turbulent fluctuations and large-scale dynamics in such settings. Examples for recent and ongoing work include the investigation of turbulence in the atmospheric boundary layer and in large wind farms. As part of the DFG Priority Program 1881 “Turbulent Superstructures" we are also investigating the interplay of turbulence and large-scale flows in turbulent convection.

Particle-laden flows are another focus of our work. The particle-based, Lagrangian view of turbulence is particularly insightful as particles sample the complexity of turbulence in space and time. Furthermore, it is highly relevant e.g. for our understanding of clouds as well as the dispersion of micro-plastics or micro-organisms in the oceans. Together with the Bodenschatz Department and collaborators from the Fraunhofer Institute for Physical Measurement Techniques (Freiburg), we recently won a competitive grant within the Max Planck–Fraunhofer Cooperation funding scheme. Starting 2019, we will investigate cloud microphysics and atmospheric turbulence in complex terrain in a joint experimental, computational and theoretical approach.

An exciting field of research that we have begun exploring is the interaction of active particles with hydrodynamic flows. Problems from

this field combine aspects of the physics of fluids and active matter. Better understanding the complex distribution of motile plankton in the oceans, for example, is one motivation for our work. In the complementary regime of high cell density, dense suspensions of motile cells constitute so-called active fluids, which exhibit a plethora of dynamical states, including meso-scale active turbulence or self-organized vortex crystals. Unraveling the origin of these phenomena is one goal of our research.

Since its founding time in early 2015, the group has expanded its scientific scope and has grown considerably to currently two postdocs, three PhD students and seven undergraduate students. Two postdoctoral alumni have already found attractive positions elsewhere: Laura Lukassen has accepted an assistant professor position for computational fluid dynamics modeling of wind energy at the University of Oldenburg, and Dimitar Vlaykov moved on to a senior postdoc position at the University of Exeter to work on astrophysical flows. Besides central funding by the Max Planck Society, our work is supported by the DFG, the BMBF, and through computational grants at the LRZ Munich.

Dr. Cristian C. Lalescu studied physics at the University of Craiova (UCv), from which he received his diploma in 2006. Supported by the SOCRATES/ERASMUS exchange program, he spent a year at the Free University of Brussels (ULB). Between 2007 and 2011 he completed a joint doctorate program, under the supervision of Prof. Daniele Carati from ULB and Prof. Bucur D. Grecu from UCv, working mostly in Brussels. He was then a postdoctoral fellow with Prof. Gregory L. Eyink at the Johns Hopkins University in Baltimore, USA, mainly within the multidisciplinary Turbulence Database Group. In 2015 he joined the Wilczek group. He is primarily interested in dynamical system theory, turbulence and the related mathematics and computer science. He is the group's supercomputing expert and main developer of turbulence simulations.

Dr. Debarghya Banerjee studied Physical Sciences at the Indian Institute of Science (IISc), Bangalore, India. He received his doctorate in physics from there in March 2015. His doctoral research under the supervision of Prof. Rahul Pandit was on studying the statistical properties of turbulence in fluids and plasmas using numerical simulations. On completion of the doctoral thesis he moved to the Lorentz Institute for Theoretical Physics, Leiden, Netherlands where he worked as a postdoctoral researcher under Prof. Vincenzo Vitelli. The work there was focused on studying the hydrodynamics of active materials. Since April 2018 he is working as a postdoctoral researcher in the group of Dr. Michael Wilczek at the MPIDS studying turbulent flows and active matter.

4.3 MAX PLANCK RESEARCH GROUP: THEORY OF BIOLOGICAL FLUIDS

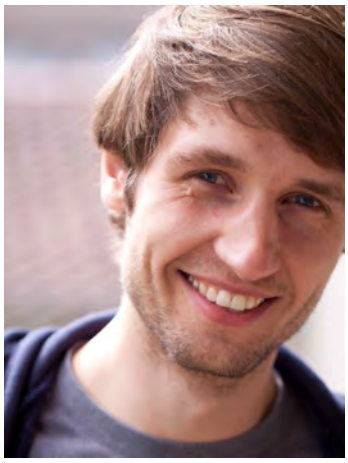

Dr. David Zwicker studied physics at the Technische Universität Dresden and Lund University (Sweden). After graduating in 2009, he worked on circadian rhythms during a short internship with Pieter Rein ten Wolde at AMOLF in Amsterdam. He then decided to pursue his PhD in Biological Physics under the supervision of Frank Jülicher at the MPI for the Physics of Complex Systems in Dresden, where he focused on theoretical descriptions of phase separation in the non-equilibrium environment of biological cells. He then joined Michael Brenner's group at Harvard University as a postdoc to work on the information theory and fluid dynamics of olfaction. In 2017, he joined the MPIDS to start his independent Max Planck Research Group. David is a faculty member at the Georg August University School of Science (GAUSS).

In contrast to most man-made machines, biological organisms are largely built from soft and fluid-like material. How is this matter controlled to fulfill precise functions? To uncover the physical principles for the spatio-temporal organization of biological fluids, we analyze theoretical models of biological processes using tools from statistical physics, dynamical system theory, fluid dynamics, and information theory. For instance, we study how liquid droplets structure the interior of biological cells and how the transport of inhaled odor molecules influences the sense of smell.

The interior of biological cells consists of thousands of different kinds of proteins that all undergo chemical reactions to fulfill their function. The resulting large chemical reaction network is controlled by spatially segregating the constituents into organelles. Typical large organelles, like the nucleus and the mitochondria, are enclosed in a membrane, but there also exist numerous smaller organelles without membranes. These membrane-less organelles form spontaneously via phase separation, much like oil droplets form in water. However, in contrast to oil in water, biological droplets exist in the non-equilibrium environment of the biological cell, where fuel molecules like ATP are constantly consumed to drive chemical reactions. Such driven chemical reactions can be used to control droplet positions, sizes, and counts. We generally study the effects of such reactions on phase separation to better understand the organization of biological cells and also learn about fundamentally new approaches for engineering soft materials.

We also study the sense of smell and the associated airflow of breathing. Despite its importance for all animals, from bacteria to humans, smell is the sense we understand the least. For instance, we do not know how our nose discerns mixtures of the about 10,000 chemicals that we can smell. Another open questions is how different concentrations of smells are distinguished. All this information about an odor must be encoded in the activity pattern of the about 300 different receptor types in a human's nose. Using information theory and statistical physics, we study various encoding strategies that the receptors could employ and compare the predictions to psycho-physical experiments. Beside the high-dimensional stimulus space, the sense of smell is also difficult to study since physical processes like advection of odorants with the airflow and their adsorption in the nasal mucus play a crucial role. In fact, the airflow itself and the surprisingly complex nasal geometry in animals are little understood. In particular, the narrow nasal geometry is prone to blockage, which leads to prevalent nasal obstruction in humans. Diagnosing and treating nasal obstruction is a challenge, in part, because the connection between the complex geometry and nasal airflow is not understood. We aim at unraveling this mystery by using both simple physical models as well as detailed numerical simulations of the airflow in the nasal cavity.

Jan Kirschbaum studied physics at the University of Münster, where he received his Master's degree in 2016. During his thesis he worked on self diffusion in amorphous silicon combining experiments and molecular dynamics. In July 2018, he joined the Research Group Theory of Biological Fluids as a PhD student, where he focuses on the theoretical description of phase separating systems with chemical reactions. His research interests are continuum dynamics, non-equilibrium thermodynamics and non-linear physics.

Ajinkya Kulkarni received his Master's degree in Applied Mechanics from the Indian Institute of Technology Madras, India. As a Master's student he worked on phase transitions in passive and active granular suspensions, with applications in controlling human stampedes. In July 2018, he joined David Zwicker's group at the MPIDS as a PhD student. The focus of his research is liquid-liquid phase separation in biological environments. In particular, he investigates dynamics of active droplets in heterogenous environments. His domains of interest are biological fluid dynamics, active matter, and granular flows.

4.4 RESEARCH GROUP: BIOMEDICAL PHYSICS

Prof. Dr. Stefan Luther studied physics at the Georg-August-Universität Göttingen, where he received his doctoral degree in 2000. Postdoctoral research on non-ideal turbulence (University of Twente, 2001-2004) and cardiac dynamics (Cornell University, 2004-2007). Since 2007, he is head of the Research Group Biomedical Physics at MPI DS, since 2008 Honorarprofessor at the Georg-August-Universität Göttingen and since 2016 Professor at the University Medical Center Göttingen. He is founding member of the Heart Research Center Göttingen, and principal investigator at the German Center for Cardiovascular Research (DZHK e.V.).

Self-organized complex spatial-temporal dynamics underlie physiological and pathological states in excitable biological systems such as heart and brain. We believe that the systematic integration of dynamics on all levels from sub-cellular, cellular, tissue, and organ to the in vivo organism is key to the understanding of complex biological systems and will open – from a long-term perspective – new paths for translating fundamental scientific discoveries into practical applications that may improve human health. Our research focuses on cardiac arrhythmias, a major cause of morbidity and mortality worldwide with sudden cardiac death taking hundred thousands of lives every year. The Research Group Biomedical Physics carries out basic evidence-based and application-oriented research, addressing fundamental scientific questions such as: What is the nature of cardiac fibrillation? Understanding the complex spatial-temporal dynamics underlying arrhythmias would answer the questions why and when they occur and how they might be treated. Towards this goal, we have provided the first visualization of three-dimensional electro-mechanical scroll waves inside the heart. Combining advanced cardiac imaging, data driven modeling and multi-modal data analysis, we aim to unravel the nature of cardiac arrhythmias and develop novel diagnostic and therapeutic approaches. To achieve this goal, we are fostering collaborations and innovation across disciplines. We also believe that science communication and education are important. Therefore, we are strongly committed to public outreach activities that share our fascination for science and make science better accessible to the large audience, ranging from education in primary schools to nation-wide science exhibitions. To attract and educate the next generation of scientists, we strive for excellence in teaching, both at the Georg-August-University and the University Medical Center.

apl. Prof. Dr. Ulrich Parlitz studied physics at the Georg-August-Universität Göttingen, where he received his PhD in 1987. After five years at the Inst. for Appl. Physics of the TU Darmstadt he returned to Göttingen in 1994 where he was habilitated in 1997 and appointed apl. Prof. of Physics in 2001. He was a visiting scientist at the Santa Fe Institute (1992), the UC Berkeley (1992), and the UC San Diego (2002, 2003). His research interests include nonlinear dynamics, data analysis and cardiac dynamics. In 2010 he joined the Research Group Biomedical Physics. He is member of the Inst. for the Dynamics of Complex Systems, GAUSS, and DZHK e.V.

Prof. Dr. Valentin Krinski studied physics at the Institute of Physics and Technology, Moscow, where he received his PhD in 1964. After 12 years at the Institute of Biological Physics in Puschino, he was appointed Head of the Autowave Laboratory in 1976, Prof. of Biological Physics at the Institute of Physics and Technology, Moscow in 1980. Since 1993, he was Directeur de Recherche, CNRS, INLN, Nice, France. His research interests include rotating vortices in biological excitable tissues and novel approaches for the termination of life-threatening chaos in the heart. In 2007 he joined the Research Group Biomedical Physics.

Dr. Jan Christoph studied physics at the Georg-August-Universität Göttingen, where he received his Diploma degree in February 2011 and his doctoral degree in October 2014. His thesis focused on multi-modal imaging and inverse imaging problems of cardiac dynamics. After receiving his doctoral degree, he worked as a postdoctoral associate in the Research Group Biomedical Physics. His research interests include cardiac dynamics, tissue electrophysiology and mechanics, mapping and imaging techniques, multi-modal fluorescence imaging, echocardiography as well as tissue engineering and morphogenesis.

Dr. Thomas Lilienkamp studied physics at the Universität Bielefeld (Germany) and the Universitetet i Bergen (Norway). He received his Diploma degree in December 2013. Afterwards he worked as a doctoral student in the Research Group Biomedical Physics at the MPI DS, where he received the doctoral degree in 2018. His current research interests include control, spontaneous termination and complexity measures of complex (chaotic) dynamics in spatially extended systems.

Dr. Alexander Schlemmer studied physics at the Georg-August-Universität Göttingen, where he received his Diploma degree in 2011. He was a research assistant at the Psychology Department of the University of Hildesheim (2011-2013) and at the Research Group Biomedical Physics at the MPI DS (2012-2017). He received his doctoral degree in 2017. His research interests focus on spatio-temporal dynamics of excitable media, time series analysis and machine learning for nonlinear systems, and semantic data management in complex heterogeneous scientific environments.

Dr. Claudia Richter studied biology at the University of Rostock, with focus on animal physiology and forensic biology (2000-2005). After graduation she worked as research associate at the department of forensic genetics at the Institute of Legal Medicine in Rostock. She received her PhD in February 2011 and since March 2011 works as a postdoctoral associate in the Research Group Biomedical Physics at the MPI DS. Her research interests include cardiac dynamics, biophysics and molecular biology, biomaterials, tissue engineering, and cardic optogenetics.

Dr. Annette Witt studied mathematics at the Humboldt-University Berlin and received her doctorate in theoretical physics from the University of Potsdam in 1996. Her thesis was awarded the Otto-Hahn-Medal of the Max Planck Society. She worked as postdoctoral researcher at several physical and geoscientific institutes in Potsdam, Florence (Italy), London (U.K.) and Göttingen. In 2014 she joined the Research Group Biomedical Physics where she is developing and improving tools for time series analysis and is using them to characterize recordings of cardiac systems.

4.5 MAX PLANCK RESEARCH GROUP: NEURAL SYSTEMS THEORY

Dr. Viola Priesemann studied physics in Darmstadt and Lisbon. For her PhD, she investigated neural information processing and collective dynamics under subsampling at the Ecole Normale Supérieure (Paris), Caltech (Pasadena) and MPI for Brain Research (Frankfurt). After her PhD in 2013, she soon became Bernstein Fellow at the Bernstein Center Göttingen, and in 2015 won an independent Max Planck Research Group, which started in 2017. Her main scientific contributions comprise the development of a subsampling theory, the characterization of collective neural dynamics and its relation to information processing. Viola is faculty member at the Institute for Nonlinear Dynamics and Graduate School GAUSS of the Georg-August University, Faculty of the Smart-Start Training Program, and since 2015 Fellow of the Schiemann Kolleg of the Max Planck Society.

Neural networks, both in the human brain as well as artificial ones, show amazing information processing capacities. Considering both side by side, we investigate the principles of neural computation with approaches from non-equilibrium statistical physics and information theory. Our major research areas comprise the development of a subsampling theory, inference about collective cortical dynamics and design of artificial networks based on information theoretic principles:

Subsampling theory. In most large systems, it is impossible to sample the activity of all units in parallel. For example, the human brain comprises 80 billion neurons, but current techniques only allow sampling the activity of some hundreds of neurons with millisecond precision. We (i) study subsampling effects, and proved that measures as basic as the correlations, or the control parameter of a critical system, are systematically mis-estimated, and (ii) derived an estimator that overcomes these biases and developed a subsampling scaling theory. This body of work is essential to make unbiased inference about large, complex systems.
Relevant publications: Levina & Priesemann, Nat Commun, 2017; Wilting & Priesemann, Nat Commun 2018

Collective cortical dynamics. Despite decades of experimental and theoretical work, the nature of collective dynamics in cortical neural networks remains enigmatic – not least due to subsampling. One popular hypothesis suggests that cortex operates at a critical state, thus at a second order phase transition, thereby maximizing computational properties like information transfer and susceptibility. Revisiting this hypothesis, we had to overturn it. Instead, we found a novel operating regime of the cortex across various species. This novel *reverberating regime* enables rapid tuning of the network to task requirements. Furthermore, we derived that the *input strength*, mediated by a central control mechanism (homeostasis), acts as a control parameter and hence determines collective dynamics and computation. Currently we investigate how the collective dynamics changes with state and how it determines processing, using information theoretic approaches.
Relevant publications: Priesemann & Shriki, PLOS Comp Biol, 2018; Wilting & Priesemann, Nat Commun, 2018; Zierenberg, Wilting & Priesemann, Phys Rev X, 2018.

Information theory. Information theory provides a natural language to quantify information processing independently of the imposed semantics, and can be harnessed in two different manners: Quantifying the processing in biological and artificial systems (inference), or *ab initio* derivation of learning mechanisms and coding principles for specific goals (design). A particularly interesting and novel framework is "partial information decomposition" (PID), which for the first time enables us to disentangle the unique, redundant and synergistic contributions to computations. We harnessed it to infer how processing self-organizes with development, to derive novel learning rules for predictive coding, and to disentangle hidden causes that have strong overlap.
Relevant publications: Wibral, Lizier, Priesemann, Front Robotics and AI, 2015; Wibral et al., Entropy, 2017; Wollstadt et al., PLOS Comp Biol, 2017.

The Neural Systems Theory Group strongly profits from close collaborations with Göttingen, Heidelberg, Tübingen, Cambridge, Beer Sheva, Bozeman and Berkeley. We contribute to teaching at the Faculty of Physics in Göttingen, as well as international summer schools. We are commited to open source pulishing and in addition drive the develop-

ment of two toolboxes (www.trentool.de, www.github.com/Priesemann-Group/mrestimator). The group is greatful for the financial support by the Max Planck Society, Bernstein Center Göttingen (BMBF), German-Israel Foundation (GIF), Gertrud-Reemtsma-Foundation, and Physics-to-Medicine initiative (VW Vorab).

Dr. Johannes Zierenberg studied physics at Leipzig University and the ETH Zürich (Switzerland). At Leipzig University, he received his Master's degree in 2011 and his PhD in 2016. During his PhD, he worked on equilibrium cluster formation in classical particle systems and polymer solutions, applying advanced Markov Chain Monte Carlo methods in generalized ensembles. In January 2017, he joined the Research Group Neural Systems Theory as a postdoc. His domains of research are phase transitions and critical phenomena, (non-)equilibrium statistical mechanics, and computational neuroscience.

Jens Wilting studied Physics and Mathematics at the University of Bonn, Imperial College London, and Göttingen University, receiving his Master's degree in 2014. He joined the Max-Planck-Institute for Dynamics and Self-Organization in the same year in the former Department for Nonlinear Dynamics. He then started his PhD studies in the Research Group Neural Systems Theory. His research focuses on the collective dynamics in cortical networks, particularly on the problem of inferring population dynamics of largely subsampled systems.

João Pinheiro Neto studied physics at the State University of Campinas (UNICAMP, Brazil), receiving his Master's degree in 2014. He joined the MPIDS in 2015, and the Neural Systems Theory Group in 2017 as a PhD student. He studies sampling effects when assessing the dynamics of neural networks, and what their presence can tell about the underlying system. His main research interests are neural network dynamics, complex systems and network theory.

Lucas Rudelt studied physics at the University of Göttingen, where he received his Master's degree in 2018. He joined the Research Group of Neural Systems Theory in October 2014 for a Bachelor's thesis on the estimation of local information quantities from limited data. During his Master's thesis in the same group, he developed and applied a temporal embedding method for the estimation of memory in neural spiking activity. Currently, he is a pre-doctoral candidate within the SmartStart Computational Neuroscience program under supervision of Dr. Viola Priesemann and Dr. Marion Silies, where his work focuses on quantifying and modeling information processing in the Drosophila motion detection circuit. His main research interests are information theory and causal inference to understand distributed computation and unsupervised learning in neural networks.

4.6 MAX PLANCK RESEARCH GROUP: STATISTICAL PHYSICS OF EVOLVING SYSTEMS

Dr. Armita Nourmohammad studied Physics at Sharif University of Technology (Iran) and moved to Cologne for her graduate studies, where she developed statistical physics approaches to study evolving populations. During her PhD with Michael Lässig, she addressed evolutionary modes of gene regulation in eukaryotes and developed an out-of-equilibrium theory for evolution of molecular phenotypes. In 2012 she won a James S. McDonnell fellowship to study complex systems and joined Princeton University as an independent biophysics theory fellow to pursue her research. There, she became fascinated by the complexity of the adaptive immune system and developed a principled framework to describe non-equilibrium coevolution of immune cells and pathogens. This work has shed light on the conditions that permit emergence of highly potent broadly neutralizing antibodies (BnAbs), which are the current hope for a universal vaccine against rapidly evolving viruses, such as HIV. In 2017 she won an independent Max Planck Research Group and in October 2017 started her group at MPIDS. Armita is an assistant professor in Physics at the University of Washington (Seattle) and a faculty member at the Institute for the Dynamics of Complex Systems and the Graduate School GAUSS at the Georg-August University, Göttingen.

Our interest lies at the interface of statistical physics, information theory, evolutionary biology and immunology. We study the adaptive immunity in vertebrates, where a highly diverse set of molecular receptors use mechanisms associated with Darwinian evolution to collectively mount a specific response against rapidly evolving pathogens. In return, pathogens evolve to escape the immune challenge and constantly form new targets for the immune system, resulting in an out-of-equilibrium stochastic process in a high-dimensional system. Recently, it has become feasible to sequence the diverse immune receptors of a host together with infecting viruses. Additionally, synthetic techniques allow for measuring functions in hundreds of thousands of genetic variants. We combine theory with such molecular data to characterize the mode and tempo of the adaptive immune response.

Information processing in immune system. The adaptive immune response is an example of information processing: limited by the diversity and maturation of immune receptors, the immune repertoire senses the pathogenic environment, adapts accordingly and keeps a memory for future infections. This process is irreversible due to a constant flow of information from changing pathogens. Our work explores limits of information processing in the non-equilibrium evolving systems, their response as a thermodynamics decision making process and memory storage, by statistically encoding the previously encountered patterns.

Predictive models of immune response to pathogens. In collaboration with Florian Klein (University of Cologne), we are tracking immune repertoire response to chronic HIV infections. HIV is a moving target for the immune system since it evolves rapidly within patients, with a turnover time of ~ 2 weeks. Despite its large depth, the immune repertoire data is a highly under-sampled representation of the receptor sequence space; inference from such incomplete information is a hallmark of statistical physics. We are developing probabilistic techniques to infer an effective low-dimensional phenotypic representation of the sequence space and characterize a predictive fitness model for the immune response. This is an inverse inference problem for immune interactions, driven out of equilibrium by evolving viruses.

Adaptive control of evolving populations. Forecasting is the first step towards controlling evolution. Recently, we have uncovered the prevalence of clonal competition and rapid turnover in immune receptors responding to HIV, which challenges the current vaccination strategies to elicit BnAbs. Directing the immune system to utilize a specific antibody is a problem of *adaptive control* to trigger a *rare event* in a non-linear stochastic system. We are developing a theory for adaptive control strategies in stochastic evolving systems with an effective dynamics inferred from molecular data.

Our group strongly benefits from close collaborations with Cologne, Paris, Philadelphia and Seattle. We contribute to the teaching effort at the university of Göttingen and at the University of Washington (Seattle)

and also at a number of international summer schools. In addition, we are involved in organizing international workshops, including the Nordita program “From molecular basis to predictability and control of evolution" to be held in July 2019 in Stockholm and the workshop "out-of-equilibrium processes in evolution and ecology" to be held in August 2019 in Casa Matematica Oaxaca (Mexico). Our group is a part of the European Biophysics Network (GDRI), “Prediction, Adaptation and Navigation". We are grateful for the support of the Max Planck Society and the DFG collaborative research center (SFB 1310).

Dr. Jakub Otwinowski studied physics at UT-Austin and obtained his Master's degree in Soft Matter physics at the University of Amsterdam. He obtained his PhD from Emory university in 2012 on a work that drew correspondence between non-equilibrium surface growth physics and evolutionary adaptation with spatial constraints. He then joined University of Pennsylvania as a postdoctoral fellow, where he worked on inferring sequence function relations from large mutagenesis experiments and studied signatures of adaptation in coevolving populations. Since August 2018, Jakub has joined MPIDS as a research associate, working on evolutionary optimization and biophysical sequence-to-function inference, relevant for the adaptive immune system.

Dr. Colin LaMont studied physics at Reed College (Oregon) and obtained his PhD in physics from the University of Washington (Seattle), where he developed a correspondence between statistics and thermodynamics. Since June 2018, he has joined our group as a postdoc within the DFG funded project of SFB1310. Colin's research focuses on developing a theory of stochastic adaptive control for co-evolving populations and to construct control strategies applicable for vaccine HIV.

Oskar Schnaack studied physics at Georg-August-University, Goettingen, where he earned his Master's degree with a thesis on information theory in quantum systems. Since February 2018, he has joined our group at MPIDS as a PhD student. Oskar's research focuses on information processing in out-of-equilibrium evolving populations. He is developing a formalism based on the thermodynamics of decision making to characterize the emergence of memory states in evolving population and especially in the adaptive immune system.

Giulio Isacchini studied physics at Trento and Oslo and obtained his Master's degree in Physics from ETH and École Polytechnique (Paris). Since October 2018, Giulio has joined our group at MPIDS as a PhD student, in a collaborative project with the group of Aleksandra Walczak and Thierry Mora at ENS (Paris). Giulio is using machine learning and thermodynamic (biophysical) modeling to construct a map between sequence and molecular function for interacting immune receptors and antigens. He is also developing methods to predict HIV escape from broadly neutralizing antibodies, using tens of thousands of molecular variants of HIV, grown in the presence of antibodies.

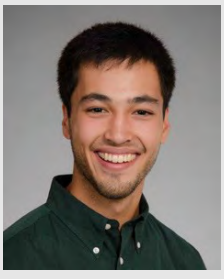

Michael Pun studied Physics at Bodwin College (Maine) and at the University of Washington (Seattle) and has joined MPIDS since July 2018 as a PhD student. Michael's research focuses on developing a statistical inference framework for analysis of immune repertoires. He is working to construct predictive models for evolutionary dynamics for populations of immune B-cell receptors, collected over time in response to distinct stimuli.

4.7 RESEARCH GROUP THEORETICAL NEUROPHYSICS

The brains of humans and animals arguably are among the most complex systems in nature. Their operation crucially depends on the cooperative dynamics of spatially distributed neurobiological multicomponent systems: Even the most elementary sensory stimulus engages large ensembles of interacting nerve cells distributed throughout the brain. The processing power of biological neuronal circuits exactly results from their collective dynamics. In addition, complex nervous systems utilize processes of dynamical self-organization to generate and maintain their processing architecture. The amount of information in a mammalian genome is by far insufficient to specify the wiring of biological neuronal networks in microscopic detail. Functionally useful processing architectures are thus dynamically generated by self-organization on the level of neuronal circuits. Finally, even an individual nerve cell is a complex dynamical system. Virtually all single neuron computations critically depend on the dynamical interaction of a multitude of subcellular components such as ion channels and other interacting biological nano-structures. It is due to this ubiquity of collective behaviors that neuroscience provides a rich source of attractive research questions for the theoretical physics of complex biological systems.

The Research Group Theoretical Neurophysics examines neurobiological and biophysical phenomena that provide challenging problems for the development of mathematical theory and which can be approached in precise quantitative experiments. Our work extends from the formulation and development of novel mathematical approaches tailored to the specifics of neuronal systems dynamics, to the development of analysis methods for turning biological experimental observations into theoretically informative quantitative data, and to the development of experimental paradigms designed to reveal cooperative and dynamic aspects of neuronal function. To achieve a close interaction of theory and experiment, many projects are pursued in collaboration with experimental biological research groups around the world. Three problems are at the core of our research agenda: (1) The self-organization of neuronal circuits in the visual cortex. In this system our analyses demonstrate that biological neural networks follow apparently universal quantitative laws predicted by our mathematical theories of neuronal self-organization. (2) The dynamics of large networks of pulse-coupled neurons and its impact on the representation of sensory information. Here the ergodic theory of network dynamical systems provides a natural language that links details of the network dynamics to information preservation, decay and flux. (3) The biophysical nature and dynamics of high-bandwidth action potential encoding. Here we are integrating concepts from non-equilibrium statistical physics with the biophysics of membranes and ion channels. The identification of dynamically realistic models of single neuron operations is essential for understanding collective computations in the brain.

Prof. Dr. Fred Wolf studied physics and neuroscience at the University of Frankfurt, where he received his doctorate in theoretical physics in 1999. After postdoctoral research at the Interdisciplinary Center for Neural Computation of the Hebrew University of Jerusalem (Israel), he became a research associate at the MPI für Strömungsforschung in 2001 and in 2004 head of the research group Theoretical Neurophysics at the MPIDS. He is a founding member and since 2013 the Chairperson of the Bernstein Center for Computational Neuroscience in Göttingen as well as faculty of several Physics and Neuroscience PhD programs at the University of Göttingen. From 2011 to 2015 he served as Section Coordinator for Computational Neuroscience of the German Neuroscience Society and from 2014-2018 on the review committee for research grants of the Human Frontier Science Program. Fred Wolf is a Fellow of the American Physical Society and received the Mathematical Neuroscience Prize 2017. He currently serves as acting founding Director of the Campus Institute for Dynamics of biological Networks and Spokesperson of the newly established German Research Foundation priority program *Evolutionary Optimization of Neuronal Processing*.

Dr. Andreas Neef obtained his Diploma in physics in 2000 from the University of Jena, Germany. After work at the MRC Laboratory of Molecular Biology, Cambridge (UK), he joined the Research Centre Jülich, Germany, where he received his doctorate in 2004 (Cologne University). After postdoctoral research he became a Bernstein Fellow at the Max Planck Institute for Dynamics and Self-Organization in 2006. Since 2013 he heads the research group Biophysics of Neuronal Computation at the Bernstein Center for Computational Neuroscience.

Dr. Elinor Lazarov studied Physics at Tel Aviv University (Israel), where she received her bachelor in 2003 and her master in 2009, working on alpha radiation cancer therapy. She obtained her PhD in a collaboration between the Hebrew University of Jerusalem and the Bernstein Center for Computational Neuroscience, combining statistical measures of neuronal information encoding and electrophysiology and superresolution imaging. Since October 2016, she is a postdoctoral researcher at the Göttingen University Medical Center and an associated scientist in the research group Theoretical Neuroscience.

Dr. Anton Unakafov obtained his diploma in applied mathematics and informatics in 2007 from the Southern Federal University, Taganrog, Russia. Following work in the biomedical electronics industry, he joined the Institute of Mathematics of the University of Lübeck in 2011 and obtained his doctorate from University of Lübeck in 2015. In 2012, he joined "Primate Cognition", a joint research focus of the Max Planck Institute for Dynamics and Self-Organization, the University of Göttingen and the German Primate Center as a Postdoctoral Fellow. His research focuses on data analysis and modelling, with topics ranging from signal processing to evolutionary game theory.

Dr. med. Jonas Franz studied physics and medicine at the University of Münster where he graduated (MD, summa cum laude) in 2016. During his MD dissertation 2012-2016 he used atomic force microscopy on inflammation with special focus on brain endothelial cells but also atopic dermatitis. In 2018 he completed his studies in Göttingen with work on the theory of quasiperiodic patterns in primary visual cortex, and experimental work using holographic stimulation of optogenetically modified neurons. He is an associated scientist with the Research Group Theoretical Neurophysics and trains as a neuropathologist at the University Medical Center of Göttingen.

Dr. Yvonne Reimann studied biology at the University of Göttingen and obtained her PhD with work at the Max Planck Institute for Biophysical Chemistry in Göttingen. From 2008 to 2009 she was a Postdoc in the Department Molecular Cell Biology at the Max Planck Institute for Biophysical Chemistry. From 2009 to 2010 she studied science management at the German University of Administrative Sciences (Speyer) and from 2010 to 2012 worked as scientific coordinator at the Leibniz Research Laboratories of Hannover Medical School and the Research Department of Göttingen University. Since December 2012, she is the administrative coordinator of the BCCN Göttingen and since 2018 of the Campus Institute for Dynamics of Biological Networks.

ASSOCIATED RESEARCH GROUPS 5

Contents

5.1 MAX-PLANCK FELLOW GROUP: MULTIFUNCTIONAL LIPID MEMBRANES ON SURFACES

Prof. Dr. Claudia Steinem born in 1967, got trained in Biology and Chemistry at the Westfälische Wilhelms-Universität Münster and received her PhD in 1997 in the group of Prof. Dr. Hans-Joachim Galla. After a post-doctoral stay at the Scripps Research Institute in La Jolla, CA (USA) in the group of Prof. M. Reza Ghadiri, she returned to the Institute of Biochemisty at the University of Münster as a Lise-Meitner fellow in 1999. Two years later, in 2001, she got a professorship for Bioanalytical Chemistry at the University of Regensburg and finished her habilitation. In 2005, she received an offer from the University of Göttingen for a professorship of Biomolecular Chemistry. Since 2006, she is full professor at the Institute of Organic and Biomolecular Chemistry and since the end of 2017 a fellow of the Max-Planck Society.

For many years the chemical complexity as well as the dynamics and function of biological membranes have fascinated scientists. My group aims at generating robust and stable planar multifunctional membranes in a bottom-up approach that mimic the natural situation as closely as possible to address pressing biochemical questions and to design chip-based assays.

More than 40 years ago, biological membranes were described for the first time as a fluid mosaic based on thermodynamic principles of organization of membrane lipids and proteins and available evidence of asymmetry and lateral mobility within the membrane matrix. Over the intervening years, there is mounting evidence that the chemical and spatial complexity of biological membranes is key to understand their dynamics and functions on various length scales. It is the heterogeneity of cellular membranes that can lead to specialized functional membrane domains, enriched in certain lipids and proteins, and the interaction between lipids and proteins that limits the lateral diffusion and range of motion of membrane components thus altering their function. To be able to understand the complex interplay within a membrane on a molecular level, my research group pursues a bottom-up approach. By developing and applying model membrane systems, we aim to understand membrane-confined processes such as fusion and fission, transport processes mediated by ion channels and protein pumps as well as protein-lipid and protein-protein interactions occurring at the membrane interface. On the one hand, we use planar supported lipid bilayers (PSLBs) and vesicles, such as giant unilamellar vesicles. On the other hand, we have developed functional lipid bilayers on highly ordered pore arrays. These so-called pore-spanning membranes (PSMs) suspend nanometer- to micrometer-sized pores in an aluminum or silicon substrate (Figure 5.1). They separate two aqueous compartments and can hence be envisioned as an intermediate between supported and freestanding membranes.

PSLBs: Protein-membrane and protein-protein interactions

Several proteins use specific lipid receptors to attach to the plasma membrane. We are interested in the molecular interaction between these membrane-confined receptors and proteins and how this interaction influences the overall membrane structure. In this context, we focus on phosphatidylinositol phosphate binding proteins such as ezrin, collybistin and epsin as well as Shiga toxin binding to the globoside Gb_3.

Ezrin is known to link the plasma membrane to the cytoskeleton. In its inactive dormant state, it is localized in the cytosol. By binding to the lipid PtdIns(4,5)P_2 at the plasma membrane and phosphorylation of a threonine, it gets activated. We have been able to elucidate the mode of ezrin binding to model membranes by surface sensitive techniques such as reflectometric interference spectroscopy, fluorescence microscopy and

atomic force microscopy as a function of its activation state. By using an active mutant of ezrin, an actomyosin network can be coupled to the membrane mimicking the actin cortex. With this system in hand, we ask the question how the actin binding sites influence the architecture of the network and how this impacts the mechanical properties of the composite system.

The epsin N-terminal homology (ENTH) domain plays an important role for membrane remodelling during clathrin mediated endocytosis. The initial step of this process is the specific binding of the ENTH domain to the plasma membrane via PtdIns(4,5)P_2. We address the question how ENTH remodels membranes and induces membrane curvature upon binding. We approach this task by combinding PSLBs with giant unilamellar vesicles adhered to a support.

Collybistin is an adaptor protein that is involved, together with the scaffold protein gephyrin, in the recruitment of $GABA_A$ receptors to the postsynaptic density of inhibitory synapses. We answer the question, which component, i.e., which phosphatidylinositol phosphate is responsible for recruiting collybistin to the synaptic membrane by using quantitative methods such as surface plasmon resonance and reflectometric interference spectroscopy as well as atomic force microscopy.

In collaboration with the group of Prof. Dr. Daniel Werz (TU Braunschweig), we elucidate, by a combination of fluorescence and atomic force microscopy on PSLBs, how the molecular structure of the lipid Gb_3 impacts the primary step of Shiga toxin internalization. This toxin, produced by *Shigella dysenteriae* and Shiga toxin producing *E. coli* strains (STECs) is known to get internalized into the cell after binding of the B-subunits to its natural receptor Gb_3 in the plasma membrane of the host. The molecular structure of Gb_3 greatly influences the membrane (re)organisation and thus the binding mode of Shiga toxin.

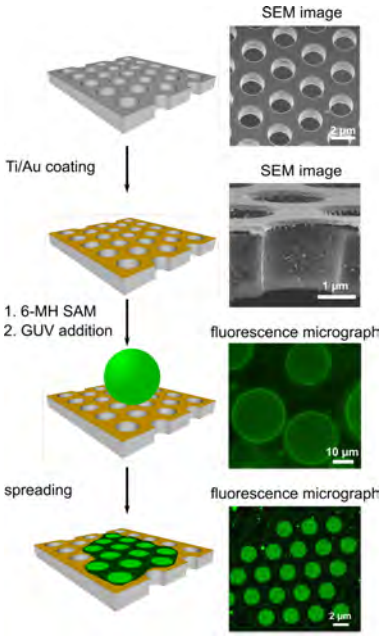

Figure 5.1: Individual steps to prepare pore-spanning membranes (PSMs) on a Si/Si_3N_4 substrate by spreading a giant unilamellar vesicle (GUV) on a 6-mercaptohexanol (6-MH) self-assembled monolayer (SAM).

PSMs: Membrane fusion and transport proteins

Membrane fusion processes, mediated by SNAREs, are a hallmark of eukaryotic life. We are especially interested in membrane fusion during neuronal exocytosis and in late endosomal fusion processes. A number of *in vitro* fusion assays with these proteins reconstituted in artificial membranes have been established in recent years. However, it has still been proven difficult to monitor intermediate states of the fusion process in a system that captures the essential features of the *in vivo* system. We develop and apply a reconstituted membrane system based on PSMs. PSMs are long-term stable and can be formed on open pore arrays as well as on cavities. These setups allow for a quantitative analysis of the different stages during fusion of a single vesicle, such as docking, hemifusion and full fusion by means of fluorescence microscopy in a time-resolved manner (Figure 5.2).

As PSMs are produced from spreading giant unilamellar vesicles, they also enable us to reconstitute ion channels and protein pumps with an appropriately high protein density. This is particularly important for ion channels and protein pumps that do not transport sufficient ions to

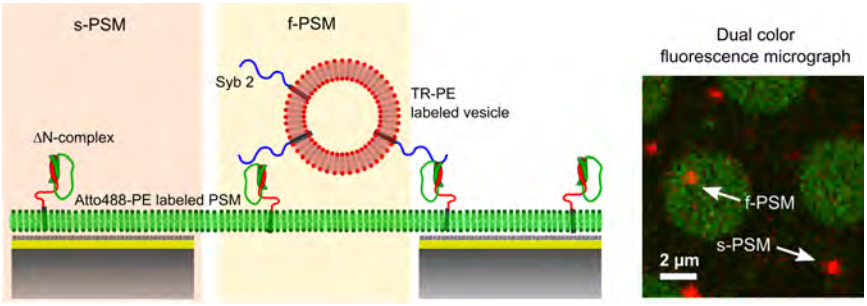

Figure 5.2: Setup to measure single vesicle fusion events (left) by means of fluorescence microscopy with high time resolution in freestanding PSMs (f-PSMs) and supported PSMs (s-PSMs) (right). The image is taken from Kuhlmann, Junius, Diederichsen, Steinem. *Biophys. J.* **112**, 2348-2356 (2017).

be detected by electrophysiological recordings on single freestanding membranes. We focus our attention on the proton transporting voltage dependent channel Hv1 and the F_0F_1 ATP-synthase that is capable of producing ATP by using a proton gradient and which can be reversed.

Silica nano- to micro-patterning at the membrane interface in vitro

Silica morphogenesis of diatoms takes place within specialized intracellular compartments, the silica deposition vesicles (SDVs), which are known to be lipid bilayer-bound compartments and which contain a number of different silica precipitating biomolecules. We investigate the impact of lipid bilayers that mimic SDV membranes on biomolecule induced silica morphogenesis. Our main interest is the protein silicanin-1, the first transmembrane protein found in an SDV, which was recently discovered.

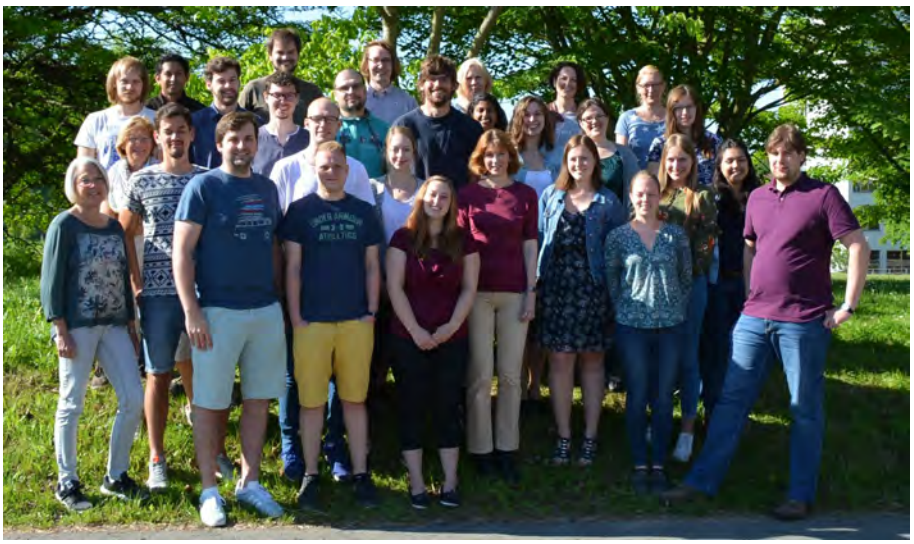

Figure 5.3: The Steinem Lab at the Institute for Organic and Biomolecular Chemistry, University of Göttingen.

5.2 EXTERNAL SCIENTIFIC MEMBER: BIOMEDICAL NMR RESEARCH

Prof. Dr. Jens Frahm is Director of Biomedical NMR at the Max-Planck-Institute for biophysical Chemistry in Göttingen, Germany. He studied physics at the Georg-August-Universität in Göttingen where he received a PhD in physical chemistry in 1977. In 1982 he founded a Biomedical NMR group at the Max-Planck-Institute for biophysical Chemistry which until 2019 operated as a non-profit research company fully financed by its MRI patents. Frahm is a recipient of the European Magnetic Resonance Award (1989), the Gold Medal of the International Society for Magnetic Resonance in Medicine (1991), the Karl Heinz Beckurts-Award (1993), the State Award of Lower Saxony for Science (1996), the Research Award of the Sobek Foundation for Multiple Sclerosis (2005), the Science Award of the Foundation for German Science (2013), the Jacob-Henle Medal (2017), and the European Inventor Award (2018). He is an ordinary member of the Academy of Science at Göttingen (2005) and was elected to the Hall of Fame of German Research (2016).

Our research is devoted to the further development and application of magnetic resonance imaging (MRI) techniques for structural and dynamic studies of biological and complex systems. Current projects focus on advanced methods that monitor human body movements and physiological functions in real time and allow for quantitative mapping of tissue parameters using model-based reconstructions. Respective applications vastly broaden the scientific and clinical potential of MRI and are expected to alter its future in coming years.

Methodological Aspects

Our breakthrough toward real-time MRI is based on spatial encoding strategies using radial trajectories, pronounced data undersampling by factors of 20 to 40, and definition of serial image reconstruction as iterative solution to a nonlinear inverse problem with temporal regularization. In practical terms, real-time MRI allows for recordings of the functional anatomy at high spatiotemporal resolution, i.e. with image acquisition times as short as 10 to 50 milliseconds – corresponding to MRI videos at 20 to 100 frames per second.

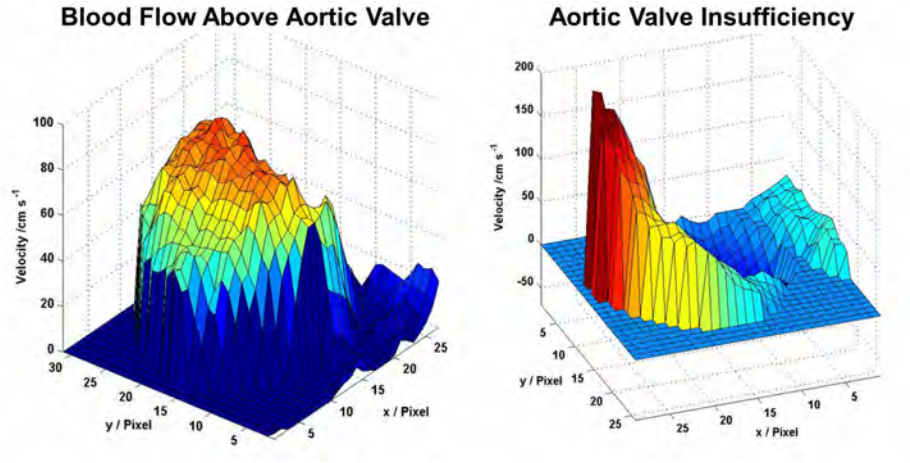

Figure 5.4: Velocity distribution of blood flow within the ascending aorta using real-time phase-contrast flow MRI for (left) a healthy subject and (right) a patient with aortic valve insufficiency. The selected frames from the systolic phase (i.e., contraction of the heart) refer to maximum blood flow in centimeter per second. Valve insufficiency doubles the peak velocity, enhances the pressure on the vessel wall and decreases blood supply to the circulation due to backward flow during diastole.

Model-based reconstruction techniques are an extension of the basic reconstruction problem posed by undersampled multi-coil MRI data. It supports quantitative mapping of physical or physiological parameters by directly estimating the parameters of a known signal model from a suitable set of raw data. Thus, instead of computing a set of images which are then used for a pixel-wise fitting of the signal model, the parametric maps are obtained directly without intermediate image reconstruction. The procedure exploits redundancy in the raw data and

– depending on the application – leads to much improved maps (e.g., almost noiseless velocity maps in phase-contrast flow MRI) or provides simultaneous access to maps from different sections (e.g., multiple maps of the T1 relaxation time).

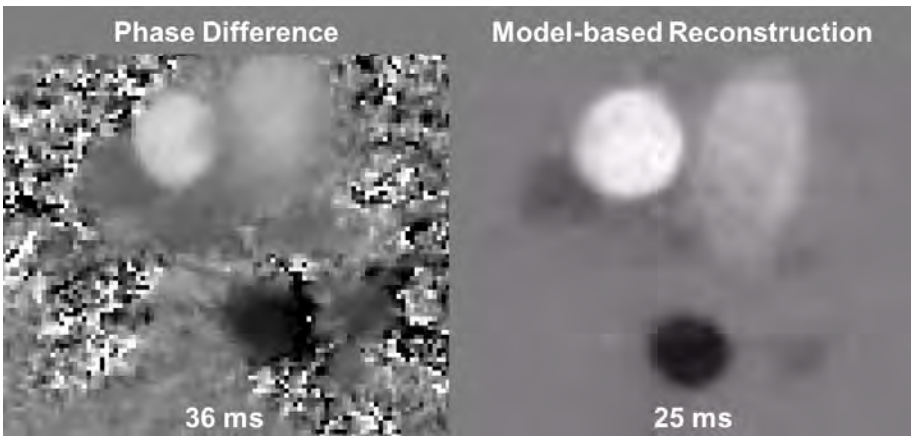

Figure 5.5: Quantitative assessment of aortic blood flow using real-time phase-contrast flow MRI. (Left) Conventional phase-difference calculation of the velocity map (28 frames per second) in comparison to (right) a model-based reconstruction with an almost noiseless floor and improved spatiotemporal resolution (40 frames per second). The selected frames refer to maximum blood flow in the ascending aorta (bright circle) and descending aorta (dark circle, opposite direction). The strength of the phase signal directly corresponds to flow velocity.

In all cases, the computational demand is met by parallelization of the corresponding algorithm and its implementation on a computer equipped with 8 graphical processing units. This computer could be fully integrated into a commercial MRI system (by a Gigabit network connection) where it serves as a by-pass system invisible to the radiological user.

Scientific and Clinical Applications

Novel real-time MRI studies address a broad range of hitherto impossible scientific and clinical questions. At this stage, a list of preliminary applications includes: joint movements (knee, wrist, temporomandibular joint), phonetic aspects of articulation (speech production, singing, whistling, stuttering), brass playing (pedagogy, dystonia), swallowing dynamics (normal physiology, dysphagia, gastroesophageal reflux disorder), cardiac function without the need for synchronization to the electrocardiogram and during free breathing, quantitative assessment of blood flow (aorta, carotid artery, peripheral veins), cerebrospinal fluid dynamics (normal physiology, hydrocephalus, flow disturbances), and quantitative mapping of T1 relaxation times (brain, heart, spinal cord).

Outlook

Ongoing methodological work mainly deals with extensions of the basic physical and mathematical concept underlying model-based reconstruc-

tions. Examples range from velocity mapping in multi-dimensional flow directions to the separation of water and fat contributions in anatomic real-time MRI videos or even the dynamic mapping of the T2* relaxation time. The latter development promises real-time access to the oxygenation of tissues such as the myocardial wall and their immediate physiological responses to stress or exercise. Moreover, "spin-off" developments exploit nonlinear inverse reconstructions for improving other techniques such as diffusion-weighted MRI which is of high clinical relevance in a variety of disorders (e.g., diagnosis of stroke and tumors).

A completely new category of applications stems from the ability to not only measure in real time, but also to reconstruct and display serial images online with minimal delay. In this sense, MRI studies with visual feedback may become a novel therapeutic option. Preliminary feedback trials with dystonic brass players demonstrate significant clinical potential as posterior portions of the tongue are without sufficient sensory feedback, while visual control during speaking or brass playing may help to improve neuromuscular control. Related applications are dynamic "search" strategies within the body using interactive control of the MRI slice position during continuous scanning. Such techniques are required for monitoring minimally invasive interventions or lead to new approaches for rapid volume coverage by moving the subject during a fixed imaging plane. Thus, scanning from feet to head with use of a transverse plane at the magnet center allows for whole-body real-time MRI in about 40 seconds.

5.3 EXTERNAL SCIENTIFIC MEMBER: PHYSICS OF FLUIDS

Prof. Dr. Detlef Lohse got his his PhD on the theory of turbulence in Marburg/Germany in 1992. As a postdoc in Chicago and later in Marburg and Muenchen he worked on single bubble sonoluminescence. In 1998 he got appointed as Chair of Physics of Fluids at the Univ. of Twente, The Netherlands, where he still is. Lohse's present research subjects are turbulence and multiphase flow, biomedical flow, granular matter, and micro- and nanofluidics. Both experimental, theoretical, and numerical methods are used in his group. Lohse is Associate Editor of J. Fluid Mechanics, Annual Review of Fluid Mechanics, and several other journals. He is Fellow of the American Physical Society, Division of Fluid Dynamics, and of IoP. He is also elected Member of the German Academy of Science (Leopoldina), the Royal Dutch Academy of Science (KNAW), the Koninklijke Hollandsche Maatschappij der Wetenschappen, and External Member of the Max Planck Society. He received various prizes such as the Spinoza Prize (2005), the Simon Stevin Prize (2009), two ERC-Advanced Grants (2011, 2017), the Physica Prize (2011), the George K. Batchelor Prize for Fluid Dynamics (2012), the AkzoNobel Prize (2012), the American Physical Society Fluid Dynamics Prize (2017), the Balzan Prize (2018), and the Max Planck Medal (2019). He also set up the Max-Planck Center Twente (2016, on Complex Fluid Dynamics).

Scientific profile and characteristics of work

Lohse's Physics of Fluids (PoF) group presently works on a variety of aspects in the fundamentals of fluid mechanics. The subjects include turbulence and multiphase flow, micro- and nanofluidics, granular matter, and biomedical flow. Both experimental, theoretical, and numerical methods are used. We closely collaborate with several companies, among them Océ and ASML. On the experimental side the key expertise of the group lies in high-speed imaging. Further information, including an updated list of publications, is available under http://pof.tnw.utwente.nl/

The main characteristics of Lohse's work is the direct interaction of experiment, theory, and numerics, all done in the PoF group. He is not method-driven, but problem-driven, and often had to acquire the required methods or knowledge from some neighboring fields to solve some particular research questions he had been obsessed with. This led to various fruitful interactions and collaborations with neighboring disciplines, such as engineering, mathematics, chemistry, acoustics, medicine, biology, or even computer science. As will be seen from the list below, various of his subjects have an "application perspective". Lohse and his coworkers also understand to visually present the scientific questions they are addressing and their results. This led to ten winning video entries to the Gallery of Fluid Motion from the American Physical Society, Division of Fluid Dynamics, and various television reports and newspaper articles on their work. It also makes Lohse's science very visual for laymen, with a positive effect on the outreach of science in general.

Overview on present main research subjects

Turbulence

Rayleigh-Bénard (RB) flow, the flow in a box heated from below and cooled from above, and Taylor-Couette (TC) flow, the flow between two coaxial, independently rotating cylinders, are the two paradigmatic systems of physics of fluids. They are the drosophilas of the field and various new concepts in fluid dynamics have been tested with these systems. In the last few years, in joint work between Göttingen and Twente, we succeeded to realise the transition from the so-called classical turbulence to the so-called ultimate turbulence for RB turbulence and TC turbulence, thanks to the Göttingen U-Boot facility and the Twente turbulent TC facility (T^3C), with which we can achieve and precisely measure an unprecedented degree of turbulence. In the ultimate state, not only the bulk of the flow is turbulent, but also the boundary layers, which for weaker driving (in the classical regime) is mainly of laminar type. The transition from one regime to the other is

so important because it dramatically changes the heat or momentum transfer properties of the system. E.g., if one used the heat transfer scaling laws of the classical regime for heat transfer estimates for large temperature differences as they occur in geophysical and astrophysical situations, one would easily be off by a factor of 10 and more! So it is crucial to understand the nature of the transition and the properties of the ultimate state of turbulence.

Next to the experiments on TC flow, we perform highly parallelized (10^5 cores) direct numerical simulations (DNS) on both TC and RB flow, and also on double diffusion convection and other related systems, also focusing on the understanding of the flow. We also look at drag reduction in these systems by adding bubbles and particles.

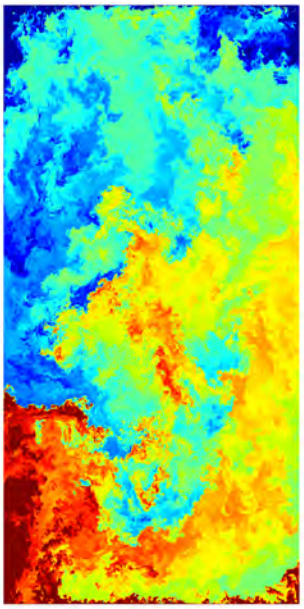

Figure 5.6: Snapshot of an numerical simulation of Rayleigh-Bénard flow at a Rayleigh number of $Ra = 1 \cdot 10^{12}$ and a Prandtl number of $Pr = 0.7$.

Multiphase flow and free surface flow

The largest setup in the PoF lab is a 8m high turbulent water channel in which bubbly turbulence or turbulence with particles is studied, accompanied by numerical work. We developed new experimental techniques to follow thousands of bubbles and particles both in time and in three-dimensional space, allowing for a better understanding of the turbulent multiphase flow organization and the dynamics of particle and bubble clusters in these flows. Recently we started to focus on multiphase flow with phase transitions.

Our research on the impact of objects on free liquid surfaces aims at revealing the mechanism of the resulting observed jet formation, combining experiments, theory, and numerical simulations. This process is very relevant for the gas exchange between the atmosphere and the ocean. Vice versa, we also study the impact of drops on solid surfaces, including superheated ones, focusing on heat exchange, splash formation, and droplet spreading.

Inkjet printing and droplet impact

On this subject the PoF group very closely collaborates with Océ Technologies. Together they revealed the disturbing role of bubbles entrained into piezoacoustic ink channels and offered solutions to resolve this problem. They also found the origin of the bubble entrainment, namely capillarity driven flow on the nozzle plate, and developed models for the droplet formation and impact of droplets on substances. Lohse's work on inkjet printing is both fundamental and applied at the same time. The present work in the PoF group includes inkjet printing of suspensions and nanoparticles (in the context of printing of solar cells and OLEDs (organic light emitting diodes)), inkjet printing of living cells, and droplet solidification. We also work on tin droplet jetting and impact in the context of extreme ultraviolet (EUV) lithography, together with ASML.

Wetting phenomena and droplet evaporation

We work on wetting phenomena on smooth, chemically, or geometrically structured surfaces and in particular on surface nanodroplets

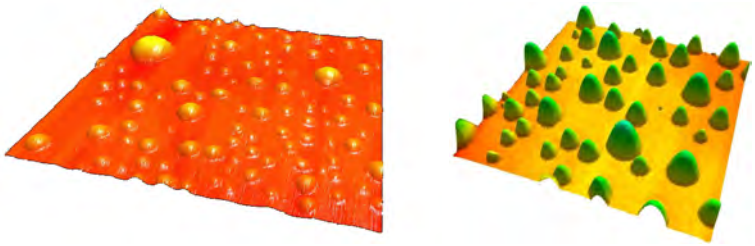

Figure 5.7: (a) AFM image of nanobubbles produced by the solvent exchange method on HOPG. The imaged area is 4x4 μm^2. (b) AFM image of nanodroplets produced by the solvent exchange method on hydrophobized silicon. The imaged area is 30x30 μm^2, and the color code is from 0 to 800 nm. Taken from Lohse, Zhang, *Rev. Mod. Phys.* **87**, 981 (2015).

and nanodroplets, whose counterintuitive stability we could account for. We try to better understand the nucleation and growth or the dissolution of nanobubbles and nanodroplets, either in another liquid or in a gas (then called condensation/evaporation). We firmly belief that major progress can be achieved at the interface between surface chemistry and fluid dynamics, by combining the methods from these two fields, both on the experimental, numerical, and theoretical side. This also holds for catalysis and electrolysis, where emerging nano-microbubbles at the surface often cause a major problem.

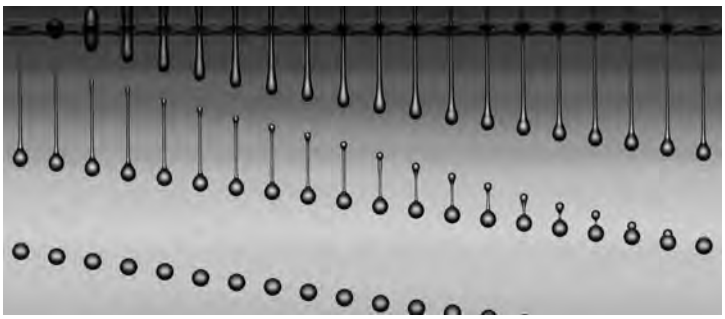

Figure 5.8: Liquid droplet formation in piezoacoustic inkjet printing generation visualized by an ultra-high-speed stroboscopic technique. Figure taken from A. van der Bos et al., *Phys. Rev. Applied* **1**, 014004 (2014)

Ultra-high-speed imaging and cavitation

The PoF group developed the world's fastest camera, the so-called Brandaris 128, allowing for 125 digital images with a frame rate of 25 million frames per second, thus enabling visualization at time scales down to 40 nanoseconds. We also pushed forward other ultra-high-speed imaging and visualization techniques, opening a totally new world of ultra-fast processes in various subfields of fluid dynamics. In particular, we have used these techniques for ultrasound diagnostics and local gene and drug delivery to cells. We also look at various cavitation phenomena, such as cavitation of vapor bubbles in micro-capillaries. These events can induce a supersonic liquid jet, which has great potential for needle-free injections in the medical context.

5.4 EXTERNAL SCIENTIFIC MEMBER: TURBULENT FLUIDS AND BIOPHYSICS

Our research is devoted to fundamental problems in hydrodynamic turbulence, with various applications to transport, as well as on biophysics problems, at the cellular and tissue level. Although theoretical and numerical by nature, our work is largely inspired by various natural (geophysics, clouds) or experimental situations. In particular, we are working in close collaborations with experimental teams, at the MPIDS and elsewhere.

Prof. Dr. Alain Pumir is Research Director at the french CNRS, working in the Laboratoire de Physique at the Ecole Normale Supérieure de Lyon, France. He studied Physics at the Ecole Normale Supérieure in Paris (1979-1983), and obtained his Doctorate in 1982 under the supervision of Prof. Yves Pomeau, on problems of nonlinear dynamics in spatially extended systems. His postdoc at Cornell University, under the supervision of Prof. Eric Siggia, was devoted to the study of singularity in the fluid equations. Back to France, he was Junior Scientist for a few years at the Ecole Normale Supérieure in Paris, before joining the Institut Non Linéaire in Nice in 1993. After a year in the Mathematics Department in Nice (2007-2008), he moved to the Laboratoire de Physique at Ecole Normale Suérieure de Lyon. He received a Humboldt Award (2013), and is a fellow of the American Physical Society since 2014. He became Chevalier de la Légion d'Honneur in 2014.

Intense structures and dynamics in turbulent flows

Direct Numerical Simulations of turbulent flows at large Reynolds numbers with a very high resolution have been used to probe our understanding of the extreme velocity gradients that can form in a turbulent flow. State-of-the-art simulations demonstrate that very large velocity gradients, which are orders of magnitude larger than their typical (averaged) value, follow a simple power-law. These extremely large gradients are typically organized in vortex tubes, which form a complex tangle in the flow, see Fig. 5.9. The magnitude of the gradients is ultimately determined by the strain acting on the tubes. As shown by the simulations, the strain is significantly weaker than vorticity itself (the conditional average of strain on vorticity grows with a power law, with an exponent smaller than 1). Elementary arguments relate this power law to the observed scaling law characterizing the most intense events. Our results provide essential data to test our theoretical understanding of turbulence, as well as guidance for experiments under way at extremely high Reynolds number at the MPIDS. (collaboration with D. Buaria, P. K. Yeung and E. Bodenschatz).

A different, but related line of research consists in studying the evolution of elementary vortex structures, and understanding how they lead to very small scales of motion. A canonical problem is provided by the head-on collision of two vortex rings. Early experiments had revealead that at low Reynolds numbers, the vortex rings reconnect and annihilate in a smooth (laminar) manner. At larger Reynolds numbers, small-scales proliferate during the collision. One of the reasons to re-visit the problem was to investigate the possibility of an iterative cascade of instabilities leading to the formation of very small scales, a possibility that has recently received much theoretical attention. The first results of a combined experimental and numerical study support the existence of a cascade of instabilities in the flow, whose mechanisms remain to be understood (joint work with R. McKeown, M. Brenner and S. Rubinstein, Harvard University, and R. Ostilla-Monico, Houston).

In an effort to understand the structure of turbulence in a realistic experimental configuration i.e. a wind tunnel, we have proposed a description of the decay of turbulence behind a grid. A generalized self-similar solution of the equations has been developed, whose results compare qualitatively well with the results obtained in the Varying

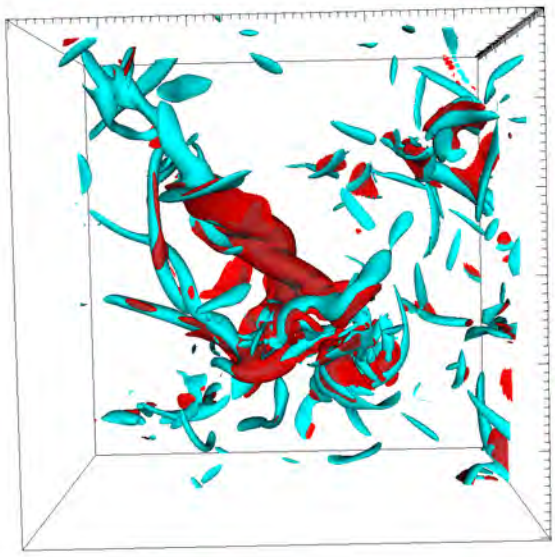

Figure 5.9: Regions of intense vorticity (cyan) and of intense strain (red) in a turbulent flow. A subdomain of size $(150\eta)^3$, where η is the Kolmogorov scale, of the full computational domain is shown. The colored regions correspond to an intensity of vorticity or strain larger than ~7 times their r.m.s.. The Reynolds number of the flow is $Re_\lambda = 650$.

Density Turbulence Tunnel at MPIDS (collaboration with H. Xu and P. Yang, Tsinghua University).

Transport in geophysical flows and collisions of Ice crystals in clouds

The enhancement of particle transport is a major property of turbulent flows. Transport of particles by a turbulent flow has been investigated in great detail in the case of the simplest possible flows, namely in flows which are istotropic and homogeneous. Although this is an enticing approximation, many flows of practical interest are more complex. As an example, geophysical flows, in the atmosphere and oceans, are affected both by stratification, and also by the rotation of the earth. Using direct numerical simulations, we investigate the transport of particles in the presence of these two effects, in situations of relevance to oceanography (collaboration with R. Marino, Lyon and A. Pouquet, NCAR).

The importance of turbulence to understand the aggregation of small particles (droplets or small crystals) in a cloud, to form rain drops, snow flakes, graupels or other precipitation particles has been known for a long time. Whereas much theoretical work has been devoted so far to droplets, we have been recently focusing on the presence of small crystal particles, that play an important role in deep clouds, which extend over a very high altitude, so the temperature in the upper part of the cloud is significantly below freezing. In such clouds, supercooled droplets coexist with ice crystals, which can be, as a first approximations, modeled as spheroids. To investigate the motion and possibility of collisions of crystals, we have simplified the problem by treating ice crystals, which are much smaller than the smallest scale

in the flow, by neglecting the inertia of the fluid (assuming locally a very small Reynolds number of the fluid). The numerical work shows that at small turbulence intensity, the collisions are dominated by differential settling velocities, induced by different orientations. Turbulence plays a more significant role at larger intensity. This can be understood by using notions recently developed to understand the properties of collisions of droplets in a turbulent flow. Our simplifying assumption concerning the motion of the spheroids, however, needs to be carefully checked. One of the issues concerns the orientational bias of settling particles, which appears to differ between the model and the available experimental information. Preliminary studies show that this effect can be partly understood by using finite (fluid) inertia corrections, an effect we are actively investigating (joint work with A. Naso, E. Lévèque, ENS Lyon, and K. Gustavsson and B. Mehlig, University of Gothenburg).

Recent effort in collaboration with the MPIDS was devoted to the nucleation of droplets in the wake of precipitation particles settling at a temperature that significantly differs from that of the surrounding medium (collaboration with MPIDS).

Actin polymerization in chemotactic amoeba

In collaboration with the group at MPIDS, we are providing a description of the dynamics of actin polymerization. The formation of actin-driven protrusion is essential in the displacement (crawling) of cells towards a source of nutrients, or other chemical signals. Previous work had demonstrated that, in the absence of any stimulation, the dynamics of actin polymerization could be spontaneously oscillating, and describable in terms of a simple oscillator in the presence of (additive) noise. In recent work, we have characterized the transient response of *Dictyostelium discoidem* cells, initially in a spontaneously oscillating regime, following a stimulation by a pulse of chemoattractant. The response involves two distinct phases. First, one observes a very strong increase of polymerization at the cells periphery (cortex) for a short time (approximately 20s). This is followed by a longer transient period, over a duration longer than ~ 100s, before the pre-existing oscillation regime is restored. A minimal elaboration of the oscillator model can reproduce the most significant features observed experimentally (collaboration with J. Negrete, Lausanne, and MPIDS).

5.5 MAX PLANCK EMERITUS GROUP NONLINEAR DYNAMICS

Prof. Dr. Theo Geisel studied physics at the Universities of Frankfurt and Regensburg, where he received his doctorate in 1975. After postdoctoral research at the MPI for Solid State Research in Stuttgart and the Xerox Palo Alto Research Center, he was appointed Heisenberg Fellow in 1983. He was Professor of Theoretical Physics at the Universities of Würzburg (1988-1989) and Frankfurt (1989-1996), where he headed the Sonderforschungsbereich (SFB) Nonlinear Dynamics of the DFG. From 1996 to 2016 he had a double appointment as director at the MPI for Dynamics and Self-Organization and as full professor in the Faculty of Physics of Göttingen University. Emeritus director since October 2016, he is a member of the Academy of Sciences and Humanities Göttingen and Inaugural Head of Faculty for Nonlinear Dynamics in the Faculty of 1000. A recipient of the Leibniz Prize (1994) and other awards, he initiated the Bernstein Center for Computational Neuroscience (BCCN) Göttingen and headed it for 9 years. His research is driven by the fascination of complex dynamics emerging in nonlinear systems as diverse as neuronal networks, nanostructures, and the population dynamics of infectious diseases.

Nature confronts us with numerous dynamical phenomena, many of which are easy to dissect for a human observer, while others have challenged theoreticians for decades. The field of nonlinear dynamics has developed tools to analyze and characterize nontrivial dynamics in complex systems. Applying these tools the Max Planck Emeritus Group Nonlinear Dynamics attempts to clarify the dynamics and function of biological neural networks, the chaotic electron transport in semiconductor and graphene nanostructures, the spatiotemporal dynamics of infectious diseases, and the role of microtiming deviations in musical performances.

In neuroscience many important problems and questions are related to dynamics and self-organization. How do the neurons in our brain cooperate when we perceive an object or perform a task? What is the role of different dynamical states for brain function? How do cortical networks quickly switch between different states, e.g. for context-dependent information routing?

Mathematical analyses of the dynamics of neural networks cannot rely on mainstream recipes but pose formidable mathematical challenges. Neural systems exhibit several features that elude standard mathematical treatment: the units of the network communicate or interact only at discrete times and not continuously as in many-body theory in physics; there are significant interaction delays that make the systems formally infinite-dimensional; and complex connectivities give rise to novel multioperator problems. Meeting such challenges has often been facilitated by cross-fertilization within the scope of problems addressed in the former Department of Nonlinear Dynamics, from diverse stochastic processes in complex environments such as Levy flight models for the spread of epidemics to wave phenomena in random and complex media such as the random focussing of rogue waves and tsunamis.

A fascinating application of the tools developed in nonlinear dynamics is the time series analysis of musical sequences. It allows us to elucidate the relation between stochastic properties of musical compositions or performances and musical perception. In particular, our group has studied fluctuations in musical rhythms and clarified the long-standing controversy on the role of microtiming deviations that were often claimed to be the essence of the swing feeling in jazz.

The former Department of Nonlinear Dynamics was created by the Max Planck Society in 1996 to initiate a scientific reorientation of the MPI for Flow Research towards modern nonlinear dynamics and complex systems. The Department founded and hosted the federally (BMBF) funded Bernstein Center for Computational Neuroscience Göttingen, in which it cooperated with experimental neuroscience labs and established a high performance computing facility. Today Theo Geisel is heading an emeritus group on nonlinear dynamics, which interacts with other research groups in the Institute.

5.6 MAX PLANCK EMERITUS GROUP MOLECULAR INTERACTIONS

Together with the late Hans Pauly (1928 - 2004) our group came to Göttingen in 1969 from the University of Bonn to establish the new research direction of molecular beam investigations of elementary collision processes between atoms and molecules. In the following years the Institute became one of the leading international centers for experimental and theoretical research in determining with unprecedented precision the van der Waals forces between atoms and molecules. These forces are of fundamental importance for understanding both the static and dynamic properties of gases, liquids and solids as well as their phase transitions. Our research led to the development of a new model for the van der Waals interaction in place of the well-known Lennard-Jones potential. The Tang-Toennies potential, which is presently widely used for accurate simulations, has been cited 1450 times since 1984.

Prof. Dr. Dr. h.c. mult. J. Peter Toennies studied physics and chemistry at Brown University, Providence,USA where he received his Ph.D.in 1957. He came to Germany in 1957 where he was a postdoc and "Assistent" 1957-1965 in Wolfgang Paul's Physics Institute in Bonn. After his habilitation (1965) he was a Dozent until becoming director at the MPI Strömungsforschung in Göttingen (1969-2002). Since 1971 he is Associate Professor at the University of Göttingen and Adjunct Professor at the University of Bonn.

In the course of these studies our group observed in the late 1970's that helium free jet gas expansions behaved in a remarkable way. Instead of the usual velocity distributions with $\delta v/v \cong 10\%$, the helium atom beams had very sharp velocity distributions and were nearly monoenergetic with $\Delta v/v \leq 1\%$. This unexpected observation was found to be related to the extremely weak interatomic forces between He atoms, with the consequence that their collision cross section, at the ultra-low ambient temperatures ($\approx 10^{-3}K$ in the expanding gas) rises to 259.000 , more than 4 orders of magnitude larger than the cross section at room temperature. These nearly monoenergetic helium atom beams have found widespread application. In expansions with small concentrations of molecules the excess of helium atoms serves to cool the molecules down to temperature of several degrees K. This became a great boon for molecular spectroscopy since at these temperatures the hot bands that otherwise obscure the molecular spectra are eliminated.

Our group exploited the helium atom beams for exploring the structures and vibrations at the surfaces of solid crystals. In complete analogy to neutrons, which are routinely used to study the structures and phonon dispersion curves inside solids, helium atoms are the ideal scattering probe method for investigating the structures and dispersion curves of phonons at solid surfaces, which are not accessible with neutrons. The study of over 200 different surfaces by helium atom scattering (HAS) and the complimentary method of inelastic electron scattering (EELS) have led to a much more profound knowledge of interatomic forces at surfaces and how atoms and molecules interact with metal surfaces, which is of basic importance for understanding catalysis. In the following years we became even more fascinated by this unusual element helium, which is the only substance which exhibits superfluidity, a collective quantum phenomena similar to superconductivity. In its superfluid state below 2.2 K liquid helium flows without friction, just as the electrons in a superconductor flow without resistance. Thus it was natural to ask if small clusters and droplets of helium might also exhibit superfluidity. In molecular beam experiments we observed that atoms

and molecules could be inserted and trapped in the droplet's interior. This opened up the possibility of employing spectroscopy to interrogate the physical properties of the trapped molecules and also the state of the helium droplets. Surprisingly the sharp spectral features of the embedded molecules indicated that the molecules rotate freely as if they were in a vacuum and not at all strongly hindered as expected for an ordinary liquid. Subsequent experiments revealed that this remarkable behavior was related to the superfluidity of these droplets. This is the first evidence that superfluidity occurs in a finite-sized system and is now called *microscopic superfluidity*.

Helium nanodroplets are now being used in more than 25 laboratories worldwide as a uniquely cold $(0.15 - 0.37K)$ and gentle matrix for high resolution molecular spectroscopic investigations of atoms, molecules, and "tailor made" clusters, their chemical reactions, and their response to photo-excitation. Our group used this technique to provide the first evidence that para-hydrogen molecules which, like He atoms are spinless bosons, can also exhibit microscopic superfluidity. Experiments were also directed at exploring the nature of small pure clusters consisting of a few helium and hydrogen molecules, which show large quantum effects. To this end we developed an apparatus to study the matter-wave diffraction of cluster beams from nanostructured transmission gratings. These experiments led to the first evidence for the existence of the very weakly bound dimer and the precise measurement of its size and of the van der Waals interactions of a number of atoms and molecules with solid surfaces. Unexpected magic numbers were found in larger clusters $(N \leq 50)$, which have led to the first insight into the elementary excitations of these nano-sized superfluids.

At present we are working in three main areas of research: (1) In the last days of 2018 our monograph with Prof. Giorgio Benedek (University of Milan) entitled "Atomic Scale Dynamics at Surfaces: Theory and Experimental Studies with Helium Atom Scattering" finally appeared. (2) We hope soon to complete the analysis of experimental data relating to the flow of solid helium through a 100 micron capillary. The data indicates that the flow is non-classical in that it does not follow the Hagen-Poiseuille law. Rather it exhibits an unexpected large velocity which is independent of the pressure gradient. This surprising phenomenon is attributed to a type of Bose-Einstein Condensation of a solid with a high concentration of vacancies. (3) In collaboration with several Bachelor students we are currently investigating a new modified Tang-Toennies model for describing the van der Waals potentials of the alkali diatomic molecules made up of the atoms Li, Na, K, Rb, and Cs in the weakly bound triplet state. These potentials are of great current interest for understanding the collisions in laser trapped ultracold gases and their Bose-Einstein Condensation. We have recently demonstrated that our model with only three parameters provides an equal or better description of all the spectroscopic data than numerical fits with up to 50 parameters. One student has recently succeeded in calculating these potentials ab initio using an elegant analytical theory, which avoids the usual numerical methods, such as with SCF, CI and DFT.

PART II

RESEARCH

SPATIO-TEMPORAL COMPLEXITY AND ORDER IN DRIVEN SYSTEMS

6

Pretty much all physical phenomena of relevance in nature occur in systems that are driven – in other words – systems that are energetically maintained out of thermal equilibrium. The driving can either be external or internal. Generic to these systems is that they break the symmetry of space and time spontaneously and that they develop spatio-temporal complexity and order. Most systems have an infinite number of degrees of freedom that condense, due to their dynamics and self-organization, to a strongly reduced number. Although it might sound contradictory, spatio-temporal complex systems have well-defined universal properties that generically describe a whole class of systems exhibiting very different physical phenomena. In other words, spatio-temporal complex systems show order within their complexity that can be captured at a universal level by the physics tools of non-equilibrium and nonlinear statistical physics. The MPIDS is and will be one of the main drivers of this rapidly developing field. In this chapter, we present our recent results on a range of systems and phenomena, which are at the frontier of our scientific knowledge and are of broad biological, societal and ecological relevance. This includes fluid turbulence, complex flow networks, neural networks, granular gases, liquid crystals and excitable media. The strong interaction between novel experimental approaches, analytical, and numerical tools is not only aimed at a better understanding of the physics but may also contribute to solving some of the most pressing challenges of our time such as climate change, the transition to renewable energies as well as leading a longer and healthier life.

Contents

6.1 TOWARDS AIRBORNE MEASUREMENTS OF CLOUD MICROPHYSICS AND TURBULENCE

G. Bagheri, F. Nordsiek, O. Schlenczek, P. Höhne, M. Schröder, E. Bodenschatz

Despite decades of research by many scientists, insufficient understanding of cloud physics is a primary source of uncertainty in weather and climate models. This uncertainty stems mainly from the unresolved processes within clouds, such as moist convection and cloud formation [1]. Resolving cloud processes is an extremely challenging task since they are turbulent over a very wide range of spatial and temporal scales [2, 3]. In order to better understand how clouds form and evolve, a comprehensive knowledge of cloud microphysics and turbulence is essential. Key questions that need to be addressed are turbulent mixing inside the cloud and the role of turbulence on the droplet spatial distribution and relative velocity statistics.

Figure 6.1: The Cloudkite.

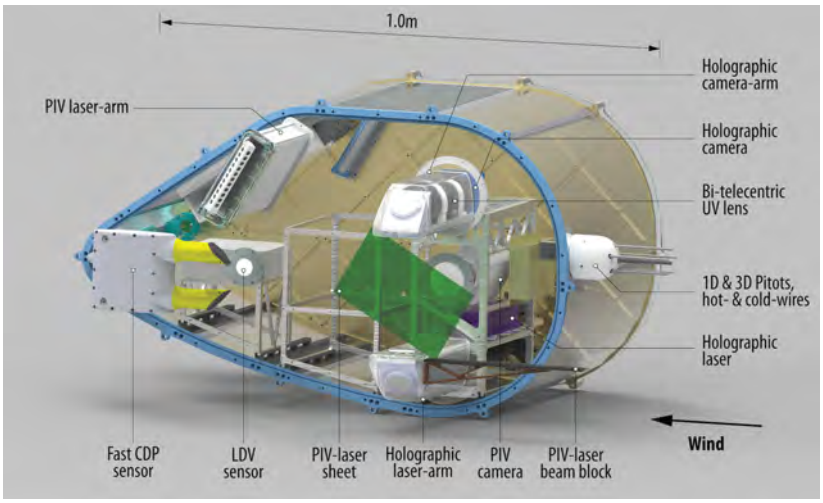

Figure 6.2: CAD visualization of the Cloudkite instrument-box. **Particle Image/Tracking Velocimetry (PIV/PTV)**: 2D velocity field and particle velocities. **holography**: 3D particle positions and sizes for particles. **Fast Cloud Droplet Probe (FCDP)**: particle counting and sizing. **Laser Doppler Velocimetry**: 1D particle velocities. **Hot-/cold-wires**: 1D air velocity and temperature. **Standard Pitot tube**: 1D air velocity. **Multi-hole Pitot tube**: air velocity and wind-direction. Humidity and Temperature sensors.

To answer these questions, we developed a unique airborne platform, the *Cloudkite*, that allows us to measure cloud features with an unprecedented level of accuracy down to the smallest relevant scales. The Cloudkite is a tethered 250m^3 helium-filled balloon-kite combination aerostat (known as a Helikite), which is 15m long and 10m wide/high. The Cloudkite provides the possibility of picking clouds of interests and performing measurements away from topographic effects. It is capable of lifting a net payload of 50kg when operating at an altitude of 1km above the sea level. The instrument box onboard the Cloudkite is designed for simultaneous acquisition of cloud-microphysics and cloud/atmospheric turbulence. Every flight, the Cloudkite will image 3 L/s of cloud for 35 min (about 6 m^3 imaged in total) while acquiring air velocity, temperature, and humidity as well as particle size counting and 1D velocities for the whole 2-3 hour flight.

[1] B. Stevens, and S. Boney, Science **340**, 1053 (2013)
[2] E. Bodenschatz, *et al.*, Science **327**, 970 (2010)
[3] A. Pumir, and M. Wilkinson, Annu. Rev. Condens. Matter Phys. **7**, 141 (2016)

6.2 FIELD MEASUREMENTS OF CLOUD DROP DYNAMICS

J. Moláček, G. Bagheri, G. Bertens, H. Xu, E. Bodenschatz
S. Risius (DLR Göttingen), H. Xi (Shenzhen, China),
S. Malinowski (U. Warsaw, Poland),
R. A. Shaw (Michigan Tech. U., USA),
H. Siebert (IfT Leipzig, Germany), Z. Warhaft (Cornell, USA)

Figure 6.3: Research station Schneefernerhaus. Our experiments are conducted on the cylindrical tower's rooftop to minimize influence of the mountain on the flow.

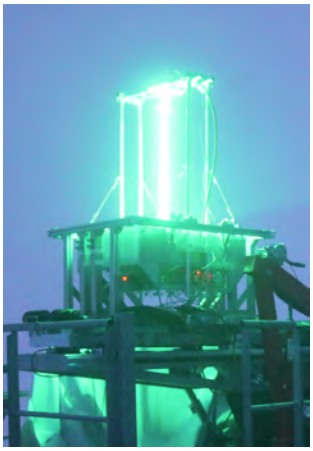

Figure 6.4: The "seesaw" during operation. Laser beam illuminates the cloud droplets from above, high-speed cameras are housed in the box underneath.

Although everyone has come into contact with a raindrop, few of us are aware of the plethora of physical processes and complex interactions that are involved in creating one. Its origins in the cloud of droplets created by condensation on aerosol nuclei suspended in the air are relatively well understood, although even here a few surprises still keep cropping up [1]. Similarly well known are the last stages of a raindrop as it falls towards the ground and gains size by coalescing with smaller droplets in its path. The mystery lies in the transition between the two stages as the time it takes for the first few collisions of a drop to happen has proven difficult to predict using simple models. It is now believed that turbulence plays a major role in speeding up this process [2] by preferentially distributing the cloud droplets in space and enhancing their collision rates by creation of high-acceleration events which "detach" droplets from their local flow velocity [4].

To complement our novel laboratory experiments [4, 5] in this area, we have built a field setup at the environmental research station Schneefernerhaus (UFS, Fig. 6.3), situated near Germany's highest mountain Zugspitze. The location was chosen for its predictable wind direction and high likelihood of being in clouds during summer months. First experiments using a set of sonic anemometers have shown [6, 7] that under typical conditions the turbulence properties measured at UFS are similar to those in free clouds and exhibit Taylor-microscale Reynolds numbers up to 10^4.

Using a stationary Lagrangian particle-tracking (LPT) system we have obtained first data on cloud droplet dynamics at smallest scales [8]. However, the best statistics require matching the velocity of the LPT system to the cloud particles as closely as possible, which led us to build an apparatus, nicknamed "seesaw" (Fig. 6.4), capable of transporting the LPT system at speeds of up to 7m/s over a 5m distance. After resolving the issues arising from the harsh local conditions, the setup has been fully functional since May 2018. Starting with extensive investigations of droplet velocity, acceleration and spatial distribution statistics, the seesaw is expected to produce insights into cloud dynamics inaccessible by DNS or laboratory measurements.

[1] J. Svensmark, *et al.*, J. Geophys. Res. Space Physics, **121**, 8152-8181 (2016)
[2] A. Pumir, *et al.*, Annu. Rev. Condens. Matter Phys., **7**, 141-70 (2016)
[3] B. J. Devenish, P. Bartello, *et al.*, Q. J. R. Meteorol. Soc., **138**, 1401 (2012)
[4] G. P. Bewley, E.-W. Saw, E. Bodenschatz, New J Phys., **15**, 083051 (2013)
[5] E.-W. Saw, G. P. Bewley, *et al.*, Phys. Fluids, **26**, 111702 (2014)
[6] S. Risius, H. Xu, F. DiLorenzo, *et al.*, Atmos. Meas. Tech., **8**, 3209 (2015)
[7] H. Siebert, R. A. Shaw, *et al.*, Atmos. Meas. Tech., **8**, 3219-3228 (2015)
[8] J. Moláček, G. Bagheri, G. Bertens, E. Bodenschatz, in preparation

6.3 LARGE-SCALE TRANSITIONS IN FULLY DEVELOPED TURBULENCE

C. C. Lalescu, M. Wilczek

In many settings, turbulence exhibits an intricate interplay between almost two-dimensional large-scale features and three-dimensional small-scale fluctuations. Our atmosphere serves as a prominent example: While large-scale weather patterns with lateral extents much larger than the height of the atmosphere can be considered as approximately planar, local phenomena such as cloud microphysics crucially depend on the three-dimensionality of the atmosphere. What determines the dimensionality of the flow, and how do two- and three-dimensional fluctuations interact? To systematically study the relation between large-scale flow structures and small-scale turbulence, we investigate a conceptually simple shear flow — a generalized turbulent Kolmogorov flow, which is maintained by a single large-scale shearing mode [1, 2] (see Fig. 6.6). By applying a large-scale drag force, controlled by the parameter μ, we can precisely tune large-scale flow features. Although turbulence fully develops in the flow, time- and height-averaged vorticity profiles exhibit a variety of coherent large-scale patterns. Increasing the drag induces a sequence of transitions (see Fig. 6.5) with rich dynamics including intermittent bursts of kinetic energy and noise-induced switching between meta-stable states.

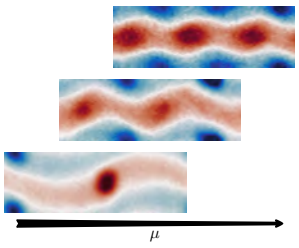

Figure 6.5: Phase diagram for generalized Kolmogorov flow showing the height-averaged vorticity (blue for clock-wise and red for anti-clock-wise vortices). For small values of μ, a single vortex pair is observed. For intermediate values, we find a coexistence of states with intermittent switching behavior. For large μ, three stable vortex pairs are observed.

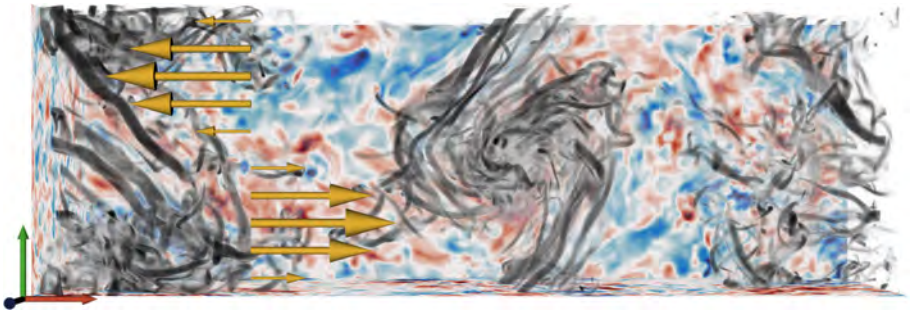

Figure 6.6: Snapshot of Kolmogorov flow structures in an aspect ratio three box. The planes show out-of-plane vorticity and the full enstrophy field is volume-rendered; yellow arrows represent the forcing.

A detailed investigation of the energetics of the system shows that the excitation of three-dimensional small-scale turbulence provides a dissipation channel for the large scales. In the absence of drag, kinetic energy accumulates at the largest scales and is quasi-periodically released into bursts of three-dimensional small-scale turbulence. This mechanism provides an important link between intermittency in the large and the small scales. The large-scale drag tames the large-scale flow, and it also reduces small-scale intermittency (see Fig. 6.7). This suggests that important flow characteristics can be assessed from the low-dimensional dynamics of the large scales, bringing a dynamical systems approach to fully developed turbulence within reach.

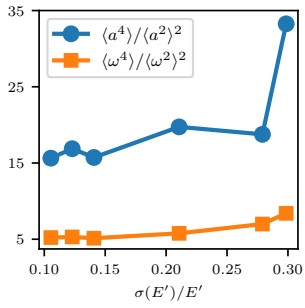

Figure 6.7: Flatness of vorticity and tracer acceleration (small-scale quantities) as a function of variance of turbulent kinetic energy, a measure for large-scale intermittency. For Gaussian statistics, the flatness is 3. The figure shows that small-scale non-Gaussianity increases with large-scale intermittency.

[1] V. Borue, S. A. Orszag, J. Fluid Mech. **306**, 293 (1996)
[2] I. E. Sarris et al., Phys. Fluids **19**, 095101 (2007)

6.4 WIND ENERGY: FROM ATMOSPHERIC TURBULENCE TO OPTIMAL POWER GRIDS

M. Wilczek
L.J. Lukassen (U. Oldenburg), C. Meneveau (Johns Hopkins U.), R.J.A.M. Stevens (U. Twente), H. Ronellenfitsch (MIT), J. Dunkel (MIT)

Figure 6.8: The turbulent fluctuations between subsequent rows in a wind farm are strongly correlated – as visualized here with data from a large-eddy simulation of a fully developed wind turbine array.

The transition to renewable energies comes with a range of challenges. For wind energy, atmospheric turbulence plays a key role: Strong wind fluctuations impose significant structural fatigue loads on wind turbines which can lead to failure. Integrating the unsteady wind energy into a decentralized power grid poses further challenges with respect to power grid stability.

To quantify the impact of turbulence on wind energy systems, it is important to characterize the velocity fluctuations in the atmospheric boundary layer as well as in wind turbine arrays. While investigations of the free atmospheric boundary layer give crucial information about the wind farm inflow conditions, investigating the flow within the wind farm helps to better understand the velocity fluctuations which ultimately translate into power output fluctuations.

In a series of works, we have investigated space-time correlations of velocity fluctuations in atmospheric boundary layers [1, 2] and wind turbine arrays [3] by means of highly resolved large-eddy simulations (see Fig. 6.8). Using concepts from fundamental turbulence theory [4], we have developed a model for space-time correlations, in which the decorrelation effects can be traced back to large-scale velocity perturbations. We used simulation data of atmospheric turbulence and wind farm flows to corroborate that such simple, physics-based models quantitatively capture trends and fluctuations of atmospheric turbulence.

Our results have shown that for typical wind farm configurations, the turbulence between subsequent rows is strongly correlated, i.e. fluctuations will not simply average out. This motivated the question whether power output fluctuations can be reduced by optimizing the underlying power grid. In fact, the question of an optimal network topology to reduce fluctuations is of much broader impact. Using tools from network theory, we devised design rules for optimal noise-canceling networks, which reduce output fluctuations by changing the wiring diagram only [5]. Interestingly, our optimal network topologies bear a strong resemblance to biological vein networks found in plant leaves, slime molds, and human vasculature, which suggests that biological design principles can be carried over to engineering applications.

[1] M. Wilczek, R. Stevens, C. Meneveau, J. Fluid Mech. **769**, 888 (2015)
[2] M. Wilczek, R. Stevens, C. Meneveau, J. Turbul. **16**, 937 (2015)
[3] L. Lukassen, R. Stevens, C. Meneveau, M. Wilczek, Wind En. **21**, 474 (2018)
[4] M. Wilczek, Y. Narita, Phys. Rev. E **86**, 066308 (2012)
[5] H. Ronellenfitsch, J. Dunkel, M. Wilczek, Phys. Rev. Lett. **121**, 208301 (2018)

6.5 SUSTAINABLE ENERGY SUPPLY AND POWER GRIDS

B. Schäfer, X. Zhang, D. Manik, M. Timme
K. Chinnow, P. Steiglechner (PIK Potsdam), D. Witthaut (FZ Julich)

The 2015 Paris climate agreement set the goal to limit global warming to a maximum of 1.5°C above pre-industrial levels. To ensure a sustainable energy system in the long term, not only do energy supply and usage need to become drastically more effective and efficient, it is also key to substantially reduce greenhouse gas emissions. Yet, enabling the transition of our electricity system to rely almost exclusively on renewable energy sources poses huge challenges for society, engineering and research: Renewable sources are smaller, more distributed, more fluctuating, less predictable and thereby force the network to become more decentral, more interconnected and, as a consequence, less centrally controllable. The impact of these changes on the robustness, stability, and even existence of a grid's operating state is barely understood. After having addressed these challenges individually in the past[1], we currently bridge them among the different branches.

Critical links and non-local rerouting. In our 2016 work [1], we investigated under which conditions and how individual infrastructure failures such as line outages influence the collective grid operating state. One rule of thumb employed in industry is to preferentially consider those links to be potentially critical for the operating state that are most highly loaded. However, such local picture turned out to be oversimplified. Our extensive model study [1] predicts a strongly non-local factor controlling how energy flows are rerouted in networks, Fig. 6.9. These insights led to us developing two predictors for critical links, by quantifying network's redundant capacity and by estimating the network-wide flow rerouting through developing a ***renormalized* linear response theory**. The proposed strategies discriminate the links that are critical for system operation (several times more effectively than local measures) from those that keep the operating state intact.

Generalized susceptibilities for network dynamical systems. Inspired by these insights, we generalized standard notions of susceptibility known from thermodynamics and statistical physics to network dynamical systems [2]. A susceptibility in general quantifies the change of a system's state following small alterations of one of its parameters. Our generalization demonstrates in how far the most sensitive parameters determining the state of a network are its topological properties, given by its coupling matrix. We proposed and analytically worked out both vertex and edge susceptibilities, providing a general theory applicable to supply, transport and flow networks. Applications to power grids included to identify links that must not be more highly loaded to keep the overall network functioning. Surprisingly, moderately loaded links may be more affected than highly loaded ones, cf. Fig. 6.9.

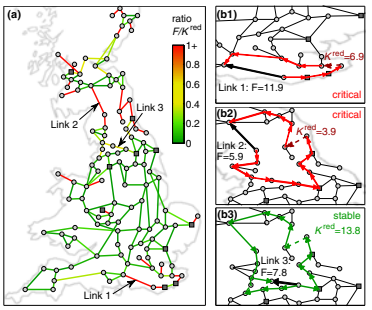

Figure 6.9: **Nonlocal rerouting and critical link prediction.** Network's redundant capacity for a failing link indicates flow rerouting options. (a) British power grid network color-coded by the ratio between loads and redundant capacities. For two of the three links (indicated by black arrows) not sufficient redundant capacity is available thus they are critical (b1,b2). For the third link the redundancy is sufficient so it is stable despite of high local load (b3).

[1] ... having initiated the research field of collective nonlinear dynamics of power grids by our 2012 *Phys. Rev. Lett.* publication and establishing a 2.9 Million joint research project with six institutions in Germany and several application partners, http://condynet.de/partner.html.

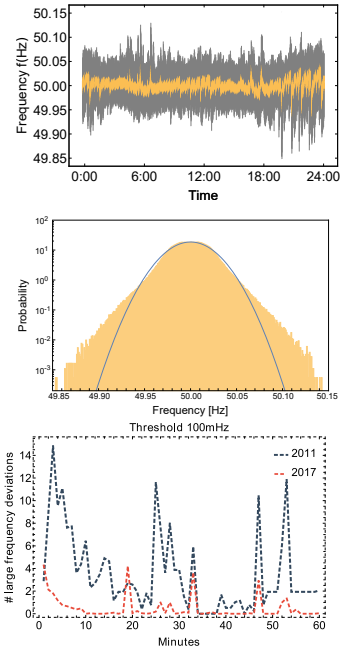

Figure 6.10: **Anomalous frequency statistics and extreme events** [4]. Top: hourly and 15 minute trading events induce irregular frequency dynamics; middle: observed non-Gaussian statistics; bottom: reducing trading intervals from hourly (2011, dashed line) to quarter-hourly (2017, solid line) reduces the number of extreme frequency excursions occurring.

Transient-induced cascades. For cascading failures in networks, the main research question in the past has been whether, after one infrastructure failed, a new stationary state exists and is stable. However, such view misses transient dynamics. We have thus proposed a new class of mathematical models of hybrid (discrete and continuous) type to account for the possibility that the transient dynamics after an initial failure already causes failures of other infrastructures, even if a new stationary operating state does exist and is stable [3]. We used the insights from this novel perspective to identify critical lines that may lead to large-scale blackouts.

Anomalous frequency fluctuations and extreme events. If power supply and demand are not balanced, the grid frequency deviates from its reference value of 50 Hz and therefore displays fluctuations. We analyzed these fluctuations in various power grids in Europe and beyond, and found non-Gaussian statistics and periodic disturbances (Fig. 6.10). The latter regular events are likely **caused by energy trading** actions. We explain the non-Gaussian statistics using (generalized) Fokker-Planck equations involving Lévy-stable noise or alternatively applying superstatistical methods. Our theory also quantifies extreme events, system-intrinsic causes and may thereby help to understand and contain fluctuation-induced risks.

Localization, spreading and spatio-temporal resonances. Spreading phenomena essentially underlie the dynamics of a wide range of natural and technological systems, from epidemics to power grids. Yet they are still far from understood, in part due to intractable difficulties in standard dynamical system's theory, e.g. transcendental equations defining signal arrival times. We introduced a complementary perspective to **capture** timing and amplitude of individual units' **deterministic trajectories by expectation values**, as in probability theory. The resulting alternative quantifiers provide dependencies of when and how strong a disturbance initiated in one unit impacts others, as an explicit function of the network's interaction patterns [6].

If a local fluctuation persists, as it often does in power grids driven by renewable power sources, its dynamical impact on the network is highly non-trivial. We uncovered three generic response regimes [7]. Most interestingly, fluctuations near some of the system's eigenfrequencies induce characteristic network resonances that may be an order of magnitude larger than those responses in the low frequency limit commonly considered important. In addition, our theory quantifies exactly how responses induced by high frequency signals decay with distance from source and frequency content. These findings may have implications on how to identify and mitigate potential systematic risks in power grids with fluctuating inputs from renewable power sources.

[1] D. Witthaut et al, Phys. Rev. Lett. **116**, 138701 (2016)
[2] D. Manik et al, Phys. Rev. E **95** (1), 012319 (2017)
[3] B. Schäfer et al, Nature Comm. **9** (1), 1975 (2018)
[4] B. Schäfer et al, Nature Energy **3** (2), 119 (2018)
[5] M. Schröder et al, Phys. Rev. Lett. **120**, 248302 (2018)
[6] J. Wolter et al, Chaos **28** (6), 063122 (2018)
[7] X. Zhang et al, arXiv:1809.03081 (2018)

6.6 EFFECTIVE DESCRIPTION OF SUPERSTRUCTURES IN TURBULENT RAYLEIGH-BÉNARD CONVECTION

G. Green, D. Vlaykov, M. Wilczek
G. Ibbeken (University of Göttingen), J.P. Mellado (MPI Meteorology)

Turbulent flows in nature often show a surprising large-scale order, even though turbulence is typically associated with chaotic, irregular motion. Better understanding this coexistence of large-scale order and turbulence is the motivation for the current work. Many physical systems, such as the ocean, the atmosphere, or the interior of stars and planets, are driven by thermal gradients leading to convection [1]. The dynamics of convective flows is characterized by a strong coupling between the temperature and velocity field. Rayleigh-Bénard convection (RBC), as illustrated in Fig. 6.11, is an idealized system which captures the main features of natural convection, including pattern formation and turbulence [1, 2]. It can be characterized by two nondimensional control parameters, the Rayleigh number Ra, which characterizes the thermal driving and the Prandtl number Pr, which is the ratio between kinematic viscosity and thermal diffusivity. Recently, slowly evolving large-scale coherent flow patterns, so-called turbulent superstructures, have been observed in turbulent RBC [3, 4, 5, 6]. Despite the presence of small-scale fluctuations, large-scale patterns are still visible in this regime, see Fig. 6.12. They are reminiscent of convection rolls which appear at the onset of convection at $Ra_c = 1708$ and can be analytically understood using pattern formation theory [1]. However, little is currently known about the origin of turbulent superstructures. It has been shown that their length scale λ is initially increasing with Ra [3, 5] and saturates for $Pr = 1$ around $Ra = 2 \times 10^7$ [6]. In order to understand this, we study the interaction of superstructures and small-scale fluctuations as well as their origin in two complementary approaches. In the first one, we investigate RBC, described by the full three-dimensional Oberbeck-Boussinesq equations, with direct numerical simulations. In the second one, we consider a reduced model for the midplane - a generalized Swift-Hohenberg (SH) equation, which was originally introduced to model the onset of convection in RBC [7].

To clarify the impact of turbulence on the large-scale patterns, we investigate the energy transfer between superstructures and small-scale fluctuations in RBC. In the statistically stationary state the averaged energy input is balanced by the mean dissipation rate $\langle\varepsilon\rangle$, in which $\langle\cdot\rangle$ is an average over time and volume. Using a filter-space technique, this can be generalized to a scale-dependent relationship, which features the energy flux between scales. On average, the resolved energy input Q_l is balanced by the large-scale dissipation ε_l (length scales $\geq l$) and the kinetic energy transfer between scales Π_l: $\langle Q_l\rangle = \langle\varepsilon_l\rangle + \langle\Pi_l\rangle$. At the scale of the superstructures, $\lambda/2$, the energy input is primarily balanced by the flux of kinetic energy, which transfers energy to the unresolved scales, see Fig. 6.13. The flux therefore acts as an additional dissipation in the resolved energy budget. In comparison, the large-

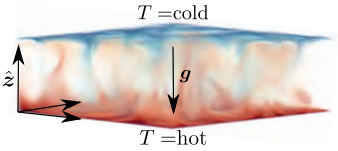

Figure 6.11: Rayleigh-Bénard Convection: a confined flow between a heated bottom plate and a cooled top plate governed by the Oberbeck-Boussinesq equations.

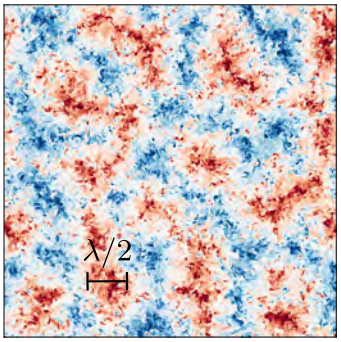

Figure 6.12: Temperature field in the midplane for $Ra = 1.1 \times 10^7$, $Pr = 1$. Even though the flow is turbulent, there are coherent large-scale flow patterns of size $\lambda/2$, reminiscent of convection rolls at onset.

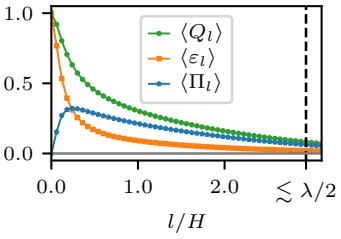

Figure 6.13: Scale-resolved decomposition of the mean power input $\langle Q_l\rangle$, the large-scale dissipation $\langle\varepsilon_l\rangle$ and the energy transfer $\langle\Pi_l\rangle$, normalized by the mean dissipation, obtained with a horizontal filter for $Ra = 1.1 \times 10^7$, $Pr = 1$.

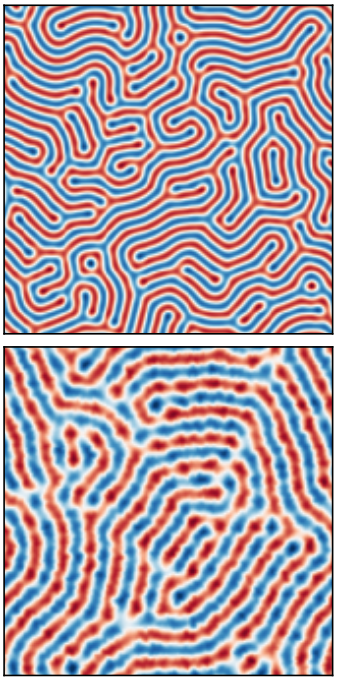

Figure 6.14: Order parameter field of the generalized SH equation without fluctuations (top) and with turbulent fluctuations (bottom). The large-scale pattern persists in presence of the fluctuations with an increased wavelength compared to the case without advection. Fluctuations therefore introduce an effective turbulent diffusion of large-scale patterns.

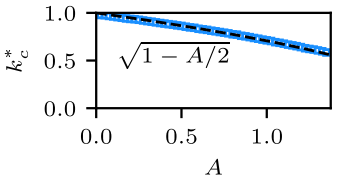

Figure 6.15: Wavenumber $k_c^* = 2\pi/\lambda_c^*$ of the mean pattern as a function of the amplitude A of the fluctuations for $r = 0.9$. The numerical results obtained from time averaging (squares) agree with the theoretical expectation (dashed line), showing that fluctuations increase the wavelength of large-scale patterns.

scale dissipation is weak at this scale. In order to understand the role of the boundary layers, we have extended the analysis to height-dependent profiles of the energy budget terms. Here additionally a spatial flux term enters, which mainly transports energy from the bulk to the wall. Locally, especially in the near-wall region, the balance has a complex structure. We find that in a layer close to the wall, the energy transfer (which on average acts as a dissipation) is a source for the resolved kinetic energy, i.e. here energy is transferred up-scale from the unresolved to the resolved scales. This shows that the dynamics in the boundary layers strongly influence the superstructures, as also observed in [5, 6]. The overall analysis points at similarities between the resolved budget of the superstructures in the turbulent regime and the fully resolved budget at much lower Rayleigh numbers, which could provide a starting point for future modeling approaches.

To study the superstructures and their origin analytically, we have investigated a generalized SH equation as a reduced two-dimensional model for the temperature in the midplane [7, 8]. The SH equation exhibits stationary large-scale patterns, which are characterized by a control parameter r, modeling the Rayleigh number. To investigate the impact of small-scale fluctuations on large-scale patterns, we have introduced an additional random advection term in the SH equation. Consistent with our computational results of the full Rayleigh-Bénard problem, we find that the fluctuations effectively add a turbulent diffusion of large-scale patterns, visible in individual realizations, see Fig. 6.14. This results in an increased length scale in presence of small-scale fluctuations. Due to the simplicity of this model, analytical statements for the resulting mean field can be obtained and verified against numerical simulations [8]. For example, we could show that the fluctuations shift the onset of convection to larger values of the control parameter and increase the wavelength $\lambda_c^* = 2\pi/k_c^*$ of the mean-patterns, see Fig. 6.15. Our model therefore shows similarities with turbulent superstructures in the midplane and qualitatively explains the growth of the wavelength of superstructures in RBC with Ra.

In future work, we plan to establish further connections to the full Rayleigh-Bénard problem by capturing the temporal dynamics of turbulent superstructures, ultimately enabling an effective description of turbulent superstructures in convection.

[1] E. Bodenschatz, W. Pesch, G. Ahlers , Annu. Rev. Fluid Mech. **32**, 709 (2000)
[2] G. Ahlers, S. Grossmann, D. Lohse, Rev. Mod. Phys. **81**, 503 (2009)
[3] T. Hartlep, A. Tilgner, F. H. Busse , Phys. Rev. Lett. **91**, 064501 (2003)
[4] M. S. Emran, J. Schumacher , J. Fluid Mech. **776**, 96 (2015)
[5] A. Pandey, J. D. Scheel, J. Schumacher , Nat. Commun. **9**, 2118 (2018)
[6] R. J. A. M. Stevens, A. Blass, X. Zhu, R. Verzicco, D. Lohse , Phys. Rev. Fluids **3**, 041501 (2018)
[7] J. Swift, P. C. Hohenberg , Phys. Rev. A **15**, 319 (1977)
[8] G. Ibbeken, G. Green, M. Wilczek, under review (2018)

DFG Turbulent Superstructures

6.7 STATISTICAL PROPERTIES OF TURBULENCE AT HIGH REYNOLDS NUMBER

C. Küchler, G. P. Bewley, E. Bodenschatz

Turbulence governs the dynamics of a variety of natural flows from blood circulation to the atmospheric boundary layer and plays and important role in a multitude of engineering disciplines. For example, turbulence is ultimately responsible for rainfall. Despite being such a common phenomenon, an efficient general theory is not in sight. Our lack of understanding of turbulence limits the accuracy of weather reports and climate models as well as the efficiency of combustion engines. Turbulent flows are commonly characterised by the Reynolds numbers R_λ - a nondimensional quantity describing the range of spatial scales that the turbulent motions span. Flows of high R_λ are of particular interest, because they shape the atmospheric dynamics and reveal a range of scales, where the statistical properties of the velocity fluctuations are predicted to follow relatively simple universal relations. However, sufficiently high R_λ are difficult to achieve in laboratory flows. In the Variable Density Turbulence Tunnel (VDTT) [1] we are able to reach R_λ of more than 5000, which is unmatched by any other wind tunnel flow. We obtain these high R_λ by using sulfur-hexaflouride at pressures up to 15 bar. At such high pressures, the kinematic viscosity ν is very small allowing the existence of very small flow structures of size $\eta \sim 10\mu$m. Recently, we have installed an active grid: an arrangement of 111 motor-controlled flaps, which we use to drive the turbulence at variable length scales and intensities larger than those of classic rigid grids as illustrated in Fig. 6.16.

The control over pressure and the large scale through the autonomous active grid allow an unusual flexibility in changing R_λ. We are exploiting this flexibility in our study of the bottleneck effect in the energy spectrum of a turbulent flow. The bottleneck effect is a pileup of energy at the small-wavenumber end of the inertial range. Its origin is subject of multiple theories [2, 4] and might contain valuable information about the scale-to-scale transfer of kinetic energy in the inertial and dissipation range. A R_λ-scaling of the effect's strength has previously been studied in direct numerical simulations [3], but no systematic laboratory study has been performed, which we attribute to the challenging measurement. From a measurement instrument perspective, it is a small effect at high frequencies, which makes the measurement very delicate. Namely, the constant temperature hot-wire anemometer we use attenuates or amplifies certain frequencies [5]. To resolve this systematic bias, we alter R_λ by changing the active grid correlations only, which influences the low-wavenumber end of the energy spectrum only. Thereby we can place the bottleneck pileup at the same frequency for different R_λ, such that the systematic frequency-dependent errors are consistent from case to case. This allows us to investigate the scaling of the bottleneck effect with R_λ. With this approach we have gained strong indications that the bottleneck effect in the energy spectrum is getting weaker with increasing R_λ shown in Fig.

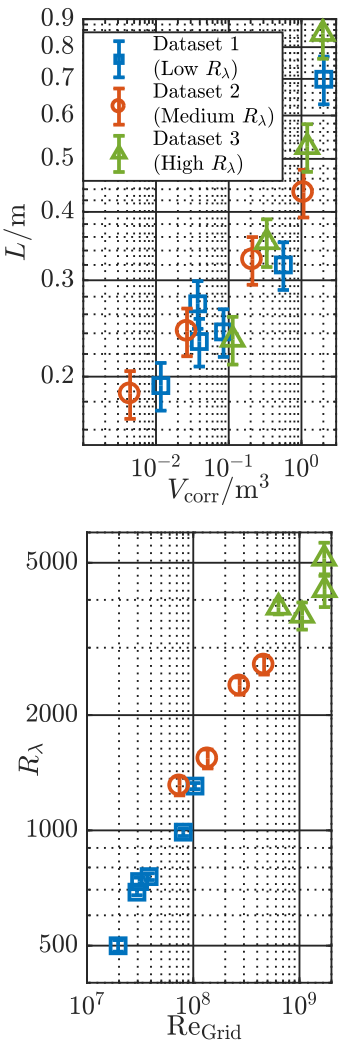

Figure 6.16: Control of large-scale forcing through the active grid. L is the size of the energy injection scale. It is mainly influenced by V_{corr}, which describes the mean volume of an active-grid induced wake. $\mathrm{Re}_{\mathrm{Grid}}$ is equivalent to the well-known large-scale Reynolds number. The scaling for homogeneous, isotropic turbulence of $R_\lambda \sim \sqrt{\mathrm{Re}}$ is almost recovered.

6.17. This has previously only been observed in numerical simulations and predicted by theories. We further find that at R_λ>3000, our data is also consistent with an absent or asymptoting bottleneck motivating further research on the topic.

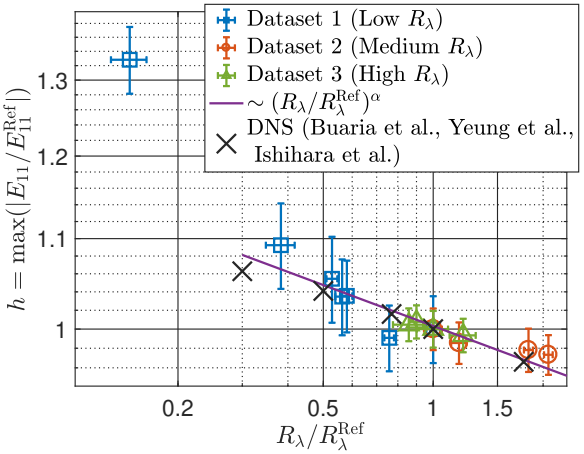

Figure 6.17: Scaling of the bottleneck effect with R_λ. To eliminate systematic instrument errors, we created three datasets, within which only the large scale forcing has been changed through the autonomous active grid. We then relate each spectrum within a dataset to a reference spectrum and measure the relative change of the bottleneck with R_λ. The effect gets weaker with increasing R_λ, follows the numerical data and is consistent with theory [2]

We have demonstrated that instrumentation that has a high spatial and temporal resolution is vital for this experiment. We are using Nanoscale Thermal Anemometry Probes provided by Princeton University, which have a spatial resolution (wire length) of 30 μm [6], and are therefore suited to investigate small-scale features of the flow in the experiment. What prevents us from measuring absolute quantities at those smallest scales are systematic errors of our instrumentation at small time scales. We are currently building a constant current anemometer that we expect to have a flat frequency response up to 10 kHz, such that we can reliably measure statistics even in the dissipative range. At the same time we will implement a two-dimensional particle tracking as an independent measurement to hot-wire anemometry and to obtain acceleration statistics. This project will be an important milestone on the path towards Lagrangian measurements using multiple cameras on a moving sled.

[1] Bodenschatz, Eberhard, et al. Variable Density Turbulence Tunnel Facility. Rev. Sci. Instrum. **85**(9), 1?45, (2014)

[2] Verma, Mahendra K., and Diego Donzis. Energy Transfer and Bottleneck Effect in Turbulence. Journal of Physics A: Mathematical and Theoretical **40** (16) (2007)

[3] Donzis, Diego A., and K. R. Sreenivasan.The Bottleneck Effect and the Kolmogorov Constant in Isotropic Turbulence. J. Fluid Mech. 657 (2010)

[4] Falkovich, Gregory. Bottleneck Phenomenon in Developed Turbulence. Physics of Fluids 6 (4) (1994)

[5] Hutchins, N., J.et al. A Direct Measure of the Frequency Response of Hot-Wire Anemometers Exp. Fluids **56** (1)(2015)

[6] Bailey, Sean C. C., et al.. Turbulence Measurements Using a Nanoscale Thermal Anemometry Probe. J Fluid Mech. **663** (2010)

6.8 TURBULENT AND MULTIPHASE CONVECTION

S. Weiss, A. Krekhov, O. Shishkina, E. Bodenschatz,
A. Pumir (ENS Lyon)
G. Ahlers (UCSB, USA), P. Prabhakaran (Michigan Tech, USA),
X. He (Harbin Inst. of Technology Shen Zhen, China)

Thermal convection is one of the most important heat transport mechanism and as such plays a crucial role in many geo- and astrophysical systems. We study convection experimentally using the Rayleigh-Bénard (RB) setup, where a fluid layer of height L, is confined by a warm plate from below and a cold one from above [1]. The dimensionless Rayleigh number (Ra) represents the strength of the thermal driving in this system, and is directly proportional to L^3. Our research focuses on different aspects of convection, such as convection at very large thermal driving (large Ra), under rotation, with fluids undergoing phase transition, or mixed convection. For this we use different experimental setups, with convection cells of heights as low as $L = 0.5\,\mathrm{mm}$, and as high as $L = 2.2\,\mathrm{m}$.

The largest convection cells are used in the "U-Boot of Göttingen", which is a 4 m long pressure vessel that is filled with Sulfur-Hexafluoride (SF_6) and pressurized up to 19 bar. Using compressed gases allows to change fluid properties and thus the relevant dimensionless control parameters over a very large range. Furthermore, SF_6 is a very dense gas, and thus well suited to achieve very large Ra ($Ra \propto \varrho^2$). With this apparatus Ra of up to 2×10^{15} can be reached and the transition to the "ultimate state" has been probed in the past [2].

Thermal convection is usually modeled using the Oberbeck-Boussinesq (OB) approximation, i.e., assuming that only the density varies linearly with temperature to generate buoyancy, while all other fluid properties are constant. In particular, for high precision measurements at very large Ra (large temperature differences between the bottom and the top), small deviations of this approximation needs to be accounted for when comparing the measured heat transport with the theoretical predictions. To achieve this, we have developed a theoretical model that considers the top and the bottom of the cell as parts of virtual convection cells with symmetric fluid properties along the vertical axis and with identical heat fluxes through each of the cells. With this model we are able to calculate the temperature at the mid-height of the cell, as this is a manifestation of non-OB effects [3, 4].

Using our $L = 2.20\,\mathrm{m}$ high convection cell inside the "U-Boot", we currently investigate the effect of rotation on the flow field and the heat transport in thermal convection, a topic particularly relevant for geo- and astrophysics. For this study, our convection cell was placed on a rotating table capable of carrying a load of 3000 kg and rotating at up to 3 rad/s (fig. 6.18). One of the questions to answer is about the heat transport under turbulent but geostrophic conditions, where Coriolis forces are balanced by pressure gradients. This regime is very difficult to access in laboratory experiments or numerical simulations, and yet important for the understanding of *e.g.*, the Earth's atmosphere

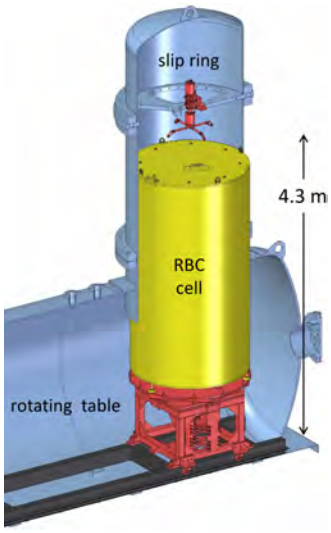

Figure 6.18: Schematic of the rotating turbulent convection setup. The convection cell (yellow) stands on a rotating table (red) inside the U-Boot (blue), which is filled with SF_6 at 19 bar. Two slip rings and a water feed through provide electrical connections as well as temperature-regulated water from the stationary into the rotating frame.

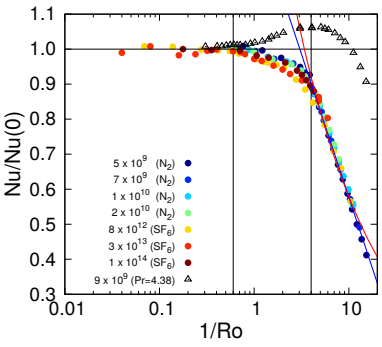

Figure 6.19: The change of the heat transport due to rotation for different Ra and Pr ≈ 0.8. Black triangles are similar data for water ($Pr = 4.38$). It can be seen that a heat transport enhancement due to Ekman pumping, as is observed for larger Pr, does not occur for $Pr \approx 0.8$.

and currents in the oceans. The Prandtl number in our experiment is $Pr \approx 0.8$, very similar to that of the Earth's atmosphere. Fig. 6.19 shows the normalised heat transport (normalised Nusselt number - Nu) as a function of the dimensionless rotation rate (i.e., the inverse Rossby number - 1/Ro) for different Ra. One can roughly distinguish three different 1/Ro-regimes based on the monotonic behaviour of Nu: (i) for small rotation rates, Nu does not change with 1/Ro, (ii) for larger 1/Ro, Nu decreases but the decreased depends on Ra, and (iii) a strong decrease for larger 1/Ro. A heat transport enhancement due to Ekman pumping as for larger Pr (black triangles in fig. 6.19) was not observed here. Another important finding is the collapse of the data for different Ra in regime (iii) when plotted as a function of 1/Ro. The decrease follows a logarithmic function of 1/Ro. This finding is very essential, as for the geostrophic regime various power-law dependencies between the various dimensionless parameters are suggested but non of them could be verified so far in experimental measurements.

In another project we study phenomena related to the dynamics of clouds by using a binary mixture of SF_6 and Helium in an RB setup. The pressure and temperatures are set such that the bottom plate is warmer and the top plate colder then the liquid-vapor transition temperature. As a result SF_6 condenses at the top plate, forming cold liquid drops that drip down to the bottom. We found that such a cold drop falling through an SF_6-saturated atmosphere causes the nucleation of new liquid droplets in its wake [5]. The droplet formation is due to homogeneous nucleation as cold saturated vapor from the drop mixes with warm saturated vapor of its environment, producing supersaturated vapor above the critical saturation ratio necessary (fig. 6.20). As the amount of liquid in the cell was reduced such that no liquid pool formed above the bottom plate, a layer of small droplets was observed in the cell, very similar to an atmospheric cloud layer (fig. 6.21). The layer marked a border between a subsaturated region in the lower part of the cell and a supersaturated region in the upper part. Small micro-droplets that slowly settle due to gravity exist in the upper part but start evaporating as soon as they reach the lower part of the cell.

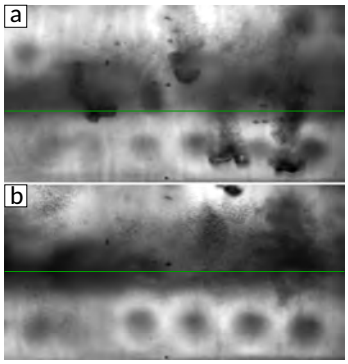

Figure 6.21: Snapshots of clouds in a SF_6-Helium binary mixture at two different times. Cold drops are falling from the top plate (a) that cause droplet nucleation in their wake (visible in b). These micro-droplets are only stable in the supersaturated region (above the green line) but evaporate in the sub-saturated region (below the green line).

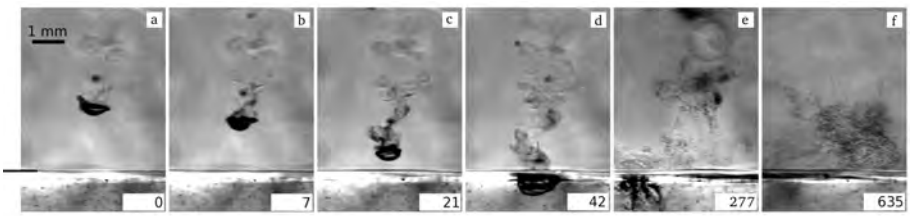

Figure 6.20: A large cold liquid SF_6 drop falls through a saturated vapor atmosphere. Due to mixing of warm and cold saturated vapors in the wake of the drop, the saturation increases above its critical value and small droplets condense due to homogeneous nucleation. The short black line at the left of (a) marks the liquid surface at the bottom.

We acknowledge financial support from the DFG Priority Program (SPP) 1881 "Turbulent Superstructures", the DFG Grant WE 5011/4-1 and the Max Planck Center for Complex Fluid Dynamics.

[1] L. P. Kadanoff, Phys. Today **54**, 34 (2001)
[2] X. He, et al., Phys. Rev. Lett. **108**, 024502 (2012)
[3] O. Shishkina, et al., Phys. Rev. Fluids. **1(6)**, 062301(R)
[4] S. Weiss, et al., J. Fluid Mech., **851**, 374 (2018)
[5] P. Prabhakaran, et al., Phys. Rev. Lett. **119**, 128701 (2017)

6.9 DISENTANGLING LAGRANGIAN TURBULENCE

C. C. Lalescu, M. Wilczek
L. Bentkamp (University of Göttingen)

The complexity of fully developed turbulent flows can be perceived either from an Eulerian or a Lagrangian point of view (Fig. 6.22). The Eulerian laboratory frame is well suited to characterize the spatial structure of turbulence, whereas following tracer particles, i.e. adopting the Lagrangian perspective, provides important insights into the dynamics of turbulence. How can we relate these complementary perspectives?

Recently, we have made progress in establishing statistical bridging relations between the Eulerian and Lagrangian frame [1]. Starting from the idea that, essentially, tracer particles sample turbulent fields in space and in time, we developed a theory which expresses Lagrangian statistics as a probabilistic mix of Eulerian statistics. Introducing an effective Lagrangian dispersion, we were able to derive time-resolved Lagrangian statistics from instantaneous Eulerian statistics. Our findings have implications for a range of problems, including turbulent mixing and transport as well as uncovering the origin of Lagrangian intermittency, i.e. the pronounced scale-dependence of Lagrangian velocity fluctuations.

Lagrangian particles frequently encounter extreme acceleration events in fully developed turbulence, which is closely related to the intermittency phenomenon. Intense small-scale structures such as vorticity filaments can give rise to acceleration events exceeding the typical root-mean-squared fluctuations by orders of magnitude (Fig. 6.23). As a first indication that the extreme acceleration events originate from the spatial fine-scale structure of turbulence, we found that systematically filtering out such spatial events reduces Lagrangian intermittency, leading to statistics much closer to those of finite-sized, neutrally buoyant particles [2]. When tracers encounter intense vortex structures, their trajectories oscillate violently in time. During these corkscrew events, the acceleration magnitude remains remarkably constant (Fig. 6.24, inset). This led us to introduce the notion of persistent Lagrangian acceleration, quantified by the squared Lagrangian acceleration coarse-grained over a viscous time scale, which forms the basis of a new Lagrangian theory of turbulence. Conditioning Lagrangian particle data from direct numerical simulations on this coarse-grained acceleration, we find remarkably simple, close-to-Gaussian statistics for a range of Reynolds numbers. As a result, we can decompose Lagrangian single-particle statistics into much simpler, Gaussian sub-ensembles. Using statistical field theory, we can then capture Lagrangian single-particle statistics as a superposition of Gaussian statistics, weighted by the frequency of persistent acceleration [3]. Our approach therefore disentangles the complex statistics of Lagrangian turbulence, laying the foundation for a comprehensive statistical theory.

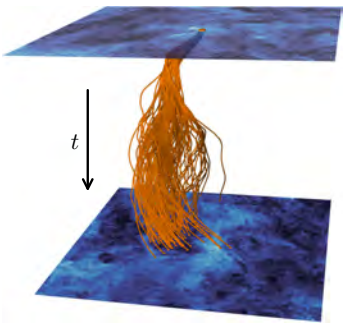

Figure 6.22: Space-time plot of Eulerian and Lagrangian turbulence (showing two out of three spatial dimensions). An initially localized cloud of particles is shown as it is advected and dispersed over time by the evolving field.

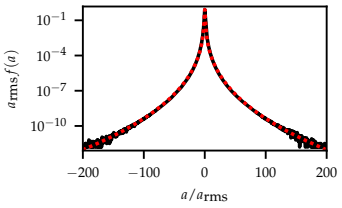

Figure 6.23: The probability density function of tracer accelerations (black curve) follows a stretched exponential form (dotted red curve). We have measured events as high as two hundred standard deviations in simulations of high Reynolds number turbulence.

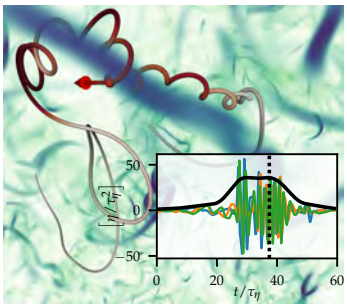

Figure 6.24: Trajectory of a particle encountering a vortex filament. The inset shows time series of acceleration components, and the black curve shows the acceleration magnitude coarse-grained over time.

[1] C. Lalescu, M. Wilczek, New J. Phys. **20**, 013001 (2018)
[2] C. Lalescu, M. Wilczek, J. Fluid. Mech. **847**, R2 (2018)
[3] L. Bentkamp, C. Lalescu, M. Wilczek, arXiv:1901.09650 (2019)

6.10 TURBULENT THERMAL CONVECTION: THEORY

O. Shishkina, E. Bodenschatz, M. Emran, S. Weiss, X. Zhang, L. Zwirner, D. Lohse (Univ. of Twente)
E. S. C. Ching (The Chinese Univ. of Hong Kong),
S. Grossmann (Philipps-Univ. Marburg), S. Horn (UCLA),
K.-Q. Xia (The Chinese Univ. of Hong Kong),

There are three classical paradigmatic systems to study thermally driven flows: Rayleigh–Bénard convection (RBC), vertical convection (VC) and horizontal convection (HC). In RBC and VC, heating and cooling of a fluid layer takes place through two different parallel surfaces of the fluid layer. In RBC the fluid is heated from the bottom and cooled from the top, while in VC the heat supply is through one and heat removal is through another vertical surface of the layer. In HC heat is supplied and removed through a single, top or bottom, surface of a fluid layer. All these flow configurations are important in geo- and astrophysical systems as well as in ingeneering applications.

We investigate turbulent thermal convection theoretically by examples of RBC [1, 5, 8, 9, 10, 11, 13], VC [4, 6, 12] and HC [2, 3, 7] and validate our results in Direct Numerical Simulations (DNS) using mainly our own finite-volume code GOLDFISH [14]. Our studies are aimed on the development of models to predict for different flow configurations (which might be enhanced by the wall roughness and/or cell rotation and/or tilting [4, 12] and/or horizontal confinement [12, 13] and/or non-Oberbeck–Boussinesq (NOB) effects [5, 11]) the main mean flow characteristics such as the self-organized turbulent wind [7, 10], the mean temperature and velocity profiles [1, 8, 10], the mean momentum and heat transport, measured, respectively, by Reynolds number (Re) and Nusselt (Nu) number, and their scaling relations [3, 6, 9] with the control parameters of the corresponding convection system, namely, Rayleigh number (Ra), Prandtl number (Pr) and Rossby number (Ro) and geometrical characteristics of the convection cell.

The highlights of our work within the last 2 years are the following:

- derivation of the boundary-layer (BL) equations in RBC [1, 8, 10], the solutions of which can perfectly approximate the mean temperature and velocity profiles;
- derivation from the BL equations of different laminar scaling regimes in VC [4];
- advancement of the Grossmann and Lohse scaling theory for HC [3] and RBC by large Pr [9];
- development of the model to predict the bulk temperature in RBC under weak NOB conditions [5, 11]).

We acknowledge the financial support of our studies by the German Research Foundation (DFG) under the grants Sh405/3, Sh405/5, Sh405/7, Sh405/8 and Sh405/10 as well as the DFG Heisenberg Programm and the DFG Priority Program 1881 (SPP) "Turbulent Superstructures". We also acknowledge the Leibniz Rechenzentrum (LRZ) for funding by providing computing time.

[1] O. Shishkina et al., Phys. Rev. Lett. **114**, 114302 (2015)
[2] O. Shishkina et al., Phys. Rev. Lett. **116**, 024302 (2016)
[3] O. Shishkina et al., Geophys. Res. Lett. **43**, 1219 (2016)
[4] O. Shishkina et al., J. Fluid Mech. **790**, R3 (2016)
[5] O. Shishkina et al., Phys. Rev. Fluids **1**, 062301(R) (2016)
[6] O. Shishkina et al., Phys. Rev. E **93**, 051102(R) (2016)
[7] O. Shishkina, J. Fluid Mech. **812**, 525 (2017)
[8] O. Shishkina et al., Phys. Rev. Fluids **2**, 113502 (2017)
[9] O. Shishkina et al., Phys. Rev. Fluids **2**, 103502 (2017)
[10] E. Ching et al., J. Stat. Phys. **167**, 626 (2017)
[11] S. Weiss et al. J. Fluid Mech. **851**, 374 (2018)
[12] L.Zwirner et al., J.Fluid Mech. **850**, 984 (2018)
[13] K.Chong et al,Phys.Rev. Fluids **3**, 013501 (2018)
[14] G.L. Kooij et al., Comp. Fluids **166**, 1 (2018)

6.11 GRANULAR CRYSTALS ARE NOT MADE OF HARD SPHERES

M. Schröter
F. Rietz, C. Radin (Austin), H. L. Swinney (Austin)

Hard spheres are a seminal model system in condensed matter. Their first order phase transition from an amorphous fluid to an ordered solid became the textbook example of entropic forces governing a multi particle system. Both colloids and granular matter are often considered to be experimental realizations of hard sphere systems. However, while the dynamics of the former is governed by Brownian motion, granular particles are orders of magnitude too large to be influenced by thermal energies. Granular spheres can therefore be considered as athermal hard spheres.

Colloids, as hard spheres, undergo a first order phase transition with a coexistence region with volume fractions ϕ between 0.49 and 0.55. The formation of new crystals is well described by the Classical Nucleation Theory (CNT) framework, which assumes that the free energy gain associated with the formation of a crystalline bulk phase has to overcome the free energy costs occurring due to the formation of interface between crystal and amorphous phase. This leads to a critical nucleus size; only above this size is it thermodynamically favorable for the crystal seed to grow.

The present work tests experimentally if the crystallisation of granular matter fits in the hard sphere paradigm. With the setup shown in figure 6.25 we cyclically shear a packing of 50000 glass spheres immersed in an index-matched liquid. Using a laser sheet scanning technique, we repeatedly identify the positions of all particles while performing 1.9×10^6 shear cycles.

Our analysis shows that driven granular packings share some of the hard sphere phenomenology. They also display a transition from an amorphous state to a regime with coexisting homogeneously nucleated crystallites (Fig. 6.26), albeit at ϕ between 0.64 and 0.74. Moreover, it is also possible to identify a critical nucleus size n_c necessary for the crystal to grow (Fig. 6.27). However, an analysis of the volume fraction in the transition zone between the nucleus and the amorphous phase shows that the formation of additional interface is energetically favorable for nuclei *smaller* than n_c.

This failure of the CNT framework demands a new approach to the crystallization in athermal sphere packings. One possible alternative explanation of the critical nucleus size is that the formation of smaller crystals is kinematically inhibited. Presently we test this hypothesis using mathematical tools from persistent homology to parameterize the geometrical configurations of groups of particles.

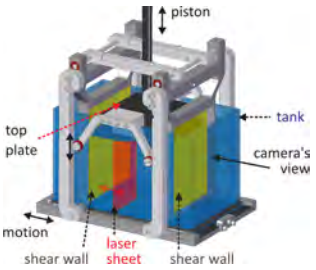

Figure 6.25: 50000 glass spheres are contained in a cubical volume with opposite side walls (green) that produce oscillating shear. The cell is filled with a liquid that is index matched to the beads. The top plate is levered to the side walls and is mounted on a piston that is constrained to move vertically. Shear is produced by periodically oscillating the cell bottom.

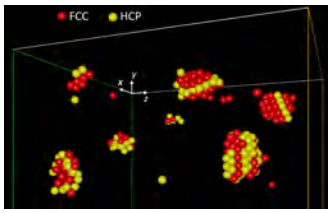

Figure 6.26: This cross section of the cell after 10^6 cycles shows crystalline regions in the cell interior; the amorphous phase is not shown. The colors of the nucleated spheres indicate crystal type [2].

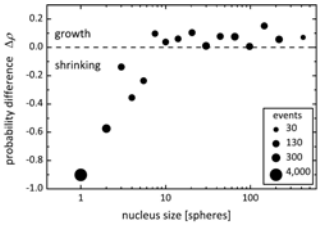

Figure 6.27: The unexplained nucleation barrier: the probability that a nucleus will grow or shrink depends on its size; nuclei with ten or more spheres predominately grow ($\Delta\rho > 0$).

[1] Frank Rietz, Charles Radin, Harry L. Swinney, and Matthias Schröter, Phys. Rev. Lett. **120**, 055701 (2018)
[2] For a video of the nucleation see: `https://youtu.be/_oV-WwtW4Xo`

6.12 EARLY-STAGE AGGREGATION IN A THREE-DIMENSIONAL CHARGED GRANULAR GAS

C. Singh, M. G. Mazza

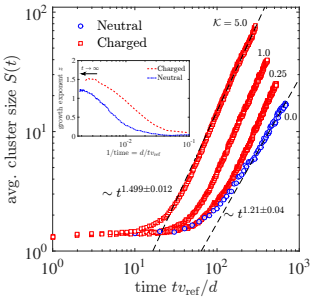

Figure 6.28: Temporal dependence of the average cluster size $S(t)$, from an average over twenty independent simulations and corresponding best fit. The granular gas with collisional charging exhibits faster growth of clusters than for neutral system. (Inset) saturation of the growth exponent z as $1/t \to 0$ using the method of local slope. A change in the ratio of characteristic Coulomb to thermal energy $\mathcal{K}$ do not alter the growth exponent z and only influences the crossover time of initiation of clustering.

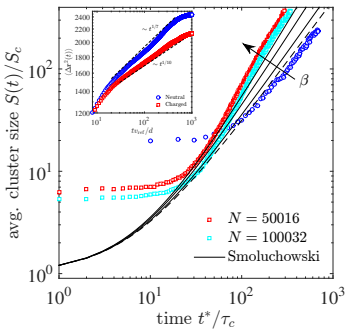

Figure 6.29: Comparison of $S(t)$ predicted by the Smoluchowski eq. with the MD results. At $\beta = 2$ (dashed line) the mean-field solution agrees reasonably well with the neutral gas, while at $\beta = 3$ (solid line) the growth rate for the charged granular gas is recovered. (Inset) Comparison of the MSD of particles between the charged and the neutral gas. The sub-diffusion due to dissipation is further suppressed by the electrostatics, (increasing β). S_c and τ_c are rescaling factors.

Since classical antiquity, lightnings have been associated with the ashes produced during volcanic activity. Collisional charging may play a significant role in particle's aggregation in the formation of planetesimals, charging in dust devils, and electric sparks in dunes.

We show [1] that the time dependent average cluster size $S(t)$ in a charged granular gas obeys the power law $S(t) \sim t^z$. To model the charged granular gas, we employ Hertzian elastic forces, non-linearly dissipative viscoelastic model and the classical Coulomb forces in the framework of granular molecular dynamics (MD) in three dimensions.

Experiments have revealed that the number of elementary charges transferred during a collision of silica particles on polished quartz and silicon wafer surfaces, on average, is proportional to a power of the relative kinetic energy, $Z_{i\leftrightarrow j} = (CE_{\rm kin})^{\kappa}$, where $E_{\rm kin}$ is the relative kinetic energy during the collision, and $C^{-1} \sim 10^{-12} - 10^{-15}$ J and $\kappa = 0.83$. Employing these empirical results, we simulate $N \sim 10^4 - 10^5$ identical, viscoelastic particles in a three-dimensional domain of volume $V = L^3$, with fixed filling fraction $\phi \equiv N\pi d^3/(6V) = 0.076$.

To investigate the statistical properties of the clusters, we calculate the average cluster size $S(t) = \frac{\sum_s s^2 N_s}{\sum_s s N_s}$, where $N_s(s)$ is the cluster size distribution. For the neutral gas, a best fit to the average over twenty independently initialized simulations reveals $S(t) \sim \left[t^{1.21\pm0.04} \approx t^{6/5}\right]$, which is close to the mean field result based on the Smoluchowski's aggregation equation. For the charged gas, we obtain $S(t) \sim \left[t^{1.49\pm0.012} \approx t^{3/2}\right]$ which clearly indicates a relatively faster cluster growth [Fig. 6.28].

To bolster our results, we consider the Smoluchowski's coagulation equation, and make a mean-field approximation by considering an initially monodisperse system

$$\frac{\partial n(i,t)}{\partial t} = \frac{1}{2}\sum_{j=1}^{i-1} K_{\rm a}(j, i-j)n(j,t)n(i-j,t) - n(i,t)\sum_{j=1}^{\infty} K_{\rm a}(j,i)n(j,t),$$

where $n(i,t)$ is the number density of aggregate of size i in the system at time t, and $K_{\rm a}(j,i)$ is the aggregation kernel. To include the effects of electrostatic interactions, we introduce the following kernel based on our MD simulation results $K_{\rm a}(j,i) \propto (i^{1/3} + j^{1/3})^2(i^{-1} + j^{-1})^{1/\beta}$, where $\beta = 2$ corresponds to the neutral aggregation, while a larger β implies a suppressed diffusion. The solution reveals that $z = 6/5$ for $\beta = 2$, and $z = 3/2$ for $\beta = 3$. The consistency of the results from numerically solving the Smoluchowski eq. MD calculations, and our mean-field approximation [Fig. 6.29] suggests that the suppression of particle diffusion due to electrostatics enhances the aggregation process.

[1] C. Singh, M. G. Mazza, Phys. Rev. E **97**, 022904 (2018).

6.13 EFFECTIVE FORCES IN JAMMED THERMAL SOLIDS

Y. G. Pollack
M. Singh, O. Gendelman, C. Rainone, I. Procaccia (Weizmann Institute of Science), E. Lerner (University of Amsterdam), G. Parisi (Sapienza Universita di Roma), B. Riechers (University of Göttingen)

The phenomenon known as jamming has historically been studied and promoted in the context of macroscopic athermal granular matter. There, loose grains can flow under stress, but compaction or shear strain can lead to a jamming transition into a disordered solid. A hallmark of the jammed state is that it can bear a load for a given direction of stress but fail for others. The reason for this becomes clear when looking at the inter-particle force chains that form in the sample with a load-dependent orientation [1] (see Fig. 6.30). These chains bear the load on the system, but obviously cannot sustain stresses orthogonal to the chain.

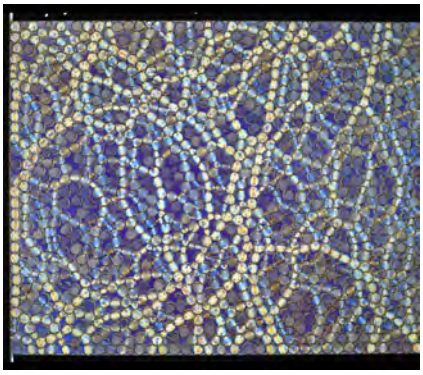

Figure 6.30: Force chains in a 2D system of photo-elastic plastic disks on a table. The vertically applied load determines the chains' orientation. Image appeared in Ref.[1]

The jamming framework has recently been suggested to extend also to slightly thermal systems [2] and to dense active matter including living matter [3] such as in epithelial cell tissues. In this spirit we have studied the effective forces in low temperature thermal amorphous solids, where particles do not mix and flow, but nevertheless move thermally within cages formed by neighboring particles. We had exposed the many-body nature of these effective forces [4] and have quantified it as a function of the proximity to jamming [5]. We have also commenced efforts to study the temporal stability of the chains of effective forces in these systems and the range of temperature and particle motility in which a rigidity framework applies.

[1] O. Gendelman, Y. G. Pollack, I. Procaccia, S. Sengupta and J. Zylberg, Phys. Rev. Lett. **116**, 078001 (2016).
[2] E. Degiuli, E. Lerner, and M. Wyart, J. Chem. Phys., **142**, 164503, (2015).
[3] L. Atia et al., Nat. Phys. **14** ,613 (2018).
[4] O. Gendelman, E. Lerner, Y.G. Pollack, I. Procaccia, C. Rainone and B. Riechers, Phys. Rev. E **94**, 051001(R) (2016).
[5] G. Parisi, Y.G. Pollack, I. Procaccia, C. Rainone and M. Singh, Phys. Rev. E **97**, 063003 (2018).

6.14 MODELING OF COMPLEX LIQUID CRYSTAL DYNAMICS

S. Mandal, M. G. Mazza

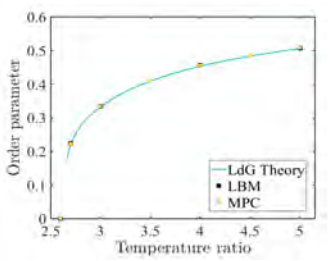

Figure 6.31: Variation of nematic order parameter with temperature ratio.

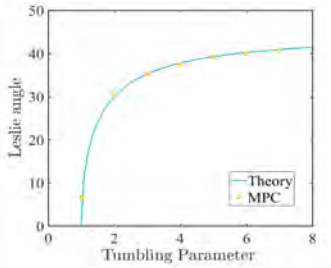

Figure 6.32: Variation of Leslie angle with tumbling parameter.

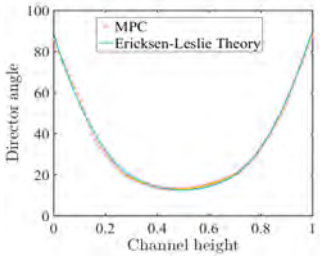

Figure 6.33: Director profile.

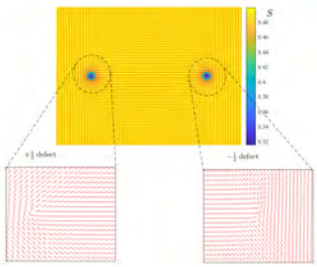

Figure 6.34: Director profile.

The study of microswimmers' dynamics in fluidic environments is of paramount importance to understand modern day applications, such as targeted drug delivery and lab-on-a-chip technologies. Recent experiments have shown a new class of microswimmers composed of nematic liquid crystal droplets suspended in an aqueous surfactant solution. The nematic microswimmers not only self-propel, but also exhibit curling or helical motion depending on the physical dimensionality. Our first goal is to understand the importance of micellar and molecular solubilization towards the genesis of the self-propelled motion of nematic swimmers. The second objective of the present project is to investigate the symmetry breaking phenomenon towards the curling or helical motion of nematic swimmers.

In this work [1], we use computer simulations to model the nematic microswimmers. The idea is to develop a full particle-based simulation scheme that includes liquid crystal molecules, surfactant molecules and aqueous solvent. Towards this, we have developed an augmented multi-particle collision dynamics (MPCD) model for nematic liquid crystals. We follow the tensorial formulation of nematodynamics given by the Qian–Sheng theory. A tensor assigned to each MPCD particle represents the orientation of the nematic director, and whose average corresponds to the macroscopic tensor order parameter. The applicability of this new method is verified by performing several physical and numerical tests.

We have tested: (a) the isotropic-nematic phase transition, (b) the annihilation dynamics of a pair of point defects, (c) the flow alignment of the nematic director in shear and Poiseuille flows, and (d) the velocity profile in shear and Poiseuille flows. Figure 6.31 shows the phase transition diagram in which we have compared our MPCD simulation with the Landau–de Genns theory and existing Lattice Boltzmann (LB) simulations. The velocity-orientation coupling is tested by studying the orientation of nematic director in shear flow using Lees–Edwards boundary condition. Figure 6.32 shows that our simulation result of the Leslie angle compares well with the existing theory. To test the combined effect of velocity-orientation and orientation-velocity couplings, we study the shear flow between two sliding walls and obtained velocity and director orientation profiles. Figure 6.33 show that our simulations compare very well with the existing theory. Additionally, we recover the dynamics of topological defects [see Fig. 6.34].

Our augmented MPCD model can have far-reaching implications not only in modeling of the hydrodynamics of nematic liquid crystals, but also to study the motion of colloids and microswimmers immersed in an anisotropic medium. To simulate the nematic microswimmers, the present model can be coupled to an isotropic solvent and surfactant molecules.

[1] S. Mandal, and M. G. Mazza, *in preparation* (2018).

6.15 THEORY OF SUPPLY IN VASCULAR NETWORKS

F.J. Meigel, K. Alim
M.P. Brenner, P. Cha (Harvard, USA)

Life and functioning of higher organisms relies on the continuous supply of metabolites to tissues and organs. Fluid flow based transport through a vascular network is the indispensable mean to supply nutrients, hormones, and metabolites to all cells in a tissue. What factors controls the supply dynamics globally throughout the tissue as well as locally in the vicinity of a single vessel? From a fluid physics perspective this is a challenging problem, as flow is globally coupled within a network. We here conquer this challenge by deriving efficient analytic approximations for the supply dynamics in a vessel with passive metabolite absorption at the vessel wall. This theoretical framework now allows us to equate what governs supply globally and locally.

Studying plant vasculature, we investigate what is required for uniform supply throughout a leaf [1], see Fig. 6.35(a). We identify the inflow rate as the key global parameter for uniform supply, a parameter that plants indeed control by water evaporation rate within the leaf. We find that in between too low and too high inflow rate there exists an optimal inflow rate for which we derive an exact expression as a function of network and vessel parameters, see Fig. 6.36 (a).

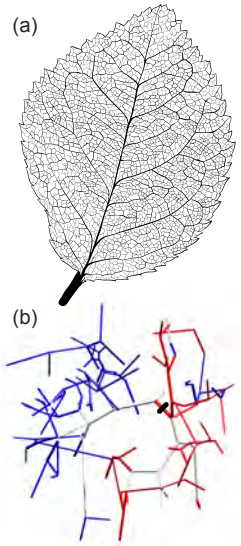

Figure 6.35: (a) Leaf xylem vasculature. (b) rat brain microvasculature excerpt from [3]. Red indicates increase, blue decrease in supply due to vessel dilation (black line).

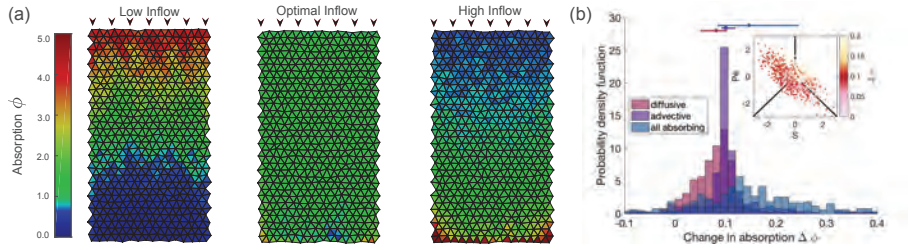

Figure 6.36: (a) Inflow rate govern uniform supply in leaf vasculature: Only the optimal inflow rate permits uniform supply [1]. (b) Local increase in supply due to dilation of a single vessel in rat brain microvasculature for three physical regimes. Vessels in advection governed regime yield a robust increase in supply [2].

Brain microvasculature needs to be set up to locally increase supply if required by neuronal activity, which is facilitated by vessel dilation, see Fig. 6.35(b). How can the local dilation of a single vessel result in a robust increase in supply? With our theory we identify three regimes of supply dynamics of which the advection governed one dominates real microvasculature [3], see Fig. 6.36(b). We justify analytically why this specific regime allows for robust increase in supply following vessel dilation independent of network architecture. Our framework is instrumental to interpet fMRI data, predict drug delivery, design blood vessel architecture in synthetic organs but may also open entire new avenues for the programming of soft robotics and smart materials.

[1] F.J. Meigel, K. Alim, J. R. Soc. Interface **15**, 20180075 (2018)
[2] F.J. Meigel, P. Cha, M.P. Brenner, K. Alim, in preparation, (2018)
[3] Blinder, P. et al., Nat. Neurosci. **16**, 889 (2013)

We acknowledge the support from the DFG Collaborative Research Center (SFB) 937 "Collective behaviour of soft and biological matter", project A19 "Morphogenesis control by mechanical stresses".

SFB 937

6.16 COMPLEX FLUID FLOW IN THE BRAIN VENTRICULAR SYSTEM

C. Westendorf, Y. Wang, E. Bodenschatz,
A. Pumir (ENS Lyon)
S. Kapoor, G. Eichele (both MPIBPC Göttingen)

We study the cilia driven fluid flow within the mammalian brain ventricular system. This system consists of 4 interconnected cavities and is filled with the cerebrospinal fluid (CSF). The beating cilia, which move and thereby distribute the CSF, line most of the ventricle surfaces. We are particularly interested in the ventral third ventricle (v3V, fig. 6.37), as it is directly connected to multiple brain nuclei (like the Hypothalamus), which communicate chemically through the CSF. In a close collaborative effort with the Eichele group, we recorded the fluid flow on the opened v3V and have shown that this flow is rather complex and possesses several distinguishable flow patterns [1]. We have further analyzed the data by averaging it to flow fields using smoothed particle hydrodynamics. These flow fields and the reconstructed ventricle geometries serve as input for numerical simulations of the 3D fluid flow in the closed ventricle. This will finally allow us to trace the transport of chemicals through the v3V. The cilia beating direction is given by its basal body orientation and the polarity of the cilia bundle patch itself (fig. 6.38). We have now shown, using immuno staining and large scale image processing, that the translational and the rotational polarity reflect the effective flow direction. Complemented with DIC imaging of beating cilia, we have now recorded the data necessary to study the origin and variability of the flow patterns (fig. 6.39).

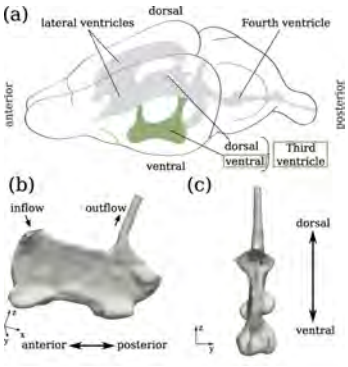

Figure 6.37: Geometry of the brain ventricular system. (a) Sketch of a mouse brain with the ventricular cavities in gray and the v3V in green [Redrawn and adapted from www.jax.org]. (b,c) 3D reconstructed geometry of the v3V. The flow direction of the CSF is indicated at the inflow/outflow.

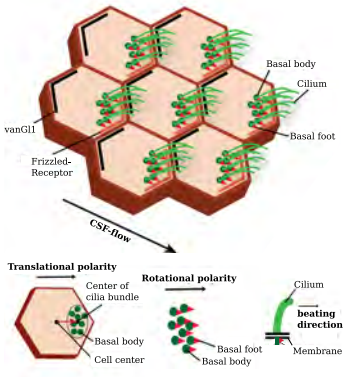

Figure 6.38: Sketch of the Planar Cell Polarity, defined by the cilia patch and the asymmetric protein distribution. The definition of the different polarities is given by the offset of the cilia patch (translational) and the orientation of the individual basal bodies (rotational), which defines the cilia beating direction.

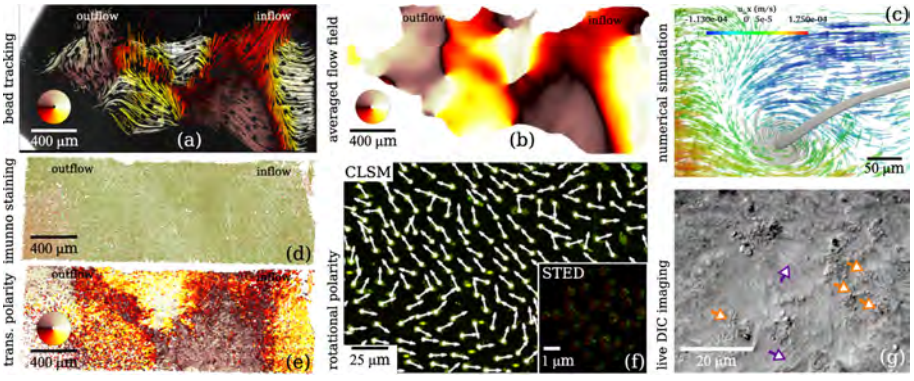

Figure 6.39: Complete analysis of the cilia driven fluid flow and the underlying cell polarity. (a) Tracking of fluorescent beads (color coded by direction) driven by the ciliated surface (background). (b) Averaged flow field of (a). (c) Example of tracer particles (gray lines) in a numerical simulation of the closed ventricle. (d) Immuno stained ventricle surface (same as in a,b) after image segmentation. (e) Translational polarity analysis of (d) of each individual cell (color coded by direction). (f) Cilia bundles immuno stained for their basal bodies and analyzed in terms of rotational polarity (arrows). The inset shows a single immuno stained patch of basal bodies recorded with STED microscopy. (g) DIC image of beating cilia on the ventricle surface. Orange arrows indicate basal body patches and purple arrows the beating cilia.

[1] R. Faubel, C. Westendorf, E. Bodenschatz and G. Eichele, Science **353(6295)** 176–178 (2016).

6.17 OVERTONES IN PERISTALTIC WAVES INCREASE PUMPING EFFICIENCY

F.K. Bäuerle, K. Alim

Wave-like patterns are ubiquitous in biological systems. From the undulatory locomotion of cells and animals, the cardiac cycle to myosin contraction cycles waves have a wide range of time and length scales. While vastly different in their use, all of these systems are governed by a wave's key quantitative parameters: amplitude, wavelength, frequency, and phase. When the environmental settings change these systems have to adapt their parameters - yet are often constrained for example in energetic cost driving the wave. Here, some systems incorporate a superposition of multiple waves, giving rise to new wave parameters. Harmonical waves in particular introduce as parameter the phase difference $\Delta\vartheta$ between its components. How can a system adjust its parameters and thereby its inherent waveform given a desired aim and its energetic constraints?

We investigate peristaltic waves and the influence of the phase difference between harmonics on the pumping efficiency, see Fig.6.40. We show that the flow rate can be tuned by adjusting the phase difference between first and second wave harmonic, while keeping the required elastic energy for deformation constant. At the optimal phase-difference the resulting wave shape occludes the tube most tightly, which optimises pumping efficiency [2]. Quantitatively analysing waves in the paradigm of living peristaltic pumps, the slime mould *P. polycephalum* [1], we find that the organims adjusts its contractions' phase difference precisely following this theoretical mechanism when evacuating an area, see Fig. 6.41, [2]. The living organism is thereby observed to self-organize it's pumping efficiency when triggered by an external stimuli without changing its energy demand - a mechanism which might be a stepping stone to unravel *P. polycephalum*'s complex behaviours. Given the abundance of wave phenomena, the strong impact of the seemingly subtle phase difference between harmonics is likely important in a broad class of biological systems. Further, the discovered mechanism can be implemented in smart materials allowing for self-organisation of pumping rates.

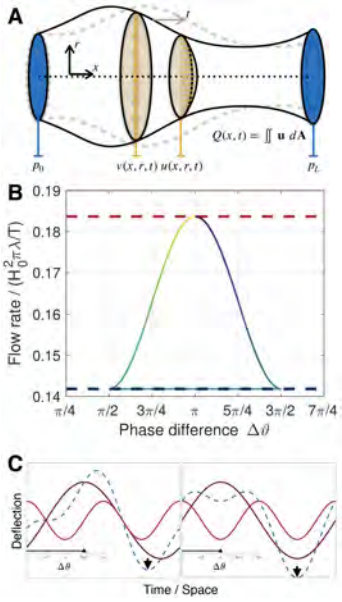

Figure 6.40: (A) Scheme of an axis symmetric tube undergoing peristaltic pumping driven by traveling wave. (B) Flow rate of a peristaltic pump as a function of the phase difference between the first and second harmonic. In red is the maximal flow rate at $\Delta\vartheta = \pi$ and in blue is the minimal flow rate for a contraction pattern without a second harmonic. (C) Sketch of the change in occlusion indicated by arrows, maximal for $\Delta\vartheta = \pi$.

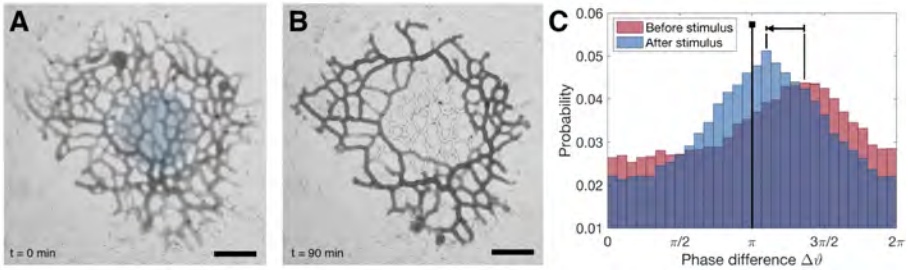

Figure 6.41: *P. polycephalum* adapts its phase difference when actively evacuating an area. (A) and (B) show *P. polycephalum* network with illuminated area (blue) at the onset of stimulus (t=0 min) and after evacuation (t=90 min). Scale bar 1mm. (C) Histogram of phase difference which shifts (arrow) toward $\Delta\varphi$ after the onset of stimulus.

[1] F. K. Bäuerle, M. Kramar, and K. Alim, J. Phys. D **50**, 434005 (2017).
[2] F. Bäuerle, K. Alim, under review (2018)

6.18 FLUID DYNAMICS OF NASAL AIRFLOW

D. Zwicker
S. Melchionna (University of Rome, Italy), M. P. Brenner,
D. E. Lieberman, R. W. Lindsay (Harvard University, USA)

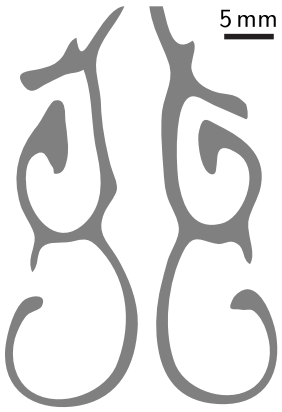

Figure 6.42: Cross section of the central part of a human nasal cavity showing the left and the right chamber.The airflow is perpendicular to the shown plane.

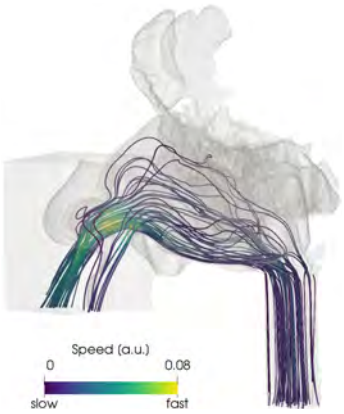

Figure 6.43: Airflow in a human nose during exhalation. The color of the shown streamlines indicates the local velocity.

Our nose not only allows us to smell but it also humidifies, heats, and cleans the inhaled air before it reaches the lungs. All these vital tasks depend critically on nasal airflow, which is driven by the pressure difference created by the lungs and depends on the complex geometry of the nasal cavity shown in Fig. 6.42. We study the relation between airflow and geometry to understand the reasons for the complex shape and to provide insight for clinicians to treat nasal obstruction.

It seems puzzling that the nasal cavity possesses a narrow geometry that is prone to obstruction. However, a simple scaling argument reveals that such a narrow geometry is necessary to efficiently heat and humidify the inhaled air [1]. Here, both heat and humidity can be described as scalar quantities that are transported with the flow and exchange with the walls of the nasal cavity. This exchange is efficient when the diffusive time scale $\tau_\mathrm{d} = \ell^2/D$ for the transport of the scalar with diffusivity D across the channel width ℓ is matched to the advective time scale $\tau_\mathrm{a} = L/v$ along the flow, where L is the channel length and v denotes the mean flow velocity. A more detailed analysis allows us to determine the pre-factor, implying that the scalar exchange is efficient when $\ell \approx 2.75\,(D\tau_\mathrm{a})^{1/2}$, where D is similar for heat and humidity [1]. Using typical values for the involved quantities from the literature, we predict $\ell \approx 3\,\mathrm{mm}$ for the human nasal cavity shown in Figure 6.42. Taken together, our analysis predicts that the observed nasal geometries are narrow to heat and humidify the inhaled air efficiently. Conversely, the overall labyrinth-like structure results from geometric constraints provided by the available space in the skull.

The narrow nasal geometry promotes obstruction, which is a common disease with strong implications on the quality of life. Yet, nasal obstruction is difficult to diagnose, mainly because the airflow cannot be measured accurately. To improve diagnostics, we propose to reconstructed the nasal geometry from CT scans and then simulated the airflow in the computer, e.g., using the Lattice-Boltzmann method [2]. We develop an automated method that combines these steps to arrive at flow data robustly [3]; see Figure 6.43. The resulting measured resistance of the nasal cavity provides an objective measure for nasal obstruction and we can identify regions significant to obstruction by considering the local viscous dissipation. Our approach could help clinicians to diagnose nasal obstruction and help to reduce the surgical failure rate.

[1] D. Zwicker, R. Ostilla-Mónico, D. E. Lieberman, M. P. Brenner, Proc. Natl. Acad. Sci. USA **115** 2936–2941 (2018)
[2] M. Bernaschi, S. Melchionna, S. Succi, M. Fyta, E. Kaxiras, J. K. Sircar Comput. Phys. Commun. **180** 1495–1502 (2009)
[3] D. Zwicker, K. Yang, S. Melchionna, M. P. Brenner, B. Liu, R. W. Lindsay, Biomed. Phys. Eng. Express **4** 045022 (2018)

6.19 MODELING HELPS FAILING HEART TO REGENERATE

Y. Wang, M. Kalhöfer-Köchling, R. Majumder, E. Bodenschatz, J. Frahm (MPIBPC), **A. Pumir** (ENS Lyon)
M. Uecker (UMG), W. Zimmermann (UMG)

Heart failure is a common, costly, and potentially fatal condition in which the heart cannot pump enough blood to meet the body's needs. In 2015 it affected about 40 million people globally [1]. It is mainly caused by myocardial infarction, and associated with changes both in structure and function of the heart. Current options for patients with end-stage heart failure include mechanical support devices and heart transplants. Alternatively, regenerative medicine may offer new avenues to remuscularize the failing heart. Tissue engineered heart repair is developing rapidly towards first-in-patient studies with the primary objective to add engineered heart muscle (EHM, Figure 6.44) to the failing heart and increase the cardiac pumping performance consequently [2, 3].

Figure 6.44: Sketch representation of the EHM implantation. The heart and the EHM are marked in black and red respectively. From Ref. [3].

Medical image (Figure 6.45) based computational modeling can be used to improve our understanding of heart mechanics and predict outcome of proposed therapeutic strategies. One of the promising applications of computational modeling is to guide personalized EHM implantation and help a failing heart to regenerate. In collaboration with the University Medical Center Göttingen and the MPI for Biophysical Chemistry, we are developing a numerical model for patient-specific heart (Figure 6.46). Employing nonlinear mechanics we analyse how different types of infarcts impair the contractile function of the left ventricle. In silico EHMs are introduced and the pump function is evaluated. Preliminary results show that EHM can improve the pump function of the left ventricle.

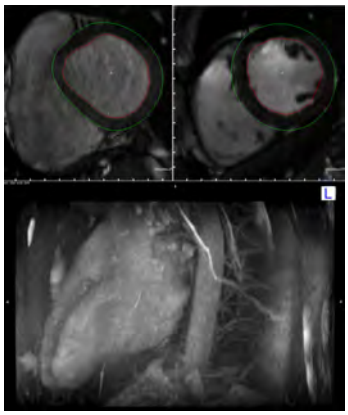

Figure 6.45: MRI image used to reconstruct the patient-specific geometry of the left ventricle. The endocardial and epicardial boundaries are marked in red and green respectively.

Since the patient-specific tissue properties and hence model parameters play a crucial role on heart function, we also investigate the passive mechanical properties of heart muscle both experimentally and numerically. Heart tissue is cut into small samples, which are sheared under different strains within a rheometer. Stress-strain curves with shearing in different directions, i.e. the fiber, sheet and normal directions, are recorded and used to measure the typical tissue properties. We also determine numerically by inverse methods the mechanical properties of heart muscle from in vivo data. Results from both approaches will be validated against each other. The numerical algorithm will be refined so that we can recover from clinical measurements for patient-specific mechanical properties. The ultimate goal of this project is to find the optimal solution of the EHM configurations, such as shape, thickness and fiber orientation, and provide the EHM construction process with a personalized EHM patch design and its placement.

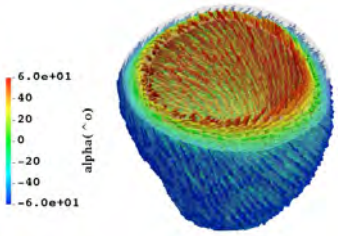

Figure 6.46: A left ventricle reconstructed from MRI images and its fiber considered in modeling.

[1] T. Vos et al., The Lancet, **388**(10053), 1545–1602 (2016).
[2] W.H. Zimmermann et al., Nature Medicine, **12**, 452-458 (2006).
[3] Y. Lei et al., Circulation Research, **113**, 922-932 (2013).

6.20 QUANTIFYING CARDIAC COMPLEXITY

A. Schlemmer, A. Witt, U. Parlitz, S. Luther

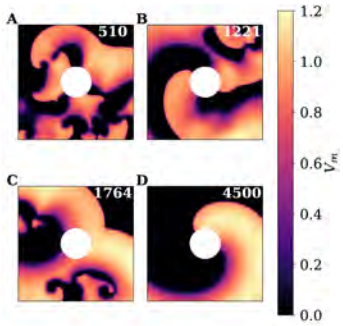

Figure 6.47: A 2D Fenton-Karma simulation of cardiac tissue exhibiting different states of spatio-temporal complexity [2].

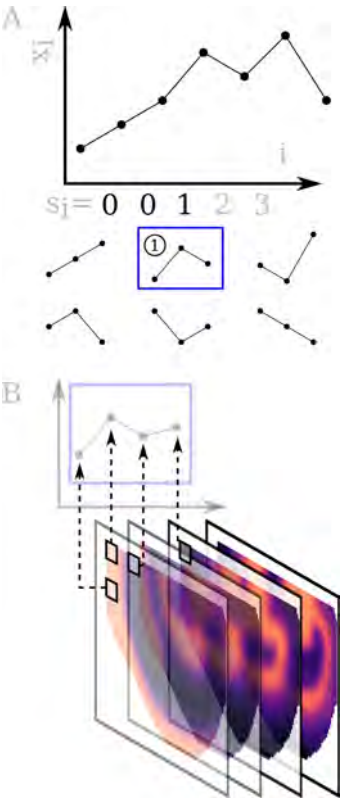

Figure 6.48: Ordinal patterns π_k within (A) a time series and (B) a video.

During lethal cardiac arrhythmias like ventricular fibrillation (VF) the dynamics on the heart is governed by complex electrical excitation waves. Understanding the structure, formation and temporal development of these waves is crucial to the development of novel therapies and diagnosis methods. During VF the complexity of the dynamics changes, which is related to the presence of a varying number of rotors and complexity fluctuations [1]. As the number of rotors may play a role in the optimization of defibrillation techniques, the development of efficient and robust mathematical methods for their quantification is desirable. In [2] we presented an application of Spatio-Temporal Permutation Entropy (STPE) to simulated dynamics of excitable media (Fig. 6.47). Usually, the number of rotors (also called spiral waves) in excitable media is estimated by the number of phase singularities. This approach, however, may become inefficient and unreliable under noisy experimental conditions. An alternative measure for quantifying complexity is Permutation Entropy $\mathrm{PE} = -\sum_k p_k \log p_k$ based on the probability p_k of ordinal patterns π_k within a time series (Fig. 6.48A). Using STPE, a spatio-temporal adaption of PE (see Fig. 6.48B) the complexity of spatio-temporal dynamics can be efficiently quantified [2]. In particular, STPE can be tuned to different spatial scales of interest as illustrated with the STPE spectrogram shown in Fig. 6.49 where scanning the spatial separation L_x is used to address different spatial scales.

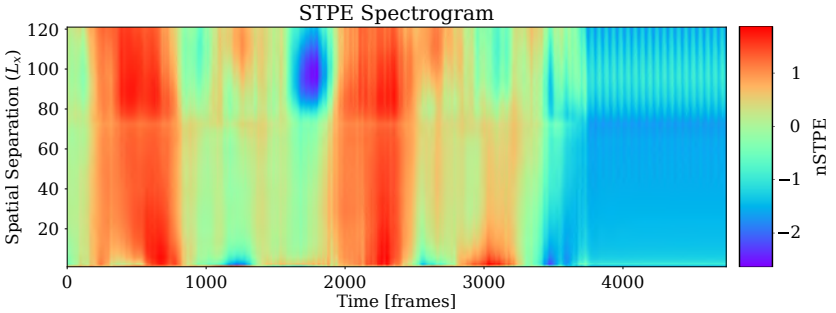

Figure 6.49: The STPE spectrogram can be used to visualize temporal changes of complexity in spatio-temporal time series at different spatial scales [2].

Time series analysis methods developed for the characterization of the temporal occurrence of extreme events have been applied to timings of Premature Ventricular Contractions (PVCs) in post-myocardial infarction (MI) patients [3]. As our main result we found that postinfarct patients older than 65 years have much more randomly timed PVCs compared to younger patients where these arrhythmic beats typically appear in clusters.

[1] A. Schlemmer, T. Baig, S. Luther and U. Parlitz, Physiol. Meas. **38**, 1561 (2017)
[2] A. Schlemmer, S. Berg, T. Lilienkamp, S. Luther, U. Parlitz, Front. Phys. **6**, 39 (2018)
[3] A. Witt, F. Ehlers and S. Luther, Chaos **27**, 093942 (2017)

6.21 FORMATION OF PERIODIC WAVE SEGMENTS IN AN EXCITABLE MEDIUM

V.S. Zykov, E. Bodenschatz

In the simplest case, a wave triggered in a two-dimensional excitable medium has a front and a back, which have no common points. If this wave is broken everywhere except a central part, a wave segment is created. Its boundary contains two phase change points, where the front coincides with the back. The segment will evolve into two counter-rotating spiral waves at a sufficiently high medium's excitability or shrink laterally and disappear in a low excitable medium [1]. At a separatrix between these two scenarios, a wave segment can be stabilized, which conserves a specific shape and moves at a constant velocity [2]. It is of great importance to identify the location of this separatrix because it determines the region within medium's parameter space, where dangerous self-sustained spiral waves can be nucleated.

For the case of a solitary propagating wave segment, this problem has been solved by using a free-boundary approach [3,4]. Namely, it was shown that the shape and the velocity of a solitary wave segment are uniquely determined by a dimensionless parameter B, specifying the medium's excitability.

Here, we consider the dynamics of a periodic sequence of the stabilized wave segments (Fig. 6.50a). The mutual interaction of the wave segments within this sequence due to the medium's refractoriness makes the problem much more difficult. The parameter B is obviously not sufficient to describe the wave sequence dynamics.

A modified free-boundary approach allows us to analyze the dynamics of a periodic sequence of the stabilized wave segments and to determine the wave segment shape and the speed as functions of the medium's parameters. First of all it was shown that a periodic segment sequence can be stabilized only in a restricted region within the parameter space. At the boundary of this region the thickness h of the wave segments measured at the symmetry axis remains constant. This motivated us to introduce a dimensionless parameter

$$H = \frac{c_0}{D} h \equiv \frac{c_0}{D} d_p(\lambda) c_t(\lambda), \tag{6.1}$$

where the translation velocity c_t and the pulse duration d_p depend on the spatial period λ. Moreover, we show that the discovered parameter H predetermines the propagation velocity and the shape of the wave segments with a high accuracy (Fig. 6.50b, c) [5].

Obviously, the elaborated approach will be helpful in a future investigation of a high-frequency spiral wave dynamics.

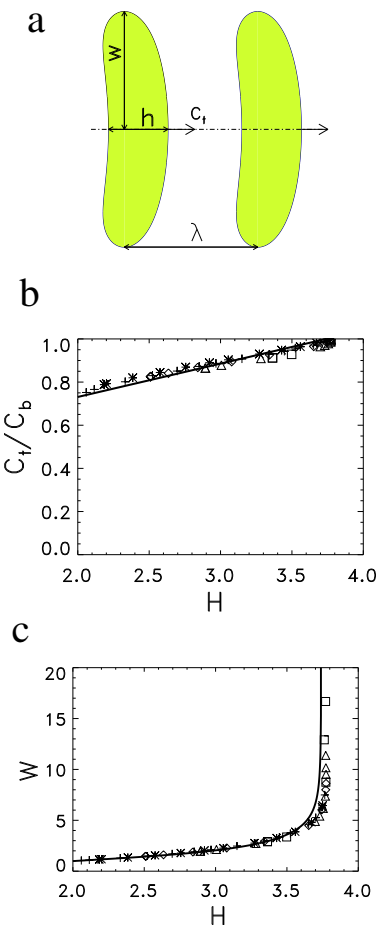

Figure 6.50: Characteristics of periodic wave segments. (a) Wave segment parameters. (b) Translational segment velocity c_t vs the parameter H. At the existence domain boundary $c_t = c_b$ and $H = H_b = 3.74$. (c) Wave segment width W vs the parameter H. The results of the free-boundary approach simulations are shown by separate symbols. Solid lines represent the corresponding analytical approximations.

[1] A.S. Mikhailov, V.N. Davydov, V.S. Zykov Physica D **7**0, 1 (1994).
[2] T. Sakurai, E. Mihaliuk, F. Chirila, and K. Showalter, Science **2**96, 2009 (2002).
[3] A. Kothe, V.S. Zykov, H. Engel, Phys. Rev. Lett. **1**03, 154102 (2009).
[4] V.S. Zykov, E. Bodenschatz, New J. Phys. **1**6, 043030 (2014).
[5] V.S. Zykov, E. Bodenschatz, Phys. Rev. E **9**7, 030201(**R**) (2018).

6.22 TRANSIENT SPATIO-TEMPORAL CHAOS IN EXCITABLE MEDIA

T. Lilienkamp, J. Christoph, S. Herzog, U. Parlitz, S. Luther

During life-threatening ventricular fibrillation we observe complex and chaotic excitation wave propagation inside the heart. This dynamics is governed by spiral/scroll waves, which can be studied in numerical simulations of the propagation of electrical excitation waves in cardiac tissue. In both, the numerical simulations of chaotic spiral waves, as well as in experimental studies of rabbit or pig hearts we observe, that the complex dynamics is often not persistent, but returns to the "resting state" without any active intervention. An exemplary episode of self-terminating spiral wave dynamics is depicted in Fig. 6.51.

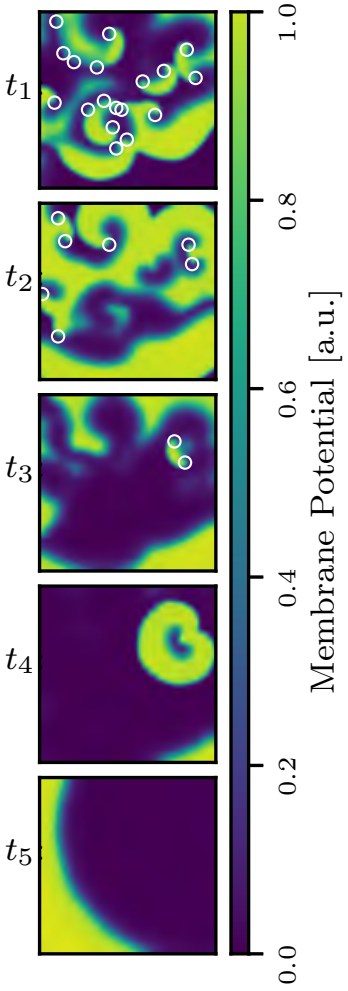

Figure 6.51: A transient episode of spatio-temporal chaotic spiral wave dynamics (Fenton-Karma model). The membrane potential is shown for different instances of time. The number of spiral waves (centers denoted by white circle) fluctuates during the episode (t_1, t_2, t_3), until all spiral waves annihilate (t_4), the remaining waves collide with the boundary (t_5) and the system returns to the resting state.

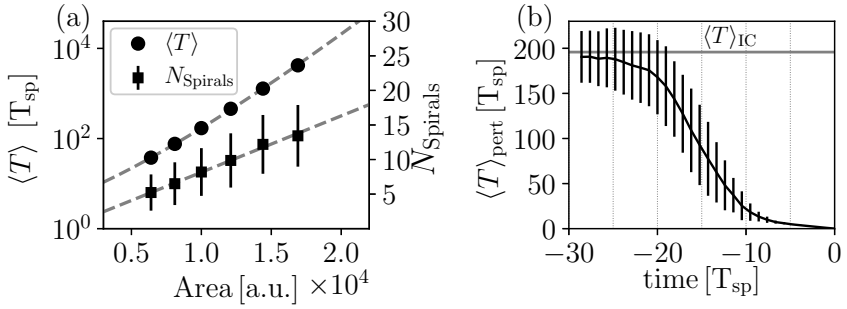

Figure 6.52: (a) The average lifetime $\langle T \rangle$ of chaotic transients is increasing exponentially, whereas the average number of spiral waves grows linearly with the domain size. (b) The quantity $\langle T \rangle_{\mathrm{pert}}$, which evaluates the state space structure, varies already a long time before the actual self-termination of typical trajectories (time = 0).

In numerical studies we found, that the average lifetime of these transients depends sensitively on the size of the domain, respectively the average number of spiral waves fitting on the domain (Fig. 6.52(a)) [1, 2]. This behavior is in agreement with clinical observations, where patients with a cardiac hypertrophy (which is accompanied by an increase of the heart muscle's volume), for instance, have a higher risk of cardiac arrhythmia.

Furthermore, we show that the structure of the state space (quantified by $\langle T \rangle_{\mathrm{pert}}$ [3, 4] in Fig. 6.52(b)) is significantly different during the final episode of self-terminating trajectories (thus nearby the "exits" of the chaotic regime), although the upcoming termination is not visible in "conventional variables". This behavior could be observed not only in high-dimensional spatially extended systems, but also in simple low-dimensional maps [3, 4]. Based on this phenomenon, we aim at predicting a possible upcoming self-termination of the dynamics, which might be relevant for future clinical applications regarding the control of cardiac arrhythmias.

[1] T. Lilienkamp, J. Christoph, U. Parlitz, *Phys. Rev. Lett.* **119**, 054101 (2017)
[2] M. Aron, S. Herzog, U. Parlitz, S. Luther, T. Lilienkamp, (under review)
[3] T. Lilienkamp and U. Parlitz, *Phys. Rev. Lett.* **120**, 094101 (2018)
[4] T. Lilienkamp and U. Parlitz, *Phys. Rev. E* **98**, 022215 (2018)

6.23 EXCITATION-CONTRACTION COUPLING

F. Spreckelsen, F. Cosi, U. Parlitz, S. Luther
F. Rehfeldt (University of Göttingen), M. Falcke (Max Delbrück Center for Molecular Medicine, Berlin), W.-H. Zimmermann (UMG, Göttingen)

Microscopically, cardiac tissue and engineered heart muscle consist of a network of coupled active and passive cells (cardiomyocytes and fibroblasts) embedded in an extracellular matrix (ECM). Beating cardiomyocytes are self-sustained oscillators interacting via viscoelastic forces [1] mediated by the ECM, whose mechanical properties are modulated by fibroblasts (Fig. 6.54). To investigate the dynamics of visco-elastically coupled excitable oscillators we implemented a pair (Fig. 6.53) and a chain (Fig. 6.55) of Mitchell-Schaeffer cell models extended by excitation-contraction coupling (ECC) and mechano-electric feedback terms. An important mechanism underlying ECC is intracellular Ca^{2+} release, which is modeled by means of stochastic PDEs (Fig. 6.56).

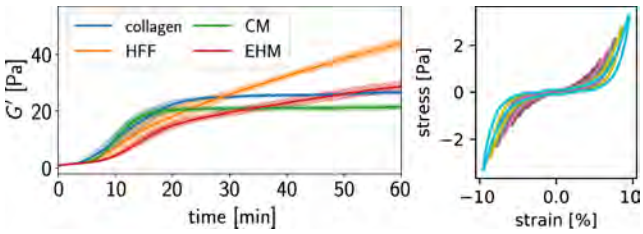

Figure 6.54: The presence of fibroblasts (HFF) or cardiomyocytes with fibroblasts (EHM) changes the time evolution of the storage modulus of the ECM [2]. In all compositions, the ECM expresses strain stiffening at $\gamma \geq 3\%$ (only collagen shown).

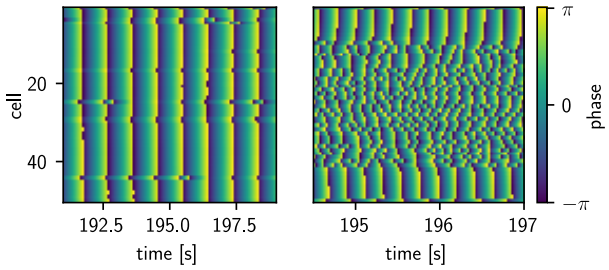

Figure 6.55: Left: A chain of 50 coupled cells exhibits almost complete synchronization at low fluidity. Right: For purely elastic coupling an anti-phasic chimera state occurs: Two groups of cells at the ends of the chain remain phase-locked with a difference π while the cells in between oscillate incoherently.

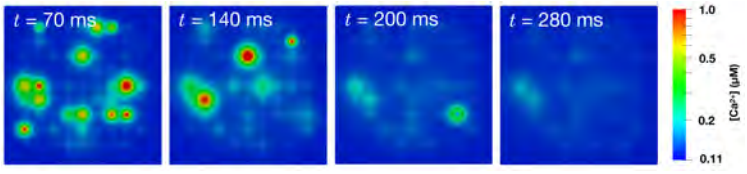

Figure 6.56: Spatial-temporal evolution of calcium concentration (color-coded) during a calcium spark in a cross-section of a cardiomyocyte. During the time course of an action potential calcium is extruded from a grid of calcium release units.

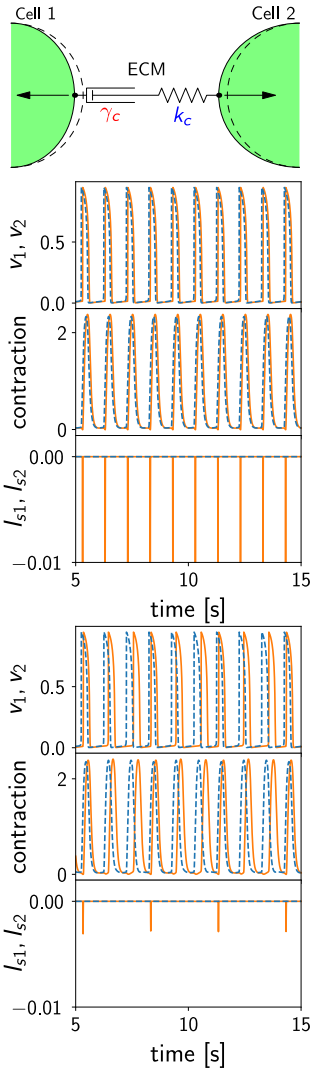

Figure 6.53: Two cells are coupled mechanically by a Maxwell element representing the extracellular matrix (ECM). For low fluidity the cells are fully synchronized, larger fluidity shows n:n synchronization (here: $n = 3$).

[1] S. Stein, S. Luther and U. Parlitz, New J. Phys. **19**, 079601 (2017)
[2] S. Schlick, F. Spreckelsen et al., Prog. Biophys. Mol. Biol. (in press)

6.24 REENTRY IN EXCITABLE MEDIA INDUCED BY FAST PROPAGATION REGIONS OF DIFFERENT SHAPES

V.S. Zykov, A. Krekhov, E. Bodenschatz

Destabilization of wave fronts propagating through an excitable medium and the subsequent initiation of reentrant excitation are known to cause cardiac arrhythmias and even sudden death [1]. The effects of the medium's heterogeneity are thought to be one of the major causes of the reentry initiation and have attracted much attention [2].

One novel scenario, which was found recently in a generic model for the excitable system, is that reentries could be nucleated in the presence of a localized fast propagation region (FPR) after application of one stimulus only [3]. It was clearly demonstrated that various geometrical factors play an important role in this scenario of rotor initiation [4,5].

We present quantitative conditions for the propagation block and demonstrate many opportunities to use FPR of quite different shapes to initiate spiral waves based on the modified Barkley model

$$\partial_t u = \nabla \cdot (D\nabla u) - Au(1-u)(u-v-b), \qquad \partial_t v = \epsilon(u-v), \quad (6.2)$$

were D, A, b and $\epsilon \ll 1$ are control parameters.

For instance, it was shown that in the two-dimensional medium the flat boundary of a rectangularly shaped FPR may block the propagation of an incoming excitation wave (Fig. 6.57a). It happens if the product DA within the FPR essentially exceeds its value outside. However, a large local curvature at the rounded corner of the FPR would prevent the blockage and thus let the outside excitation penetrate into the FPR causing the initiation of a phase change point (PCP) (white dot in Fig. 6.57b) and then a reentry generation (Fig. 6.57c). If the FPR size is below a critical one, the initiated PCP would vanish when it approaches the medium's boundary and no reentry will be generated [5].

We investigate in detail the critical length L of the FPR and the radius of the rounded corner R needed to initiate a reentry and determine the boundaries of the non-penetration and non-blockage regions for various D and A inside the FPR (Fig. 6.57d). The two boundaries of the reentry initiation region could be estimated by the analytical equation for the bistable distributed system and the simulations for a circular FPR, respectively [4,5].

Our findings indicating crucial geometrical factors of the FPR obtained for the generic model might be applicable to describe the dynamics of excitation in heterogeneous cardiac tissue.

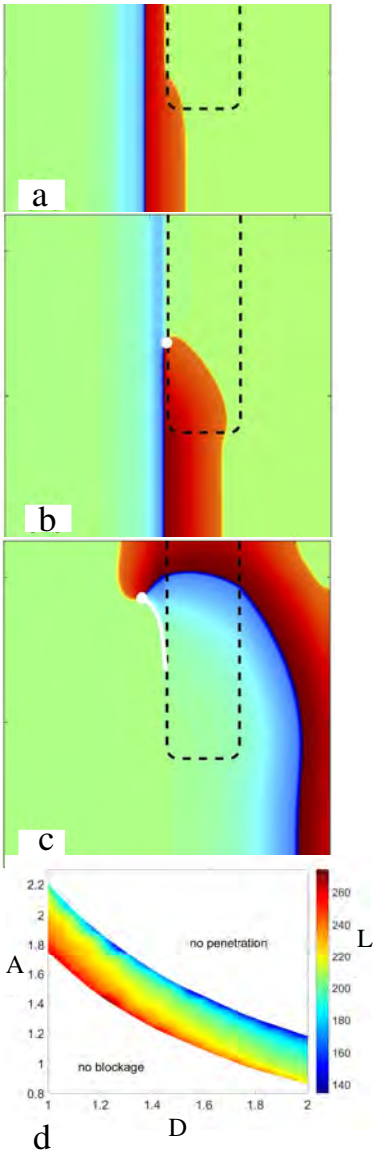

Figure 6.57: Dynamics and conditions of reentry initiation in an excitable medium containing a rectangularly shaped fast propagation region, where the parameter A is fixed to $A = 2$, while $A = 1$ everywhere else. Rounded corner radius R=15.

[1] E. Carmelite and J. Vereecke, Cardiac Cellular Electrophysiology, Springer 2002).
[2] V. Zykov and E. Bodenschatz, Annu. Rev. Condens. Matter Phys. **9**, 435 (2018).
[3] V. Zykov and A. Krekhov and E. Bodenschatz, PNAS, **114**, 1281 (2017).
[4] V. Zykov and A. Krekhov and E. Bodenschatz, Chaos, **27**, 093923 (2017).
[5] X. Gao, A. Krekhov, V. Zykov and E. Bodenschatz, Frontiers in Physics, **6**, 8 (2018).

6.25 ELECTRO-MECHANICAL IMAGING

J. Christoph, J. Schröder-Schetelig, V. Kappadan, U. Parlitz, S. Luther
A. Karma (Northeastern U., Boston), G. Hasenfuss (UMG, Goettingen)

What is the nature of cardiac fibrillation? While it has been hypothesized that fibrillation is driven by vortex-like rotating scroll waves, the experimental characterization of three-dimensional waves inside the heart muscle remains a major scientific challenge. Our research aims to address this fundamental question by developing advanced electro-mechanical imaging methodologies. Recently, we have introduced a tri-modal, panoramic fluorescence imaging system (Fig. 6.58) for the simultaneous measurement of membrane potential, intracellular calcium, and mechanical deformation (strain). The simultaneous measurement of electrical and mechanical waves is a demanding experimental task, which requires reliable imaging registration and motion tracking in order to disentangle the corresponding fluorescence signals [1, 2]. Using this imaging system, we observed the co-localization of phase singularities associated with rotating membrane potential, calcium, and deformation waves on the epicardial surface of intact, Langendorff-perfused rabbit and pig hearts during ventricular arrhythmias [3]. We confirmed the optically measured mechanical rotors on the surface using high-resolution ultrasound. Using 4D ultrasound, we were able to track the filaments of mechanical rotors deep inside the ventricular wall during ventricular tachycardia and fibrillation [3, 4] (Fig. 6.59). In collaboration with A. Karma, we are developing models of cardiac electro-mechanics to further investigate the dynamics and interaction of electrical and mechanical rotors. In a first patient study in collaboration with G. Hasenfuss, we will translate the ultrasound-based imaging approach to clinical application. We expect that our findings will significantly enhance the understanding of cardiac fibrillation, and will lead to novel diagnostic and therapeutic approaches.

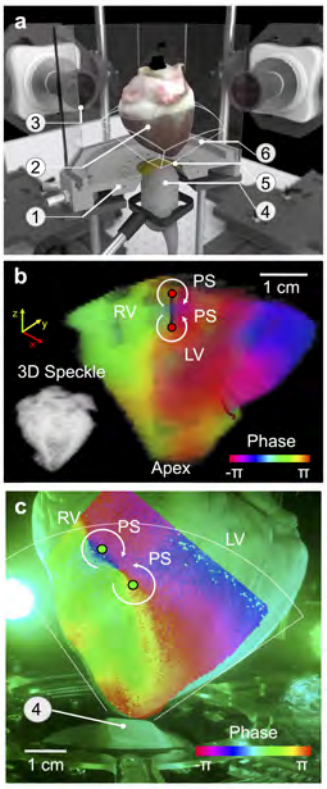

Figure 6.58: Imaging of electro-mechanical rotors. (a) Experimental setup for simultaneous 4D ultrasound and fluorescence imaging of isolated, intact pig hearts. 1 – tissue bath, 2 – Langendorff-perfused pig heart, 3 – fluorescence camera, 4 – ultrasound transducer, 5 – acoustic window, 6 – field of view (b) Three-dimensional U-shaped filament of a mechanical scroll wave inside the ventricular wall. Phase singularities on surface are indicated by red circles. (c) Corresponding electrical phase singularities (green circles) on surface obtained from fluorescence imaging using potentiometric optical dye [3].

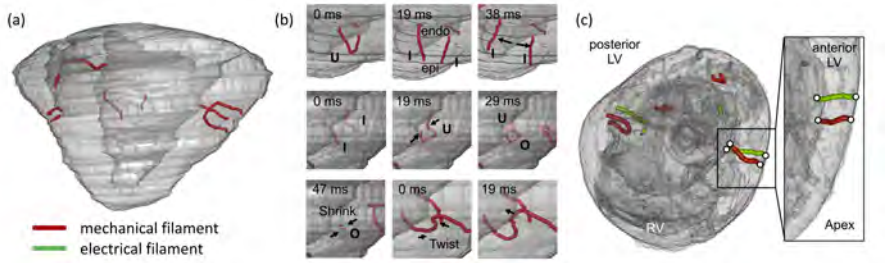

Figure 6.59: Electromechanical rotors during cardiac fibrillation. (a) Mechanical filaments (red) observed in an isolated intact pig heart (ventricles shown in gray) during ventricular fibrillation. (b) Dynamics of U-, I-, and O-shaped mechanical filaments in pig ventricle. (c) Numerical simulation showing co-localization of electrical (green) and mechanical (red) filaments.

[1] J. Christoph et al., *Prog. Biophys. Mol. Biol.* **130**, 150–169 (2017)
[2] J. Christoph, S. Luther, *Front. Physiol.* **9**, 1483 (2018)
[3] J. Christoph et al., *Nature* **555**, 667-672 (2018)
[4] J. Christoph, S. Luther, Patent Application PCT/EP/2015/077001 (2015)

6.26 LOW-ENERGY CONTROL OF ELECTRICAL TURBULENCE IN THE HEART

C. Richter, H. tom Wörden, S. Berg, E. Boccia, U. Parlitz, S. Luther

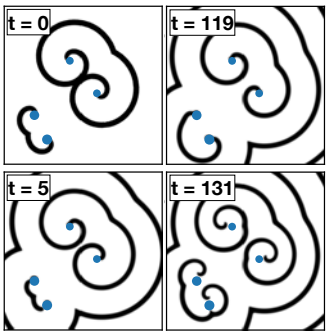

Figure 6.60: Successful simultaneous unpinning of four pinned spirals using the synchronization approach [7] ($t = 0$ initial state, $t = 5$ state after the first synchronization pulse, $t - 119$ immediately after the last synchronization pulse, $t = 131$ about one spiral period after the unpinning pulse).

During cardiac fibrillation, coherent mechanical contraction of the heart is disrupted by unstable vortex-like rotating waves that interact with each other and the complex anisotropic and heterogeneous anatomical substrate. For a lack of a better strategy, high-energy electric shocks are applied to terminate cardiac fibrillation, which may have severe side effects, including traumatic pain and tissue damage indicating a significant medical need.

Both molecular and dynamical mechanisms contribute to electro-mechanical instabilities that induce and sustain electrical turbulence in the heart [1, 2]. In order to control cardiac arrhythmias such as ventricular and atrial fibrillation, we have developed Low-Energy Anti-Fibrillation Pacing (LEAP) [1]. Currently, we are optimizing the pacing protocol and the electrode configuration in large animal disease models of cardiac infarction and heart failure. We have shown that the electrode placement has a significant impact on the energy reduction in vivo (Fig. 6.61). Our recently developed high-resolution electro-mechanical mapping system [3] will be employed to visualize three-dimensional scroll waves and their the interaction with heterogeneities before, during, and after applying LEAP. In two-dimensional models of excitable media, we have studied the role of heterogeneities on the emergent spatio-temporal dynamics [4], the interaction of rotating waves with heterogeneities due to myocardial infarction [5, 6], and the unpinning of multiple spirals using weak electric field pulses ([7], Fig. 6.60).

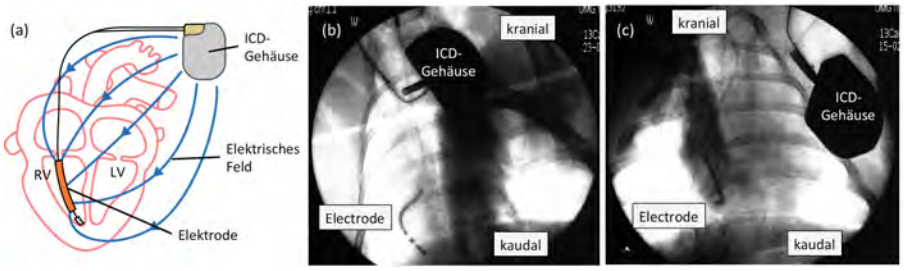

Figure 6.61: (a) Schematic of an implantable cardioverter/defibrillator (ICD). RV – right ventricle, LV – left ventricle. (b) Electrode placement I: Catheter electrode in RV, ICD housing cranial in vivo experiment (pig). (c) Electrode placement II: Catheter electrode in RV and ICD housing ventral in vivo experiment (pig).

[1] S. Luther, F.H. Fenton et al., *Nature* **475**, 235-239 (2011)
[2] B. Mohammed et al., *Science Trans. Med.* **10**, eaan0724 (2018)
[3] J. Christoph et al., *Nature* **555**, 667-672 (2018).
[4] P. Bittihn, S. Berg, U. Parlitz and S. Luther, *Chaos* **27**, 093931 (2017)
[5] E. Boccia, U. Parlitz and S. Luther, *Commun. Nonlinear Sci. Numer. Simulat.* **48**, 115-122 (2017)
[6] E. Boccia, S. Luther and U. Parlitz, *Phil. Trans. R. Soc. A* **375**, 20160289 (2017)
[7] H. tom Wörden, U. Parlitz and S. Luther, *Phys. Rev. E* (under review)

6.27 OPTOGENETIC ARRHYTHMIA CONTROL

C. Richter, R.A. Quinonez, S. Hussaini, L. Diaz-Maue, S. Luther
P. Ruther (IMTEK, Freiburg), R. Hinkel (DPZ, Göttingen)

The control of spatio-temporal dynamics in excitable media is a challenging task. In cardiac tissue, rotating excitation waves are associated with cardiac arrhythmias, such as ventricular fibrillation or tachycardia. Cardiac optogenetics is a technique that allows to control cardiac cells with light, i.e. through the activation of light-sensitive ion channels resulting in the depolarization of the membrane potential. We use optogenetic tools and optical technology to control excitation waves in cardiac tissue [1, 2, 3]. Figure 6.62 shows successful termination of ventricular tachycardia in a transgenic murine heart *ex vivo* by epicardial illumination [4]. Experiments are complemented by numerical simulations of the murine electrophysiology based on the Bondarenko model [5], with the light-activated Channelrhodopdsin-2 function being modeled following [6]. Using epicardial μLED arrays embedded in stretchable polymers developed by P. Ruther (Department of Microsystems Engineering, IMTEK, Freiburg), we have demonstrated successful photostimulation (Figure 6.63). We will continue to employ cardiac optogenetic tools to further explore the mechanisms underlying arrhythmia control using multi-site pacing strategies, such as LEAP [7].

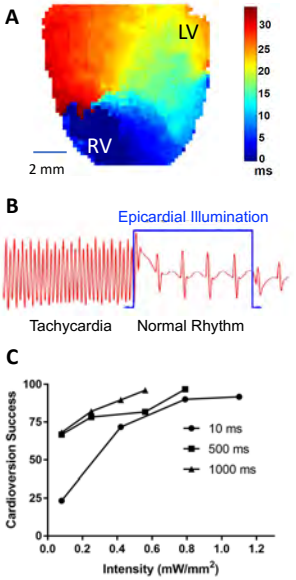

Figure 6.62: Optogenetic arrhythmia termination in an intact, Langendorff-perfused transgenic murine heart. **A** Activation maps of ventricular tachycardia (color indicates activation time in ms). **B** Volumentric ECG signal showing arrhythmia termination by a light pulse (duration 1s, indicated by blue line) of global epicardial illumination. **C** Dose-response curve for optogenetic arrhythmia termination. Data show mean values, N=6 hearts [4].

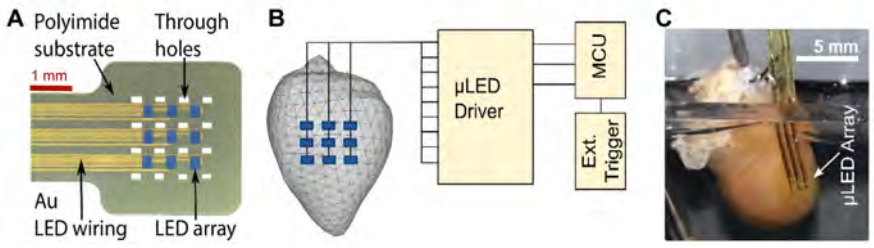

Figure 6.63: **A** Micrograph and driver block diagram of a two-dimensional μLED array on a flexible polyamide substrate. Rectangular through-holes for optional electrodes (not shown). **B** Schematic of the μLED control unit (MCU) including μLED driver and external trigger input. **C** Transgenic Langendorff-perfused murine heart with epicardial μLED array for photostimulation [8].

[1] L. Diaz-Maue, S. Luther and C. Richter, Proc. SPIE 10482G, doi: 10.1117/12.2288976 (2018)
[2] C. Richter, J. Christoph, S.E. Lehnart and S. Luther, in *Optogenetics - Methods and Protocols*, Methods in Molecular Biology **1408**, 293-302 (2016)
[3] T. Zaglia et al., PNAS **112**, E4495-4504 (2015)
[4] R.A. Quinonez Uribe, S. Luther, L. Diaz-Maue and C. Richter, *Front. Physiol.* **9**, 1651 EP (2018)
[5] V.E. Bondarenko et al., *Am J Physiol Heart Circ Physiol* **287**, H1378-H1403 (2004)
[6] J.C. Williams and E. Entcheva, *Biophysical Journal* **108**, 1934-1945 (2015)
[7] S. Luther, F.H. Fenton et al., *Nature* **475**, 235-239 (2011)
[8] L. Diaz-Maue, M. Schwaerzle, P. Ruther, S. Luther and C. Richter, *Conf. Proc.* IEEE *Eng. Med. Biol. Soc.* (2018)

6.28 LINKING THE FUNCTION OF CORTICAL NETWORKS TO TEMPORAL DYNAMICS

J. Dehning, V. Priesemann
N. M. Dotson (UC Berkeley),
S. J. Hoffman, C. M. Gray (Montana State University)

It is widely accepted that neural information processing is organized in a hierarchical manner. However, the organization principles still remain debated. First evidence for a functional hierarchy were recently identified in a compiled data set from different macaque monkeys, which showed a systematic increase of intrinsic timescales[2] across seven areas [1]. We investigated a unique dataset [3] that encompasses up to 39 areas recorded simultaneously in a macaque monkey (Fig. 6.64 A). We identified a clear hierarchy of intrinsic timescales, which is in agreement with the visual processing hierarchy: Visual cortex exhibits the shortest timescales, prefrontal and posterial parietal intermediate ones and motor and somatosensory cortex the highest (Fig. 6.64 B).

2. **Intrinsic timescales**: The autocorrelation of spiking activity of neural networks decays exponentially in a first approximation [2]. The intrinsic timescale is defined as the time constant of this decay (see Sec. 8.3).

More importantly, we found a dependence of the intrinsic timescales on the type of task performed: timescales are higher during visual memory tasks than during fixation periods. Furthermore, neurons inside the visual field tend to increase their timescale when confronted with a task, whereas the ones that are outside decrease theirs. One can link the intrinsic timescale to other computational properties like the sensitivity, dynamic range and transmission of the network [4]. In this scope, we interpreted the increase of timescale of the circuits in the visual field as a *tuning-in to task requirement*, increasing their sensitivity, whereas the others tune-out, decreasing sensitivity. Thereby we did not only expand on earlier insights about a hierarchy of information processing, but also showed that neural circuits may adapt their intrinsic timescale depending on task requirements.

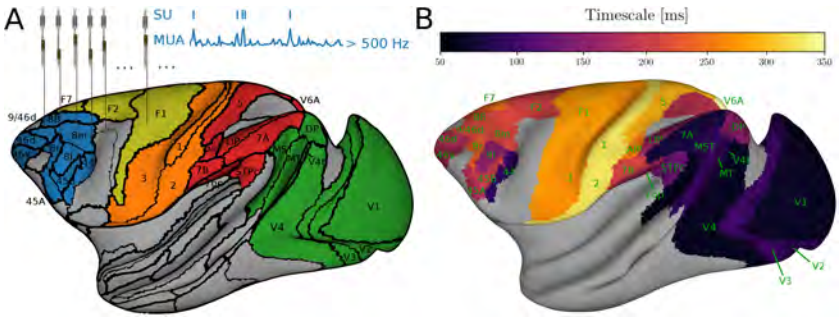

Figure 6.64: **A.** Large-scale single unit (SU) and local field potential recordings (up to 107 channels in parallel) were obtained with individually movable electrodes. **B.** A surface plot of the intrinsic timescales showing a clear increase from occipital to frontal to parietal areas [5].

[1] J. D. Murray et al., Nature Neuroscience **17**, 1661–1663 (2014)
[2] J. Wilting, V. Priesemann, Nat. Commun. **9**, 2325 (2018)
[3] N. M. Dotson et al., Neuron **96**, 769-782 (2017)
[4] J. Wilting et al., Front Syst Neurosci. **12**, 55 (2018)
[5] J. Dehning, N. M. Dotson et al., *in preparation*

6.29 RECAPITULATING 100.000+ YEARS OF BRAIN EVOLUTION IN A TABLETOP EXPERIMENT

M. Schottdorf, J. Franz, J. Vogel, A. Neef, F. Wolf
W. Stühmer (MPIEM)

The trajectory of brain evolution is composed of long periods of continuous refinement interrupted by key innovations in neural circuit design. Examples of key innovations are the transformation of the brain's episodic memory center at the origin of mammals or the radical change of the architecture of the visual cortex near the origin of primates. Although quick on geological timescales, these qualitative transitions are believed to require thousands of generations to unfold. For instance, the evolution of the first primate brain from its non-primate ancestors during the Paleocene-Eocene transition presumably progressed over a period on the order of 100.000 years and led to the emergence of cortical networks composed of densely interconnected functional domains.

Comparative studies can reconstruct likely scenarios for these fundamental transitions but the identification of the evolutionary benefits that might have driven them appeared beyond the scope of experimentally controlled scientific studies. To start addressing such questions, we established a synthetic biology approach that links computational models of neural circuits to living neural networks using neural interface technology.

In a first study we employed this approach to assess a prominent scenario for the emergence of the primate visual systems from a rodent-like ancestral condition. The central feature of this transition is the emergence of macroscopic neuronal modules called orientation domains. We use our synthetic biology approach to explore the consequences of shrinking and enlarging orientation domains, which are absent or extremely miniaturized in the rodent visual cortex, and by analogy in the reconstructed stem-primate ancestors. We constructed a hybrid in silico - in vitro model of the retino-cortical pathway, in which the scale of orientation domains can be freely modified. In this system, we found that miniaturizing orientation domains below their natural scale range largely preserves the number of orientation-tuned neurons but reduced the level of orientation selectivity. Miniaturizing orientation domains below a critical size induced a switch from the classical Hubel-and-Wiesel mechanisms of orientation selectivity to an emergent selectivity generated within the in vitro cortical network and arranged in a sparse salt-and-pepper layout. In the presence of orientation domains, optimal orientation selectivity requires matching domain size to the scale of lateral interactions among cortical neurons. These findings offer an explanation for the invariance of orientation domain size across primates and demonstrate that a synthetic biology approach can elucidate aspects of brain evolution previously considered fundamentally inaccessible.

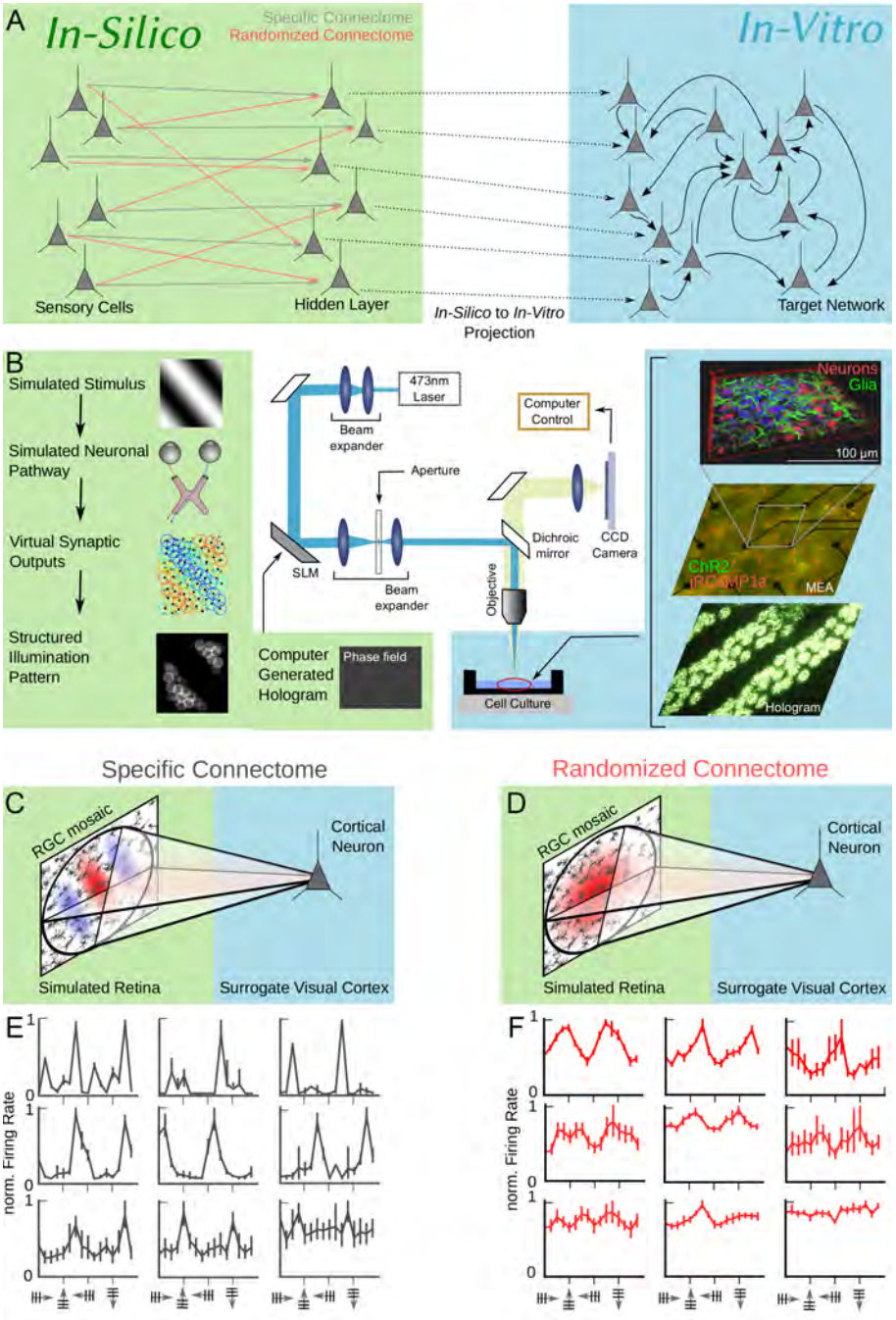

Figure 6.65: A synthetic biology approach recapitulates brain evolution A) Schematic structure of a neuronal sensory system and how to re-engineer it with a hybrid of biological and artificial elements. B) Simulating the activity of sensory cells and the hidden layer, we calculate synaptic input currents into the target network. Using a holographic projection system, spatio-temporal light patterns are generated that induce these currents in neurons, expressing a light gated ion channel, *in vitro*. The living target network forms a surrogate cortex. C, D) *In vivo*, the specific connectome of afferent projections create complex, asymmetric receptive fields. Those can be maintained in the *in silico* pathway (C), or they can be randomized/homogenized to cancel all pathway contributions to orientation selectivity (D). E) Example tuning curves, recorded from cultured neurons. F) Tuning curves obtained with the randomized/homogenized connectome. Surprisingly, we find a substantial degree of orientation tuning that is an emergent property of the recurrent circuit.

[1] D. Keppeler, R.M. Merino ,D. Lopez de la Morena, B. Bali, A.T. Huet, A. Gehrt, C. Wrobel, S. Subramanian, T. Dombrowski, F. Wolf, V. Rankovic, A. Neef, T. Moser. EMBO J 37 e99649.(2018)

[2] R. Samhaber, M. Schottdorf, A. El Hady, K. Broeking, A. Daus, C. Thielemann, W. Stuehmer, F. Wolf. J Neurosci Methods 257:194–203. (2016)

[3] M. Schottdorf, W. Keil, D. Coppola, L.E. White, F. Wolf. PLoS Comput Biol 11:e1004602 (2015)

[4] A. El Hady, G. Afshar, K. Bröking, O.M. Schlüter, T. Geisel, W. Stühmer, F. Wolf. Front Neural Circuits 7:1–15. (2013)

[5] M. Kaschube, M. Schnabel, S. Loewel, D.M. Coppola, L.E. White, F. Wolf. Science 330:1113–1116. (2010)

6.30 UNDERSTANDING DIFFERENCES BETWEEN NEURAL DYNAMICS IN VITRO AND IN VIVO

J. Zierenberg, J. Wilting, M. Schottdorf, A. Neef, V. Priesemann

Comparing experimental spike recordings from cultured neural networks (*in vitro*) and from the living brain (*in vivo*) reveals striking differences in their neural activity: Networks *in vitro* develop strong bursts separated by periods of very little spiking activity, whereas *in vivo* cortical networks show continuous activity (Fig. 6.67, bottom). This difference is quite puzzling considering that both networks presumably share similar single-neuron dynamics and plasticity rules. As defining difference, we identified the strength of external input and investigated how this may lead to differences in neural activity.

We derived analytically and verified numerically that the difference in neural activity can be attributed to the difference in external input combined with a homeostatic regulation mechanism [1]. For neural networks, homeostatic plasticity is known to regulate the average neural activity on long timescales [2]. However, its functional benefits for neural computation have been debated. We built on a generic description of recurrent spiking networks that can reproduce statistics of cortical recordings, see Sec. 8.3, and incorporated homeostatic plasticity as a generic negative feedback that adapts the recurrent activation strength to mediate external activation and target activity (Fig. 6.67, top). Our hypothesis is supported by (i) a mean-field theory, (ii) numerical simulations of stochastic activity on structured networks (Fig. 6.66), and (iii) experimental recordings.

A. Neef and M. Schottdorf addressed the same question experimentally. Inspired by propagating waves that emerge during development, they exposed cultured neural networks to long-term input [4]. In line with the predictions, first results showed that long-term stimulation decorrelates neural activity and reduced the occurrence of bursts.

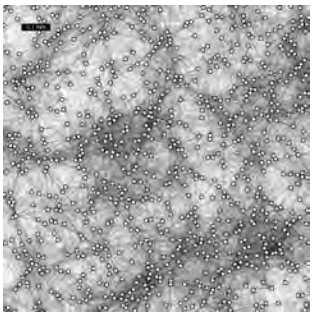

Figure 6.66: Illustration of a spatially-clustered topology (1.4×1.4 mm^2 cutout) generated by axonal-growth rules [3] to mimic realistic neural connectivity.

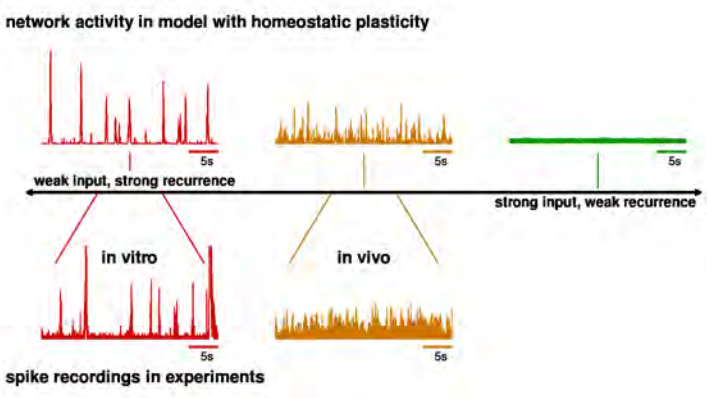

Figure 6.67: Difference between neural activity recorded *in vitro* and *in vivo* can be explained by the difference in external input combined with a homeostatic regulation mechanism. Top row shows activity in a numerical model, bottom row shows spike recordings in experiments. For a full theory see our recent results [1].

[1] J. Zierenberg, J. Wilting, V. Priesemann, Phys. Rev. X **8**, 031018 (2018)
[2] G. G. Turrigiano and S. B. Nelson, Nat. Rev. Neurosci. **5**, 97 (2004)
[3] J. G. Orlandi et al., Nat. Phys. **9**, 582 (2013)
[4] M. Schottdorf, A. Neef et al. *in preparation*

ACTIVE MATTER

7

The living cell and many of its components, life-forms large and small, and artificially energized mimics of motility are all examples of Active Matter, in which free energy is taken up and consumed at the level of each particle, generally leading to systematic movement. An understanding of the individual and collective behaviour of active particles is one of the grand challenges of nonequilibrium statistical physics, and holds the key to a physical grasp of the mechanics and statistics of living matter. It is now widely appreciated that mechanics, through the exertion, detection, modulation and transduction of forces, plays a crucial role in cellular processes, decisions and fate. Fluctuations, flow, instabilities, and ordering phase transitions are seen over an enormous range of length scales in the living world. The success of agent-based flocking models, theories of the swimming of individual microorganisms, fundamental experimental and theoretical advances in catalytic self-propulsion, hydrodynamic theories of self-driven fluids, and increasingly quantitative experiments on extracts, cells and organisms testify to the extraordinary ferment created by the rise of active-matter physics.[1]

Contents

[1] Adapted from: R. Golestanian & S. Ramaswamy, Eur. Phys. J. E **36**, 67 (2013)

7.1 SOLUBILISATION KINETICS OF ACTIVE EMULSIONS

C. C. Maaß, K. A. Baldwin, B. V. Hokmabad
A. Mathijssen (Stanford), M. Jalaal (Twente)

We study an experimental microswimmer model of self-propelling oil droplets gradually dissolving in a micellar surfactant solution. In these swimmers, the flow driving their propulsion is determined by micelles incorporating oil molecules diffusing into the bulk medium and the resulting surfactant depletion at the interface [1]. Since their propulsion is directly driven by processes at the interfaces (Marangoni stresses), they bear a natural correspondence to hydrodynamic spherical squirmer models, where long range hydrodynamic interactions are derived from an interfacial velocity profile $\vec{v}_i(\theta)$. Squirmer approximations are commonly used to model aggregation and wall interactions of front and back driven microorganisms, i. e., in the context of the squirmer model's expansion to second order polynomials, pullers ($\beta > 0$), pushers ($\beta < 0$) or neutral squirmers [2], for $\vec{v}_i(\theta) = U_0\,(\sin\theta + \beta \sin 2\theta)\,\hat{\vec{e}}_\theta$ (droplet speed U_0). For our droplets, a comparison of PIV data around 50 μm pinned droplets with an analytical approximation of the flow field in Hele-Shaw geometries [3] suggests an increased posterior interfacial flow, i. e. a pusher, which is consistent with their stable wall attraction and collective behaviour.

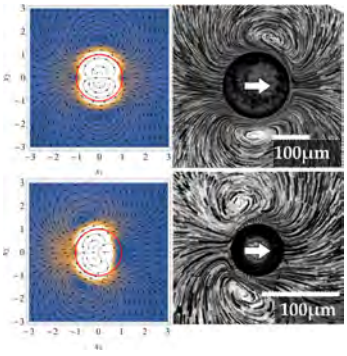

Figure 7.1: left: calculated flow fields for neutral (top)/pusher (bottom) type squirmers in Hele-Shaw cells, right: streak images of colloidal tracers around pinned droplets of different size resembling puller (top) and pusher (bottom) flow fields.

We propose that the reason for this shift towards the posterior lies in the time scale of micellar filling. Assuming that the oil uptake initially grows with the micellar surface and that micelles saturate at a finite size for larger times, there is a saturation time T and length $L = U_0 T$ independent of the droplet radius, such that we can tune droplet swimmers from pusher to puller simply by increasing their radius R. However, for $R \gg L$, large squeezed droplets ($R \gtrsim 1\,\text{mm}$) develop multiple Marangoni instabilities, (Fig. 7.1). Moreover, such droplets are, due to their smaller Laplace pressure, more deformable. As opposed to the stably spherical 50 μm droplets, they develop pulsating swimming states reminiscent of keratocytes [4] (cf. Schlieren image of the droplet trail in Fig. 7.2 c); and toroidal stationary states leading to self-division cascades as well as intermittent behaviour like symmetric "dumbbell"

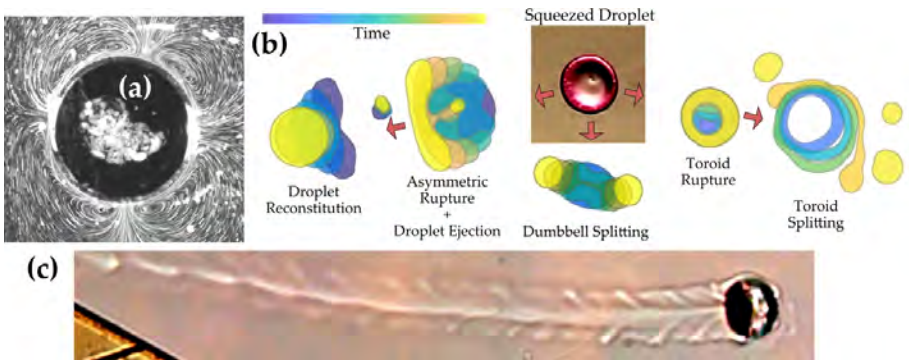

Figure 7.2: (a) Quadrupolar flow around squeezed droplet. (b) Squeezed droplet self-division pathways during multi-polar solubilization. Left: periodic asymmetric rupture, sheddding daughter droplets. Middle: dumbbell splitting. Right: central rupture into a growing toroid, which splits into smaller droplets. (c) Schlieren image of a pulsating droplet and trail

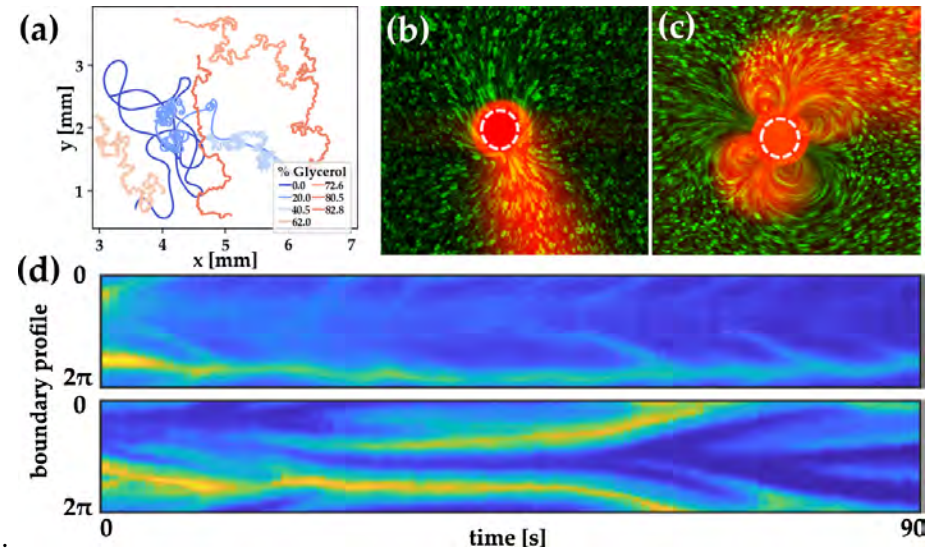

Figure 7.3: (a) change of trajectory morphology with glycerol fraction. Simultaneous mapping of flow field (green) and filled micelle (red) distribution around swimmers at glycerol fractions of 0 (b) and 50% (c) (d) Kymographs of filled micelle profiles around a droplet vs. time for persistent (no glycerol, top) and noisy swimming (>50% glycerol, bottom)

splitting and the asymmetric ejection of daughter droplets. We have summarised the shape evolution of such states in Fig. 7.2 b.

We are also currently investigating the behaviour of swimmers in non-Newtonian and highly viscous media. Recent results using water/glycerol mixtures suggest that increasing the viscosity of the swimming medium results in noisier propulsion, which is notable since increased viscosity usually leads to dampened fluctuations. The propulsion dynamics can be tuned from persistence over 'run-and-spiral' to 'stop-and-go' states (Fig. 7.3 a) without a discernible change in the average speed. We attribute these unsteady Marangoni flows at the interface to different modes of chemical (filled micelles) secretion from the swimmer causing chemical and hydrodynamic instabilities. This is demonstrated in Fig. 7.3 b–d, showing the transition from persistent (no glycerol) to noisy swimming at high glycerol concentration, in simultaneous multichannel fluorescent micrographs of the chemical and hydrodynamic fields (section 7.7), and in Fig. 7.3 d, showing azimuthal fluorescence, i. e. the concentration of the chemical field around the droplet, vs. time. In the low viscosity case, the droplet self-propels in a steady squirmer motion with a front-aft broken symmetry in the chemical concentration (the single peak in Fig. 7.3 d, top indicates the trail). In contrast, at higher viscosity, slower diffusion and longer fluid entrainment cause a transient heterogeneity in the chemical field at the interface (Fig. 7.3 d, bottom). This causes continuous shifts between dipolar and quadrupolar squirming modes as shown in Fig. 7.3 b–c.

[1] S. Herminghaus et al., "Interfacial mechanisms in active emulsions", *Soft Matter*, **10**, 7008 (2014).

[2] M. T. Downton and H. Stark, "Simulation of a model microswimmer", *JPCM*, **21**, 204101 (2009).

[3] R. E. Pepper et al., "Nearby boundaries create eddies near microscopic filter feeders", *J R Soc Interface*, **7**, 851 (2010).

[4] K. Keren et al., "Mechanism of shape determination in motile cells", *Nature*, **453**, 475 (2008).

7.2 DYNAMICS OF DROPLETS DRIVEN BY CHEMICAL TURNOVER

J. Kirschbaum, A. Kulkarni, D. Zwicker

Droplets driven by chemical turnover are a class of active matter where phase separation is combined with non-equilibrium chemical reactions. In the simplest case, droplets are formed by building blocks B, which are created from precursors P in a chemical reaction. In this binary system, B and P phase separate while also being converted into each other; see Figure 7.4. We simulate such systems numerically by extending the classical Cahn-Hilliard equation that describes phase separation by chemical reactions. Additionally, we develop analytical solutions based on a thin-interface approximation [1]. Here, the chemical reaction outside the droplet creates a supersaturation of B, which drives a diffusive influx that scales with the droplet radius. Conversely, the chemical reaction degrading B inside implies an efflux that scales with the droplet volume. Taken together, the different scalings of these fluxes allow for stationary droplets, whose size is controlled by the chemical reaction rates [2].

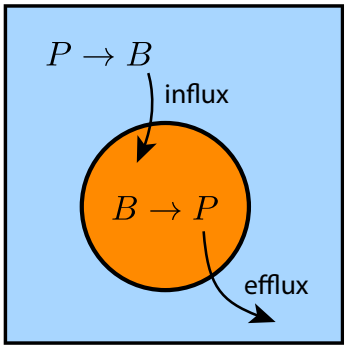

Figure 7.4: Droplets (orange) enriched in building blocks B form by phase separation from the solvent phase (blue) enriched in precursors P. Non-equilibrium chemical reactions between B and P imply diffusive fluxes of B (arrows) that persist in stationary states and affect the droplet dynamics.

Droplets driven by chemical turnover have been studied in simple environments, where they do not interact with other droplets, concentration gradients, or walls [1]. To understand the behavior of such droplets in more complex environments, we study how they migrate and grow in an external concentration gradient. This also informs the dynamics of two droplets in close proximity, where one droplet creates a concentration gradient for the other. Understanding the pair-wise interaction will allow us to simulate emulsions of many droplets without solving the numerically challenging Cahn-Hilliard equation.

The droplets can also divide spontaneously when the chemical driving is strong enough [3]. These division events mimic the exponential growth of cell colonies, so the droplets quickly occupy the entire system. In such dense emulsions, droplets compete for the building blocks produced in the solvent and will thus be smaller than calculated from the simple scaling argument presented above. To determine how the model parameters affect the stable states, we investigate hexagonal packings that have been observed in numerical simulations; see Figure 7.5. Using an analogy with a thermodynamic system with long-ranged interactions and exploiting the symmetry, the problem can be reduced to minimizing a functional in the triangular unit cell. With this approach, we determine the pattern length scale and the droplet size in the stationary state as a function of the model parameters.

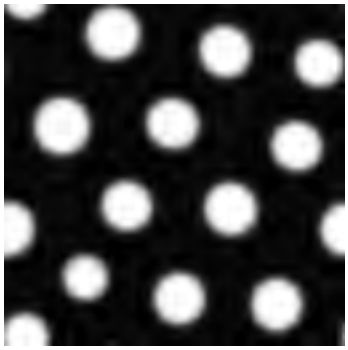

Figure 7.5: Numerical simulation of droplets driven by chemical reactions using an extended Cahn-Hilliard model. The simulation has not yet reached the stationary state, but the hexagonal lattice is clearly visible.

Understanding the dynamics of droplets driven by chemical reactions will help to unravel how cells could use chemical reactions to control their membrane-less organelles.

[1] D. Zwicker, A. A. Hyman, F. Jülicher, Phys. Rev. E, **92** 012317 (2015)
[2] C. A. Weber, D. Zwicker, F. Jülicher, C. F. Lee, under review
[3] D. Zwicker, R. Seyboldt, C. A. Weber, A. A. Hyman, F. Jülicher, Nat. Phys. **13** 408–413 (2017)

7.3 DYNAMICS OF CONFINED PHORETIC COLLOIDS

K. R. Prathyusha, S. Saha, R. Golestanian

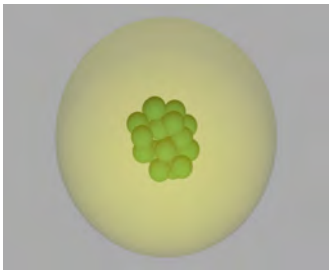

Figure 7.6: Snapshot of the colloids in a cluster formed by chemotactic collapse. Colloids coated with catalysts when placed in a medium with reactants produce non-uniform chemical fields that can be sensed by other colloids. The interactions between these colloids are through long ranged chemical fields, falling inversely with separation. Due to the boundary condition of chemical field at container wall, a dynamic cluster of colloids forms at the center of the spherical container.

Phoretic colloids are known to form clusters by mechanisms similar to those in black holes formed by long ranged gravitational forces [1]. Here the long ranged interactions are driven by phoretic response [1] of one colloid to the chemical field generated by others. We systematically study the dynamics of a colloid in such an assembly by gradually increasing the total number of colloids and the strength of interactions.

Brownian dynamics simulations are used to study the time evolution of the system. The self avoiding colloids are placed in a spherical container of radius much larger than particle size. Zero-flux boundary conditions lead to the formation of a dynamic cluster at the center of the container, see Figure 7.6. The radial distribution function reveals that for a given number of colloids, the structure of clusters changes from being fluid like to more layered geometries as the interaction strength, quantified by a dimensionless number vo, is increased. We study the slow relaxational dynamics in the steady state by calculating the mean square displacement (MSD), see Figure 7.7. For large enough interactions we see a plateau in the MSD, a characteristic feature of glassy systems.

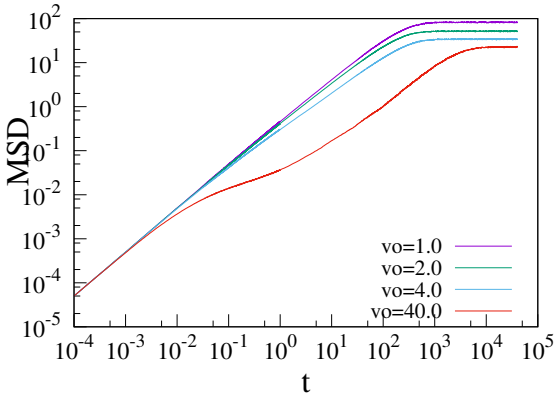

Figure 7.7: Mean squared displacement in steady state obtained by averaging over all colloids in the cluster and initial conditions, for various vo.

We have also identified several dynamical regimes leading finally to a clustered steady state. In the beginning, colloids diffuse normally, then transition to super-diffusive behaviour driven by phoretic interactions. The rich dynamics in steady state is currently being investigated further by studying step size distributions and cage breaking dynamics. This study is also motivated by processes inside a cell, as the cellular interior is a non equilibrium environment that constantly produces and destroys high energy molecules, creating chemical gradients within the cell.

[1] R. Golestanian, Phys. Rev. Lett. **108**, 038303 (2012)

7.4 STABILITY, TOPOLOGY AND SELF-PROPULSION IN ACTIVE NEMATIC DOUBLE EMULSIONS

C. C. Maaß, Ch. Bahr,
B. V. Hokmabad, K. A. Baldwin

The capability to produce controllable, self-propelled microcapsules would present a leap forward in the development of artificial cells, microreactors, and microsensors. One example of *inactive* microcapsules are double emulsions, which have been applied as, *e.g.*, reactive microcontainers, food and drug capsules, cosmetics, optical devices, biotic sensors, and synthetic cell membranes [2]. Despite the wide utility of double emulsions as a platform for synthetic biology and microchemistry, a significant challenge remains in combining activity, stability, and control. Building on the established system of active *single* emulsions [1] (see section 7.1), we approach the problem of encapsulation by using active nematic double emulsions, where a solubilization mechanism induces motility and the nematic structure provides stability [4].

Since the convective flow inside a self propelling double emulsion droplet or shell drives the aqueous core towards the outer interface (fig 7.8 a), there has to be a barrier against coalescence with the outer phase. In the case of nematic shells, this barrier is provided by an elastic force associated with the distorted nematic director field driving the core towards the centre of the shell. We have estimated this force by numerical integration to be on the order of the force enacted by the internal flow, and established in experiments that active shells are significantly less stable above the clearing point (fig 7.8 a). Nematic shells survive down to shell thicknesses on the order of 1 μm, at which point they coalesce into an active single emulsion droplet. Within one experiment, burst events are sharply clustered around a common bursting time and shell thickness (fig 7.8 b, e).

In single core double emulsions, we observe a curious "shark-fin meandering" motion in quasi-2D (Fig. 7.9) We have found a related behaviour in active nematic single emulsions [3] caused by a surface-flow induced distortion of the nematic director field inside the droplet. In contrast, for active shells the underlying instability lies in the different viscosities of oil shell and aqueous core, with $\eta_{\text{shell}} \approx 50\eta_{\text{core}}$. In a moving shell, a toroidal convective flow inside the droplet, which is imposed by the moving interface, traps the core on one side of the shell and causes it to rotate. Fig. 7.9 (a) shows this circulation as analysed by colloidal tracers. This rotation causes the droplet trajectory to bend back on itself, the droplet to slow down due to chemotactic repulsion (cf. sec. 7.7) and eventually reverse direction.

At this point, the 'shark fin' tip, the chemotactic force gives positive feedback, restarts the core circulation and makes the droplet accelerate away from its own trail at first, until it is turned back again by the core circulation and the cycle starts anew.

Similar to single emulsions, the chemotactic repulsion forces shells on helical traejctories in density matched 3D. We note that the helices are more tightly wound, which suggests a higher asymmetry torque,

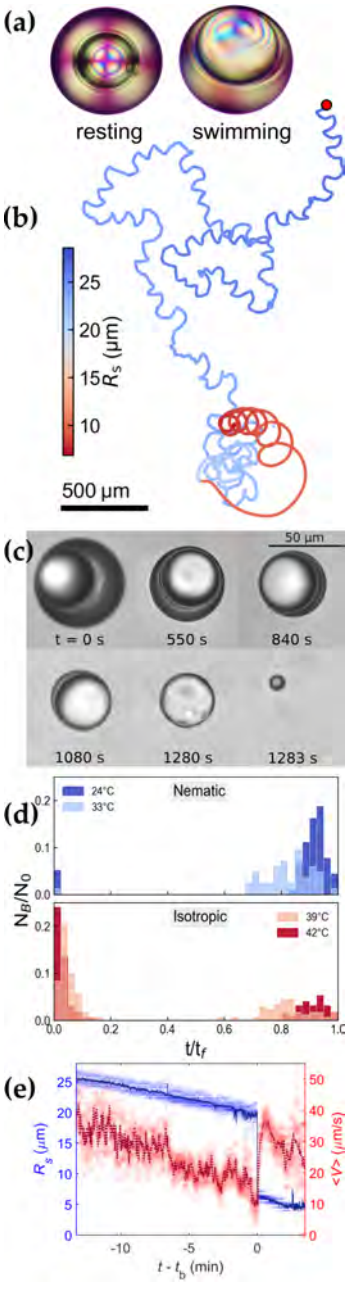

Figure 7.8: (a) polarised images of resting and moving nematic shells; (b) burst statistics above and below the clearing point; (c) life stages of 1-core shell; (d) trajectory colour coded by shell radius; (e) radius and speed around bursting

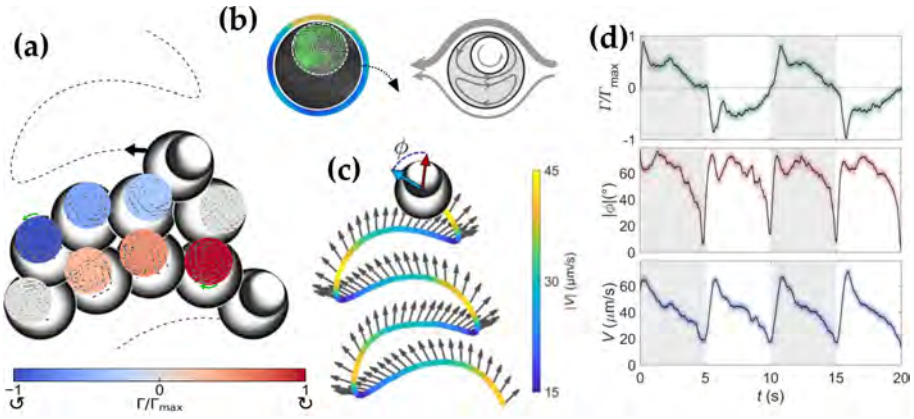

Figure 7.9: periodic 'shark-fin' meandering: (a) core circulation stopping and reversing at a kink; (b) PIV of core circulation and interfacial flow speed (left) and flow field schematic (right); (c) speed and core orientation; (d) measured circulation Γ, core orientation ϕ and speed v vs. time

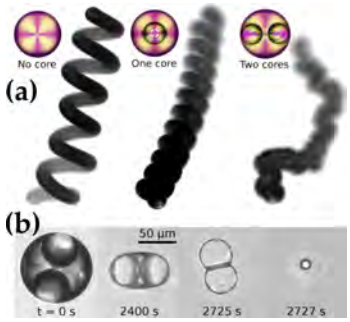

Figure 7.10: (a) 3D motion of 0-, 1-,and 2-core droplets; (b) life stages of a 2-core droplet

probably due to the stronger viscous anisotropy. We were also able to produce double core emulsions, which have a fixed symmetry axis suppressing the meandering asymmetry. In this case, the shells propel perpendicular to the core axis, with some rotational fluctuation, as we can expect if the cores are trapped on opposite sides of the internal convection roll.

If we want to use shells for transport and targeted release applications, we need reliable guidance mechanisms. In Fig. 7.11 (a) we demonstrate stable wall attachment, even around convex and concave corners, with the core constantly rotated outwards, driving the shell into the wall. As demonstrated for single emulsions, the shells can also follow fuel gradients, which speed the shells up and rectify their trajectories (fig 7.11 (b)).

[1] C. C. Maass et al., "Swimming Droplets", *Annu. Rev. Condens. Matter Phys.*, **7**, 171 (2016).

[2] J. Petit et al., "Vesicles-on-a-chip: A universal microfluidic platform for the assembly of liposomes and polymersomes", *EPJ E*, **39**, 59 (2016).

[3] C. Krüger et al., "Curling Liquid Crystal Microswimmers: A Cascade of Spontaneous Symmetry Breaking," *PRL*, **117**, 048003 (2016).

[4] B. V. Hokmabad et al., "Active double emulsions", *arXiv*, 1810.07223 (2018).

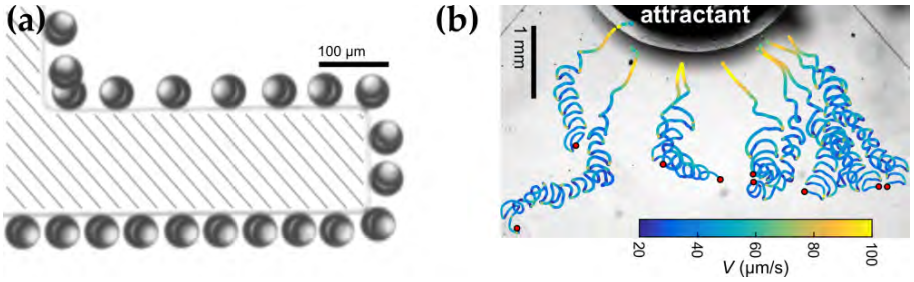

Figure 7.11: Guidance by topographical features (c) and a surfactant gradient (d)

7.5 PARTICLE CENTERING IN DROPLETS DRIVEN BY CHEMICAL TURNOVER

D. Zwicker
F. Jülicher (MPIPKS Dresden)

Phase separation has recently emerged as an important concept for organizing membrane-less compartments inside biological cells. One example for such compartments are centrosomes, which organize the mitotic spindle at cell division. During this process, it is paramount that exactly two droplets of the same size form simultaneously and dissolve in a later stage of the cell cycle. We showed that non-equilibrium chemical reactions affecting the droplet material can explain these properties of centrosome growth [1]. More generally, we have shown that the chemical reactions turning over droplet material provide much more control over the droplet morphology than is possible in classical, passive droplets [1, 2].

The driving chemical reactions create concentration gradients inside and outside the droplet; see Figure 7.12. These gradients imply diffusive fluxes, which persist even in stationary states, revealing the non-equilibrium nature of these systems. Besides stabilizing multiple droplets, these fluxes can also control the positioning of solid-like particles inside the droplets [3]. Interestingly, whether such particles are centered in the droplet or expelled from it depends on the direction of the fluxes induced by the chemical reactions. Moreover, a catalytic activity on the surface of the particles, which is for instance present in centrosomes, can further affect the particle dynamics. Taken together, we have shown that driven chemical reactions allow to control the droplet morphology by varying the reaction rates.

Figure 7.12: Schematic picture of a droplet driven by chemical turnover enclosing a solid particle (gray). Compositional gradients inside (red) and outside (blue) indicate fluxes that restore the symmetric state (dotted line) and thus center the particle.

Applying this model to centrosomes directly explains why the solid-like centrioles are found at the center of the liquid-like centrosome; see Figure 7.13. Judging from light microscopy and electron micrographs alone, it has been a puzzle how the small centrioles could locate the center despite the large thermal fluctuations that are present at these small length scales. Our model suggests that concentration gradients created by chemical reactions center the centrioles without any additional assumptions beyond the ones necessary to explain centrosome growth [1]. More generally, our work shows that driving droplets with chemical reactions might allow biological cells to control droplet formation to structure their interior.

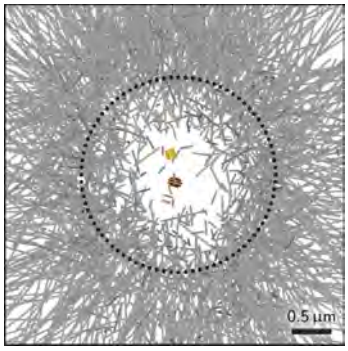

Figure 7.13: Centrosomal microtubules reconstructed from electron micrographs of a *C. elegans* embryo [4]. The colored microtubules in the center mark the two centrioles, while they gray microtubules emanate out of the surrounding pericentriolar material (dotted circle), which can be described as a liquid droplet [1].

[1] D. Zwicker, M. Decker, S. Jaensch, A. A. Hyman, F. Jülicher, Proc. Natl. Acad. Sci. USA **111** E2636–45 (2014)
[2] D. Zwicker, A. A. Hyman, F. Jülicher, Phys. Rev. E, **92** 012317 (2015)
[3] D. Zwicker, J. Baumgart, S. Redemann, T. Müller-Reichert, A. A. Hyman, F. Jülicher, Phys. Rev. Lett., **121** 158102 (2018)
[4] S. Redemann, J. Baumgart, N. Lindow, M. Shelley, E. Nazockdast, A. Kratz, S. Prohaska, J. Brugués, S. Fürthauer, T. Müller-Reichert, Nat. Commun., **8** 15288 (2017)

7.6 ENHANCED DIFFUSION AND CHEMOTAXIS OF NANOSCALE ENZYMES

J. Agudo-Canalejo, R. Golestanian
T. Adeleke-Larodo (U. of Oxford), P. Illien (ESPCI Paris)

Biological enzymes catalyze the transformation of a chemical substrate into a product. Interestingly, many experimental studies in recent years have shown that the activity of enzymes is not just chemical: enzymes also exhibit motion in the presence of their corresponding substrate [1]. In a uniform substrate background, experiments have observed an increase in the undirected motion of the enzymes or *enhanced diffusion*. In a substrate gradient, enzymes moreover undergo biased motion in the direction of the gradient or *chemotaxis*. Understanding enzyme motion in response to chemical cues is important both in applied biomedical research, e.g. in the design of biocompatible nano-sized vehicles for directed drug delivery; as well as in basic biology, in the context of self-organization of the different enzymes that participate in a metabolic pathway (metabolon formation). Our project aims to elucidate the underlying mechanisms through microscopically-detailed modelling [1].

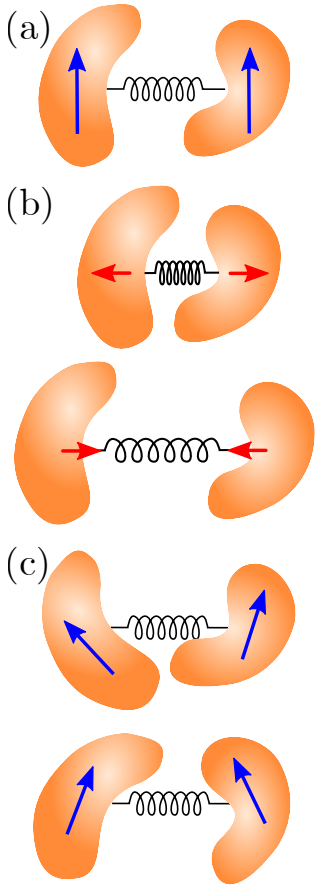

Figure 7.14: A flexible dumbbell-like enzyme can fluctuate around its equilibrium conformation (a), undergoing extensional (b) and orientational (c) fluctuations. From Ref. 1.

Early experiments suggested a link between the exothermicity of the catalytic reaction and the strength of enhanced diffusion, implying an *active*, non-equilibrium origin for the enhancement. However, careful consideration of several candidate active mechanisms [2], including kinetic energy boosts, stochastic swimming, and self-thermophoresis showed that none of them could explain the observed magnitude of enhanced diffusion. Collective heating of the sample by the enzymes seemed a plausible candidate, but no such heating has been observed experimentally. Subsequent experiments with aldolase, a slow and endothermic enzyme, surprisingly showed a diffusion enhancement not only in the presence of substrate but also in the presence of a competitive inhibitor that simply binds to the enzyme but is not catalyzed [3]. The latter observations demanded a paradigm shift towards *passive* mechanisms for enhanced diffusion that depend on binding-unbinding of the substrate (or inhibitor) rather than on the catalytic step.

One intriguing possibility is that binding-induced conformational changes of the enzyme affect its diffusion coefficient. As a minimal model for a modular enzyme that can undergo conformational changes, we considered a flexible dumbbell-like enzyme, consisting of two subunits that are subject to extensional [3, 4] and orientational [5] fluctuations; see Fig. 7.14. Our calculations showed that the effective diffusion coefficient of such a flexible object has the form $D_{\text{eff}} = D_{\text{avg}} - \delta D_{\text{fluc}}$ where the first term is the thermal average of contributions from translational modes, and the second term with $\delta D_{\text{fluc}} > 0$ is a correction due to the conformational fluctuations. Binding-induced stiffening of the enzyme would lead to a reduction in the fluctuation-induced correction, and ultimately to a higher effective diffusion coefficient in the bound state. Assuming that binding-unbinding occurs much faster than catalysis, we found that the dependence of the diffusion coefficient

on substrate concentration c_s will go as

$$D(c_s) = D_0 + \Delta D \frac{c_s}{K + c_s} \tag{7.1}$$

where K is the binding constant; see Fig. 7.15 for a fit of this expression to experimental data for aldolase.

In order to understand the observations of chemotaxis, we considered a passive model in line with our model for enhanced diffusion; see Fig. 7.16 [6]. The enzyme interacts with the substrate *via* (i) hydrodynamic interactions, (ii) non-contact direct interactions (electrostatic, van der Waals, etc.), and (iii) specific binding to form a complex, involving conformational changes. We obtained an expression for the time evolution of the enzyme concentration

$$\partial_t c_e = \nabla \cdot \left\{ D(c_s) \cdot \nabla c_e - [\boldsymbol{V}_{ph}(c_s) + \boldsymbol{V}_{bi}(c_s)] c_e \right\} \tag{7.2}$$

which includes three important contributions to the motion of the enzyme. The first term corresponds to enhanced diffusion with the diffusion coefficient $D(c_s)$ as in Eq. 7.1. The second term is the phoretic velocity due to non-contact interactions with the substrate, with a typical form $\boldsymbol{V}_{ph}(c_s) = \mu(c_s)\nabla c_s$ where $\mu(c_s)$ is a substrate-dependent phoretic mobility which encodes the strength of the interactions. The last term is a chemotactic velocity due to binding-induced changes in diffusion, given by $\boldsymbol{V}_{bi}(c_s) = -\nabla D(c_s)$. Importantly, for a typical enzyme, we find that the phoretic and binding-induced velocities point in opposite directions and compete against each other. At high substrate concentration, the phoretic velocity dominates and the enzyme is directed towards the substrate, whereas at low concentration, the binding-induced velocity dominates and the enzyme is directed away from the substrate. This competition could explain contradictory experimental observations for the direction of urease chemotaxis [6].

In ongoing work, we are considering the effects of shape anisotropy and conformational fluctuations on chemotaxis, by studying the flexible dumbbell model in the presence of a substrate gradient. We find that phoretic interactions can lead to alignment of the dumbbell with the gradient, and that conformational fluctuations induce corrections to the phoretic velocity [7]. Further work is concerned with the collective self-organization of many enzymes, either spontaneously or in externally-imposed substrate gradients. The formation of dense enzyme clusters may be related to the clusters of phoretic colloids studied in Rep. 7.3.

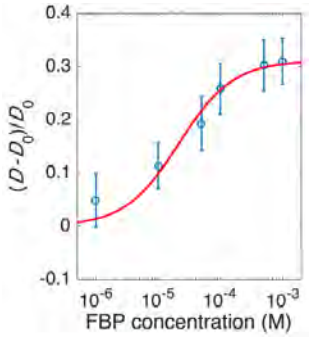

Figure 7.15: Experimental data and fit to Eq. 7.1 for the enhanced diffusion of aldolase in the presence of its substrate FBP. From Ref. 3.

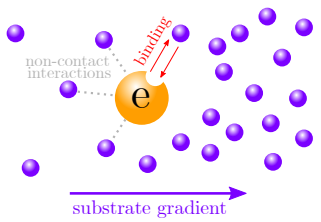

Figure 7.16: An enzyme in a substrate gradient interacts with all substrate molecules through non-contact interactions, and can also bind one-on-one with a substrate to form a complex. From Ref. 6.

[1] J. Agudo-Canalejo, T. Adeleke-Larodo, P. Illien, R. Golestanian, Acc. Chem. Res. **51**, 2365 (2018)
[2] R. Golestanian, Phys. Rev. Lett. **115**, 108102 (2015)
[3] P. Illien, X. Zhao, K. K. Dey, P. J. Butler, A. Sen, R. Golestanian, Nano Lett. **17**, 4415 (2017)
[4] P. Illien, T. Adeleke-Larodo, R. Golestanian, EPL **119**, 40002 (2017)
[5] T. Adeleke-Larodo, P. Illien, R. Golestanian, arXiv:1712.06418
[6] J. Agudo-Canalejo, P. Illien, R. Golestanian, Nano Lett. **18**, 2711 (2018)
[7] T. Adeleke-Larodo, J. Agudo-Canalejo, R. Golestanian, arXiv:1811.09631

7.7 "GHOST CAGING": AUTOCHEMOTACTIC ARREST IN ACTIVE EMULSIONS

C. C. Maaß, M. G. Mazza,
C. Jin, B. V. Hokmabad, F. J. Schwarzendahl

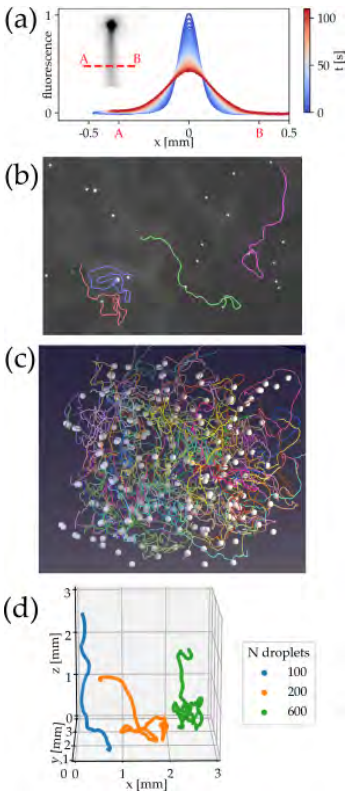

Figure 7.17: (a) 2d: droplets getting entangled in each other's trails, (b) diffusion profiles of fluorescent micelles in the trail (c) reconstruction of 200 droplets in a $(3\text{mm})^3$ volume (light sheet microscopy) (d) 3D trajectories for increasing number densities

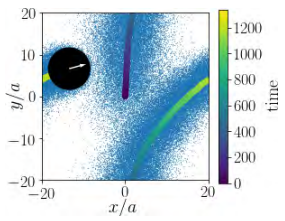

Figure 7.18: Simulation of a squirmer (●) with micellar interaction: "filled micelle" trail of the swimmer (•) and its time colour coded trajectory.

Chemotaxis and autochemotaxis drive a myriad of collective behaviours in the microbial world. However, clear physical mechanisms are difficult to isolate due to the complexity of biological interactions. Emulsions of active droplets with precisely tunable chemotactic interactions provide an ideal testing bed of current theories.

The propulsion of our active oil droplets (sec. 7.1) is driven by the local density of empty surfactant micelles in the aqueous phase. Due to the slow micellar diffusion, which is on the order of the droplet speed, droplets leave very persistent trails of oil-filled micelles acting as an autochemotactic repellent: an effect that is not common in e. g. H_2O_2 catalysis driven Janus colloids, where the fuel diffuses much faster than the swimmers. We have established [1] that the chemotactic repulsion scales with the gradient of filled micelles, ∇c_f, and can directly image c_f by adding a fluorescent dye to the oil phase. The fluorescent intensity in the wake of a swimming droplet matches Gaussian diffusion (Fig. 7.17 a).

In the collective interactions of multiple swimmers in quasi 2D (Fig. 7.17 b) and density matched 3D environments (Fig. 7.17 c), autochemotaxis leads to an interesting phenomenon. While droplets swim persistently at the start of the experiment, they develop a network of repulsive trails (Fig. 7.17 b), with droplets trapped in the interstices. We have seen trapping in 2D and 3D, shown here with example trajectories for increasing number densities from a 3D experiment(Fig. 7.17 d). This phenomenon is reminiscent of caging effects in glassy systems, however, it occurs at much lower volume fractions since the droplets here interact with the trails left by other droplets.

We also developed a theoretical and numerical scheme to simulate active droplets. We employ active squirmer particles that self propel by imposing a velocity field on their surface. We implemented a hybrid molecular dynamics – multiparticle collision dynamics method for the squirmers and the fluid. In addition to the velocity field on the surface, fluid particles that collided with the squirmer can turn into "filled micelles". Once a fluid particle is turned into a "filled micelle" the imposed surface velocity upon collision with a squirmer becomes repulsive. In Fig. 7.18 we show a quasi 2D simulation of a single neutral squirmer with periodic boundary conditions in the x-y direction. Starting from the center of the simulation domain, as the squirmer moves it deflects in order to avoid its own trail of filled micelles. The qualitative behavior of our model squirmer is similar to the experimental picture observed in Fig. 7.17 b. While this preliminary work is promising, a statistical analysis will be necessary to make a quantitative comparison between experiment and simulations.

[1] C. Jin et al., "Chemotaxis and autochemotaxis of self-propelling droplet swimmers", *PNAS*, **114**, 5089 (2017).

7.8 PAIRING, WALTZING AND SCATTERING OF CHEMOTACTIC ACTIVE COLLOIDS

S. Saha, R. Golestanian
S. Ramaswamy (Indian Institute of Science)

Two interacting chemotactic active colloids, which move autonomously along their polar axes [1] can rotate their polar axis to align with an imposed chemical gradient [2], form new bound states by cancellation of velocities rather than by minimisation of a free energy. The non-central and non-reciprocal interactions are dynamical in origin, resulting due to an interplay of self-propulsion and phoretic response to chemical field generated by each other. The bound states, defined when distance between swimmer centres remains finite at long times, are formed only when the chemotactic response of one of the swimmers is positive, i.e. it points up a linear gradient.

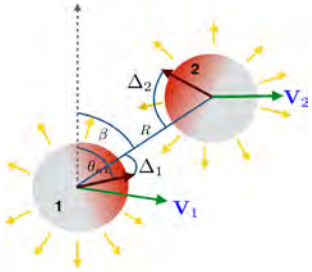

Figure 7.19: The swimmer velocities point in directions different from the line joining their centers, leading to non-central and non-reciprocal interactions. State diagram showing dynamical behaviour as the mobility and total surface activity.

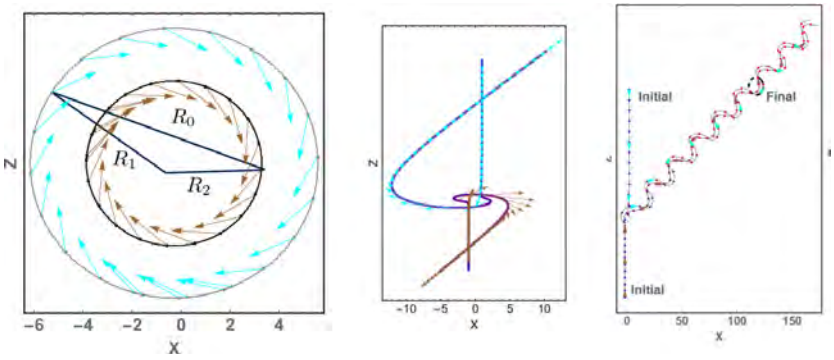

Figure 7.20: Interaction between two swimmers results in varied dynamical behaviour: synchronous ornits (left), scattering (middle) and oscillatory dimers (right).

These states fall in two broad categories – (i) active dimers, polar axes line up (ii) orbits, relative inclination of the polar axes fixed. Swimmers unbind and scatter away depending on initial conditions or with an increase of self-propulsion; while mutually anti-chemotactic swimmers always scatter away. These findings can be summarized in state diagrams 7.21 and representative trajectories are calculated to illustrate the rich dynamics 7.20.

These interactions are mediated by a diffusing field and are therefore naturally long-ranged. The short-range interparticle repulsion is also dynamically generated by phoretic mechanisms. The orientation vector carried by each particle sets the direction of persistent motion. This endows the colloids with a kind of inertia which is why, despite their vanishingly small Reynolds number, their behaviour bears some similarity to scattering in Newtonian mechanics. We expect our work to inspire efforts to fabricate particles with a range of catalytic and mobility coat patterns, using shape as an additional control parameter.

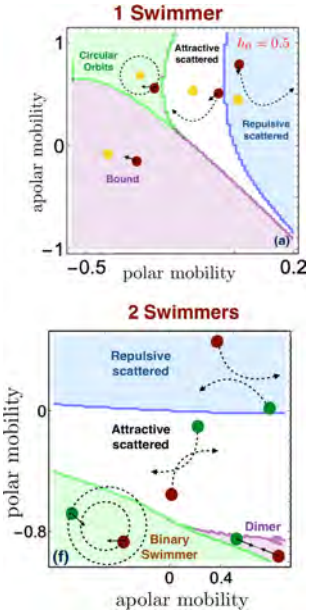

Figure 7.21: The total catalytic activity and the first and second harmonic of the mobility pattern as parameters are chosen to constriuct state disgrams illustrating the dynamical behaviour.

[1] R. Golestanian, T. B. Liverpool, and A. Ajdari, Phys. Rev. Lett., **94**, 220801 (2005).
[2] S. Saha, R. Golestanian, and S. Ramaswamy Phys. Rev. E **89**, 062316 (2014).

7.9 MAXIMUM IN DENSITY HETEROGENEITIES OF ACTIVE SWIMMERS

M. G. Mazza, F. J. Schwarzendahl

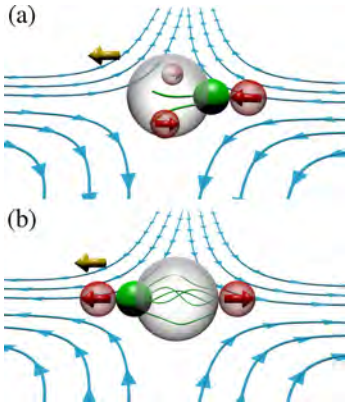

Figure 7.22: Schematic representation in a perspective view of the active swimmer model for (a) a puller-type, and (b) a pusher-type microswimmer.

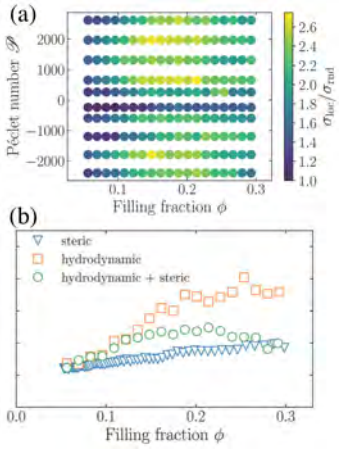

Figure 7.23: Standard deviation of local Voronoi volume $\sigma_{\rm loc}$ compared to standard deviation $\sigma_{\rm rnd}$ of a homogeneous configuration. (a) The Péclet number $\mathcal{P}$ as well as the global filling fraction ϕ are varied. Positive Péclet numbers correspond to pusher-type and negative to puller-type swimmers. (b) The Péclet number is fixed to $\mathcal{P} = 2.4 \times 10^3$ for puller-type swimmers. The circles include hydrodynamic and steric interactions; the squares include only hydrodynamic interactions; and the triangles include only steric interactions.

Suspensions of unicellular microswimmers such as flagellated bacteria or motile algae can exhibit spontaneous density heterogeneities at large enough concentrations. Based on the relative location of the biological actuation appendages (*i.e.* flagella or cilia) microswimmers' propulsion mechanism can be classified into two categories: (i) pushers, like *E. coli* bacteria or spermatozoa, that generate thrust in their rear, push fluid away from them and propel themselves forward (see Fig. 7.22(b)); (ii) pullers, like the microalgae *Chlamydomonas reinhardtii*, that have two flagella attached to their front, pull the fluid in and thereby generate thrust in their front (see Fig. 7.22(a)).

We introduce [1] a novel model for biological microswimmers that creates the flow field of the corresponding microswimmers, and takes into account the shape anisotropy of the swimmer's body and stroke-averaged flagella. By employing the multiparticle collision dynamics technique in combination with molecular dynamics, we directly couple the swimmer's dynamics to the fluid's.

We characterize the nonequilibrium phase diagram (Fig. 7.23(a)), as the filling fraction and Péclet number are varied, and find density heterogeneities in the distribution of both pullers and pushers, due to hydrodynamic instabilities. We find a maximum degree of clustering at intermediate filling fractions and at large Péclet numbers. Using additional simulations that include only hydrodynamic interactions or only steric interactions (Fig. 7.23(b)) we show that the maximum in density heterogeneities results from a competition of hydrodynamic and steric interactions between the swimmers [1].

We also develop an analytical theory that supports these results, in which we include steric and hydrodynamic based on a Fokker-Planck approach. Using a linear stability analysis we come to the same conclusion as in the simulations: hydrodynamic interactions destabilize the system, causing density heterogeneities which are tempered by steric interactions are higher filling fraction.

The density heterogeneities that we find are different from motility-induced phase separation, as they are induced by hydrodynamic interactions. Importantly, our maximum in density heterogeneities occurs at much lower filling fraction as opposed to motility-induced phase separation and can therefore have an ecological effect.

By including (*i*) an elongated shape of the swimmer, (*ii*) steric effects, and (*iii*) hydrodynamic interactions we find a behavior that might represent an optimum for the microorganisms' colonization of their environment and thus be relevant for the formation of biofilms.

[1] F. J. Schwarzendahl, and M. G. Mazza, Soft Matter **14**, 4666 (2018)

7.10 LIVING FOAMS – A ROUTE TOWARDS ARTIFICIAL TISSUE

H. Witt, H. Kim, F. Cavallini, S. M. F. Dannenberg, C. Steinem (Univ. of Göttingen), **M. Tarantola, E. Bodenschatz**
Y. E. Portillo C., K. J. M. Kramer, J. F. E. Bodenschatz, H. Hubrich, P. Nietmann, T. Oswald, A. Janshoff (University of Göttingen), M. Schröter, I. Platzmann, J. Spatz (MPI for Medical Research, Heidelberg)

The evolution of multicellularity was critical for the success of life on earth. We want to follow the steps from unicellular microbes to multicellular life using the tools of synthetic biology by creating artificial tissues, so called *living foams*. The living foam project is funded by the LIFE initiative of the Volkswagen foundation and consists of groups from Göttingen and Heidelberg (Fig. 7.24A). We seek to realize collective behavior of the multicellular state by implementing the essential biology in actively driven artificial biomimetic systems.

Our strategy for the creation of living foams is the use of polymersomes and giant unilamellar vesicles (GUVs) as the basis for minimal cell compartments (MCCs) - equipped with reconstituted biological proteins - which self-assemble into artificial tissues or hybrid tissues together with living cells (Fig. 7.24B). The creation of living foams imposes several challenges: We need a reliable way to produce minimal cell compartments (MCCs) with a defined size distribution, that are equipped with proteins allowing for adhesion as well as connectivity to enable mechanical and chemical communication between MCCs and living cells. To address these challenges we use microfluidic techniques to create MCCs based on hollow Poly(N-isopropylacrylamide) (PNIPAm) shells (Fig. 7.24C) or droplet-stabilized GUVs (dsGUVs), a continuous lipid bilayer inside droplets of water in biocompatible oil (Fig. 7.24D) [1]. In parallel, we are establishing protocols for the isolation and reconstitution of the required proteins [2].

Living foams will not only aid in our understanding of collective processes in multicellular assemblies but might eventually even be used in clinical applications to replace missing cells in wounded tissue. As a lab model for the creation of a wound and the subsequent healing we established electrical wound healing assays of cultured cardiac myocyte and fibroblast cells [3]. This assay allows the creation of a well-defined wound by applying a high voltage (see Fig. 7.24E), while the impedance of the cell layer also is a powerful tool to monitor the wound healing process. This method will allow us to examine the effect of living foams within hybrid tissues.

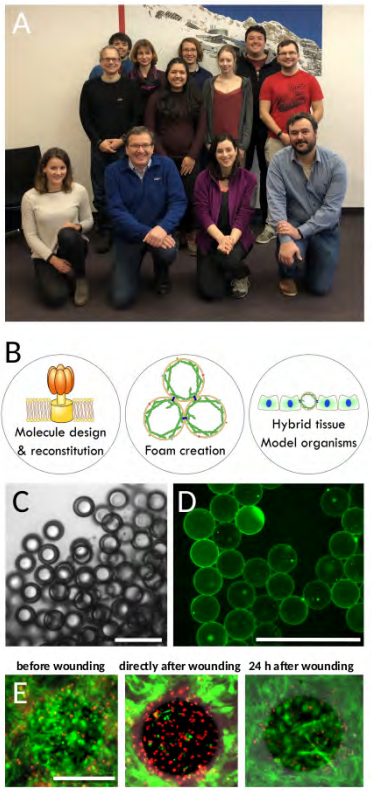

Figure 7.24: A) The living foams team B) Outline of the living foams project C) Microgels based on PNIPAm. D) Droplet stabilized GUVs. E) ECIS based wound healing. Scale bar is 200 micrometer.

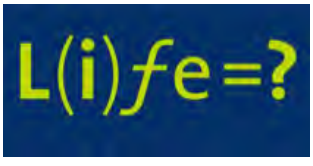

[1] M. Weiss, J. P. Frohnmayer, L. T. Benk, B. Haller, J.-W. Janiesch, T. Heitkamp, M. Börsch, R. B. Lira, R. Dimova, R. Lipowsky, E. Bodenschatz, J.-C. Baret, T. Vidakovic-Koch, K. Sundmacher, I. Platzman, J. P. Spatz, *Nat. Mat.* **17** (2018)
[2] H. Nöding, M. Schön, C. Reinermann, N. Dörrer, A. Kürschner, B. Geil, I. Mey, C. Heussinger, A. Janshoff, C. Steinem, *J. Phys. Chem. B* **122**, 16 (2018)
[3] F. Cavallini, M. Tarantola, *Prog. Biophys. Mol. Biol. (in press)*

7.11 LIGHT DEPENDENT CELLULAR MOTILITY INDUCES PATTERN FORMATION IN CONFINEMENT

A. Fragkopoulos, J. Vachier, J. Frey, F.-M. Le Menn, M. Wilczek, M.G. Mazza, O. Bäumchen

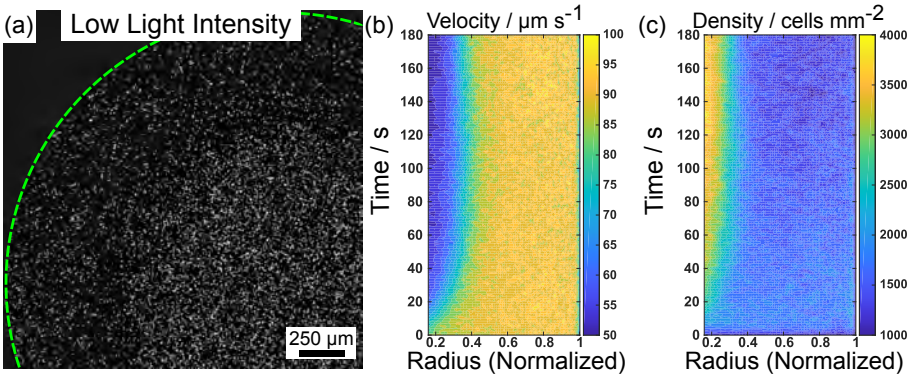

Figure 7.25: (a) A suspension of *Chlamydomonas* cells confined in a quasi-2D circular chamber display cellular aggregation in the center of the compartment (pattern configuration) at low light intensity. At high light intensities the suspensions exhibits a homogeneous distribution. (b-c) Temporal evolution of the radial dependence of the local cell velocity and density during pattern formation.

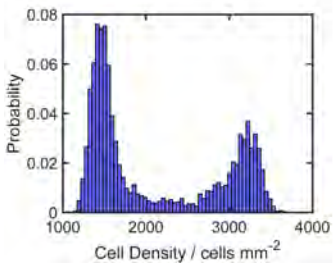

Figure 7.26: Probability distribution function of the cell density in the pattern configuration exhibits a bimodal distribution.

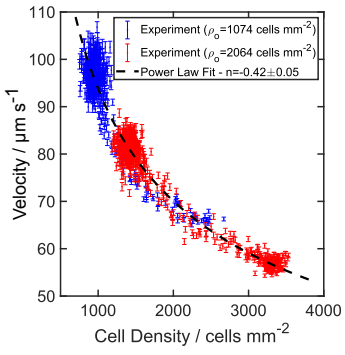

Figure 7.27: Cell velocity as a function of cell density for two experiments exhibiting a pattern at low (blue) and high (red) cell densities. The dashed line represents a best fit to a power-law behavior.

A collection of self-propelled particles can undergo complex dynamics due to hydrodynamic and steric interactions. In highly concentrated suspensions, it is possible for such particles to form large-scale concentration patterns, where the suspension separates into regions of high and low particle concentrations. This can be attributed to the interactions of the particles with boundaries, their specific particle-particle interactions, or other particle specific motility behavior [1].

Our research focuses on the collective behavior of concentrated suspensions of the unicellular microalgae *Chlamydomonas reinhardtii*, a biflagellated puller-type microswimmer, confined in a quasi-2D circular chamber. In ambient light conditions, the suspension appears uniform, but a pattern forms for low light conditions ($< 10^{19}$ photons m^{-2} s^{-1}) and sufficiently high cell densities (> 500 cells/mm^2), where a high density region appears at the compartment's center, see Fig. 7.25(a).

Since *Chlamydomonas* are sensitive to a number of external stimuli, we investigated if this phenomenon is related to its phototactic, gravitactic, or chemotactic behavior. We found that these properties are not the origin of the pattern formation, and another mechanism is involved, for example the motility of the cells. By tracking the cells during the pattern formation, we observe that, initially, the cell velocity and density is constant throughout the compartment and quickly develops a region of high density at the center accompanied by a decrease of the cell velocity, see Fig. 7.25(b,c). By looking at the probability density function of the cell density when the pattern has formed, we observe a bimodal distribution, indicative of a phase separation (see Fig. 7.26). This behavior appears to be similar to a Motility Induced Phase Separation (MIPS), where active Brownian particles phase separate due to the dependence of their motility (velocity or diffusion) to the local concentration.

As a result, we perform experiments at different cell densities and light intensities to determine their role on the cell motility. The velocity of the cells initially increases with increasing cell density for both light intensities, probably due to hydrodynamic interactions [2]. Above a threshold density, the same needed for the pattern to form, steric interactions become important and the velocity of the cells decreases significantly for low light intensities, while there are minor changes for high light intensities instead. As shown in Fig. 7.27, we find a generic coupling between the cell velocity and the cell density, which can be described by a power-law behavior. An additional feature of the pattern formation is the effect of the confinement to the shape of the pattern itself. The region of high cell density appears consistently a distance of about 1.5 mm from the edge. As a result, the shape of the pattern transition from a disk to a ring as we progressively increase the radius of the compartment. These observations raise the question of the mechanism of light-switchable pattern formation and how light affects the motility of the cells. Here, we find that the velocity probability function for individual cells exhibits a characteristic modulation: at low light intensities the distribution is rather symmetric, while we observe high velocity tails for high light intensities, see Fig. 7.28.

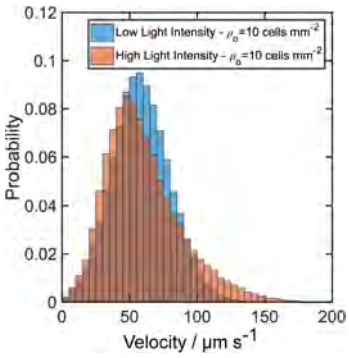

Figure 7.28: Probability density function of cell velocities at low (blue) and high (red) light conditions.

The observed pattern formation is switchable by light and depends on the geometry of the confinement, both of which are not captured by current models and thus require a revision of the state-of-the-art theoretical approaches. In a first step, we devise a simple model based on two Langevin equations, to study the emergence of collective behavior. We treat the motion of interactive active particles, confined in a quasi-2D box, by considering active Brownian particles moving with a self-propulsion speed v_{loc} that depends on the local cell density. The particles are subject to random fluctuations modeled with Gaussian white noise, whose diffusion coefficient also depends on the local cell density. In order to take into account the light-switching ability, the speed and the diffusion coefficient are lower at "low-light intensity" compared to the "high-light intensity" state, similar to the experimental values. Finally, the steric interactions between the particles are included using a hard-core repulsion potential.

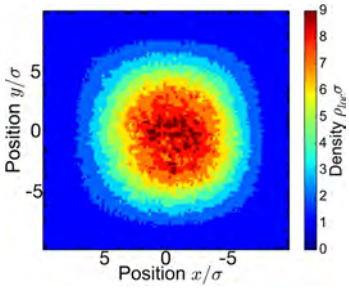

Figure 7.29: Density map of the pattern formation. Top view of a quasi-2D box, with 500 particles, in the steady state regime

For the low-light intensity parameter space, we observe the emergence of a dense region at the center of the simulated box similar to the experiments (see Fig. 7.29). By changing the parameters between low- to high-light intensity, we observe the emergence and annihilation of the pattern (see Fig. 7.30), which we quantify using the clustering coefficient, $C_M = \exp S/M$, where S is the Shannon entropy [3]. From this we can quantify the time scale of the dynamics, which for the pattern formation is ~ 30 s and ~ 50 s for the simulation and experiment, respectively, showing that the model can capture multiple aspects of this phenomenon. These observations support our hypothesis that the interplay between the local cell density and the cell motility is pivotal for unraveling the mechanism of light-switchable pattern formation.

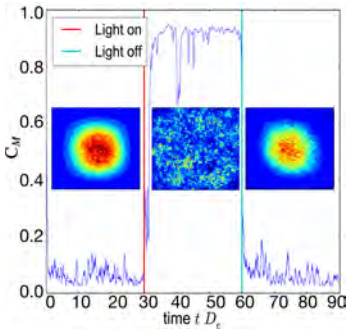

Figure 7.30: Clustering coefficient as a function time and light switchability.

[1] D. Saintillan and M.J. Shelley, *Phys. Fluids* **20**, 123304 (2008).
[2] D. Krishnamurthy and G. Subramanian, *J. Fluid Mech.* **781**, 422-466 (2015).
[3] C. López, *Phys. Rev. E* **72**, 061109 (2005).
[4] M.E. Cates and J. Tailleur, *Annu. Rev. Cond. Matt. Phys.* **6**, 219-244 (2015).

7.12 MAGNETIC ACTIVE MATTER - POSITIONING, SWIMMERS AND ROTORS

F. Meng, R. Golestanian
D. Matsunaga (Osaka), A. Zöttl (ESPCI), J. M. Yeomans (Oxford),
J. Hamilton (Exeter), F. Ogrin (Exeter)

Magnetic active or driven matter offers the possibility to control the collective responses of the particles and future applications by applying an external magnetic field.

Magnetic ellipsoid in a Hele-Shaw cell

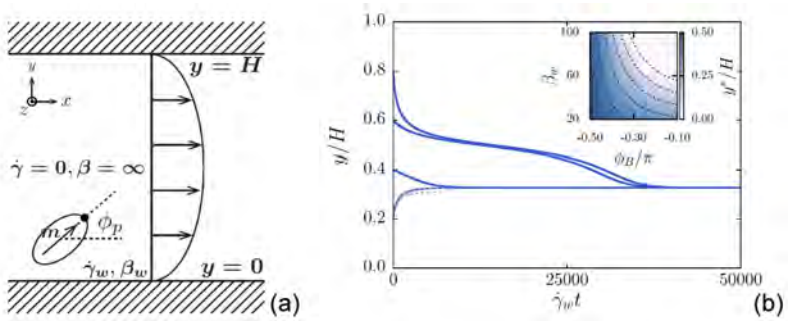

Figure 7.31: (a) System geometry. (b) Time history of particle position $y(t)$ from boundary element simulations. The inset shows stable fixed point y^*/H for ellipsoids ($\alpha = 3$) as a function of the magnetic field β_w and ϕ_B obtained by far-field theory. Parameters: $\beta_w = 60$ $\phi_B = -0.4\pi$ and channel width $H/a = 20$.

A permanent magnetic particle with prolate shape of volume $4\pi a^3/3$, is suspended in a Newtonian fluid of viscosity η. The particle is assumed to be neutrally buoyant for simplicity. It has one semi-axis of length $a\alpha^{2/3}$ and two of length $a\alpha^{-1/3}$, where α is the particle's aspect ratio.

There is a dimensionless parameter comparing the strength of the magnetic torque and the hydrodynamic torque: $\beta(y) = mB/[\eta a^3 \dot{\gamma}(y)]$, where m is the amplitude of the ellipsoid magnetic moment, B is the strength of the magnetic field, and $\dot{\gamma}(y)$ is the local shear rate of the flow. If the particle is placed in a Hele-Shaw cell, the background flow speed is $v_x^\infty(y) = \dot{\gamma}_w y(H-y)/H$, where $\dot{\gamma}_w$ is the local shear rate at the wall and H is the height of the cell. By considering the hydrodynamic interaction between the particle and the confining walls to the lowest order, i.e., the effect of the image stresslets due to the walls, the ellipsoid can be positioned stably to

$$\frac{y^*}{H}(\alpha, \beta_w, \phi_B) = \frac{1}{2} \pm \frac{\beta_w F(\alpha)}{8\pi[1+J(\alpha)]} \cos\phi_B \tag{7.3}$$

where β_w is the value of β at the wall, ϕ_B is the angle of magnetic field, $F(\alpha)$ and $J(\alpha)$ are functions of the particle aspect ratio. This model [1] can be utilised for particle separation in a lab-on-a-chip device.

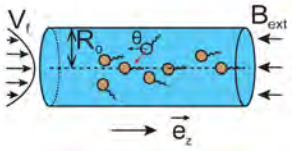

Figure 7.32: Magnetic swimmers in a microfluidic channel.

Magnetic swimmers in a microfluidic channel

A magnetic swimmer possesses a permanent magnetic moment $\mathbf{m}_0$ and self-propels with velocity $\mathbf{v}_0$. Under an external magnetic field, $-B_{\text{ext}}\mathbf{e}_z$, if the magnetic swimmers of uniform number density ρ_0 are suspended in a Poiseuille flow with velocity profile as $\mathbf{V}_\text{f}(r) = \mathbf{e}_z v_\text{f}(R_0^2 - r^2)/R_0^2$, i.e., in a microfluidic circular channel, the swimmers will be focused into the centre of the channel and can form clusters if satisfying the critical condition.

This applies to magnetic swimmers of small magnetic moment, such as magnetotactic bacteria, between which the magnetic dipole-dipole interaction between the swimmers are comparable with the thermal energy. Clustering here can be mapped to Cahn-Hilliard type phase transition, and hydrodynamic interaction between swimmers is also incorporated. For swimmers of large magnetic moment, our preliminary results show that the swimmers can be condensed into the centre of the channel, which constitutes as another new dynamic regime apart from the regime of focusing and clustering.

Clustering condition:

$$\frac{\mu_0 \rho_0 m_0^2}{4 k_B T} \frac{m_0 B_{\text{ext}}}{k_B T} \frac{v_f}{v_0} \geq 1. \quad (7.4)$$

where μ_0 is vacuum permeability, k_B is the Boltzmann constant, and T is the temperature.

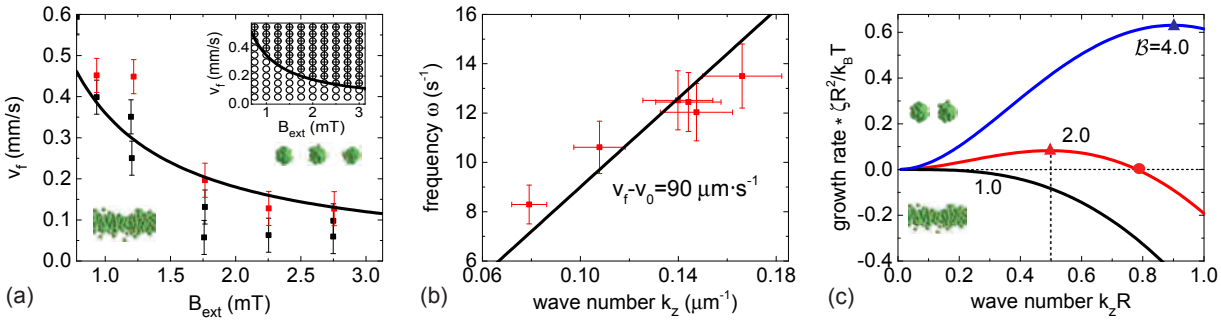

Figure 7.33: (a) Comparison between the prediction of Eq. (7.4) for the threshold of clustering (solid line) and the experimental data extracted from *Waisbord et al.* (where the black/red squares denote the experiments that led to non-clustering/clustering, respectively), in (v_f, B_{ext}) space. Upper inset: comparison between the theoretical prediction and our Brownian dynamics simulation for the threshold of clustering ($\circ$ for non-clustering and $\oplus$ clustering). (b) Fitting of the dispersion relation $\omega = k_z(v_f - v_0)$ with propagation speed $(v_f - v_0) = 90^{-}\text{m} \cdot s^{-1}$, corresponding to $B_{\text{ext}} = 2.8\text{mT}$ and $v_f = 180^{-}\text{m} \cdot \text{s}^{-1}$. (c) Growth rate versus wave number in systems of different conditions.

Magnetic rotors under an oscillating magnetic field

We designed the setup where magnetic rotors are subjected to an oscillating magnetic field. By performing experiment, numerical simulation and analytic modelling, our preliminary results show that the system has several dynamic regimes including quarter, stripe, staggered, mixed and chaotic patterns.

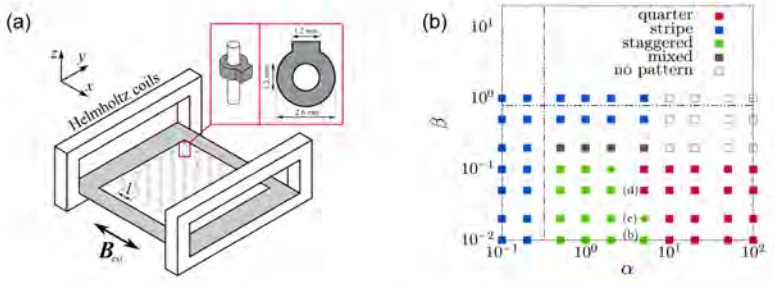

Figure 7.34: (a) Schematic of the experimental setup, consisting of a Helmholtz coil system, with the 3D printed pin system placed in the centre. The inset shows a rotor mounted on a pin and indicates its dimensions. (b) Phase diagram from theoretical prediction (dash lines) and simulation (squares).

[1] D. Matsunaga, F. Meng, A. Zöttl, R. Golestanian, J. M. Yeomans, Phys Rev Lett **119**, 198002 (2017).

[2] F. Meng, D. Matsunaga, R. Golestanian, Phys Rev Lett **120**, 188101 (2018).

[3] J. Hamilton, D. Matsunaga, F. Meng, R. Golestanian, F. Ogrin, J. M. Yeomans, under preparation (2018).

7.13 CURVATURE-GUIDED MOTILITY OF MICROALGAE IN CONFINEMENT

T. Ostapenko, J. Cammann, F.J. Schwarzendahl, T.J. Böddeker, C.T. Kreis, D. Lavrentovich, M.G. Mazza, O. Bäumchen

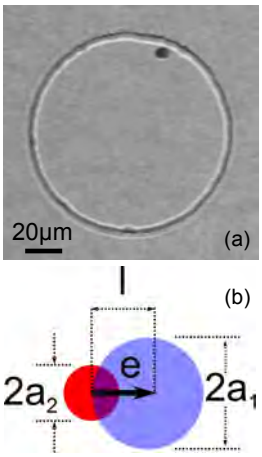

Figure 7.35: (a) Optical micrograph of a single microalga contained in a quasi-2D circular confinement. (b) Asymmetric dumbbell model representing the *Chlamydomonas* cell.

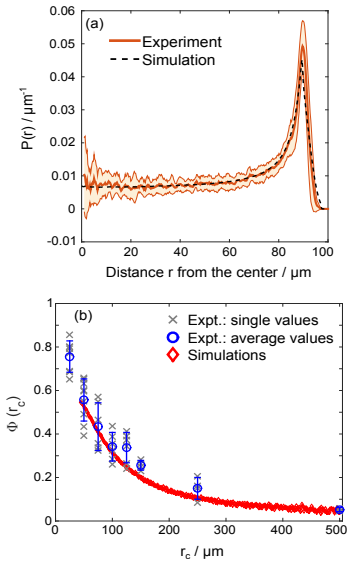

Figure 7.36: (a) Radial probability distribution $P(r)$: experiment (orange) and simulation (black dashed line). (b) Near-wall swimming probability $\Phi(r_c)$: experiments (blue circles) and simulations (red diamonds).

The characteristics of active fluids, such as suspensions of active colloids, droplets and biological microswimmers, may not only originate from the mutual interactions between the constituents, but also from their interactions with interfaces and confining walls. Such interactions have raised interest among researchers from several perspectives. First, the natural habitat of many living organisms are complex surface-dominated environments, e.g. liquid-infused soil, rather than bulk situations. Second, the confinement and, in particular, the exposure to solid/liquid interfaces plays an important role with regard to the adhesion of cell populations and, subsequently, the formation of biofilms.

Using experiments and Brownian dynamics simulations, we report on the motility of a single *Chlamydomonas* microalga in tailor-made microhabitats to elucidate the effects of geometric confinements on cellular motility [1]. We employed optical microscopy techniques and particle tracking to study the motility of a single wild-type *Chlamydomonas* cell contained within an isolated quasi-2D microfluidic compartment (Fig. 7.35a). We study precisely a single isolated cell in order to dissect the effect of boundaries on the motility, and to exclude any cell-cell interactions and collective effects.

In our Brownian dynamics simulations, the *Chlamydomonas* cell is modeled as an active asymmetric dumbbell consisting of two rigid spheres (Fig. 7.35b). The smaller sphere represents the cell body, and the larger sphere mimics the stroke-averaged area covered by the two anterior flagella during their beating. The Langevin equation represents a balance of forces, both deterministic and stochastic, experienced by the microswimmer [2]. All geometric and dynamic parameters that entered the simulations were either measured directly from our experiments or extracted from the literature.

We provide evidence for a pronounced near-wall swimming effect inside the circular compartment, for which we find excellent agreement between our experiments and simulations (Fig. 7.36a). We quantify the swimming statistics by defining the near-wall swimming probability, $\Phi(r_c)$, as the relative probability of finding the cell towards the wall as compared to the center. Fig. 7.36b displays $\Phi(r_c)$ for experiments and Brownian dynamics simulations, which all agree quantitatively and show a monotonic decrease for increasing compartment radius r_c.

To uncouple the effects of curvature from size-dependent geometric factors, we also consider elliptical chambers. We find in both experiments and simulations (Fig. 7.37) that the near-wall swimming probability in elliptical chambers increases monotonically with the corresponding local wall curvature [1]. The apex regions represent the regions of high near-wall swimming probability. In conclusion, we have established unambiguous evidence that the (local) wall curvature controls the motility of *Chlamydomonas* in confinement.

The relative probability density (see Fig. 7.37) provides information about the likelihood of the cell being found at a particular location within the microhabitat. However, the rates of change of the microstates, i.e. the probability fluxes of the swimmer, give an indication of where the swimmer is likely to move in the future. For an equilibrium system the transition rates between multiple microstates are equal, this fact is commonly referred to as “detailed balance". The hallmark of non-equilibrium physics is the imbalance of these transition rates, hence a “broken detailed balance” [3]. Since a living *Chlamydomonas* cell represents an out-of-equilibrium system, this leads us to the investigation of broken detailed balance.

We calculate the probability fluxes of the cell as it traverses locations of high and low curvature in elliptical microchambers. For circular compartments, rotational symmetry forbids a preferred angular direction, yielding no net probability fluxes. However, Fig. 7.39 demonstrates that gradients in wall curvature drive probability fluxes and conservation of probability leads to flux loops with net fluxes in the bulk. Again, we find excellent qualitative agreement between experiments and Brownian dynamics simulations. The dynamics inside the chamber appears to be dominated by the local wall curvature. As the natural habitats of *Chlamydomonas* involve a plethora of irregularly shaped interfaces, simulations (Fig. 7.38) indicate that shapes with even higher gradients of curvature appear to produce larger probability fluxes than shapes with lower gradients of curvature. By elucidating how boundaries statistically affect the behavior of microswimmers, we aim to understand how microbial colonies grow in complex environments and to develop new concepts for microfluidic technologies of living matter.

[1] T. Ostapenko, F.J. Schwarzendahl, T. Böddeker, C.T. Kreis, J. Cammann, M.G. Mazza, O. Bäumchen, *Phys. Rev. Lett.* **120**, 068002 (2018).
[2] J. Elgeti, R. G. Winkler, G. Gompper, *Rep. Prog. Phys.* **78**, 056601 (2015).
[3] C. Battle, et al., *Science*, **352**, 604–607 (2016).

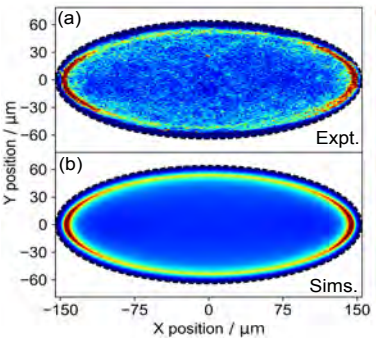

Figure 7.37: Relative probability density in an elliptical compartment with eccentricity = 0.91: (a) experiments and (b) simulations.

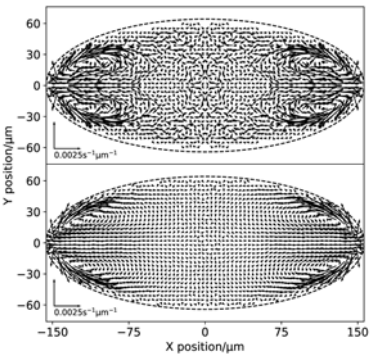

Figure 7.39: Probability fluxes for a single *Chlamydomonas* cell in an elliptical compartment with eccentricity = 0.91 for experiments (top) and simulations (bottom).

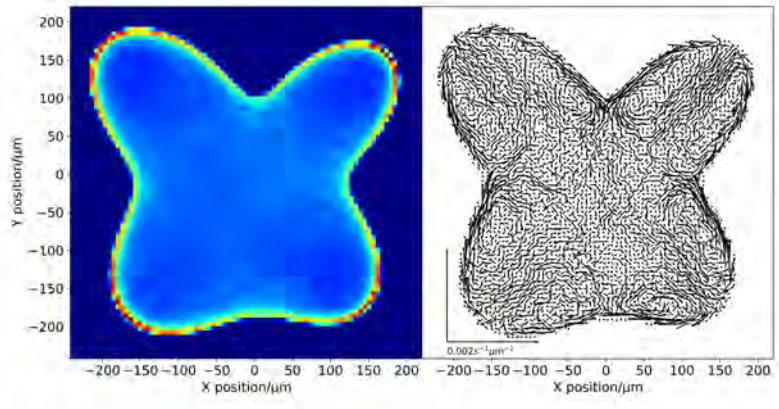

Figure 7.38: Relative probability density for the cell’s position (left) and probability flux (right) for simulations in a flower-shaped compartment with petals, each of which exhibits a different curvature gradient.

7.14 PERTURBATION OF PATTERN FORMATION IN D. DISCOIDEUM: EFFECTS OF OBSTACLES, FLOW, ELECTRIC FIELD AND CELL-TO-CELL VARIABILITY

A. Gholami, T. Eckstein, E. Vidal, I. Guido,V. Zykov, E. Bodenschatz
A. Bae (Rochester), K. H. Prabhakara (Illinois)

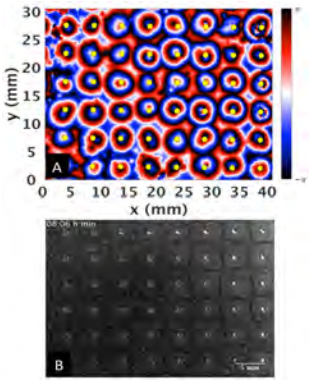

Figure 7.40: (A) Phase map of of the circular waves and (B) periodic domains around the pillars.

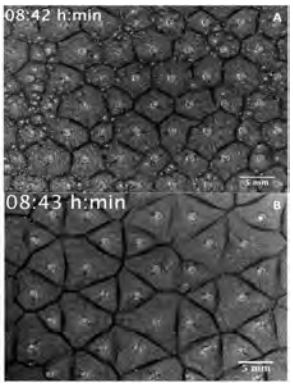

Figure 7.41: Hexagonal and triangular domains formed around the pillars with A) triangular and B) hexagonal arrangement, respectively.

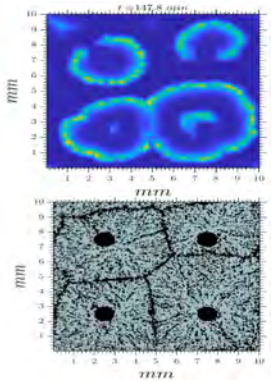

Figure 7.42: Numerical simulations of cAMP waves with four pillars as obstacles.

Upon starvation, Dictyostelium discoideum (D.d.) exhibit social behavior mediated by the chemical messenger cyclic adenosine monophosphate (cAMP). Large-scale cAMP waves synchronize the population of starving D.d. cells and enable them to aggregate and form a multicellular organism. In nature, D.d. cells are exposed to **external obstacles**, which can significantly influence the wave generation process. Here, we investigate the pattern formation of signaling D.d. amoeba in the presence of a periodic array of millimeter-sized pillars. In our experiments with caffeine treated cells, we observe concentric cAMP waves that initiate almost synchronously at the pillars and propagate outwards (Fig. 7.40). These waves have higher frequency than the other firing centers and dominate the system dynamics. The cells respond chemotactically to these circular waves and stream towards the pillars, forming periodic domains that reflect the periodicity of the underlying lattice. This phenomenon is also observed for triangular and hexagonal arrangement of the pillars leading to the formation of hexagonal and triangular domains, respectively (Fig. 7.41).

We performed comprehensive numerical simulations of a reaction-diffusion model to study the role of caffeine and characteristics of the boundary conditions given by the obstacles (Fig. 7.42). Our simulations show that a critical minimum accumulation of cAMP around the obstacles is required for the pillars to act as the wave source. This critical value depends on the cAMP production rate, a variable which we can experimentally decrease by adding caffeine. Experiments and simulations also show that in the presence of caffeine the number of firing centers is reduced which is crucial in our system for circular waves emitted from the pillars to successfully take over the dynamics. Moreover, our simulations reveal that caffeine reduces the excitability threshold of the cells and increases the sensitivity to cAMP accumulation around the obstacles. In the absence of caffeine, non-treated cells are less sensitive to cAMP accumulation around the pillars and ignore them. Another mechanism for wave creation observed in our simulations was a higher local density around the pillars. This can be achieved either by inhomogeneous initial conditions or by adhesion to the pillar after colliding due to random movement. These locally high density cell clusters then act as aggregation centers. Our results suggest that in nature the excitability threshold of the cells is tuned by an adaptation process that optimizes the sensitivity to waves while ignoring the cAMP accumulations around spatial heterogeneities which can interrupt the development process of the cells in complex environments [1].

Moreover, in their natural habitat in the forest soil, D.d. cells are subjected to **flows** which advect cAMP, thus affecting the signaling

process. We investigate the pattern formation of D.d. cells in a microfluidic setup under a constant buffer flow. The external flow advects the cAMP downstream, while the chemotactic cells attached to the solid substrate are not transported with the flow. At high flow speeds, elongated cAMP waves are formed that cover the whole length of the channel and propagate both parallel and perpendicular to the flow direction. While the wave period and transverse propagation velocity are constant, parallel wave velocity and the wave width increase linearly with the imposed flow (Fig. 7.43). We also observe that the acquired wave shape is highly dependent on the wave generation site and the strength of the imposed flow (Fig. 7.44) . We compared the wave shape and velocity with numerical simulations and found excellent agreement. We tested the dynamical state of the cells by abruptly setting the flow velocity to zero and observing the response of the waves. As the flow is turned off, we observe that the waves still propagate further downstream at slower speed of 0.4 mm/min. This type of response is expected in excitable systems where a pulse has defined characteristics given by the system to which the wave would return in the absence of flow [2].

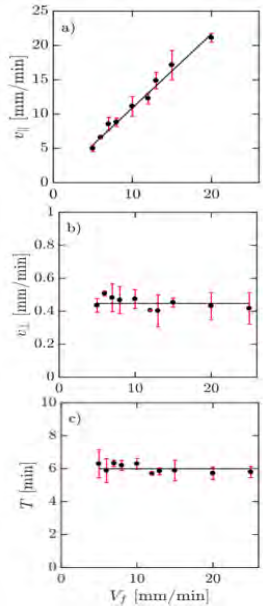

Figure 7.43: a-c) Wave speed and the wave period.

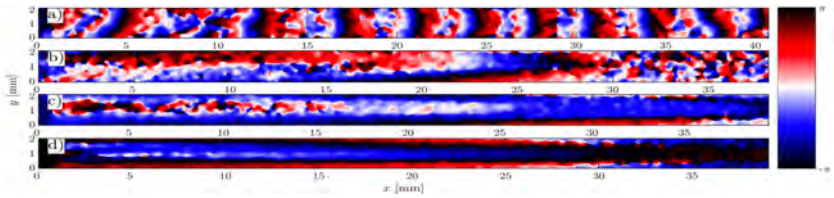

Figure 7.44: Phase map of the flow-driven waves showing different wave shapes at different imposed flow velocities. a-d) V_f = 0.5, 5, 10 and 15 mm/min.

Moreover, we explore the effect of **cell-to-cell variability** [2] in the production of cAMP on aggregation. We create a mixture of extreme cell-to-cell variability by mixing a few cells that produce cAMP (haves) with a majority of mutants that cannot produce cAMP (have-nots). Surprisingly, such mixtures aggregate, although each population on its own cannot aggregate. We show that a lack of divalent ions kills the haves at low densities and the have-nots supply the cAMP degrading enzyme, phosphodiesterase, which, in the presence of divalent ions, enables the mixture to aggregate. Our results suggest that a range of degradation rates induces optimal aggregation [3].

Cells have the ability to detect **DC electric fields** and respond to them with a directed migratory movement. Here we show that besides triggering a directional bias, the electric field influences the cellular kinematics of cells by accelerating their movement along their paths. We found that the migratory velocity of the cells in an electric field increases linearly with the exposure time. This finding opens new insights into the understanding of the mechanisms [3] that transduce the external stimulus into directed cell migration in an electric field and may offer a novel perspective towards wound healing assays.

[1] T. Eckstein*, E. Vidal*, A. Bae, and A. Gholami (under review)

[2] T. Eckstein*, E. Vidal*, A. Bae, V. Zykov, E. Bodenschatz, and A Gholami, Plos ONE, **13(3)**, e0194859 (2018)

[3] K. Prabhakara, A. Bae, and E. Bodenschatz (under review)

2. Essential to the survival of D.d. is its ability to self-organize by chemical signaling. However, in a population, there is significant cell-to-cell variability in cAMP production. How then is the signaling mechanism so robus. We intensified the cell-to-cell variability by mixing two kinds of cells, those that can produce cAMP, and mutants that cannot produce cAMP and thus cannot aggregate. Puzzlingly, when we add a small number of haves to a high density of have-nots, the mixture aggregates, whereas neither population aggregates on its own.

3. By analysing the effect of electric field on vegetative and briefly starved cells we found evidence that conditioned medium factor (CMF), a protein secreted by the cells, when they begin to starve, is an essential factor for triggering the electric sensing of the cells.

7.15 ACTIVE MATTER CLASS WITH SECOND-ORDER TRANSITION TO QUASI-LONG-RANGE POLAR ORDER

B. Mahault
X.-c. Jiang, X.-q. Shi (Soochow Univ., China), E. Bertin (Univ. Grenoble Alpes, France), A. Patelli, H. Chaté (CEA Saclay, France)

Dry active matter (DAM) refers to systems of motile agents for which the surrounding fluid can be neglected. When the dominating interactions between particles take the form of velocity alignment, a minimal description of such systems in the dilute limit can be achieved through Vicsek-style models [1]. The latter consider constant-speed point particles in 2 dimensions aligning their velocities locally in competition with noise. The symmetries of alignment (ferromagnetic or nematic) and motion (polar or apolar) then determine the class to which the model belongs. All three main classes studied thus far[4] display a transition to (quasi-)long-range order occurring via phase separation between a disordered gas and an ordered liquid [2].

In this work, we have shown that a nontrivial critical behavior can nevertheless be found in a new class of aligning DAM in which particles carry an intrinsic polarity $\mathbf{p}$ that they align ferromagnetically, and move at constant speed with stochastic reversals in the directions given by $\pm\mathbf{p}$. Like in all Vicsek-style models, the main control parameters governing the dynamics are the mean density of particles ρ_0 and the strength of the noise η. We numerically determined the phase diagram of the model (Fig. 7.45), and found a transition from a disordered gas to a quasi-ordered phase, in which the time-averaged global magnetization of the system decreases algebraically with system size with continuously varying exponents. Moreover, our simulations do not show any sign of phase separation at the transition, which looks continuous. This observation is supported by an analysis of kinetic and hydrodynamic equations derived from the microscopic dynamics in Ref. [3]. Because, in this case and contrary to the other classes, velocity and order fields are no more identical, we find that this problem exhibits a qualitatively different analytic structure. Therefore, no phase separation can occur at the transition, in qualitative agreement with microscopic simulations.

Despite these apparent similarities with the equilibrium XY model, a numerical study of the transition, detailed in [3], leads to conclude that it does *not* belong to the Berezinskii-Kosterlitz-Thouless universality class [4]. Our results, on the contrary, are consistent only with the assumption that the correlation length diverges algebraically at the critical point. We rationalize these findings by showing that the role of defects is deeply modified by the interplay of density and order (see Fig. 7.46), characteristic of aligning DAM. Indeed, in this system defects can no more be considered as singularities of the order field, such that the equilibrium Coulomb gas picture breaks down.

4. Polar particles with ferromagnetic interactions define the *polar* class, the same particles that align their velocities nematically constitute the *self-propelled rods* class, finally apolar particles with nematic alignment form the *active nematics* class.

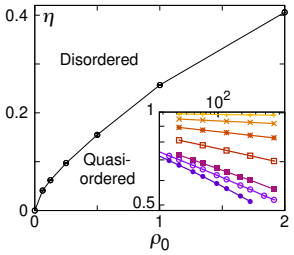

Figure 7.45: Phase diagram of the model in the (ρ_0, η) plane showing a single transition line. Inset: magnetization as function of system size for $\rho_0 = 1$ and, going downwards, $\eta = 0.05$, 0.1, 0.15, 0.2, 0.24, 0.25, and 0.26.

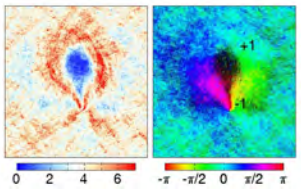

Figure 7.46: Snapshot of density and polarity orientation fields from a simulation of the microscopic model starting with a pair of ± 1 defects deep in the quasi-ordered phase. Because of the coupling between density and order, the $+1$ defect expels particles from its core such that it always forms a sparse disordered region whose diameter grows deterministically like $\sqrt{t}$. I can thus no more be considered as a point-like object.

[1] T. Vicsek *et al.*, Phys. Rev. Lett. **75**, 1226 (1995).
[2] A.P. Solon, H. Chaté, J. Tailleur, Phys. Rev. Lett. **114**, 068101 (2015).
[3] B. Mahault *et al.*, Phys. Rev. Lett. **120**, 258002 (2018).
[4] J.M. Kosterlitz, D.J. Thouless, J. Phys. C **6**, 1181 (1973).

7.16 TURBULENT PATTERN FORMATION IN ACTIVE FLUIDS

M. James, M. Wilczek
W.J.T. Bos (École Centrale de Lyon)

Biological flows are among the most feature-rich flows in nature. For example, active fluids such as dense bacterial or microtubule suspensions exhibit a fascinating range of dynamical states ranging from well-ordered patterns to spatio-temporal chaos. The fundamental properties and dynamics of such non-Newtonian fluids can be studied through continuum models. A fairly general class of models combines hydrodynamic equations of motion with aspects of pattern-forming systems. In these models, active stresses and free-energy-minimizing dynamics give rise to linear instabilities and nonlinear saturation which couple to nonlinear advection.

We investigate a class of continuum models of the form $\partial_t \omega + \lambda \boldsymbol{u} \cdot \nabla \omega = L(\nabla; \alpha)\omega + N(\omega)$ in two dimensions. Here, ω is the vorticity, and $\boldsymbol{u}$ is the velocity of the active fluid. L and N denote linear and nonlinear operators, respectively. The linear operator L introduces an instability, whose strength is controlled by the parameter α. The parameter λ controls the relative strength of advection as compared to the nonlinearity N. By choosing different forms for L and N, we analyze the properties of the active fluid system. This description captures a variety of phases including classical lattices, active turbulence and a novel self-organized quasi-stationary hexagonal lattice state, which emerges from an extended turbulent transient [1, 2]. Figure 7.47 maps out the phase diagram. The active turbulent phase, shown in Fig. 7.47 (d), is reminiscent of two-dimensional hydrodynamic turbulence, which inspired us to employ tools from turbulence theory to develop a statistical theory for active fluids. The eddy-damped quasi-normal Markovian (EDQNM) closure theory enabled us to clarify the role of upscale energy transfer in two-dimensional active fluids and to quantitatively capture their correlations (Fig. 7.48). Surprisingly, the upscale energy transfer mediated by background fluctuations also plays an important role in the emergence of the vortex lattice (Fig. 7.47 (e)): It leads to the emergence of the pattern on a length scale corresponding to the neutral mode of the dispersion relation rather than the fastest growing one. The turbulent pattern formation underlying the emergence of the vortex lattice is therefore markedly different from classical pattern formation mechanisms. Currently, we investigate how this phenomenon depends on the type of active fluids and parameters like system size. Preliminary results point at intriguing analogies to ferromagnetic spin systems as well as to the occurrence of phenomena such as supertransients. Experimental realizations of the turbulent lattice phase and theoretical investigations into its properties are exciting directions for future research.

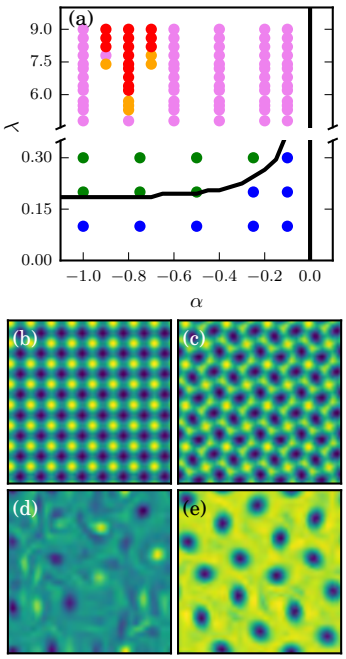

Figure 7.47: (a) Phase diagram of the active fluids model. The blue, green, violet and red dots correspond to phases (b), (c), (d) and (e), respectively. The orange dots correspond to the intermittent patterns. The black curve is the marginal stability line for the classical square-lattice state.

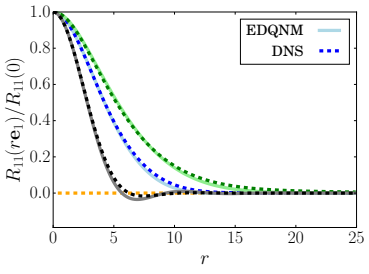

Figure 7.48: The spatial correlation function of the active turbulence velocity field as computed through direct numerical simulations (dashed curve) and the EDQNM closure theory for different choices of parameters. [2]

[1] M. James, M. Wilczek, Europ. Phys. J. E **41**(2), 21 (2018)
[2] M. James, W.J.T. Bos, M. Wilczek, Phys. Rev. Fluids **3**(6), 061101 (2018)

7.17 CILIA DRIVEN FLOWS AND THE ESTABLISHMENT OF LEFT-RIGHT ASYMMETRY IN EMBRYONIC DEVELOPMENT

A. Vilfan
R. R. Ferreira, J. Vermot (IGBMC Strasbourg),
F. Jülicher (MPIPKS Dresden), W. Supatto (Paris)

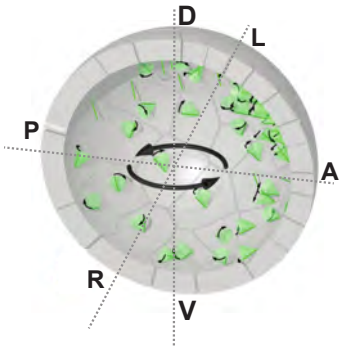

Figure 7.49: Schematic view of Kupffer's vesicle. Cilia (green) beat in a way that they describe tilted cones in clockwise direction, leading to a global rotational flow (black arrows). Directions: **D**orsal, **V**entral, **A**nterior, **P**osterior, **L**eft, **R**ight.

Chirality is the property of asymmetry between an object and its mirror image. Most biomolecules are chiral, but the mechanism that transfers this nano-scale chirality to the macroscopic body asymmetry is still not well understood. Among the many mechanisms for left-right asymmetry establishment that exist in animals and plants, the most studied is certainly the vertebrate left-right organizer. In zebrafish, a common model organism in developmental biology, it is called Kupffer's vesicle (KV) and forms a fluid-filled cavity with a diameter of $\sim 60\,\mu$m, surrounded by cells that together contain some 70 cilia (Fig. 7.49). These cilia rotate clockwise – a sense of rotation that is determined by the chirality of their molecular structure – and thereby induce a rotational flow in the cavity. Two questions where physics is central for understanding the function of the left-right organizer concern the flow generation and the flow detection [1].

There are theoretically two possibilities how rotating cilia can generate global flow: (i) Cilia can move along cones perpendicular to the surface. If they have the maximal density at the dorsal pole, they can produce a net rotational flow around the dorso-ventral axis. (ii) Similar rotational flows can be achieved if cilia are uniformly distributed, but tilted in meridional direction towards the dorsal pole. A coarse-grained approach that only considers the far-field flows induced by dense ciliary carpets shows that mechanism (i) leads to a flow that is weaker by a factor $(3L/8R)\cos\psi/\sin\theta_0 \approx 0.1$, where L is the length of a cilium, R the radius of the cavity, ψ the opening angle of the cone and θ_0 the maximal tilt of a cilium. Imaging in live embryos confirmed a consistent tilt of cilia, but no dorso-ventral density gradient. We then used experimentally obtained cilia maps to compute the flow patterns in individual embryos in more detail. The average flow in mature KVs is shown in Fig. 7.50A. We quantified the intensity of the rotational flow

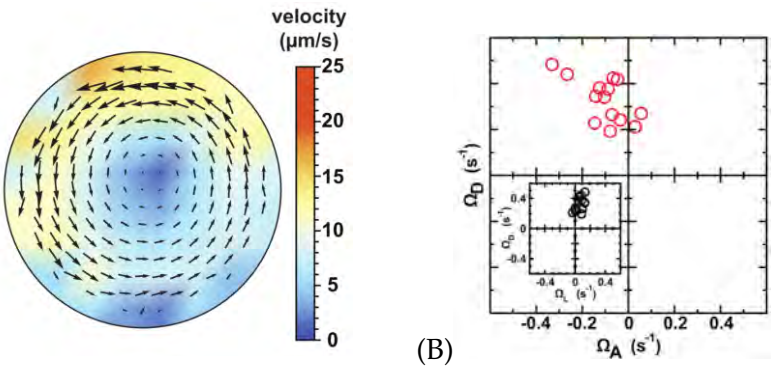

Figure 7.50: (A) Average flow profile in a KV, calculated from experimental 3D cilia maps. Robust rotational flow is visible. (B) The effective angular velocity vector from individual embryos, as seen from the right (main panel) and from posterior (inset). Despite great variability, all embryos display rotational flow, approximately around the dorso-ventral axis.

using the effective angular velocity, defined through the total angular momentum of the fluid. Circulatory flow around the dorso-ventral axis is a robust feature of all KVs, although there is also substantial variability from embryo to embryo (Fig. 7.50B).

A more precise analysis of cilia orientations shows that at later stages cilia orientations are already asymmetric and that this asymmetry even arises in mutants without ciliary motility [2]. This could indicate the existence of some tissue-scale chirality that is already present before the symmetry breaking event in the left-right organizer takes place. However, an alternative explanation is that the cells are still symmetric, but that the cilia orientation does not directly follow the direction of cell polarity.

The flow detection mechanism that recognizes the left side and triggers the signalling cascade has not yet been identified. Possible suggestions include direct detection through mechanosensitive cilia and transport of particles by the cilia driven flow. We therefore investigated the physical limits of the proposed flow detection mechanisms and compared them with the conditions found in the KV. The reliability of mechanosensory flow detection is severely restricted by the weakness of the flow and by its spatial variability. Figure 7.51 shows the distribution of torques on hypothetical immotile sensory cilia. Robust side detection is only possible if the signal is not only time-averaged, but also ensemble-averaged over at least 3 sensory cilia on each side. However, most KVs have fewer than 3 immotile cilia on each side. Our analysis therefore does not support the mechanosensory hypothesis.

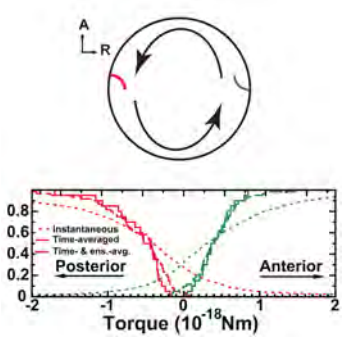

Figure 7.51: Test of the mechanosensory hypothesis. The lines show cumulative histograms of torques acting on immotile sensory cilia on the left (red) and right (green) side of the KV, calculated from N=20 experimentally mapped embryos. A gap around 0 is a pre-requisite for mechanosensory flow detection, and it only exists for time- and ensemble-averaged torques.

Alternatively, signalling particles could be secreted in the anterior region, carried to the left by the rotational flow, and then captured by the cilia. Simulations combining Brownian motion with drift in the calculated velocity field show that particles with a Stokes radius above $\sim 2\,\mathrm{nm}$ can provide a reliable readout.

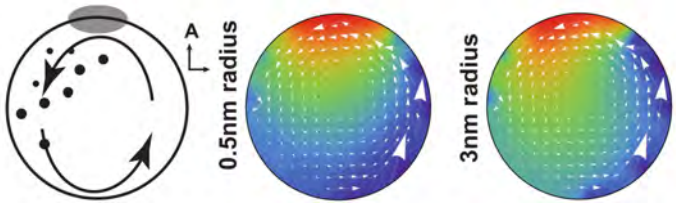

Figure 7.52: Test of the chemical hypothesis: particles are released in the anterior and move diffusively in the rotating flow. Particles with Stokes radius larger than a few nanometers can establish a robust left-right asymmetry.

Although the molecular nature of the flow detection remains obscure, our analysis of physical limitations provides strong evidence to rule out mechanical flow sensing and at the same time shows that morphogene transport can provide a robust side discrimination mechanism. It also allows us to predict the minimum size of the signaling particle, which will eventually facilitate the search for it.

[1] R. R. Ferreira, A. Vilfan, F. Jülicher, W. Supatto and J. Vermot, eLife **6**, e25078 (2017)

[2] R. R. Ferreira, G. Pakula, L. Klaeyle, H. Fukui, A. Vilfan, W. Supatto and J. Vermot, Cell Reports **25**, 2008-2016 (2018)

7.18 OUT-OF-PLANE BEATING COMPONENTS OF ACTIVE AXONEMES ISOLATED FROM C. REINHARDTII

A. Gholami, E. Bodenschatz
S. Mojiri, S. Isbaner, J. Enderlein (Göttingen University)
A. Bae (Rochester)

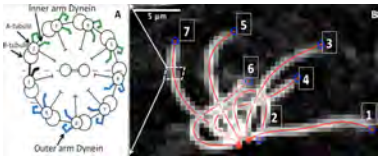

Figure 7.53: A) Structure of an axoneme formed of nine microtubule doublets at the periphery and two microtubule singlets at the center. (B) Wave-like deformations of an axoneme isolated from C. reinhardtii, demembranated and reactivated in the presence of ATP. This axoneme is attached from one side to the substrate and rotates around the anchoring point.

Cilia and flagella are slender cellular protrusions composed of a microtubule based structure called the axoneme. To mediate motility, the axoneme undergoes regular oscillatory bending waves that propel cells through fluids, and fluids across the surfaces of cells. These bending waves emerge from the interplay of active internal stresses generated by dynein motor proteins within the structure, which induce locally a relative sliding of microtubules. In addition to sliding forces, axonemal dyneins can also generate torques, which rotate microtubules in *in vitro* assays [1]. In the axoneme, this rotation will lead to twist. It is thought that both shear stresses (associated with sliding forces) and transverse stresses (associated with torques) can be used to regulate motors and generate periodic beating patterns. The twist stiffness of axoneme is provided by the doublet sliding stiffness κ_s. Since twisting the axoneme involves bending of the microtubule doublets, their bending stiffness κ couples to the twist stiffness κ_s. The competetion of sliding and bending of the axoneme during twist is characterized by the length scale $d \sim \sqrt{(\kappa/r^2\kappa_s)}$, where $r = 100$ nm is the radius of axoneme and d is estimated to be between 3.5 and 10 μm [2]. At this length scale twist deformations decay along the axoneme in response to spatially localized motor forces or torques. Note that the torsional stiffness of the

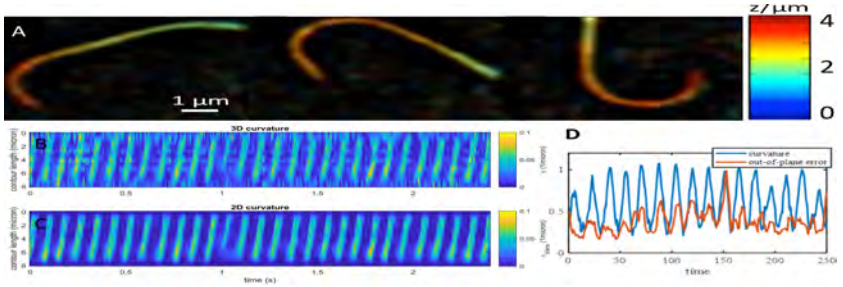

Figure 7.54: (A) Different configurations (B, C) 2D and 3D curvature and (D) out of plane error measured for an active axoneme. Images are captured at 150 Hz using multi-plane imaging technique in which color code indicates the depths of the axoneme in z direction.

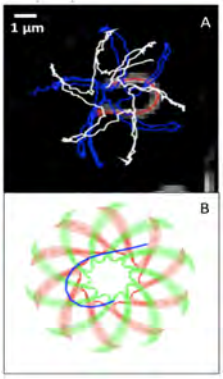

Figure 7.55: (A) The red curve represents the tracked centerline of an actively beating axoneme in 2D. The white path depicts the trajectory of the basal end, which is the leading end during swimming. The tip is tracked with the blue line. (B) Simulated trajectories based on resistive force theory.

axoneme could also have contributions from the torsional stiffness κ_3 of individual microtubule doublets. This contribution becomes relevant when doublets are constrained not to rotate around their axis, and results in a net torsional stiffness $\kappa_3 + r^4 k_s$. Estimating $\kappa_3 \sim \kappa$, we have that $\kappa/(r^4\kappa_s) \sim (d/r^2) \sim 10^3$. Here we use the novel multi-plane phase contrast imaging technique to record the three dimensional beating pattern of isolated axonemes from C. reinhardtii that beat in the vicinity of a substrate. We measure the curvature and the torsion of the axoneme along the contour length with high spatio-temporal resolution. These measurements show that torsion of the axoneme is with a factor of 10^3 smaller than curvature, consistent with the rough calculations above.

[1] Furuta, A., et al., J. Biological Chemistry, 284(9), 5927-5935 (2009).
[2] Sartori, P., et al. Phys. Rev. E., 94, 042426 (2016).

7.19 HYDRODYNAMIC INTERACTIONS OF CILIA ON A SPHERICAL BODY

B. Nasouri
G. J. Elfring (UBC, Vancouver)

To propel themselves in an inertialess environment, many microorganisms use small whip-like extensions, called flagella (when they possess one or two) or cilia (when they possess many). The cyclic motion of each cilium in a chain can form a coordinated pattern of beating, wherein each pair of neighboring cilia are orbiting with a constant, nonzero, phase difference [1]. As a result of this synchrony, the tips of cilia form a moving wave, known as a metachronal wave, which may arise from their hydrodynamic interactions [2]. Here, we investigate such interactions in ciliary chains of microorganisms such as *Paramecia* and *Volvox* in which the ciliate body is curved and imposes a periodicity to the dynamical system.

To model such a system, we consider a chain of identical cilia, uniformly distributed around a spherical ciliate body, as shown in Fig. 7.56. We use the bead and spring model to capture the motion of the cilia, which allows each cilium to elastically deviate from its prescribed circular trajectory in response to the background flow induced by the other cilia [3]. In the asymptotic limit where the cilia are far from one another and also their lengthscale is much smaller than the size of the ciliate body, we find that the chain evolves to a stable state of full synchrony. The cilia eventually beat with identical frequencies and zero phase differences at equilibrium, as shown for chains of 10 and 15 cilia in Fig. 7.57. Our results suggest that the natural periodicity embedded in the geometry of the ciliate body, along with the elasticity of the cilia, prevents formation of any metachronal waves [4]. Thus, introducing an asymmetry to the system (see for example Rep. 7.17) may be necessary to capture a wave-like behavior.

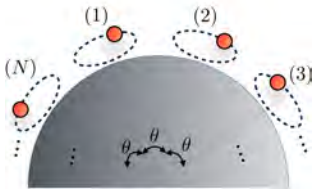

Figure 7.56: Schematic of a chain of N cilia around a spherical body

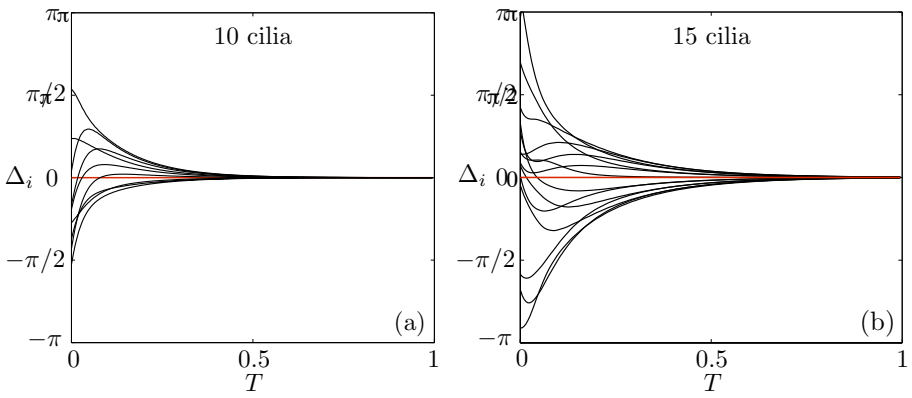

Figure 7.57: Synchronization of a chain of (a) 10 and (b) 15 identical cilia distributed uniformly around a spherical body, with random initial phases. Each line indicates the evolution of the phase difference for cilium i compared to a reference cilium (Δ_i), over a dimentionless time period T.

[1] E. W. Knight-Jones, J. Cell Sci. **s3-95**, 503 (1954)
[2] M. C. Lagomarsino, P. Jona, B. Bassetti, Phys. Rev. E **68**, 021908 (2003)
[3] T. Niedermayer, B. Eckhardt, P. Lenz, Chaos **18**, 037128 (2008)
[4] B. Nasouri, G. J. Elfring, Phys. Rev. E **93**, 033111 (2016)

7.20 RECONSTITUTION OF SYNTHETIC CILIA

I. Guido, R. Golestanian, A. Vilfan, E. Bodenschatz
K. Oiwa (NICT, Kobe)

Cilia are microtubule-based organelles, hair-like structures that protrude from the surface of many eukaryotic cells. They exhibit a rhythmic waving or beating motion and generate flow by exerting mechanical force. Motile cilia are present on the surface of several cell types such as epithelial cells in airways and reproductive tracts or on the ependyma and choroid plexus in brain [1]. Although more than 200 proteins were identified in the motile cilia, their motility is driven by outer and inner arm dyneins with the innen arm dyneins being responsible for the wave form and the outer arm dyneins adjusting ciliary beat frequency [2, 3]. Although cilia are the oldest observed cell organelles, discovered by Van Leeuwenhoek in 1657[5], the mechanism underlying their beating is still unknown.

5. *In September 1675 Antony Van Leeuwenhoek, using a simple mounted lens and a method of observation known only to himself, possibly darkfield microscopy, saw a living protozoan in rain water whose belly was flat, "provided with divers incredibly thin feet, or little legs, which were moved very nimbly". On June 28, 1713, concerning cilia, Leeuwenhoek wrote: "One can't be satisfied with just looking at so wonderful a structure: chiefly because one can't get clear on how such an unbelievable motion is brought about".* From [5].

Our work focuses on building synthetic biomimetic beating structures that resemble the natural cilia and therefore allow us to get an insight into the mechanism that drives cilia to beat with a stroke and a recovery phase. These structures rely only on few biological cilia constituents such as the framework of microtubules and the motor proteins for force generation. This bottom-up approach has the advantage of reducing a complex structure such a cilium to a minimal system that we can study in terms of biopolymers and force generators. Although the basic function of cilia has been the topic of many theoretical studies, to our knowledge an appropriate experimental setup constituted by biofilaments and motor proteins does not exist yet.

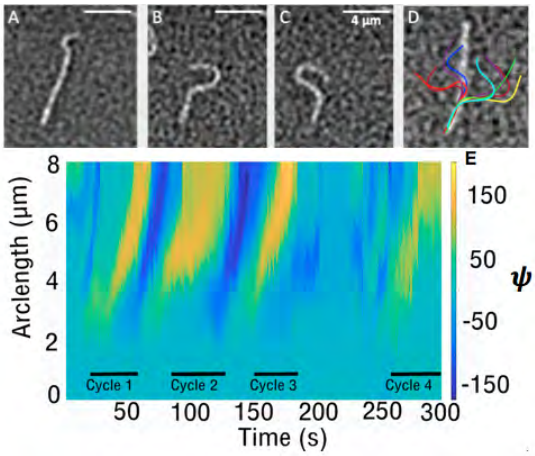

Figure 7.58: A-C. One oscillation cycle of a single microtubule decorated with motor proteins. D. Filament tracking shows the time evolution of the emergent oscillations. E. Kymograph of the tangent angle along the filament over time.

In Fig. 7.58 A-D we show our proof of concept of a 2D minimal beating structure. We synthetically assembled a system made of one microtubule clamped to a fixed point and decorated with few motor proteins (Kinesin-1), organized as clusters in a tetrameric configuration. This structure performed sustained oscillations when the motor

proteins interact with surfaces where the protein adsorption is drastically reduced by a polylysine grafted polyethyleneglycol (PLL-g-PEG) functionalization. The movement can be modulated by tuning the concentration of motor proteins and it is inhibited by removing the surface functionalization. The propagation of the tangent angle along the filament over time is shown in the kymograph in fig. 7.58-E.

By adding a non-adsorbing polymer, polyethylene glycol (PEG), an attractive interaction between microtubules is induced that leads to the assembly of bundles. The reduced distance between microtubules increases the probability that the motor proteins clusters simultaneously bind and walk along close microtubules [4]. We used this approach and assembled microtubule bundles which show continuous bending and buckling in 3D (Fig. 7.59). Besides these beating structures which resemble ciliary behavior without using the cilia components, we aimed to get closer to the natural cilia by using axonemal dynein as force generator. We assembled an active system made of microtubules and outer arm dynein, which was extracted from flagella of *Chlamydomonas Reinhardtii* [6, 7]. The system presents continuous beating involving association and dissociation cycles similar to the sliding of a pair of doublet microtubules from a frayed Chlamydomonas flagellum [8] as can be seen in fig. 7.60.
To our knowledge this system can be considered the first synthetic axoneme which presents a behavior that resembles the natural system and can provide insight into the complex mechanism of ciliary beating.

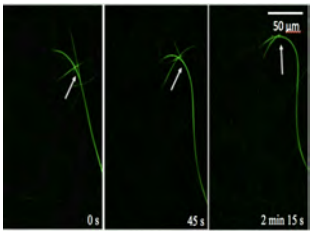

Figure 7.59: Time series depicting bending of long, actively beating microtubule bundle.

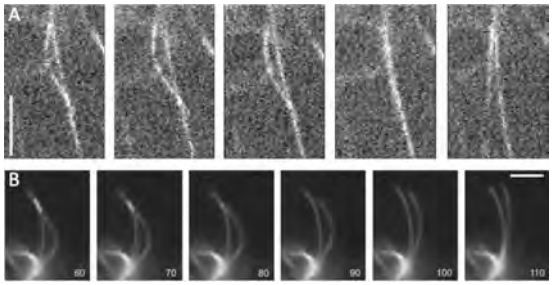

Figure 7.60: A. Cycle of a synthetically assembled system composed of microtubules and axonemal dynein. Scale bar: 3 μm. B. Sliding of a pair of doublet microtubules from a frayed Chlamydomonas flagellum [8]. Scale bar: 5 μm.

[1] I. Ibañez-Tallon, N. Heintz, H. Omran, Hum Mol Genet. **12**, R27 (2003)
[2] R. Hard, K. Blaustein, L. Scarcello, Cell Motil. **21**, 199 (1992)
[3] C. J. Brokaw, R. Kamiya, Cell Motil. **8**, 68 (1987)
[4] T. Sanchez, D. Welch, D. Nicastro, Z. Dogic, Science **333**, 456 (2011)
[5] P. Satir, Cell Motil. **32**, 90 (1995)
[6] H. Sakakibara, H. Kojima, Y. Sakai, E. Katayama, K. Oiwa, Nature **400**, (1999)
[7] I. Takashi, H. Sakakibara, K. Oiwa, J. Mol. Biol. **368**, 1249 (2007)
[8] S. Aoyama, R. Kamiya, Biophys J. **89**, 3261 (2005)

7.21 BACTERIAL TRAIL-MEDIATED SELF-ORGANIZATION AND SURFACE SENSING

R. Golestanian
A. Gelimson, W.T. Kranz, R.R. Bennett (Oxford),
C.K. Lee, J. de Anda, Y. Luo, E.Y. Lee, J.A. Keefe, J.S. Helali, J. Ma,
K. Zhao, G.C.L. Wong (UCLA),
A.E. Baker, G.A. O'Toole (Dartmouth)

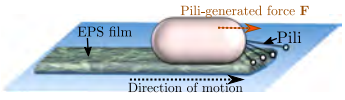

Figure 7.61: Schematic depiction of a microscopic model system such as *P. aeruginosa* that uses pili for motility and sensing. The surface-moving microorganism leaves behind an exopolysaccharide (EPS) trail that will be sensed by others.

For many animals and microorganisms it is advantageous to know where their companions or they themselves have been. To this end, many creatures leave trails of some characteristic substance; see Fig. 7.61 for a schematic of a bacterial trail. For bacteria, these trails are often subsumed as exopolysaccharides (EPS). To be evolutionarily favorable, the (energetic) costs incurred by trail formation should balance the advantages gained through this form of communication.

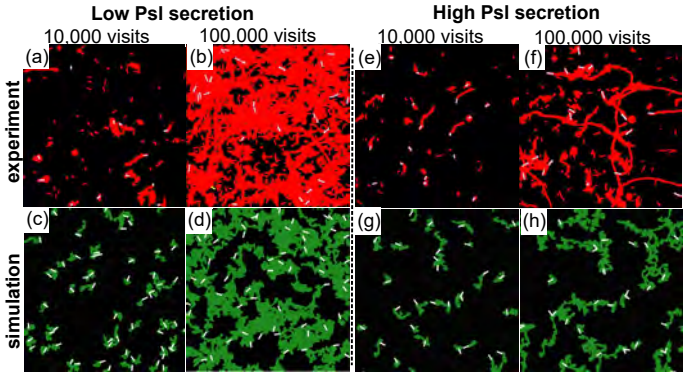

Figure 7.62: Snapshots of bacterial positions (blue and white) and a typical cumulative surface coverage i.e. surface areas visited by bacteria over time from experiments (red) and simulations (green) for the case of low Psl deposition (a)–(d) and high Psl deposition (e)–(h).

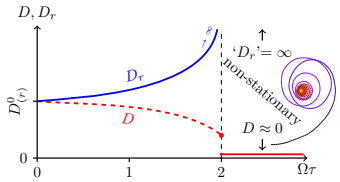

Figure 7.63: Phase diagram of the dynamics of the microorganism with trail-mediated self-interaction, as a function of the dimensionless turning frequency $\Omega\tau$ that is a measure of the rate of trail deposition.

Trail secretion provides a medium for communication between bacteria, leading to a mechanism whereby single-bacterium motion determines large-scale colony structure [2]. A model system for this are the pathogenic bacteria *P. aeruginosa*, which secrete the polysaccharide Psl and propel themselves using appendages called Type-IV pili. Following experimental data for the motion of single bacteria, we have derived and adjusted a mechanistic model for the interaction between pili and Psl. In the collective limit, without further adjustments, the same model also explains the experimentally observed large-scale structures in the early stages of biofilm formation; see Fig. 7.62. Trail-mediated self-interaction could also play a significant role in the behavior of microorganisms. In particular, it provides a mechanism to tune the effective translational and orientational diffusivities as a function of the trail deposition rate (see Fig. 7.63 and note a novel localization transition at a finite threshold). This can help bacteria modify their search strategy. A nontrivial perpendicular alignment mechanism is responsible for modulating the orientation of bacteria [1] resulting on the aforementioned control.

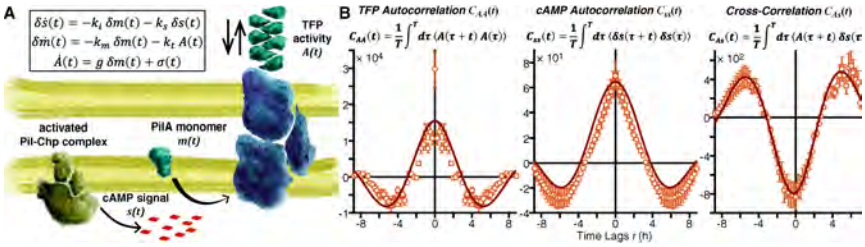

Figure 7.64: Multigenerational cAMP-TFP signal transduction drives memory and memory loss. (a) Schematic of the stochastic model that describes multigenerational cAMP-TFP signal transduction, illustrating the model components (PilA monomer $m(t)$, cAMP signal $s(t)$, and TFP activity $A(t)$). Inset shows the equations relating these components. (b) Comparison of model and experiments using the correlation functions $C_{AA}(t)$ (left), $C_{ss}(t)$ (center), and $C_{As}(t)$ (right) calculated from data for one wild-type family.

Using multigenerational, single-cell tracking we have explored the earliest events of biofilm formation by *P. aeruginosa* [3]. During initial stages of surface engagement, the surface cell population of this microbe comprises overwhelmingly cells that attach poorly with little increase in surface population. If we harvest cells previously exposed to a surface and direct them to a virgin surface, we find that these surface-exposed cells and their descendants attach strongly and then rapidly increase the surface cell population. This "adaptive," time-delayed adhesion requires determinants we showed previously are critical for surface sensing: type IV pili (TFP) and cAMP signaling via the Pil-Chp-TFP system. We find that these surface-adapted cells exhibit damped, coupled out-of-phase oscillations of intracellular cAMP levels and associated TFP activity that persist for multiple generations, whereas surface-naïve cells show uncorrelated cAMP and TFP activity. These correlated cAMP–TFP oscillations, which effectively impart intergenerational memory to cells in a lineage, can be understood in terms of a stochastic model based on the Pil-Chp-TFP framework (see Fig. 7.64). Importantly, these cAMP–TFP oscillations create a state characterized by a suppression of TFP motility coordinated across entire lineages and lead to a drastic increase in the number of surface-associated cells with near-zero translational motion. The appearance of this surface-adapted state, which can serve to define the historical classification of "irreversibly attached" cells, correlates with family tree architectures that facilitate exponential increases in surface cell populations necessary for biofilm formation.

The studies are related to the general question of structure formation in early forms of life [4], and the morphology of growing bacterial colonies and biofilms (cf. section 7.28).

[1] W.T. Kranz, A. Gelimson, K. Zhao, G.C.L. Wong and R. Golestanian, Phys. Rev. Lett. **117**, 038101 (2016)

[2] A. Gelimson, K. Zhao, C.K. Lee, W.T. Kranz, G.C.L. Wong and R. Golestanian, Phys. Rev. Lett. **117**, 178102 (2016)

[3] C.K. Lee, J. De Anda, A.E. Baker, R.R. Bennett, Y. Luo, E.Y. Lee, J. Keefe, J. Helali, J. Ma, K. Zhao, R. Golestanian, G.A. O'Toole, and G.C.L. Wong, Proc. Natl. Acad. Sci. U. S. A. **115**, 4471 (2018)

[4] R. Golestanian, Nature Phys. **13**, 323 (2017)

7.22 MICRO-SWIMMERS IN A SIMPLE VORTEX FLOW: FROM HAMILTONIAN DYNAMICS TO CLUSTERING

J.A. Arguedas-Leiva, M. Wilczek

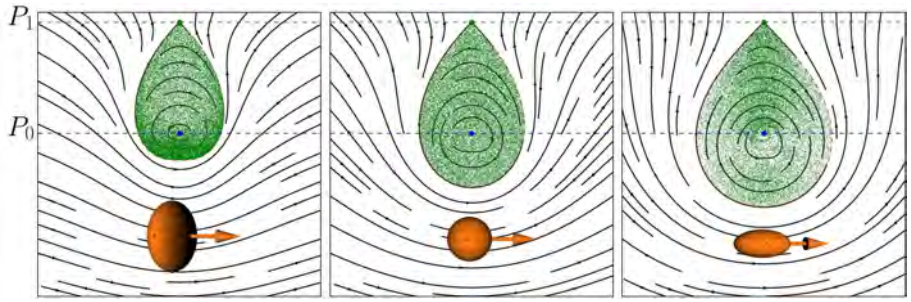

Figure 7.65: The phase space of swimmers in an axisymmetric flow is effectively two-dimensional and features a center (P_0) and saddle (P_1) fixed-point pair. The homoclinic orbit of the saddle-point encloses the area of closed bound orbits. Introducing an effective swimming velocity for different swimmer shapes allows us to map different shapes to topologically equivalent phase spaces.

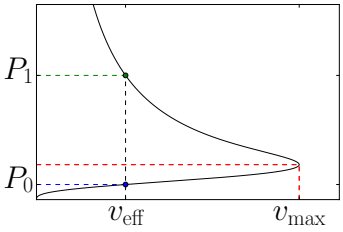

Figure 7.66: The dissapearance of the homoclinic orbit by a saddle-node bifurcation illustrates the role of the effective swimming velocity v_{eff}. After it exceeds v_{max}, the fixed points annihilate and no swimmers remain near the vortex core.

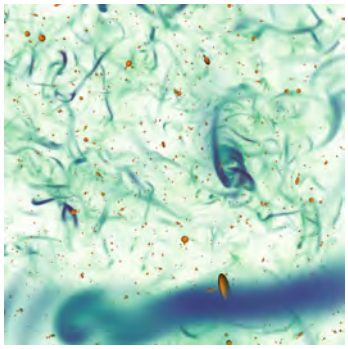

Figure 7.67: Microswimmers in three-dimensional turbulent flows exhibit complex dynamics, which we are currently investigating.

Motile plankton in the ocean [1] and bacteria in laboratory flows [2] are two examples of microscopic swimmers interacting with hydrodynamic flows. Even in simple settings, phenomena such as preferential concentration of (otherwise neutrally buoyant) cells can occur as a consequence of motility and shape-dependent hydrodynamic interactions. Here, we consider swimmers in a two-dimensional axisymmetric vortex flow and address the ecologically relevant problem of preferential concentration. We idealize swimmers as ellipsoidal particles with a swimming direction and constant self-propulsion speed v, which are advected in a flow field. Vorticity and shear induce particle rotation and tumbling [3]. This simple setting reveals surprising insights: Due to the axisymmetry of the problem, the phase space is two-dimensional and can be parameterized by the radial position and an orientation angle (relative to the position vector). Topologically, the phase space features a saddle point and a center (see Fig. 7.65). If any, clustering can occur in regions bounded by the homoclinic orbit of the saddle point. Cell shape plays a decisive role: For spherical swimmers, we showed that the dynamics is Hamiltonian, excluding preferential concentration as a result of phase-space conservation. However, non-spherical particles break the Hamiltonian structure, hence enabling shape-induced clustering. By introducing an effective swimming velocity $v_{\mathrm{eff}} = v/(1-\alpha)$, where α is a shape parameter, we were able to map different particle shapes to topologically equivalent phase spaces. Figure 7.65 shows the phase space of swimmers in a Lamb-Oseen vortex with three different shapes but equal effective velocities. Increasing the effective velocity ultimately leads to a merging of the center and the saddle point (see Fig. 7.66), such that all swimmers escape from the vortex.

In a related project (see Rep. 7.30), we have also investigated clustering in more complex, time-dependent flows. The results helped to clarify the role of turbulence and particle-particle interaction, which is also the topic of ongoing investigations (see Fig. 7.67).

[1] Jumars et al., Mar. Ecol. **30**, 133-150 (2009)
[2] Sokolov, A. and Aranson, I.S., Nat. Commun. **7**, 11114 (2016)
[3] Jeffery, G.B., Proc. R. Soc. Lond. A **102**, 161-179 (1922)

7.23 COLLECTIVE DYNAMICS OF ACTIVE SEMI-FLEXIBLE FILAMENTS

K. R. Prathyusha
S. Henkes (University of Aberdeen),
R. Sknepnek (University of Dundee)

Biological systems like actin or microtubule filaments driven by molecular motors inside a cytoskeleton and bacteria gliding on a substrate are flexible slender bodies which can consume energy locally and are capable of spontaneous directed motion. They can exhibit non-equilibrium collective behaviour which is absent in conventional passive polymers, where the dynamics are dominated by thermal fluctuations.

Motivated by the biological examples, we study the dynamics and pattern formation of self-propelling filaments (see Figure 7.68) on a substrate, using Langevin dynamics simulations [1]. The two dimensionless numbers are, the relative filament stiffness $\frac{\xi_p}{L}$, where ξ_p is the thermal persistence length, a measure of flexibility and the active Péclet number, $Pe = \frac{f_p L^2}{\sigma k_B T}$, which gives a measure of the propulsion.

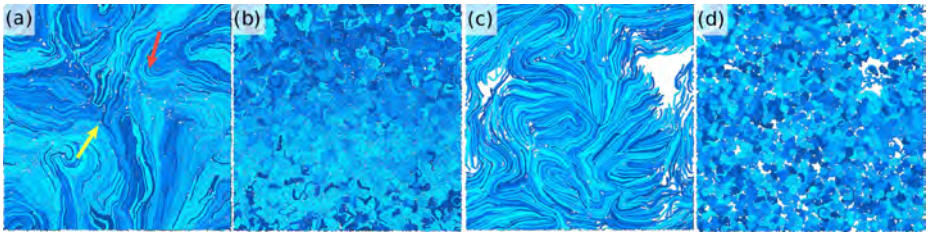

Figure 7.69: Snapshots of simulations for $N = 50$ in four non-equilibrium phases: (a) flowing melt ($\frac{\xi_p}{L} = 0.2$, $P_e = 35.5$), (b) swirl ($\frac{\xi_p}{L} = 0.04$, $P_e = 177.58$), (c) segregated phase ($\frac{\xi_p}{L} = 0.82$, $P_e = 355.16$) and (d) spirals ($\frac{\xi_p}{L} = 0.04$, $P_e = 17757.8$). Arrows in (a) are $+1/2$ (red) and $-1/2$ (yellow) topological defects.

Snapshots of various phases are shown in Figure 7.69. We created a phase diagram in $\frac{\xi_p}{L}$ vs. P_e plane as shown in Figure 7.70. For low activity, steric repulsions dominate and the system resembles a conventional polymer. Activity, introduces flow leading to flowing melt phase. When $\frac{\xi_p}{L} \geq 0.2$), at sufficiently high P_e the system crosses over into a phase-segregated state characterised by fila- ments aligning and flowing as a coherent bundle. For $P_e \approx 10^2 - 10^4$ and $\frac{\xi_p}{L} \leq 0.2$ the system enters the swirling state in which the dynam- ics is dominated by large fluctuations of filament shapes with individual filaments forming shot-lived spirals that quickly uncoil. For $P_e \geq 10^3$, the most filaments curl into long-lived rotating spirals.

We show that the combination of self-avoidance and flexibility of active filaments leads to interesting collective behaviour in dense limit. This model can be extended to study any filamental self-propelling system when the hydrodynamics is less important.

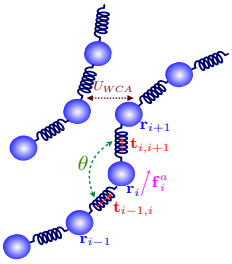

Figure 7.68: The active force on bead i is modelled as $\mathbf{f}_i^a = f_p(\mathbf{t}_{i-1,i} + \mathbf{t}_{i,i+1})$, which mimics active driving produced by a homogeneous distribution of molecular motors [2]. f_p is the strength of the force and $\mathbf{t}_{i,i+1} = \mathbf{r}_{i,i+1}/r_{i,i+1}$ is the tangent vector along the bond connecting beads i and $i+1$; end beads have only contributions from one bond. with the choice of the self avoidance interaction (U_{WCA}), the stretching and bending potentials we have an inextensible, semi-flexible non-penetratable polymer chain.

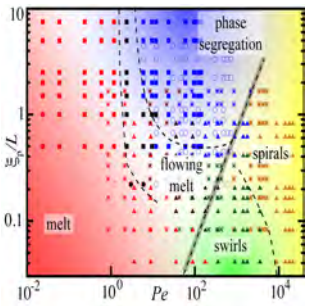

Figure 7.70: Non-equilibrium phase diagram for ξ_p/L vs. Pe at packing fraction $\phi = 0.64905$. No of beads in a given polymer $N = 5$ (square), $N = 10$ (circles), $N = 25$ (stars) and $N = 50$ (triangles).

[1] K. R. Prathyusha et al, Phys. Rev. E, **97**, 022606 (2018)
[2] R. E. Isele-Holder et al, Soft Matter **11**, 7181 (2015)

7.24 FILAMENTOUS CYANOBACTERIA: ALIVE POLYMERS

S. Karpitschka

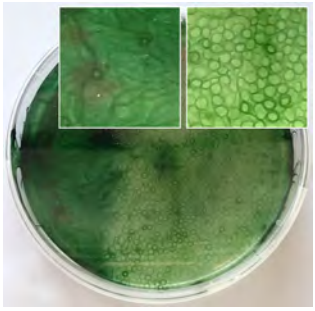

Figure 7.71: Light-responsive patterns in filamentous cyanobacteria on agar: only the right part was illuminated, leading to circular structures.

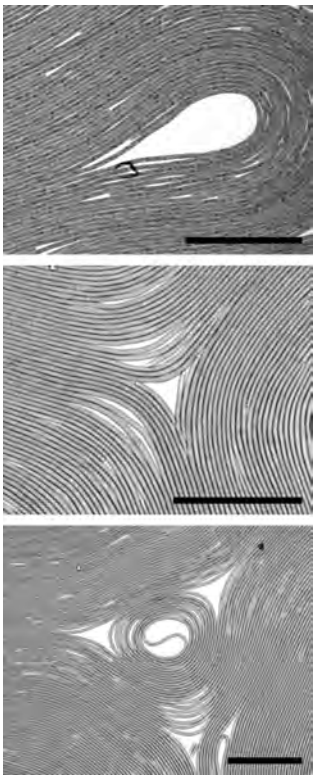

Figure 7.72: Topological defects in monolayers of filamentous cyanobacteria (scale bar $= 100\mu$m). All filaments continuously glide along their contour in either direction. $+1/2$ defects can be stationary or motile.

Cyanobacteria of the order Oscillatoriales form flexible, multicellular trichomes that are a few um in diameter but can grow up to millimeters in length. The natural habitat of these phototrophic organisms ranges from benthic soils to open fresh or sea water. Individual filaments do not swim, but glide over compliant surfaces at speeds of several um/s. Together with their photo-responsitivity, such motility is believed to support optimizing light exposure for photosynthesis [1, 2].

In this new project we started investigating flocking and colony-scale structures that emerge from such active polymers. Observed patterns depend on species and environmental conditions, most notably, light exposure (see Fig. 7.71). Confining the filaments to quasi-two-dimensional layers (see Fig. 7.72) reduces complexity and allows for examining both, the properties of individual filaments, as well as the emerging long-range order. This way, signatures of both polar and nematic symmetries could be found. Topological defects appear and disappear spontaneously due to the activity of the filaments.

In contrast to systems studied in recent literature, where agents typically had compact (frequently spherical) shape, here the active agents are long and flexible, equivalent to the worm-like-chain model used for semiflexible polymers. Active nematic microtubuli suspensions [3] exhibit similar patterns, but cyanobacterial colonies differ significantly. Their mesoscopic size allows us to fully resolve the microstate. Different species cover a wide range of passive and active properties, such that their influence on the emergent patterns can be revealed experimentally. The gliding motion bears spontaneous direction reversals, both stochastic and in response to spatial light gradients [2]. This presumably impacts pattern formation, but also permits manipulation of flocks: Light patterns may provide a *virtual confinement* that can be changed arbitrarily. Lastly, active forces are manily generated relative to the substrate and not to other filaments, altering the stability of topological defects [4]. Indeed we frequently observe transient half-integer charges which are absent in the confined microtubuli suspensions from [3].

We expect the findings of this project to be relevant far beyond the domain of active matter research since fliamanetous cyanobacteria belong to the oldest known forms of life on earth and played a key role in the oxygenation of our atmosphere. Current ecological relevance ranges from toxic blooms to renewable energy sources, where formation and properties of biofilms have great impact on reactor efficiency.

[1] B. A. Whitton (ed.), Ecology of Cyanobacteria II, Springer Netherlands (2012)
[2] E. Hoiczyk, Arch. Microbiol. **174**, 11 (2000)
[3] S. J. DeCamp, G. S. Redner, A. Baskaran, M.F. Hagan, Z. Dogic, Nat. Mater. **14**, 1110 (2015)
[4] A. Maitra, P. Srivastava, M. C. Marchetti, J. S. Lintuvuori, S. Ramaswamy, M. Lenz, Proc. Natl. Acad. Sci. USA **115**, 6934 (2018)

7.25 TRANSPORT AND SELF-ORGANIZATION AT BIOMEMBRANES

J. Agudo-Canalejo, R. Golestanian
R. Lipowsky (MPIKG)

Biological membranes are not just passive boundaries providing compartmentalization to the cell. They are also host to a great number of embedded and adsorbed proteins; they are essential players in all morphological changes of the cell; and they actively mediate transport of substances between the different compartments, both of small ions and molecules (through membrane channels) as well as of larger objects such as viral capsids or nanoparticles (through endo- and exocytosis). In this project, we study theoretically different instances of transport and protein self-organization at membranes, that may be observed both in biological cells as well as in model systems such as giant unilamellar vesicles.

During endo- and exocytosis of solid particles, the membrane adheres to the particle until it completely engulfs it, see Figure 7.73. This process is governed by a competition between adhesion and bending of the membrane, and is extremely sensitive to the properties of the membrane. In particular, we have shown that asymmetries in the composition of the two membrane leaflets strongly affect engulfment, and can explain the observed size-dependence of particle endocytosis by cells. [1] Moreover, we found that adhesive particles can sense the local curvature of the membrane, [2] and are subject to membrane-mediated forces that direct them towards regions of low curvature. [3] Once a particle is completely engulfed, the narrow neck [4] that connects the engulfed particle to the mother membrane is actively severed by cytosolic proteins such as the ESCRT complexes. [5]

Similarly to an adhering particle, embedded or adsorbed proteins also induce curvature on the membrane, and are thus subject to membrane-mediated attractive interactions. We have shown [6, 7] that the interplay between bending, entropic forces, and the geometric constraints on the membrane can result in the formation of patterns of highly-curved, protein-rich and weakly-curved, protein-poor domains, which may be related to protein self-organization in processes ranging from protocell division to the formation of membrane rafts, see Figure 7.74. In future work, we will couple non-equilibrium processes to the membrane, such as the activity of catalytic enzymes (see Chapter 7.6) as well as transport of ions by channel proteins.

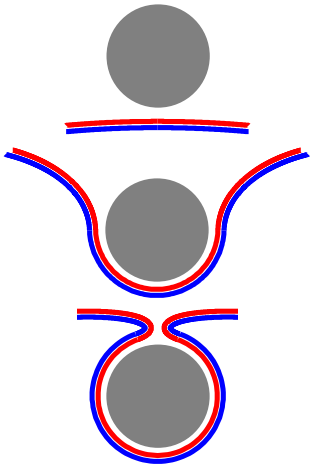

Figure 7.73: A nanoparticle in contact with a membrane may remain free, be partially engulfed, or be completely engulfed (which involves the formation of a narrow neck). From [1].

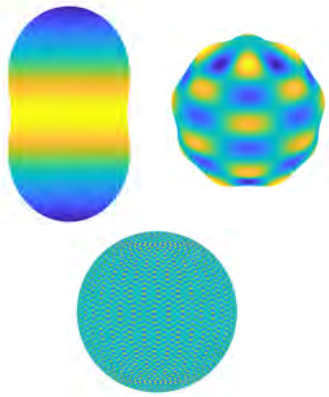

Figure 7.74: Curvature-inducing proteins form patterns of highly-curved, protein-rich and weakly-curved, protein-poor domains on the membrane. The size and number of the domains is controlled by the protein density and the geometric constraints on the membrane. From [7].

[1] J. Agudo-Canalejo, R. Lipowsky, ACS Nano **9**, 3704 (2015)
[2] J. Agudo-Canalejo, R. Lipowsky, Nano Lett. **15**, 7168 (2015)
[3] J. Agudo-Canalejo, R. Lipowsky, Soft Matter **13**, 2155 (2017)
[4] J. Agudo-Canalejo, R. Lipowsky, Soft Matter **12**, 8155 (2016)
[5] J. Agudo-Canalejo, R. Lipowsky, PLOS Comput. Biol. **14**, e1006422 (2018)
[6] J. García-Lara et al., Proc. Natl. Acad. Sci. U.S.A. **112**, 15725 (2015)
[7] J. Agudo-Canalejo, R. Golestanian, New J. Phys. **19**, 125013 (2017)

7.26 ADHESION OF PHOTOACTIVE MICROBES TO SURFACES IS SWITCHABLE BY LIGHT

C.T. Kreis, C. Linne, M. Le Blay, M.M. Makowski, O. Bäumchen

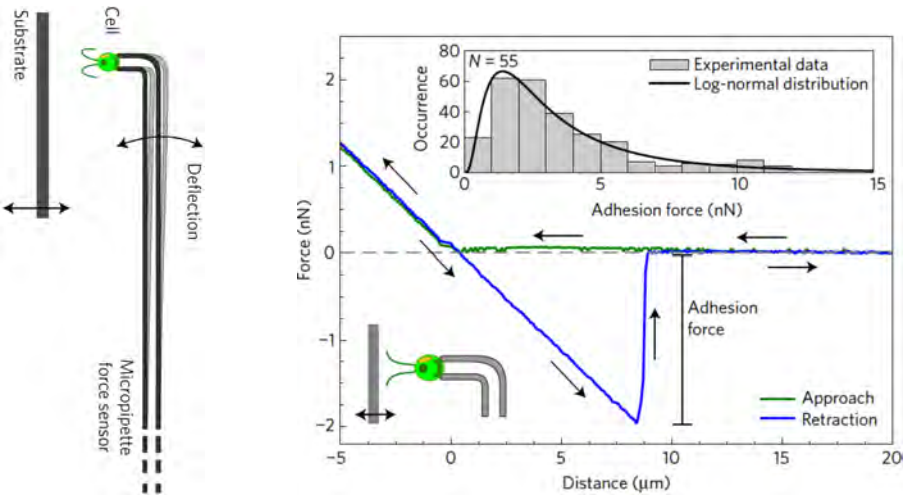

Figure 7.75: (Left) The adhesion of the unicellular microalga *Chlamydomonas* to a surface is measured with a micropipette force sensor. A single cell is immobilized at the tip of the micropipette force sensor by applying a small suction pressure. (Right) Force-distance curves obtained *in vivo* from the micropipette's deflection upon retraction of the substrate from the cell in white light yield adhesion forces of several nanonewton (inset) [1].

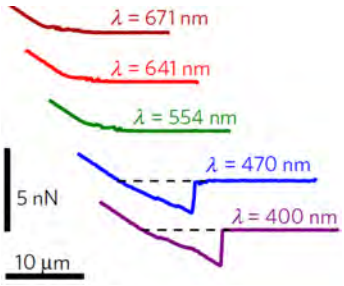

Figure 7.76: Adhesion force measurements in different light conditions provide evidence that a blue-light photoreceptor is involved in light-switchable adhesion [1].

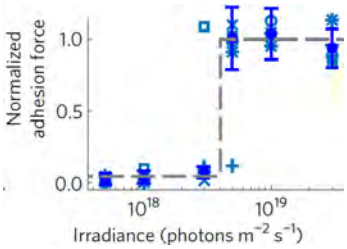

Figure 7.77: Variation of the light intensity in blue light reveals a sharp irradiance threshold for the adhesion of *Chlamydomonas* [1].

Bioadhesion is a ubiquitous phenomenon in nature. For microbial life, the adhesion to surfaces is ultimately linked to the formation of dense microbial populations called biofilms, which have profound implications in a variety of natural, physiological and technological scenarios. While the adhesion strategies of bacteria and mammalian cells have been widely studied over the past years, the biological mechanisms and interfacial forces involved in microalgal adhesion to surfaces in aqueous environments remained elusive. Microalgae are photoactive microbes that often live in liquid-infused porous environments, such as wet soils and moist rocks, where they encounter and colonize a plethora of surfaces. They inherit abundant ecological and technological relevance, e.g. in water purification systems and photo-bioreactors for the sustainable production of biofuels and pharmaceutical agents. The biflagellated microalga *Chlamydomonas* is a model organism in cell biology to study a wide range of phenomena including photosynthesis, phototaxis, light receptors, cell metabolism among others.

We discovered that the adhesion of photoactive microalgae to surfaces can be reversibly switched on and off by light [1]. Using a novel micropipette force sensor technique [2], we measured *in vivo* adhesion forces of individual cells and show that the microalga's flagella provide adhesive contacts with the surface, yielding typical adhesion forces of a few nanonewton (see Fig. 7.75). We find that the cells can switch the adhesiveness of their flagella in response to blue light (see Fig. 7.76, 7.77), as inferred from micropipette force-distance experiments in different light conditions [1]. Time-resolved micropipette force measurements of cells in close proximity to a surface provide access to the time scales associated to flagella-surface interactions: Within a few seconds after switching to white light, the flagella become sticky and start to pull the cell body towards the surface (see Figs. 7.78, 7.79) [1].

Ultimately, these results suggest that light-switchable adhesion to surfaces is a natural functionality of photoactive microbes to regulate their transition from the freely swimming (planktonic) state to the surface-associated state, which presumably represents an evolutionary adaptation to their habitat. In the heterogeneous and variable light conditions of their natural habitats, the cells can optimize their photosynthetic efficiency by actively searching for light sources (phototaxis) and clinging to surfaces that are illuminated.

Our discovery has opened a plethora of interesting avenues for applied and fundamental research. Currently, we are exploring whether the light-switchability of the flagella adhesiveness is a generic trait of soil-dwelling photosynthetic microbes. Furthermore, we aim at identifying the functional photoreceptor underlying light-switchable adhesion and work on dissecting chemical inhibitors of the signal transduction pathways as well as the protein synthesis and transport machinery that might be involved in the flagella-mediated adhesion to surfaces. These aspects are essential ingredients to obtain a biomolecular picture of the light-sensitive adhesion mechanism. Moreover, these fundamental insights are of outstanding relevance for the regulation of microbial biofilm formation in technological applications.

Besides genetic and metabolic control of adhesive functionalities, we test the influence of the substrate properties on microbial adhesion by employing different sets of model substrates exhibiting tailored interfacial forces. Remarkably, we find that *Chlamydomonas* does not show any significant difference in the adhesion force statistics on substrates for which we have systematically varied the (short-range) hydrophobic as well as the (long-range) van der Waals interactions. Flagella adhesion of *Chlamydomonas* to surfaces has been attributed to a single type of flagella membrane glycoprotein, called FMG-1B, which is rather underexplored from a biomolecular perspective. Further structural and functional characterization of this membrane protein and its glycosylation might not only help to understand microalgal adhesion to surfaces, but also advance the development of new design principles for synthetic glues that are effective in aqueous environments.

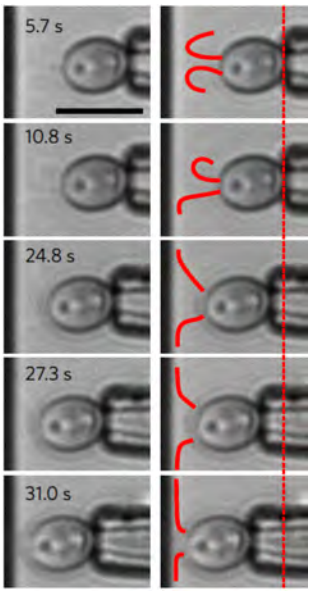

Figure 7.78: Series of optical micrographs illustrating the auto-adhesion behaviour of *Chlamydomonas*. The cell uses dynein motors to actively pull itself towards the substrate (gliding configuration) [1].

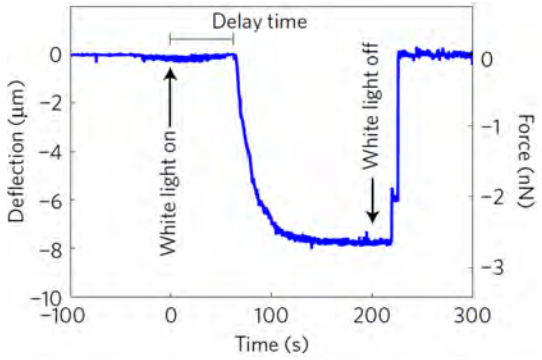

Figure 7.79: Auto-adhesion of *Chlamydomonas*. The deflection of the micropipette is continuously monitored, while the light is switched from red to white. Within a few seconds the flagella establish adhesive contact and the cell starts to pull itself towards the substrate, see Fig. 7.78 [1].

[1] C.T. Kreis, C. Linne, M. Le Blay, M.M. Makowski, and O. Bäumchen, *Nature Physics* **14**, 45 (2018).

[2] M. Backholm and O. Bäumchen, *Nature Protocols*, **14**, 594 (2019).

7.27 SUBSTRATE EFFECTS ON BACTERIAL GROWTH

Y. G. Pollack, R. Golestanian
A. Amiri (MPIPKS)

Starting from an initial colony "seed", bacteria on a substrate form self-organized biofilms through division, motility and swarming. The type of organization that the colony attains and the mechanisms that control its formation can depend on genetics, available nutrients, chemical/mechanical cell-cell interactions [1], etc (cf. Reps. 7.28, 7.21). The mechanical properties of the substrate can also have a great effect on cells (sometimes quite surprisingly so, as in the related example of substrate stiffness affecting differentiation in embryonic stem cells [2]).

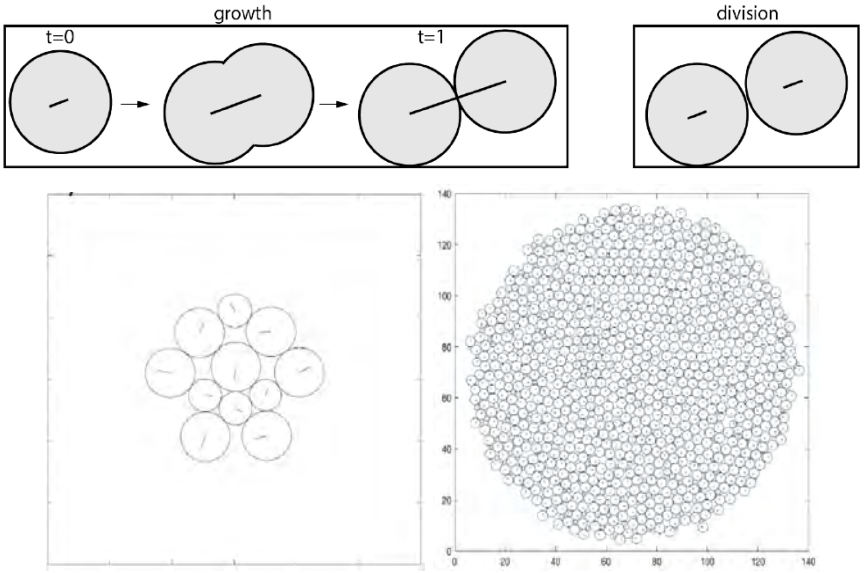

Figure 7.80: Top: Illustration of the model used to simulate bacterial growth and division. Bottom: Snapshots from a simplistic simulation of a bacterial colony using active disks. Bottom left: Zoom-in on the initial colony seed. Bottom right: The same colony after 13 generations.

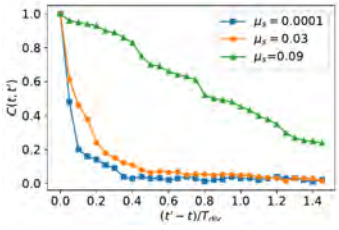

Figure 7.81: Time decay of C the orientational autocorrelation of cells for different static friction coefficients μ_s (time normalized by the cell division time T_{div}). Beyond a certain μ_s threshold, the correlation switches to a slow glassy decay (in green).

We are currently studying the implications of varying the cell-substrate adhesion, that results in effective friction, on biofilm growth and organization. Naively, greater cell-substrate adhesion suggests improved attachment of colony to substrate, but studies suggest the opposite: bacterial colonies become adapted to a given substrate and thrive on it better over time after an initial period of mixing and exchanging neighbors [3]. Our preliminary numerical results show that when the cell-substrate friction coefficient grows beyond a certain threshold, the cell dynamics show a marked slow-down reminiscent of a glass transition and an aging process. This in turn is indicative of arrested growth of the colony and reduced neighbor exchanges that should result in lesser substrate compatibility of the colony and a reduced degree of attachment.

[1] M. E. Anyan, A. Amiri, C. W. Harvey, G. Tierra, N. Morales-Soto, C. M. Driscoll, M. S. Alber, and J. D. Shrout, Proc. Natl. Acad. Sci. **111**, 18013 (2014).
[2] N. D. Evans, C. Minelli, E. Gentleman, V. LaPointe, S. N. Patankar, M. Kallivretaki, X. Chen, C. J. Roberts, and M. M.Stevens, Eur. Cell Mater., **18**, e13 (2009).
[3] C. K. Lee, , J. de Anda, , A. E. Baker, , R. R. Bennett, ,Y. Luo, , E. Y. Lee, J. A. Keefe, J. S. Helali, J. Ma, K. Zhao, R. Golestanian, G. A. O'Toole, G. C. L. Wong, Proc. Natl. Acad. Sci., **115**, 201720071 (2018).

7.28 BACTERIAL POPULATION DYNAMICS AND PATTERNS

P. Bittihn, R. Golestanian
S. R. Scott, A. Didovyk, L. S. Tsimring, J. Hasty (UC San Diego)
X. Wang (University of Oxford), H. A. Stone (Princeton)

Desipite their designation as unicellular organisms, bacteria are not only influenced by mechanical and chemical interactions with their environment (cf. [1] and Reps. 7.21, 7.27, 7.13). Due to their fast growth, a single bacterium also quickly turns into an entire, spatially structured, population. Understanding the involved feedback processes is not only of fundamental scientific interest as a prime example of emergent dynamics and self-organization. It is also a necessary prerequisite for advanced synthetic biology applications, where artificial gene regulatory networks ("gene circuits") are designed to create novel behavior in genetically engineered bacterial populations [2].

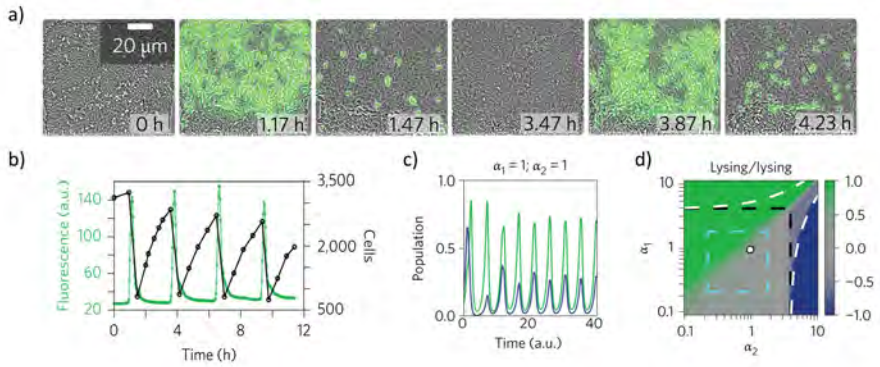

Figure 7.82: Engineered population dynamics. **(a)**, **(b)** Fluorescence microscopy snapshots and graph showing alternating growth and lysis. Activation of quorum-sensing triggered lysis shown in green. **(c)** Numerical simulation of two co-cultured populations (green, blue) with cross-talk between the two population control circuits. **(d)** Stability diagram showing stable coexistence (gray) or dominance of green or blue strain for different growth rates α_1, α_2. Adapted from [3].

A prominent mechanism bacteria use to coordinate collective behavior is quorum sensing (QS), by producing molecules of a QS agent that diffuse through the cell membrane into the environment where they can be "sensed" by other bacteria. We harnessed this mechanism in an artificial population control circuit that is designed to initiate lysis (killing cells) upon detecting a suprathreshold QS signal, thereby artificially limiting population size. Modeling this system in the confined environment of a microfluidic trap we showed that, by tuning experimental parameters, the system goes through a Hopf bifurcation leading to alternating phases of growth and lysis, which were experimentally confirmed (Fig. 7.82a, b). The self-limiting nature of this circuit can be used to suppress dynamical instabilities in multi-strain ecologies that would usually lead to the dominance of the fastest-growing strain. We investigated different interaction topologies between two strains, with or without chemical crosstalk between QS systems, and examined the robustness of each scheme, one example of which is shown in Fig. 7.82c, d. We also explored the effects of periodic population dynamics on the fate of mutations and thus the genetic composition of the population. Our analytical approximations show that beneficial mutations are suppressed by a factor that depends both on the severeness of the population reduction as well as the growth rate increase the mutation confers (Fig. 7.83), thus stabilizing the original genotype and growth rate of the population.

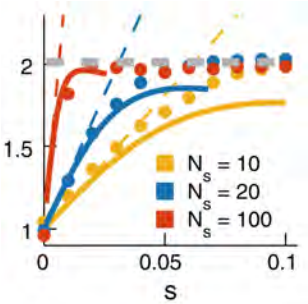

Figure 7.83: Factor by which mutations with selective advantage s are suppressed in a population undergoing periodic reductions in population size with different seed population sizes N_s [4].

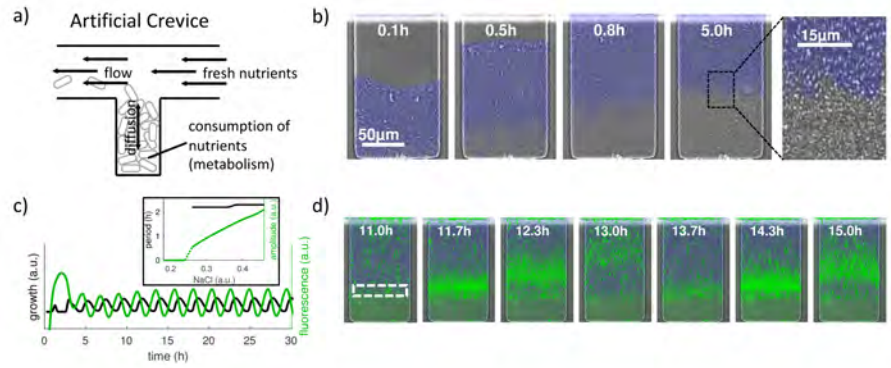

Figure 7.84: Growth patterns in diffusion-limited environments. **(a)** Schematic of microfluidic cell trap with supply of nutrients by diffusion and spillover-removal. **(b)** Colonies of *E. coli* filling the traps. Active growth (blue) can only be sustained in region with sufficient nutrients. **(c)** Theoretical prediction of oscillatory instability leading to alternating phases of growth and growth arrest close to no-growth boundary (white rectangle in d). Bifurcation diagram shown as inset. **(d)** Experimental observation of growth instability. Green fluorescent marker is activated during growth arrest. Adapted from [5].

Even without QS, bacterial metabolism leads to chemical gradients of metabolites in the environment that feed back on cellular physiology to create specific growth patterns in large enough environments. We used artificial microfluidic crevices (Fig. 7.84a) with precisely controlled nutrient supply to observe steady-state growth patterns shaped by diffusion-limitation (Fig. 7.84b). A model incorporating cell metabolism, diffusion and advection due to cell division and growth shows that the stability of this pattern critically depends on the cells' response to nutrient deprivation. If metabolism is shut down prematurely, nutrient supply to deeper layers is effectively increased, which transiently resume growth until the process repeats. These growth oscillations with a characteristic amplitude-independent period (Fig. 7.84c) were indeed observed with a gene circuit that implements premature growth arrest (Fig. 7.84d). Interestingly, oscillations in growth that allow the passage of metabolites to "inner" cells has recently been observed as an evolutionarily beneficial strategy in natural biofilms of *B. subtilis* [6].

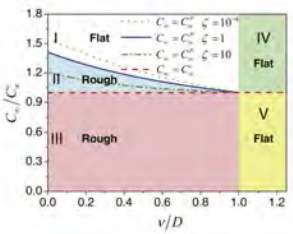

Figure 7.85: Stability diagram for the front shape of a growing biofilm as a function of nutrient level C and surface tension ν normalized by the diffusion coefficient D. In regions labeled "flat", perturbations of an initially straight front decay, whereas in "rough" regions they grow [7].

The same chemical gradients also manifest as a layer of growing cells that push the front of the colony forward during unconstrained growth (e.g., during initial biofilm development). We theoretically investigated the mechanical stability of a growing front that approaches a fixed nutrient source (similar to the first snaphots of Fig. 7.84b). A perturbative analysis shows that a combination of front velocity, mechanical cell-cell interactions and diffusion leads to different regimes with transient or sustainable long-term growth, having either a flat or a rough biofilm surface (Fig. 7.85) [7]. Our analytical results shed new light on the relevant parameters for this bacterial self-organization process and could also help to constrain parameters and growth conditions in biofilm experiments.

[1] R. R. Bennett, C. K. Lee, J. De Anda, K. H. Nealson, F. H. Yildiz, G. A. O'Toole, G. C. L. Wong, R. Golestanian, *J. R. Soc. Interface* **13**, 20150966 (2016)
[2] P. Bittihn, M. O. Din, L. S. Tsimring, J. Hasty, *Cur. Op. Microbiol.* **45**, 92 (2018)
[3] S. R. Scott, M. O. Din, P. Bittihn, L. Xiong, L. S. Tsimring, J. Hasty, *Nature Microbiol.* **2**, 17083 (2017)
[4] P. Bittihn, J. Hasty, L. S. Tsimring, *Phys. Rev. Lett.* **118**, 028102 (2017)
[5] P. Bittihn, A. Didovyk, L. S. Tsimring, J. Hasty, *in preparation*
[6] J. Liu *et al.*, *Nature*, 550 **523** (2015)
[7] X. Wang, H. A. Stone, R. Golestanian, *New J. Phys.* **19**, 125007 (2017)

7.29 MECHANICS OF PLANT ORGAN OUTGROWTH

J. Khadka, J.R.D. Ramos, J.D. Julien, K. Alim
A. Maizel (Heidelberg)

Development of life relies on robust and reproducible moulding of organs. Particularly, at the fast time scales and the large spatial scales during development, biochemical signalling is not sufficient to coordinate robust growth. In plants, mechanical forces provide the missing link that may be pivotal in coordinating organ growth. We and others have shown that tissue-wide mechanical stresses feed back on individual cell growth [1] and on the patterns of the omnipresent plant growth hormone auxin [2]. Yet, the power of even the simple feedback between stress and cell growth is unknown, let alone of the more complex cycle between auxin promoting cell growth through loosening cell walls and resulting mechanical stress changing auxin patterns, see Fig. 7.86.

The plant shoot tip is the stem cell niche for all upper plant organs. Robust organ formation by outgrowth here is crucial for plant development. We develop a three-dimensional vertex model for the tissue mechanics at the shoot tip and investigate what drives robust organ outgrowth, see Fig. 7.87. Quantifying organ outgrowth initially triggered by a patch of faster growing cells, we find that organ outgrowth gets more and more efficient with the cell's ability to respond to mechanical stresses within the tissue, see Fig. 7.88, [3].

The root is for all lower plant organs what the shoot is for all upper plant organs. Here, lateral root outgrowth is a model system allowing us to probe how tissue mechanics self-organize patterns of auxin [4], see Fig. 7.86. In particular, want to uncover how the feedback between auxin patterns and cell mechanics gives rise to the dynamic patterns throughout organ outgrowth. Here, we include PIN protein mediated auxin patterning on top of the vertex model describing tissue mechanics. With this model, we find that increased pressure in the lateral root founder cells is sufficient to sustain initial auxin accumulation, see Fig. 7.89 A and drives the subsequent swelling of founder cells, see Fig. 7.89 B. Moreover, "down-the-gradient" patterns in later stages of organ outgrowth, can dynamically self-organise due to competition between mechanical feedback and auxin/PIN patterning.

Understanding the role of cell mechanics not as sole output but as a key for the self-organisation of tissues is crucial to alter plant development for crop production and serves as a physical principle for organism development beyond the realm of plants.

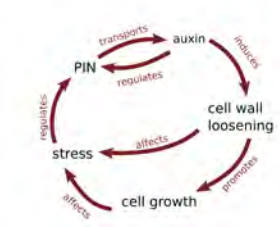

Figure 7.86: Growth hormone auxin controls its patterns by feedback on tissue mechanics.

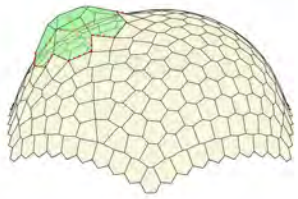

Figure 7.87: Vertex simulation result of organ outgrowth at the tip of the plant shoot.

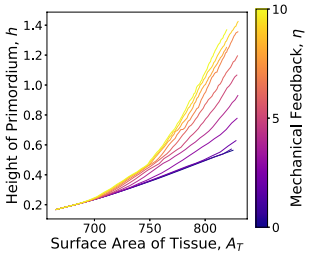

Figure 7.88: Increasing the ability of cells to respond to mechanical stresses leads to efficient organ growth.

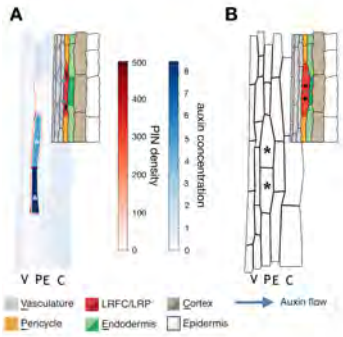

Figure 7.89: Early stage of lateral root formation of (A) auxin accumulation followed by (B) cell swelling captured by model.

[1] M. Uyttewaal, A. Burian, K. Alim, et al., Cell, **149(2)**, 439-451 (2012)
[2] M. G. Heisler, O. Hamant, P. Krupinski, M. Uyttewaal, C. Ohno, et al., PLoS Biol. **8**, e1000516 (2010)
[3] J. Khadka, J.-D. Julien, K. Alim, submitted (2018)
[4] A. Vilches-Barro, A. Maizel, Curr. Op. Plant Biol. **23**, 31 (2015)

SFB 937

PLANT FOR 2581 MORPHODYNAMICS

7.30 EMERGENCE OF PHYTOPLANKTON PATCHINESS: THE ROLE OF TURBULENCE

R. E. Breier, C. C. Lalescu, M. Wilczek, M. G. Mazza

Algal blooms, which can stretch for tens or hundreds of km, are caused by countless microscopic organisms called phytoplankton, microscopic organisms that use sunlight to produce energy. They are the base of the marine food chain, and produce 50% or more of the oxygen in the atmosphere. Additionally, they fix carbon and thus contribute to the carbon budget in the atmosphere. Recent observations found that swimming phytoplankton species have a patchy spatial distribution down to the millimeter scale in oceans and lakes. This is rather surprising because it goes against the intuitive expectation that the turbulent flow mixes the microorganisms and spreads them rather homogeneously.

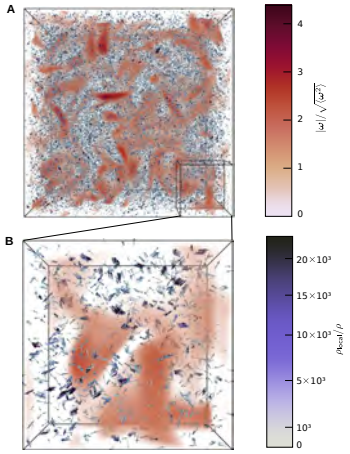

Figure 7.90: (A) Typical steady-state configuration of the motile cells in the Navier–Stokes flow field (at $\mathcal{S}_\omega = 86.52$). Cells are shown as arrows whose color indicates the normalized local density (obtained from a Voronoi tessellation), and whose orientation indicates the local alignment. The background (red) color represents the value of the normalized turbulent vorticity. The elongated, dark red regions correspond to the vortex cores moving through the system. (B) Close-up of the system where the clusters are discernible.

In this work [1], we combine particle simulations and continuum theory to study the emergence of patchiness in motile microorganisms in three dimensions. By addressing the combined effects of motility, cell–cell interaction, and turbulent flow conditions, we uncover a general mechanism: the coupling of cell–cell interactions to the turbulent dynamics favors the formation of dense patches. Identification of the important length and time scales, independent from the motility mode, allows us to elucidate a general physical mechanism underpinning the emergence of patchiness.

Numerous phytoplankton species are motile, and the vast majority of harmful algal blooms are caused by motile phytoplankton. Thus, a comprehension of the consequences of active motion in a turbulent environment can clarify important aspects of the phytoplankton ecology. We explore the microhydrodynamics characterized by a Taylor-based Reynolds number of the order of $\mathcal{R}_\lambda \approx 20$ which matches the typical conditions found, e.g., in the pycnocline. We model the cells as particles with swimming speed v_0 and orientation $\boldsymbol{e}$. The cells' reorientation is subject to two torques: (*i*) $\frac{1}{2}(\boldsymbol{\omega} \times \boldsymbol{e})$ induced by the fluid vorticity $\boldsymbol{\omega} = \nabla \times \boldsymbol{u}$, where $\boldsymbol{u}$ is the fluid velocity, and (*ii*) a torque representing the short-range cell-cell interactions with up-down symmetry. The interaction is restricted to particles within the range ϵ and takes place on a time scale $1/\gamma$. Rotational diffusion is introduced through a stochastic noise $\boldsymbol{\xi}$. For the sake of comparison we also consider select simulations with extended particles to examine the impact of repulsive contact forces.

To model the turbulent flow, we combine results from two complementary techniques. First, we use kinematic simulations; that is, the turbulent velocity field is modeled by a sum of unsteady random Fourier modes which obey a prescribed energy spectrum (the "Kraichnan fluid"). Second, we perform direct numerical simulations (DNS) of the incompressible Navier–Stokes equations with a pseudospectral method to model the turbulent flow directly.

To quantify the degree of patchiness in the spatial distribution of swimming cells we calculate the patchiness factor Q, which is a

normalized local density based on a 3D Voronoi tessellation. We define the vortical Stokes number as $\mathcal{S}_\omega = \tau_{\text{turb}}/\tau_{\text{int}} = 2\gamma/\omega_K$, where τ_{turb} and τ_{int} are the characteristic times of the turbulent field and of the cell-cell interaction.

Figure 7.91 shows the nonequilibrium phase diagram obtained from our molecular dynamics simulation of swimming cells immersed in a Kraichnan fluid. At fixed Péclet number, as the vortical Stokes number $\mathcal{S}_\omega$ increases to values larger than unity (indicating a dominant reorientational dynamics of the cells), we find that the patchiness factor Q exhibits a sharp increase. At $\mathcal{S}_\omega \approx 10$ a well-defined maximum occurs. This maximum is robust upon variation over a wide range of Péclet numbers and upon replacing point-like with extended particles. At large values of $\mathcal{S}_\omega$ the patchiness always saturates to a finite value.

To characterize the relevant length scales, we define a dimensionless number $\zeta \equiv L_{\text{turb}}/L_{\text{int}}$ that compares the length scale associated to the turbulent vortical motion $L_{\text{turb}} = \tau_{\text{turb}} u_{\text{rms}}$ with the length scale $L_{\text{int}} = \tau_{\text{int}} v_0$ associated to the cell-cell interactions. The region of enhanced patchiness is delimited by the two loci described above, and as visible from Fig. 7.91A. In the current setting, we find that the condition $\zeta \approx 1$ marks the emergence of strong patchiness for our system of motile cells for both point-like particles and extended ones. This fact points to a general mechanism underpinning the emergence of patchiness. The region where cell-cell interactions considerably change cells' swim directions has characteristic size L_{int}. When L_{int} roughly matches the size L_{turb}, where turbulent vortical motion acts most strongly, dense patches emerge.

Our results indicate that the coupling of cell-cell interactions with mildly turbulent flows controls the emergence of a patchy spatial distribution of motile phytoplankton. This finding [1] can complement discussions of the influence of physical forces on marine ecology.

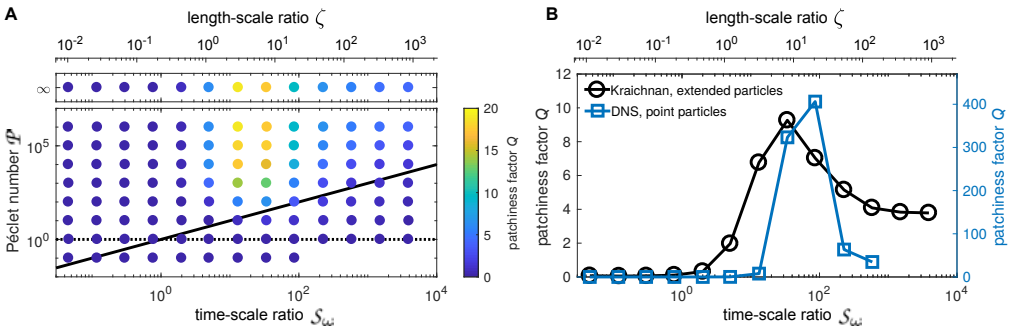

Figure 7.91: (A) Nonequilibrium phase diagram of point-like swimming cells immersed in a Kraichnan turbulent flow field. As the reorientation of the swim direction due to cell-cell interactions increases its strength with respect to the turbulent vorticity (i.e., increasing vortical Stokes number $\mathcal{S}_\omega$) small-scale patchiness emerges. (B) The maximum in patchiness does not depend on the microscopic details of the interaction, as the emergence of patchiness is robust upon replacing point-like with extended particles (both cases for $\mathcal{P} \to \infty$); nor does the maximum in patchiness depend on the details of the flow field.

[1] R. E. Breier, C. C. Lalescu, D. Waas, M. Wilczek, M. G. Mazza, Proc. Natl. Acad. Sci. USA, doi:10.1073/pnas.1808711115 (2018)

7.31 ACTIVE COORDINATION AND STATE SWITCHING IN MORPHOGENESIS

S. Eule, N. Lenner, M. Haering, A. Neef , F. Wolf
J. Grosshans, D. Kong, P. Richa (UMG)

Perhaps the most spectacular example of self-organization in living matter is developmental morphogenesis, the process by which a fertilized oocyte transforms itself into a complex organism composed of a multitude of differentiated cells, tissues, and organs. Many aspects of morphogenesis are genetically specified but whenever multiple cells have to work together to transform a complex tissue, the dynamics of morphogenesis requires that embryonic cells sense the states of their neighbors and coordinate their active mechanics. While mechanical forces in morphogenesis have been extensively studied in developing systems, studies of information transfer and dynamical coordination in developing systems are in their infancy.

To elucidate the dynamics of intercellular coordination in morphogenesis we are developing methods to detect and quantify signatures of intercellular coordination from large-scale *in vivo* imaging, in order to infer effective dynamical laws governing cells and groups of cells. We also develop experimental methods and paradigms to causally test intercellular coordination by temporally precise, single cell resolution control of cellular activity *in vivo*. We apply and test these methods on paradigmatic morphogenetic transformations in *Drosophila* gastrulation: axis elongation, by which the embryo elongates in anterior-posterior direction, and dorsal closure by which the exterior body surface of the developing animal is sealed at its back.

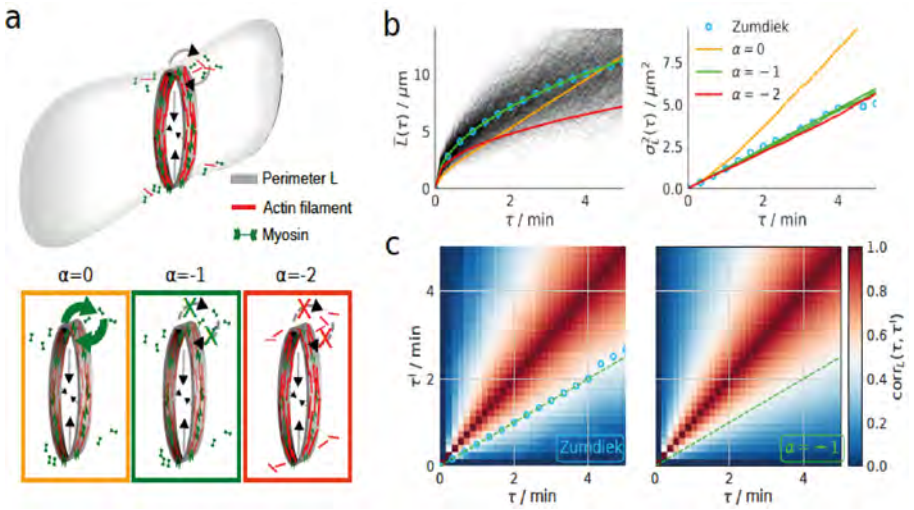

Figure 7.92: Actomyosin turnover model inferred from observed dynamics in cytokinetic ring constriction. (a) Scenarios for the turnover of force generating molecules (b) Mean and variance for the inferred, target-state aligned dynamics and two rejected alternatives. (c) The two-time correlation functions from data and effective stochastic model.

To enable a defined perturbation of individual cells, we recently introduced a novel opto-chemical technique *Calcium mediated Light-*

activation of Myosin (CaLM), by which active contractions of epithelial cells can be induced noninvasively with single cell precision and high temporal accuracy. Using this technique we showed that synchronized contraction of anterior-posterior (AP) pairs of cells in the germband is sufficient to drive the extension and stabilization of new cell contacts, the elementary process in tissue elongation. In large-scale quantitative analyses of the dynamics of axis elongation we demonstrate that also spontaneously *in vivo* AP cell pairs actively synchronize in advance of elementary axis elongation steps, and that in a mutant in which axis elongation is impaired cells have a specific disability to effectively coordinate and synchronize. We also discovered a coordination phenotype in dorsal closure when putatively force-sensitive calcium ion channels were genetically deleted. This strongly suggests that cellular calcium also serves as a key messenger in the active mechanical synchronization of developing epithelial cells.

A central problem in obtaining large-scale quantitative data on cellular dynamics within its natural *in vivo* setting is the automated segmentation of images from time lapse movies. Recently, convolutional neural networks, such as the U-Net, have substantially simplified such segmentation tasks. An inherent disadvantage of this approach, however, is the prerequisite of large numbers of manually prepared training samples, i.e. pairs of image - ground truth mask. We found that this costly and time-consuming task can be circumvented by segmentation based on cycle consistent generative adversarial networks. These networks can be trained without pre-prepared image - mask pairs. We demonstrated [4] that this approach successfully realizes large-scale image segmentation even for samples with substantial defects.

Dynamical processes in developmental systems, such as those studied here, are not only thermodynamically out of equilibrium but they are typically non-stationary and in a strong sense irreversible as they progress in a directed manner towards functionally important target-states. In addition, cells will typically actively alter their dynamical behavior when approaching and progressing through such target states. To infer the underlying directional dynamics from data, we developed a theory of target-state-aligned ensembles (TSA) that reveals whether and when a system can be represented by a single, effective stochastic equation of motion [5]. We show how, in this equation, genuine biological forces can be separated from spurious forces, which, invariably arise from target-state-alignment. These theoretical, experimental, and data driven studies open new avenues for analyzing the smart dynamics of active matter in morphogenesis.

[1] Y. Zhang, D. Kong, L. Reichl, N. Vogt, F. Wolf, J. Grosshans. Developmental Biology 390:208–220. (2014)

[2] D. Kong, F. Wolf, J. Grosshans. Mech Dev 144:11–22. (2017)

[3] D. Kong, F. Wolf, J. Grosshans. bioRxiv:255372. (2018)

[4] M. Haering, J. Grosshans, F. Wolf, S. Eule. bioRxiv:311373. (2018)

[5] N. Lenner, S. Eule, F. Wolf. Bulletin of the American Physical Society (2019)

DYNAMICS, GEOMETRY AND INFORMATION

8

Life depends as much on its constituting matter as on efficient processing of information. How does the geometry of matter, and the topology and interactions within a complex network impact dynamics and processing? How can we quantify these collective properties in large systems despite imperfect experimental assessment? To unravel the mutual dependencies among dynamics, geometry and information, we study the flow of matter and information, information transformation for efficient processing, adaptation and optimization principles, and the role of singularities and phase transitions. Systems being researched range from stochastic processes and inanimate porous media to living systems like Physarum, complex transport networks, the immune system, and the human brain. Although these systems widely differ in their components and mechanisms, information theory provides a common language to describe the principles of how they are organized to achieve high efficiency.

Contents

8.1 INFORMATION THEORY OF OLFACTION

D. Zwicker

The olfactory system faces the difficult task of identifying an enormous variety of odors independent of their intensity. In humans, odors are sensed by about 300 receptor types in the nasal cavity and information from all receptors of a given type is accumulated in a single glomerulus; see Figure 8.1. The odor information is encoded by the excitation pattern of all glomeruli, which can be thought of as a 300-dimensional vector. These high-dimensional stimulus space and encoding spaces proved to be a major roadblock in studying olfaction, both experimentally and numerically.

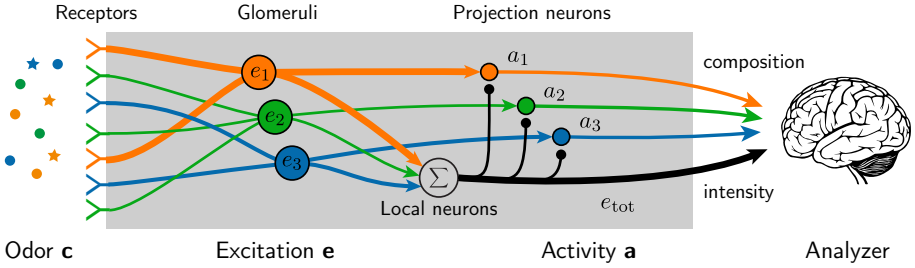

Figure 8.1: Schematic picture of the olfactory system, where information about odors is processed by glomeruli and projection neurons before it is analyzed by the brain.

We study olfaction theoretically by combining methods from information theory and statistical physics. In particular, we developed a simplified model of the olfactory system, where the receptor sensitivities are represented by random matrices [1]. Performing numerical simulations for small systems, we were able to verify our analytical predictions for the behavior of the olfactory system; see Figure 8.2. These analytical formulas naturally extend to the interesting regime of high dimensionality and thus overcome numerical difficulties.

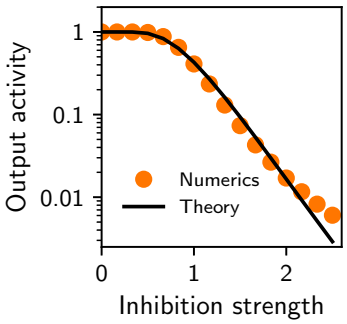

Figure 8.2: Predicted output activity as a function of the projection neuron inhibition strength in a model of normalized odor signals [2].

Comparing the performance of three different coding schemes, we uncovered the following general behavior: a simple binary coding, where all channels are independent, typically leads to dense signals and cannot account for the observed olfactory performance over large ranges of odor intensities [1]. Normalizing the signal by its average removes the strong correlation with the odor intensity, which is not necessary for determining the odor identity. Normalized signals can be sparse, but they fail at identifying mixtures of many odors [2]. Conversely, representations based on the most strongly excited receptor types can discriminate odors with observed performances for all intensities and mixtures sizes [3]. Our statistical model therefore identifies this primacy coding as a promising candidate and it links the microscopic parameters of such a model with the psycho-physical quantities that are measured in experiments.

[1] D. Zwicker, A. Murugan, M. P. Brenner, Proc. Natl. Acad. Sci. USA **113** 5570-75 (2016)
[2] D. Zwicker, PLoS One **11** e0166456 (2016)
[3] D. Zwicker, under review

8.2 THE DIMENSION OF NEURAL ACTIVITY IN EFFECTIVE LEARNERS

E. Tang
M.G. Mattar, C. Giusti, S.L. Thompson-Schill, D.S. Bassett
(Univ. of Pennsylvania, PA)

A fundamental cognitive process is the ability to map value and identity onto objects as we learn about them. Exactly how such mental constructs emerge and what kind of space best embeds this mapping remains incompletely understood. Here we develop tools to quantify the space and organization of such a mapping, thereby providing a framework for studying the geometric representations of neural responses as reflected in functional MRI.

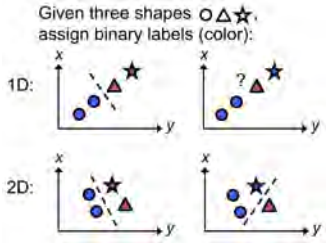

Figure 8.3: A higher-dimensional representation (bottom row) allows different categories (here denoted as shapes) to be more easily separated; x and y are the activation on different brain regions.

Dimensional estimation is performed using a linear classifier to separate assigned binary labels on the data [1]. When the data are arranged in a low-dimensional manner, some binary assignments will result in poorer separability, whereas in a higher dimension, these binary assignments can be more easily separated (see Fig. 8.3). The average performance of separability over different possible binary assignments gives the separability dimension. The stimuli dimension is estimated on the data with their original object labels, while embedding dimension is estimated on the null model with shuffled object labels. This embedding dimension reflects the distribution of neural responses without the task-relevant labels, and hence the neural activity used in the task. We apply this method to the evoked neural responses of 20 participants measured as they learned the value of twelve computer-generated shapes, with each shape assigned a distinct monetary value (see Fig. 8.4; [2]).

Figure 8.4: Adult subjects learned the monetary value of novel computer-generated objects through feedback.

We show that quick learners have a higher dimensional geometric representation than slow learners, and hence more easily distinguishable whole-brain responses to objects of different value [3]. Furthermore, we find that quick learners display a more compact embedding of the stimuli information and hence have a higher ratio of stimuli dimension to embedding dimension, consistent with a greater efficiency of cognitive coding. This and other recent work show that changes in various types of dimension can reflect the effectiveness of learning, even within the same experiment or the same neural network [4]. Lastly, we investigate the neurophysiological drivers of high dimensional patterns at both regional and voxel levels, and complete our study with a complementary test of the distinguishability of associated whole-brain responses. Our results demonstrate a spatial organization of neural responses characteristic of learning, and offer a suite of geometric measures applicable to the study of efficient coding in higher-order cognitive processes more broadly.

[1] M. Rigotti et al., Nature **497**, 585–590 (2013)
[2] M.G. Mattar et al., Network Neuro. **2**, 128 (2018)
[3] E. Tang et al., Nat. Neuroscience (in press)
[4] S. Chung, D.D. Lee, H. Sompolinksy, Phys. Rev. X, **8**, 031003 (2018)

8.3 CHARACTERIZING THE DEFAULT STATE OF CORTICAL SPIKING DYNAMICS

J. Wilting, J. Dehning, A. Hagemann, J. de Heuvel, L. Leppin, J. Pinheiro Neto, L. Rudelt, P. Spitzner, J. Zierenberg, V. Priesemann
M. Wibral (University of Göttingen)

What can we learn about a dynamical system if we can only observe a small part of it? The problem of subsampling is common to the study of many complex, spatially extended systems in nature. For example, in many diseases the number of reported infections may be much lower than the unreported ones. In the financial system only a subset of all banks is evaluated when assessing the risk of developing system-wide instability. Subsampling is particularly severe in neuroscience, because electrophysiological recordings of spiking activity can only access a small fraction of all neurons simultaneously [1] (Sec. 8.17). This limitation has hindered characterizing even most basic properties of collective spiking dynamics in cortical networks. In particular, two contradictory hypotheses prevailed for over a decade: the first proposes an asynchronous-irregular, the second a critical state. While distinguishing them is straightforward in models, we showed that in experiments classical approaches fail to correctly infer network dynamics, because subsampling can bias measures as basic as correlation strengths.

I. We developed a novel estimator, which can correctly characterize network dynamics even under strong subsampling, in principle even from the activity of a single neuron (Fig. 8.5) [2, 3]. First, we showed that whenever any of two populations is subsampled, the *observed* spike count cross correlation between the populations is smaller than the actual correlation. Likewise, the strength of autocorrelation of activity within one population is decreased. These limitations hinder the correct inference of the underlying network dynamics. The average number m of postsynaptic spikes triggered by one presynaptic spike characterizes the dynamics of first-order autoregressive systems. For these systems, the autocorrelation function is exponential, $C(t) = m^{t/\Delta t}$, or equivalently $C(t) = \exp(-t/\tau)$ with the event propagation timescale Δt and the intrinsic timescale $\tau = -\Delta t / \log m$. Our novel estimator for m relies on our analytical result that the network timescale is preserved in the tail of the autocorrelation function even under subsampling (Fig. 8.6). Thereby it overcomes the systematic subsampling bias.

II. We used this estimator to infer the default state of cortical spiking dynamics [4]. We investigated recordings from monkey prefrontal cortex, cat visual cortex, and rat hippocampus. For all experiments, collective dynamics are in a narrow, reverberating regime (median $m = 0.98$, Fig. 8.7**A**, also Sec. 6.28). This reverberating regime is clearly distinct from asynchronous-irregular ($m = 0$) and critical ($m = 1$) states.

III. We first cross-validated our results on the default state of cortical dynamics, and then predicted properties that are currently hard or impossible to obtain experimentally (see [4]). In detail, using a generic model, and matching m and the mean activity to each experiment, we could correctly reproduce network properties like interspike interval

Activity Propagation: We here investigated systems whose dynamics can be interpreted as propagation of activity A_t. This propagation can be quantified by m, the *mean number of units that are causally activated by any active unit*. To first order, activity propagation then follows the autoregressive representation $\langle A_{t+1}|A_t\rangle = m\,A_t + h$, where additional units are externally activated by input with rate h.

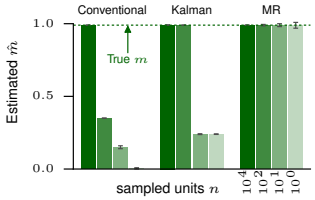

Figure 8.5: Whereas estimators for m based on conventional linear regression or Kalman filters are strongly biased under subsampling, our novel multi-step regression (MR) estimator is invariant to subsampling.

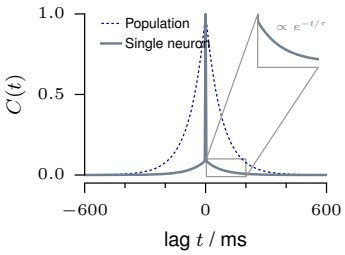

Figure 8.6: The autocorrelation strength $C(t)$ is strongly reduced under subsampling, except for zero lag. The tail of the autocorrelation function still unveils the expected, exponential decay, even for single neuron activity.

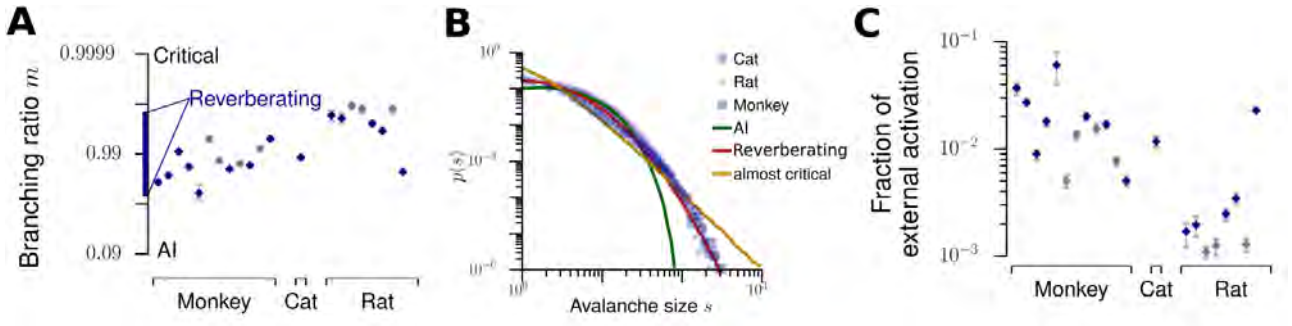

Figure 8.7: **A**. The propagation or branching ratios m of cortical spiking activity in three species are in a reverberating regime around $m = 0.98$, which is neither critical nor asynchronous irregular (AI). **B**. A generic model which reproduces the distribution of avalanche sizes s of cortical networks if tuned to the experimentally observed m, but not if tuned to AI or almost critical states. **C**. The validated model predicts that only between 0.1% and 7% of cortical activity are generated by external input, implying that the majority of spiking ($> 90\%$) is generated recurrently.

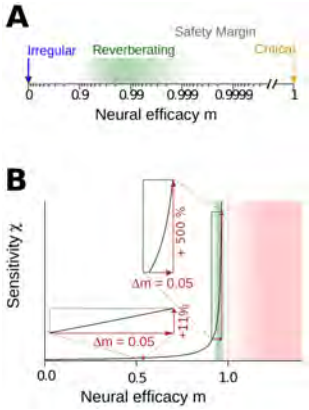

Figure 8.8: **A**. The reverberating regime has a larger m than the irregular state, but maintains a safety margin to criticality (yellow), and thus to the instability associated with the supercritical regime. **B**. The reverberating regime allows large tuning of the sensitivity by small changes of the neural efficacies, in contrast to states further away from criticality.

distributions, Fano factors, activity distributions, cross-correlations, and distributions of durations and sizes (Fig. 8.7**B**). After this cross-validation, we used the model to predict yet unknown network properties. These include the Fano factor of population activity, the total response to small perturbations, and the fraction of external activation (drive), compared to internal propagation (Fig. 8.7**C**).

IV. The reverberating regime, which characterizes cortical dynamics, is particularly versatile for information processing because: (i) already small changes in synaptic strength allow for large changes in the sensitivity, amplification and network time scale, because the reverberating regime is in the vicinity of the critical state, where many dynamical properties diverge (Fig. 8.8**B**); (ii) networks can adapt the timescale over which they integrate stimuli according to task-specific requirements; (iii) networks retain a safety margin from the instability associated with a supercritical regime (Fig. 8.8**A**); (iv) networks can strike a balance between opposing computational requirements, like trial-to-trial variability versus amplification [5].

We suggest self-organization to the reverberating regime as a central organization principle of cortical networks. We are currently developing an open-source toolbox for our estimator, which we are already using to investigate the transition to instability in human epilepsy patients; and are furthermore extending our estimator in order to compensate for non-stationary input and to infer activity propagation between two interacting populations.

[1] A. Levina, V. Priesemann, Nat. Commun. **8**, 15140 (2017).
[2] J. Wilting, V. Priesemann, Nat. Commun. **9**, 2325 (2018).
[3] F. P. Spitzner, Toolbox for the Multistep Regression Estimator. `https://github.com/Priesemann-Group/mrestimator`.
[4] J. Wilting, V. Priesemann, preprint, available at http//arxiv.org/abs/1804.07864.
[5] J. Wilting et al., Front. Syst. Neurosci. **12**, 55 (2018).

8.4 CONTROLLABILITY OF BRAIN DYNAMICS ACROSS DEVELOPMENT

E. Tang
C. Giusti, G.L. Baum, S. Gu, E. Pollock, A.E. Kahn, D.R. Roalf, T.M. Moore, K.Ruparel, R.C. Gur, R.E. Gur, T.D. Satterthwaite, D.S. Bassett (Univ. of Pennsylvania, PA)

While much of the study of neural dynamics and their control has focused on single neurons or ensembles of neurons, we explore processes and dynamics that occur across spatially distributed systems in neural tissue. To investigate how connectivity between brain regions constrains the transfer of information, we use network control theory, which provides energetic considerations for the ability to affect the activity of one part of the network from another (Fig. 8.9, [1]).

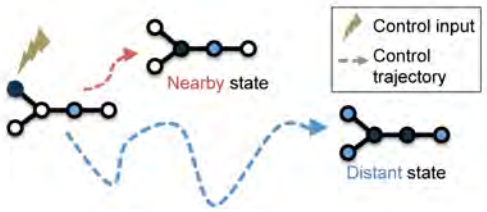

Figure 8.9: Network control models how input to a specific node in the network can change the network state along various control trajectories; magnitude of dynamical activity is represented with node color.

We study networks of white matter tracts, the strength and direction of which were inferred using diffusion tensor imaging in MRI. This enabled us to construct structural brain networks, where the edges represent white matter fiber bundles connecting these brain regions. Using network controllability metrics [2], we characterize changes in brain connectivity and supported dynamics during the period from 8 to 22 years old. We find that compared to a child's brain, an adult brain displays increased controllability, suggesting a more diverse repertoire of specialized and stereotyped dynamics, and lower synchronizability (see Fig. 8.10, [3]). In addition, we observe that improved cognitive performance (above that predicted by age) is tied to the relative strength of subcortical controllers to cortical controllers, suggesting that global or network level effects subserve functions as complex as intellectual and mental acuity.

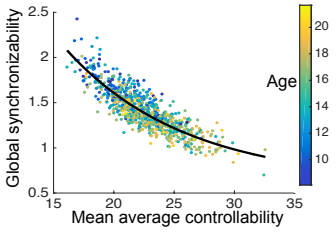

Figure 8.10: We find an adult's brain network (yellows) exhibits increased controllability and decreased synchronizability as compared to a child's brain (blues), suggesting a more diverse repertoire of specialized and stereotyped dynamics at the expense of flexibility.

Lastly, we examine if network controllability could suggest a mechanism for development, through the use of forward modeling tools for network evolution such as Pareto-optimization [4]. This method stipulates a set of growth rules towards the optimization of certain properties such as increased controllability and decreased synchronizability. These simulations provide predictions for comparison with neuroimaging data, and evidence that network controllability is being optimized across healthy neurodevelopment.

[1] F. Pasqualetti, S. Zampieri, F. Bullo, IEEE Trans. on **1**, 40–52 (2014)
[2] E. Tang, D.S. Bassett, Rev. Mod. Phys., **90**, 031003 (2018)
[3] E. Tang et al., Nat. Comm. **8**, 1252 (2017)
[4] A. Avena-Koenigsberger et al., Phil. Trans. R. Soc. B **369**, 20130530 (2014)

8.5 UNIVERSALITY AND OPTIMIZATION IN PRIMATE BRAIN EVOLUTION

M. Schottdorf, J.F. Weidinger, W. Keil, J. Liedke, B. Feulner, J. Franz, W. Wu, F. Wolf
D. Huber (U Genf)

Biological brains have the capability to build their structure by dynamical self-organization. However, unlike inanimate systems, they are *evolved* self-organized systems: although self-organization can dispense the detailed genetic specification of their structure and wiring diagram, their dynamics itself is subject to Darwinian evolution. Our prior research indicated that the self-organizing dynamics of neural circuits in the visual cortex evolved through a phase-transition-like transformation during the evolutionary path towards modern primate brains [1, 2, 3]. What drove that transition? When in mammalian evolution did it happen? And is the brain's evolutionary dynamics fast enough that selection can drive its architecture towards a functional optimum?

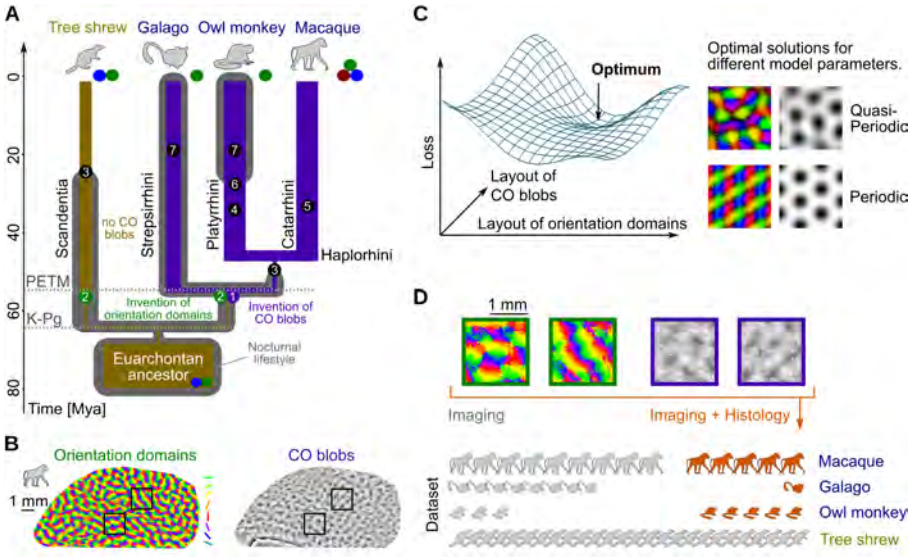

Figure 8.11: Using large-scale data from a wide phylogenetic sample and optimization theory to analyze the evolutionary remodeling of V1. A The selected lineages of supraprimate phylogeny. Key evolutionary transitions: 1: CO-domains, 2: Orientation columns, 3: Transition to diurnal lifestyle. 4: Dispersal to South America. 5: Opsin gene duplication and transition to constitutive trichromacy. 6: Secondary transition to nocturnality 7: Loss of M opsin. B Example of Macaque orientation and CO domains. C Sketch of the utility landscape of the optimization model. D Magnified regions from B and total numbers of intrinsic signal / CO-histology cases from different species.

To address these questions we formulated an analytically tractable optimization theory for the design of key features of primate visual cortex: the positioning of orientation domains, a core element of form vision circuitry, and cytochrome oxidase (CO) domains, spatial compartments that are closely associated with color vision. We tested the predictions of this theory against a large-scale data corpus of primate brain imaging data, spanning all major primate lineages and including

the smallest living primate, the mouse lemur, a classical model of the primate common ancestor.

Our studies confirm that the complex spatial structure of the form vision core circuit likely emerged in a phase-transition-like, disruptive innovation of neural circuit architecture at the origin of primates. We find a reconfiguration of CO domains during primate evolution that achieves near optimal matching to the form vision core circuit in diurnal trichromatic macaques. This observation provides direct evidence that the time scales of mammalian brain evolution are sufficient to achieve convergence to near ideal circuit architectures. In contrast, we find that the structure of the form vision core circuit was apparently maintained near invariant with exquisite precision over the past 55 Million years of primate evolution. We view this as evidence for a strong and specific selective pressure favoring and stabilizing this architecture. Mathematically we find that large-scale optimization of neuronal diversity in V1 is a functional optimization principle that can account for the invariant structure of the form vision core circuit.

Did the invariant architecture of the form-vision core circuit really emerge in an all-or-nothing transition? To test this scenario we characterized the architecture of visual cortex in one of the most basal primate lineages and we asked whether orientation prevalence maps exist in V1 of one of the smallest living primates, the miniature 60g mouse lemur Microcebus Murinus. Using chronic intrinsic signal imaging we found that visual cortical circuits in the mouse lemur are functionally organized into orientation preference domains arranged in a pinwheel-like fashion [4]. The size of orientation domains and pinwheels is smaller than previously found in any mammal. They are, however, only marginally smaller than in macaque and other large primates, suggesting that the size of these circuit elements is nearly incompressible. Intriguingly, the spatial organization of pinwheels in mouse lemur V1 was indistinguishable from macaque and precisely adheres to the design mathematically predicted by us to emerge from the self-organization of large scale V1 circuitry [4, 5]. V1 in mouse lemurs covers one fifth of the cortical surface and thus exhibits one of the largest V1/cortex ratios found in primates, which might be related to their relatively high visual acuity. Taken together, these results indicate substantial limitations to a miniaturization of primate-type visual cortical circuitry and corroborate that it evolved by disruptive innovation rather than by gradual change.

[1] M. Schottdorf, W. Keil, D.M. Coppola, L.E. White, F. Wolf. PLoS Comput Biol 11:e1004602 (2015)

[2] W. Keil, M. Kaschube, M. Schnabel, Z.F. Kisvarday, S. Lowel, D.M. Coppola, L.E. White, F. Wolf. Science 336:413–413. (2012)

[3] M. Kaschube, M. Schnabel, S. Lowel, D.M. Coppola, L.E. White, F. Wolf. Science 330:1113–1116. (2010)

[4] C.L.A. Ho , R. Zimmermann, J.D.F. Weidinger, B. Tia, F. Pifferi, F. Aujard, F. Wolf, D. Huber Cosyne (2019)

[5] F. Wolf. Phys Rev Lett. 95:208701 (2005)

8.6 DYNAMICAL MECHANISMS OF FLEXIBLE INFORMATION ROUTING IN THE BRAIN

A. Palmigiano, T. Geisel, F. Wolf, D. Battaglia

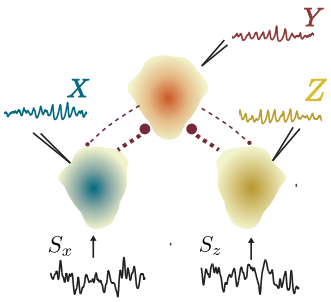

Figure 8.12: We consider realistic models of multi-area cortical circuits near the onset of oscillatory synchrony that are symmetric with respect to X and Z.

The efficiency of our brain depends on its ability to flexibly select relevant information and to route it along different paths, e.g. under selective attention. How can it switch this routing in a fraction of a second, if the wiring of neurons can be reconfigured only slowly? We have recently uncovered a highly flexible mechanism which uses transient synchrony to dynamically reroute information paths in a few hundred milliseconds [1].

The discovery of correlated oscillatory neuronal activity three decades ago has led to a plethora of theoretical work on neuronal synchronization, but so far its functional role, e.g. for the so-called binding problem has not been confirmed rigorously. More recently a communication-through-coherence (CTC) hypothesis was proposed, which posits that inter-areal coherence may selectively favor inter-areal communication. The stochastic and transient nature of neuronal oscillations in vivo, however, appeared hard to reconcile with such a function. We have shown [1] that models of cortical circuits near the onset of oscillatory synchrony selectively route input signals despite the short duration of gamma bursts and the irregularity of neuronal firing. In canonical multi-area circuits with realistic anatomy we found that gamma bursts spontaneously arise with matched timing and frequency. They gate information flow by large-scale routing states depending on relative phase differences, as exhibited by mutual information and transfer entropy. Specific self-organized routing states can be induced by minor modulations of background activity.

[1] A. Palmigiano, T. Geisel, F. Wolf, and D. Battaglia, Nature Neurosci. 20, 1014 (2017).

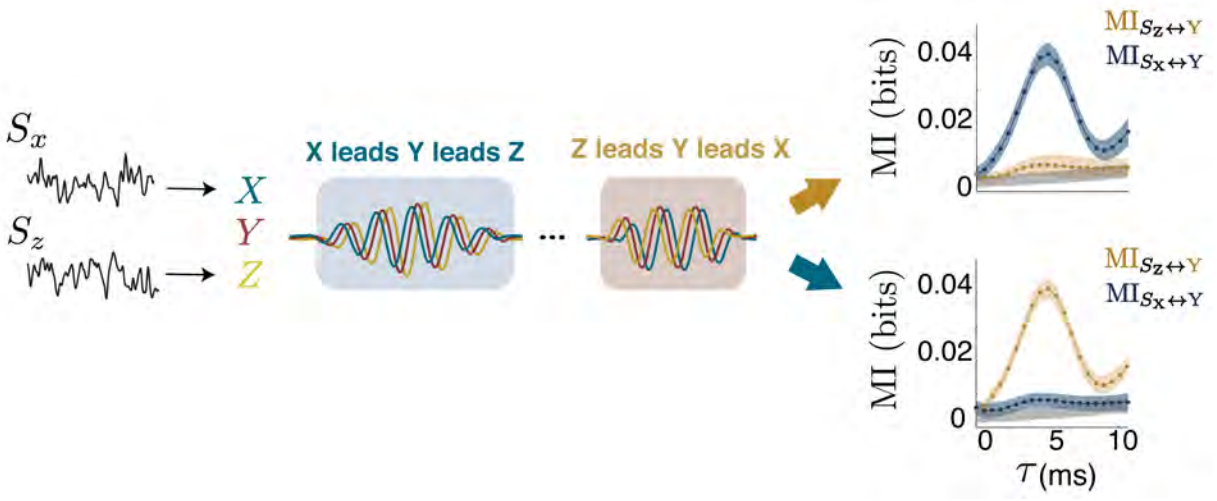

Figure 8.13: Relative phase differences can flexibly gate information flow (S_x or S_z into Y) as exhibited e.g. by the time-delayed mutual information.

8.7 DYNAMICAL STATES OF A LIVING NETWORK

P. Fleig, M. Kramar, M. Wilczek, K. Alim

In living systems, behaviour is the result of complex information processing and decision making. Unraveling how information translates into distinct actions is important to understand animal behaviour and may inform us about useful design principles for smart materials and soft robots. Specifically very simple organisms allow a novel perspective to understand the physical principles of information processing driving behaviour. Non-neural organisms like the slime mould *Physarum polycephalum* show remarkably complex behaviour including growth, adaptation of the network morphology and foraging for food - while still being a single, giant, network-shaped cell. Behavioural dynamics, here, emerge from information processing in living matter namely the coordinated contractions of the cell's tubular shaped acto-myosin cortex undergoing rhythmic contraction every 100 seconds, see Fig. 8.15(a). Understanding how behaviour results from contraction patterns in *P. polycephalum* may inform us both about the physics of behaviour and the dynamics of living matter.

To characterise behaviour of animals, a fruitful statistical approach has been to decompose the behaviour and represent it by a relatively small set of distinct stereotyped 'modes' with transitions between them, for example [1]. In *P. polycephalum* the generation of behaviour lies in the active control of contraction patterns across the network. Decomposing spatiotemporal contraction dynamics into principal components, see Fig. 8.14, we indeed find a reduced set of 'modes' corresponding to characteristic large-scale contraction patterns [2]. Yet, the organism intermittently, reproducibly switches to incoherent, higher frequency contraction patterns for short periods of time, see Fig. 8.15(b). These surprising dynamics are accompanied with our observation of a power law distribution of relative mode amplitudes, see Fig. 8.15(c), which may be key to allow for the switching between coherent and incoherent dynamics to unfold. Our findings now connect behaviour with characteristic states of living matter.

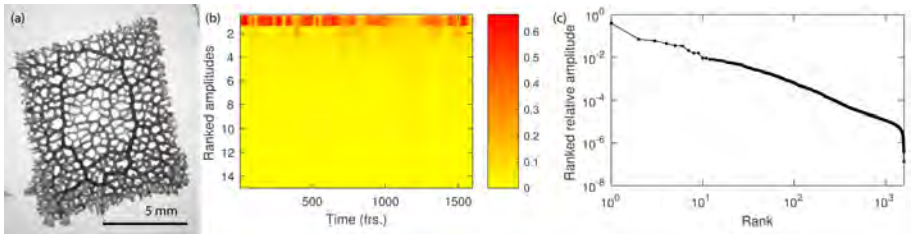

Figure 8.15: (a) Example frame of bright-field data. (b) The ranked relative values of mode amplitudes over time and (c) the spectrum of ranked relative amplitudes at one point in time.

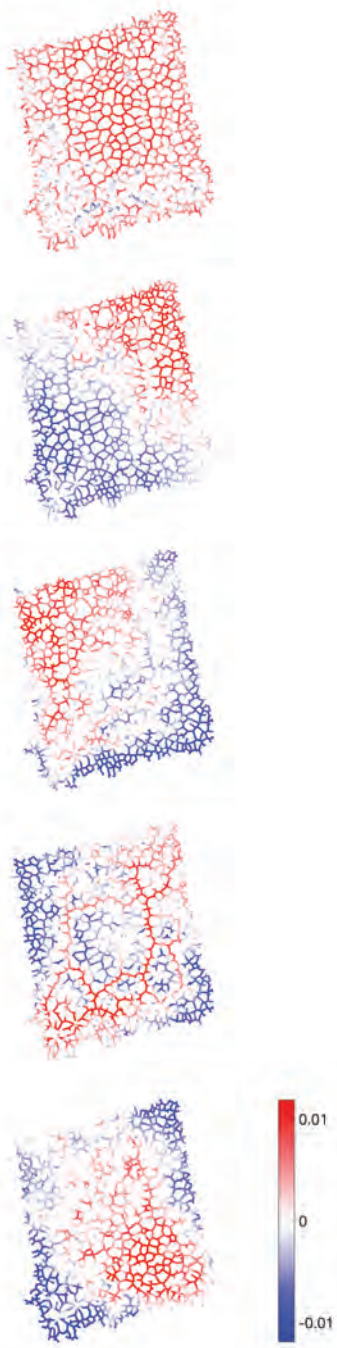

Figure 8.14: The five top ranked principal components of network contractions ordered by magnitude top to bottom.

[1] G.J. Stephens et al., PLoS Comput Biol 4(4): e1000028 (2008).
[2] P. Fleig, M. Kramar, M. Wilczek, K. Alim, in preparation (2019).

8.8 COLLECTIVE DYNAMICS OF HUMAN MOBILITY

M. Schröder, D. Manik, N. Molkenthin,
N. Beyer, P. Marszal, A. Sorge, S. Herminghaus, M. Timme
J. Nagler (ETH Zurich & Frankfurt)

How we are mobile and transport goods is rapidly changing. Since the end of the 19th century, the average European is constantly spending about 7 hours a week traveling. Yet, the paths we take as well as the vehicles and services we use have become different, and the distances we travel have increased dramatically. Urbanization, world population growth, and the omnipresent digital services put additional constraints on and add various new options to how we organize mobility.

Today, we more easily combine different modes of transport such as walking, biking and driving, request more flexible, publicly available transportation on demand and during the act of being mobile more and more favor to communicate or work rather than drive ourselves.

Despite such options and desires, traffic in large cities further slows to a crawl and public transport systems are often too inflexible to meet demand due to their predefined timetables and stopping locations, or simply overwhelmed by the number of passengers. Staying mobile in a flexible way becomes a pressing issue also in rural areas, currently addressed by (too) many pricate cars. Such forms of human mobility imposes substantial financial, ecological and societal costs that are likely to increase even more in the future. Moreover, local non-systemic solutions to mobility problems may result in substantial rebound effects. For instance, establishing improved streets in a city may attract even more traffic.

The changing mobility and transport systems thus exhibit a number of research challenges on how to organize and optimize mobility patterns and finally decrease overall traffic volume. How can we systematically evaluate non-standard forms of mobility, understand distributed and correlated demand patterns (e.g. distributed interlocked "rush hours"), the consequences of electrified and autonomous vehicles on mobility patterns, the effects of the transport infrastructure, and especially the interplay of all these aspects? In the network dynamics team, we aim to advance the fundamental understanding of the complex patterns and interactions between the different aspects of human mobility to help develop efficient and scalable solutions for public, shared and individual transport.

***EcoBus* – Physics of shared mobility.** One significant milestone in this direction is the ongoing collaborative project we enabled at the MPIDS through scientific research, tool development, public relations and a major EU/Lower Saxony grant support via the European fund for regional development (EFRE). Please see also http://ecobus.jetzt and Rep. 8.21. EcoBus realizes a project rooted in applied fundamental science on the **physics of shared mobility**, addressing how ad hoc and pre-planned origin-destination requests can be efficiently met by shared (small) busses that flexibly offer door-to-door service. In close collaboration with local government and mobility service providers, the

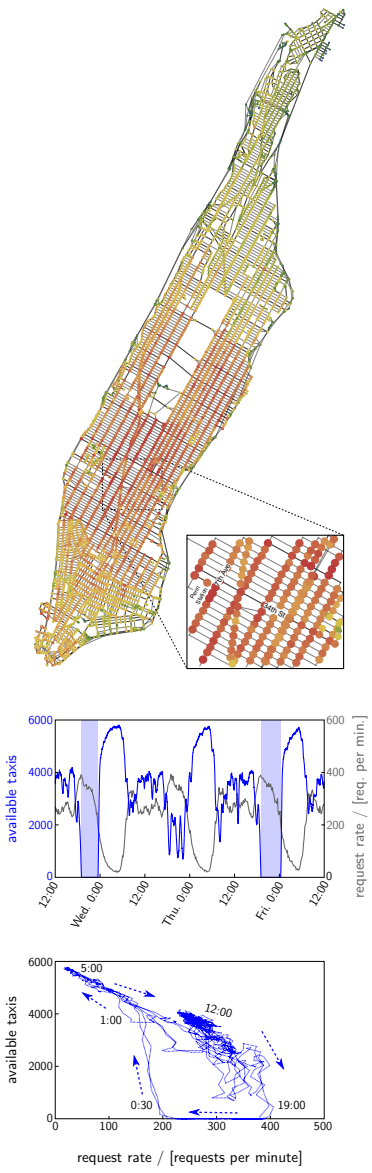

Figure 8.16: **Dynamic hysteresis and overload of inefficient ride hailing.** Simulation results based on actual request data in Manhattan from 2015.

ongoing pilot project aims to provide a proof of concept for on-demand shared mobility in rural areas.

The data and experience gained during this test phase helps to improve the performance of such systems. To further support this project, we developed a general simulation framework and logical structure build to study the problem of efficient vehicle routing under different conditions and to develop, evaluate and compare routing algorithms, see, e.g. [1, 2, 3].

Inherent inefficiencies in standard collective ride-hailing. How efficient can ride hailing services be and how can they be optimized to reach their best performance? Combining our simulation tools with the analysis of mathematical models, we studied the efficiency of different algorithms to assign transporters (e.g. taxis or buses) to origin-destination requests by passengers in space-time. We reveal inherent inefficiencies of ride hailing systems if they exploit commonly used first-come-first-serve (fair) assignment schemes [2]. In statistical physics and nonlinear dynamics terms, these systems exhibit **hysteresis in their dynamics**, see Fig. 8.16. Hysteresis is essentially unavoidable, because it relies on a simple fundamental mechanism. In the high-load state, transporters becoming available appear individually within a crowd of busy transporters, thus on average drive a relatively long distance until they pick up a new passenger and thereby need a large total time to serve one request. In contrast, in the low-load state, there are many transporters available to serve an incoming request, such that on average the nearest transporter has to drive a relatively short distance to realize the pick-up, thereby becoming available again earlier.

If a system is overloaded, it stays overloaded even when the request rate decreases. This state of high load is intrinsically collective and disappears only if the requests rate drops substantially (middle panel of Fig. 8.16). Importantly, this hysteresis in almost **unavoidable**: it emerges independent of the details of the traffic networks or request patterns, prevails across taxi and ride-sharing services and disappears only if *all* service providers (a fraction of one, almost surely) use a collectively more efficient assignment scheme. These results may help selecting an efficient and fair assignment method and developing suitable algorithms guided by insights about the *collective* dynamics.

Unavoidable hysteresis explained. Hysteresis is essentially unavoidable, because it relies on a simple fundamental mechanism. In the high-load state, transporters becoming available appear individually within a crowd of busy transporters, thus on average drive a relatively long distance until they pick up a new passenger and thereby need a large total time to serve one request. In contrast, in the low-load state, there are many transporters available to serve an incoming request, such that on average the nearest transporter has to drive a relatively short distance to realize the pick-up, thereby becoming available again earlier.

Scaling and quantifying ride-sharing efficiency. We also developed models for ride-sharing in on-demand bus services mimicking those of the ***EcoBus*** project. Combining stochastic mean field theories with direct numerical simulations, we revealed a scaling relation between the waiting and driving times of the passengers and the overall utilization of the system that is independent of the specific transport network and route assignment algorithms. Extending these results, we developed quantifiers to evaluate and compare transport and route assignment algorithms in terms of their utilization and ride-sharing efficiency, as well as fairness to the passengers [3].

[1] A. Sorge et al., *Towards a unifying framework for demand-driven directed transport (D3T)*, Proc. Winter Simul. Conf., 2800-2811 (2015)

[2] P. Marszal et al., *Hysteresis and inefficiency in ride-hailing systems*, in prep.

[3] N. Molkenthin et al., *A universal measure for ride-sharing efficiency*, in prep.

8.9 SAMPLING BIAS IN NEURONAL DYNAMICS WITH COARSE MEASURES

J. Pinheiro Neto, V. Priesemann

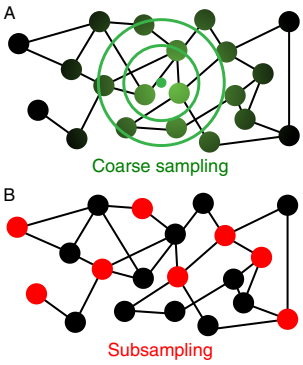

Figure 8.17: **A.** Under coarse sampling, a weighted representation of all neurons in a region is recorded. This is the case for LFP, EEG, and MEG signals. **B.** Under subsampling, only a fraction of all neurons is recorded.

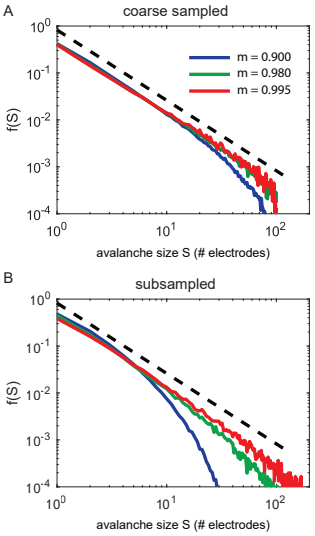

Figure 8.18: Avalanche size distributions: **A.** Coarse-sampling hinders separating dynamical regimes with varying branching ratio m. **B.** Subsampled (spike) data show a much better separation. Dotted line corresponds to $f(S) \sim S^{-3/2}$.

A popular hypothesis about large-scale brain activity is that it self-organizes to a critical point of a phase transition [1]. There are two main criteria used to pinpoint criticality: i) a *branching ratio* of $m = 1$, which means that, on average, neurons induce as many spikes as they receive (see Sec. 8.3), and ii) an *avalanche size* S — the total number of neurons active between periods of silence (see Sec. 8.17) — follows a probability distribution of $f(S) \sim S^{-3/2}$.

Most evidence for criticality originates from *coarse-sampled* activity, which measures a weighted sum of activity of a large population (Fig. 8.17A). For example, this is the case for local field potentials (LFP), or electric and magnetic signals measured at the scalp level (EEG, MEG). Alternatively, one can record spiking activity, but this captures only a fraction of all neurons. This limitation is called *subsampling* (Fig. 8.17B). In contrast to coarse-sampled results, analysis of subsampled data typically indicate subcritical dynamics [2, 3], which is characterized by $m < 1$ and $f(S)$ with an exponential cut-off.

We showed that the origin of these contradicting hypotheses may lie in the sampling approach: under coarse sampling, it is not possible to distinguish between $f(S)$ from states at different distances to criticality (Fig. 8.18A). In contrast, this is possible with subsampled (spike) data (Fig. 8.18B). We identified the *inter-electrode distance* d as a key parameter that can influence analysis of coarse-sampled data. A small d can introduce spurious correlations into the system, biasing $f(S)$ and the measured m (Fig. 8.19). Thus, a system may appear critical for subcritical underlying dynamics.

We provided an explanation for the contradictory results. Our findings support results from spike recordings regarding criticality, in particular, that cortical activity is in a subcritical state — a state that offers the computational advantages associated with criticality but maintains a safety margin from unstable, supercritical dynamics [4].

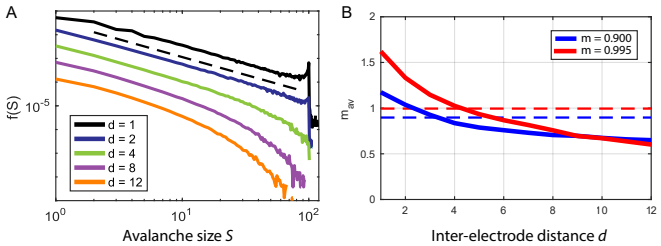

Figure 8.19: **A.** Effect of the inter-electrode distance d on $f(S)$ with $m = 0.900$, under coarse sampling. Dotted line corresponds to $f(S) \sim S^{-3/2}$, expected for criticality ($m = 1$). **B.** Measured branching ration m_{av} for a model with $m = 0.995$ and $m = 0.900$.

[1] M. A. Muñoz, Rev. Mod. Phys. **90**, (2018)
[2] V. Priesemann et al., Front. Syst. Neurosci. **8**, 108 (2014)
[3] J. Wilting & V. Priesemann, Nat. Commun. **9**, 2325 (2018)
[4] J. Wilting et al., Front. Syst. Neurosci. **12**, (2018)

8.10 QUANTIFYING INFORMATION PROCESSING TO INFER CODING STRATEGIES IN NEURAL CIRCUITS

L. Rudelt, V. Priesemann

The brain is capable of processing huge amounts of sensory information using orders of magnitude less energy than human-made computing devices. This has inspired the theory of efficient coding, which proposes that the neural code quenches temporally and spatially redundant input information to save resources. The theory has proven very successful in predicting receptive field and physiological properties of neurons in early sensory processing. However, it remains an open question whether efficient information transmission and redundancy reduction shape the neural code also at later stages of information processing. Since at later stages, i.e. in higher cortical areas, a clear correspondence between neural responses and encoded information is no longer available, we used information theory to quantify how much temporal redundancy (TR) in neural spiketrains limits their transmission capacity, irrespective of the encoded content [1].

Technically, estimating single neuron information capacities subject to temporal redundancy is an extremely challenging inference problem. This is because spiking occurs on the timescale of milliseconds, whereas past dependencies may extend over seconds. Consequently, considerable temporal coarse graining through binning of past activity (Fig. 8.20) is required to keep estimation bias in check. We developed and bench-marked a novel binning method that preserves as much statistical dependencies as possible under the constraint of reliable estimation, and we controlled potential mis-estimations due to the curse of dimensionality using a Bayesian bias criterion (BBC) [2].

When comparing recordings from retina [3] (sensory input) and hippocampal CA2 [4] (memory), we found that TR reduced single neuron transmission capacity by about 25%, and that the past range of TR extended over hundred milliseconds in retina, and up to seconds in CA2 (Fig. 8.22).

In contrast to the prevalent view on TR reduction, we showed that past information is maintained in the form of neural spikes at the cost of redundancy, and thus limits information transmission capacity. Importantly, clear differences of TR between hippocampus and retina point at distinct requirements on information transmission at different stages of information processing. The higher past range and TR of CA2 can support its memory function, whereas retina as a sensory input shows signatures of fast transmission and fast forgetting.

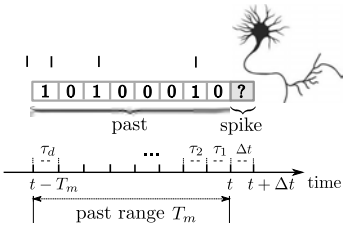

Figure 8.20: Binary representation of spiking activity and its past using temporal binning.

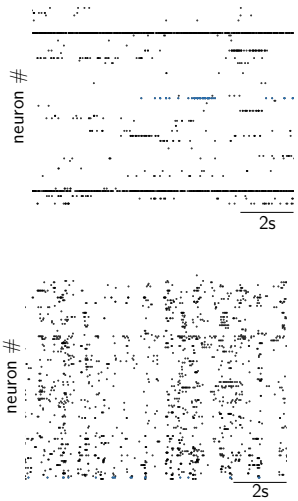

Figure 8.21: Excerpt of recorded spiking activity in hippocampus (top) and in retina (bottom).

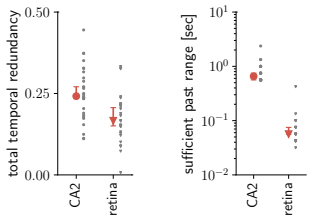

Figure 8.22: Total estimated TR (BBC) for all analyzed neurons and median as well as 5 % and 95 % percentiles using bootstrapping (left) and the same for sufficient past range required to account for 98% of the total TR (right).

[1] M. Wibral, J. Lizier, V. Priesemann, Frontiers in Robotics and AI **2** (2015).
[2] L. Rudelt, M. Wibral, V. Priesemann, *in preparation* (2018).
[3] J. S. Prentice, O. Marre, M. L. Ioffe, A. R. Loback, G. Tkačik, M. J. Berry II, PLOS Computational Biology **12**(11), e1005148 (2016).
[4] K. Mizuseki, A. Sirota, E. Pastalkova, G. Buzsáki, Neuron **64**, 267-280 (2009).

8.11 PSYCHOPHYSICS OF MUSICAL RHYTHMS AND MICROTIMING DEVIATIONS IN JAZZ

G. Datseris, M. Sogorski, V. Priesemann, T. Geisel
A. Ziereis, T. Albrecht, Y. Hagmayer (Univ. Göttingen)

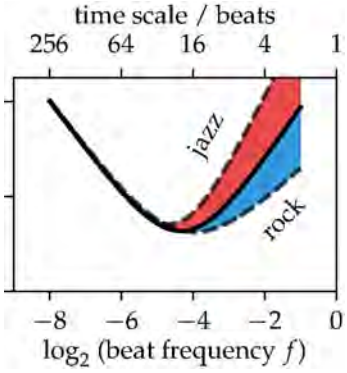

Figure 8.23: Summarizing sketch of typical genre-induced differences in the power spectral density.

Musical rhythms performed by humans typically show temporal fluctuations. While they have been characterized in simple rhythmic tasks, it is an open question what is the nature of temporal fluctuations, when several musicians perform music jointly in all its natural complexity. To study such fluctuations in over 100 original jazz and rock/pop recordings played with and without metronome we developed a semi-automated workflow allowing the extraction of cymbal beat onsets with millisecond precision [1]. Analyzing the inter-beat interval (IBI) time series revealed evidence for two long-range correlated processes characterized by power laws in the IBI power spectral densities (Fig.8.23). One process dominates on short timescales (t < 8 beats) and reflects microtiming variability in the generation of single beats. The other dominates on longer timescales and reflects slow tempo variations. Whereas the latter did not show differences between musical genres (jazz vs. rock/pop), the process on short timescales showed higher variability for jazz recordings, indicating that jazz makes stronger use of microtiming fluctuations within a measure than rock/pop [1]. These results elucidate principles of rhythmic performance and can inspire algorithms for artificial music generation.

In particular in jazz performances, the so-called swing feeling has puzzled musicologists and jazz critics for decades. For a long time it was believed that one can feel it, but one cannot explain it. More recently discussions focused on the role of microtiming deviations. Some musicologists claim that they are substantial for the swing feeling, others deny such a role. In an attempt to resolve this controversy we carried out an online survey using jazz recordings in which we had systematically manipulated microtiming deviations – exaggerating, deleting, and inverting them [2]. We found that the presence of microtiming deviations is not essential for the "swing" feeling as versions without microtiming deviations were preferred (Fig. 8.24), in contrast to the common belief of many musicians.

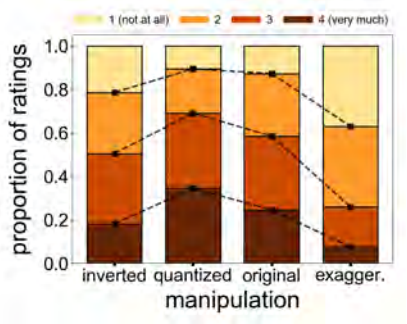

Figure 8.24: Result of the online survey. Proportion of ratings averaged across 12 pieces and 160 participants for 3 different manipulations of microtiming deviations and for the original jazz recordings. Dashed lines are guides to the eye for the cumulative distributions of ratings.

[1] M. Sogorski, T. Geisel, V. Priesemann, PLoS ONE, 0186361 (2018).
[2] G. Datseris, A. Ziereis, T. Albrecht, Y. Hagmayer, V. Priesemann, and T. Geisel, to be publ.

8.12 OSCILLATORY FLOW DRIVE SCALING OF CONTRACTION WAVE WITH SYSTEM SIZE

J.-D. Julien, S. Lafon, K. Alim

Flows over remarkably long distances are crucial for the functioning of many organisms, across all kingdoms of life. Coordinated flows are fundamental to power deformations, required for migration or development, or to spread resources and signals. A ubiquitous mechanism to generate flows, particularly prominent in animals and amoebas, is actomyosin cortex-driven mechanical deformations that pump the fluid enclosed by the cortex. However, it is unclear how cortex dynamics can self-organize to give rise to coordinated flows across the largely varying scales of biological systems.

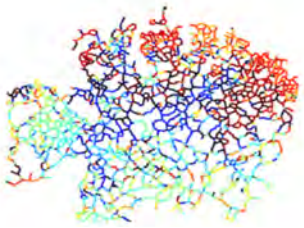

Figure 8.25: A single wave of contractions scales with network size in *P. polycephalum*, as shown here by a phase map of the contractions.

A particularly striking example are the long-wavelength cortex contractions of the tubular networks of the slime mould *Physarum polycephalum* [1], see Fig. 8.25. We observed that in *P. polycephalum* stimulants that alter cortex contractility are advected with the fluid flow within the tubes [2]. This observation suggested that the physical transport by fluid flows is the key to long-range spatial coordination of cortex contractions and fluid flows. We therefore developed a mechanochemical model of actomyosin cortex mechanics coupled to a contraction-triggering, soluble chemical. The chemical itself is advected with the flows generated by the cortex-driven deformations of the tubular-shaped cell. We show that this system exhibits spontaneous waves of contractions and flows, see Fig. 8.26(a), and that those waves are stable up to a scale of several centimeters, seven times beyond the analytical prediction λ_{lin} [3], see Fig. 8.26(b). Patterns can be robustly generated in a growing system or by flow-generating boundary conditions. We therefore identify oscillatory flows as the key for the scaling of contraction waves with system size. Our work shows the importance of active flows in biophysical models of patterning, not only as a regulating input or an emergent output, but also as a full part of a self-organized machinery. Considering the ubiquity of actin-driven contractions and cytoplasmic flows, this mechanism is likely to be relevant for other biological systems.

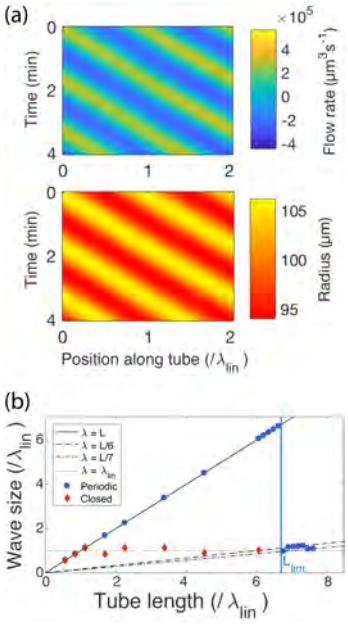

Figure 8.26: (a) Simulation of our model for self-organized contractions coupled by cytoplasmic flows in a single tube. (b) Contraction waves scale with system size up to several centimeters in a growing tube, with periodic boundary conditions (blue dots).

The key principle of advection driven scaling with system size applies generally beyond the specific system of cortex contraction driven flows. To show this we extend the FitzHugh-Nagumo model by an advection term and analytically solve for the pulse width. We find that the advection term leaves the pulse velocity untouched but linearly varies the pulse width [4]. These findings substantiate that flows are of important function in active patterns in general.

[1] K. Alim, G. Amselem, F. Peaudecerf, M.P. Brenner, A. Pringle, Proc. Natl. Acad. Sci. U.S.A. **110**, 13306 (2013)
[2] K. Alim, N. Andrew, A. Pringle, M.P. Brenner, Proc. Natl. Acad. Sci. U.S.A. **114**, 5136 (2017)
[3] J.-D. Julien, K. Alim, Proc. Natl. Acad. Sci. U.S.A. **115**, 10612 (2018)
[4] S. Lafon, J.-D. Julien, K. Alim, in preparation (2019)

8.13 THE DYNAMICS OF ADAPTIVE IMMUNE RESPONSE TO HIV

A. Nourmohammad

The adaptive immune system in vertebrates is an evolving cellular population, constantly challenged by diverse populations of co-evolving pathogens. It consists of diverse B- and T-cells, whose unique surface receptors are generated through genomic rearrangement, mutation, and selection. The maturation of B-cells is a *somatic Darwinian evolution* that occurs within an individual: During infections, B-cell receptors (BCRs) undergo mutations and are selected based on their binding affinity to pathogens, forming genetically related BCRs and antibodies (lineages), and secrete these receptor as antibodies in the blood; see Fig. 8.27.

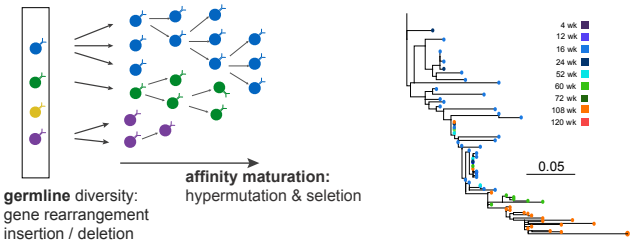

Figure 8.27: Left: Maturation of diverse B-cell receptors (colors) by somatic mutations forms genealogies of genetically related cells (lineages), selected based on their affinity against pathogens. Right: Maximum likelihood phylogeny for a lineage in an HIV patient over time (colors) shows a skewed topology, indicative of positive selection [3].

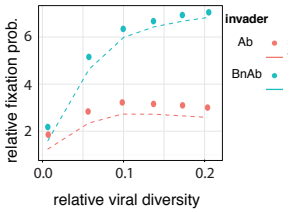

Figure 8.28: BnAbs (blue) are more likely to dominate the immune response against a diversified viral population compared to neutralizing antibodies (red) [1]. Fixation probability of lineages and the outcome of coevolution can be estimated from the inferred fitness parameters.

Our goal is to characterize the efficacy of adaptive immune strategies and the evolutionary constraints that shape the immune response. To this end, we study the statistical structures of large amounts of immune repertoire sequence data in different biological conditions. There is an ongoing effort to collect repertoires and viral populations from HIV patients over many years. Aside from the significant public health component of research on HIV, the BCR repertoire-HIV interaction is an attractive model system to quantify adaptive immune responses against adapting pathogens in coevolving ecologies.

Chronic viruses like HIV-1 engage in a rapid coevolutionary arms race with the host's adaptive immune system. We have developed a principled framework to describe the non-equilibrium coevolutionary dynamics of immune cells and pathogens, based on their biophysical interactions [1]. Our theory indicates that measuring interactions between immune and pathogen populations sampled from different time points provides a signature for immune-pathogen coevolution, and is predictive of their dynamics. This work has shed light on the conditions that permit emergence of highly potent broadly neutralizing antibodies (BnAbs), which trap the virus by targeting its vulnerable regions (Fig. 8.28). Eliciting such BnAbs is the current goal for a universal vaccine against rapidly evolving viruses, such as HIV.

While it is clear that pathogens exert strong selection on the adaptive immune system, the modes of immune response are still unknown. Recently, we have characterized the dynamics of the immune response by analyzing high-throughput BCR repertoire sequences from a number of HIV-1 infected individuals, over 2.5 years of infection [3]; data from ref. [4]. Despite its large depth, the immune repertoire data is a highly under-sampled representation of the receptor sequence space; statistical inference from such incomplete information is a hallmark of statistical physics. Our statistical approach involves constructing advanced evolutionary models and population genetics statistics suitable for the dynamics of the highly structured immune (B-cell receptor) repertoire data (Fig. 8.27).

We show the prevalence of clonal interference, where multiple beneficial mutations simultaneously arise on different genetic backgrounds and result in a stochastic, non-linear competitive dynamics: this evolutionary regime is common to rapid adaptation of asexual populations of microbes and viruses. We show that positive selection and clonal interference among beneficial mutations escalate as the viral population expands, resulting in its rapid evolution (Fig. 8.29). Clonal competition among BCRs reduces the efficacy of selection, leading to a less predictable fate for good clones, as they can be outcompeted by new mutants before they dominate the immune response. On the positive side, we hypothesize that, due to dominance of selection with a large supply of beneficial mutations, it should be feasible to infer *fitness models* to forecast immune responses, based on receptors' selection differences. Constructing predictive models for immune response is an ongoing effort in my group.

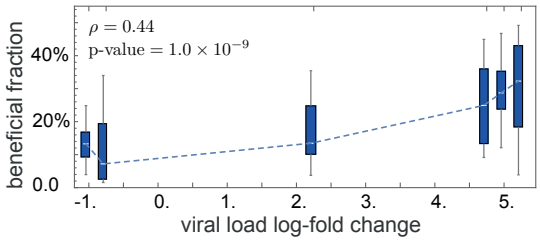

Figure 8.29: B-cell response traces the evolution of HIV-1. Fraction of positively selected mutations in pathogen-engaging regions of B-cell receptors strongly correlates with the log-fold change in the viral load [3].

[1] Nourmohammad A, Otwinowski J, Plotkin JB. Host-pathogen coevolution and the emergence of broadly neutralizing antibodies in chronic infections. PLoS Genet. 2016; 12: e1006171.

[2] Richman DD, Wrin T, Little SJ, Petropoulos CJ. Rapid evolution of the neutralizing antibody response to HIV type 1 infection. Proc Natl Acad Sci USA. 2003; 100: 4144–4149.

[3] Nourmohammad A, Otwinowski J, Mora T, Walczak AM. Clonal competition in B-cell repertoires during chronic HIV-1 infection. bioRxiv 2018; 10.1101/271130.

[4] Hoehn KB, Gall A, Bashford-Rogers R, Fidler SJ, Kaye S, et al., Dynamics of immunoglobulin sequence diversity in HIV-1 infected individuals. Philos Trans R Soc Lond B Biol Sci. 2015; 370(1676): 20140241.

8.14 A KEY INNOVATION DURING THE EARLY EVOLUTION OF NERVE CELL DESIGN

E. Lazarov, B. Feulner, C. Zhang, M. Puelma-Touzel, A. Palmigliano, R. Engelken, A. Neef, F. Wolf
M.J. Gutnick (Hebrew U), I.A. Fleidervish (Ben Gurion U),

Nervous systems are large-scale multi-component dynamical systems evolved to process information. Compared with most dynamical systems in physics they are special in that they continuously transform their dynamical state variable between two representations: analog and digital. The digital spike output of the individual nerve cells mediates all causal interactions with other nerve cells. Internally, however, nerve cells - like most other cells - use analog variables such as ion concentrations and electrical potentials for computation. Synapses are the nervous system's tools for converting the spike sequences arriving at a neuron back to this internal analog code. The nerve cell's biological AD converter, the spike generator situated in the initial segment of the axon (AIS), thus plays a critical role in the dynamics of biological neuronal networks. Over the past decade, it was discovered that the biological AD converter used in the human brain was a relatively late evolutionary invention: specialized scaffold proteins increased the density of ion channels in the AIS. Which advantage drove this invention and whether its dynamics is tailored to optimize the neuronal code had, however, remained elusive. To answer these questions we employ a combination of stochastic dynamics, and *ex vivo* and *in vitro* experiments to determine the quality of this encoding, its molecular biophysical basis and the advantages of the specific biophysical design found in mammals.

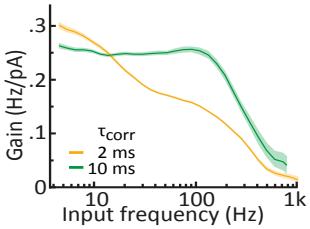

Figure 8.30: Spiny stellate cells have a narrow encoding bandwidth (≈10Hz) if the background input is rapidly fluctuating (orange), as is the case for cortical pyramidal neurons, where we observed an input correlation time τ_{corr} of 2ms . However, due to special synaptic NMDA receptors, spiny stellate cells feature an input correlation of τ_{corr}=10ms, which endows them with 200Hz encoding bandwidth.

Our most recent results establish a near ideal, single action potential sensitivity of the stellate cell network in barrel cortex [1]. Combining theoretical and experimental approaches we found direct quantitative evidence that dynamic encoding by a CNS neural population code is functionally optimized (Fig. 8.31). Slight modifications of the dynamics of synaptic transmission or of spike generation greatly decreased encoding quality (Fig. 8.30). The native bandwidth of the system is so high that the number of neurons in the circuit is large enough to allow near perfect detection of every spike reaching cortex from the sensory pathway. This picture is complemented by our results from a novel experimental approach to reduce the channel density at the spike generator while maintaining its regular nanoscale structure [2]. For the first time, we demonstrated that even with a low density of sodium channel in the AIS, spike initiation still occurs in the axon, albeit with compromised temporal precision. Hence, the main benefit of the high ion channel density is precise spike timing and an increased bandwidth of the neuronal population code. Theoretical results on the impact of spike generation in recurrent networks [4, 5] demonstrate that the impact of increasing the temporal precision of spike generation is orders of magnitude stronger than the information rate of a noninteracting neuronal population [6, 7]. Together our studies indicate that

optimizing the function of a neuronal circuit at the level of its collective dynamics creates a selective pressure that reaches down to the most subtle details of the nerve cells' bio-molecular organization. We thus propose that benefits in the collective dynamics of neuronal information processing were the likely drivers of the evolutionary innovation of the spike generation mechanisms.

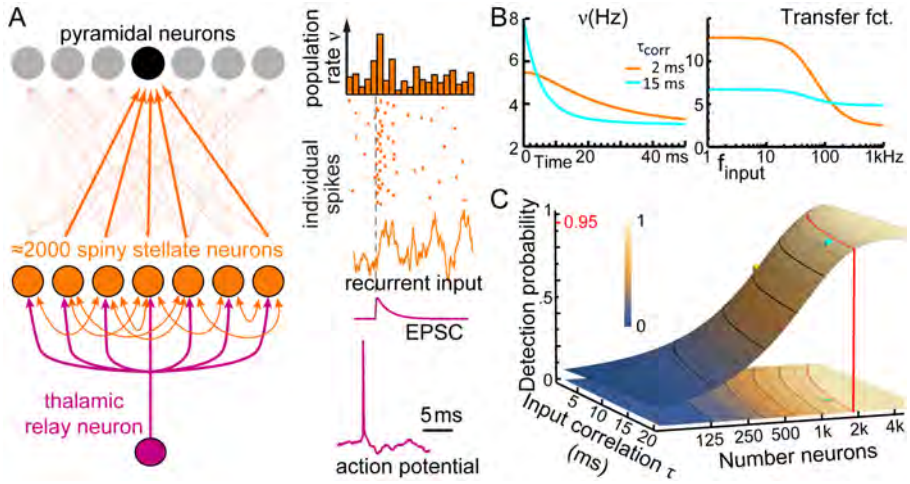

Figure 8.31: Neuronal information encoding A) Simplified barrel cortex layout: Sensory information from the thalamus enters as spikes, strongly diverging (1:1000) onto spiny stellate cells (orange), where they trigger synaptic currents (EPSC). The recurrent network of spiny stellates creates fluctuating, uncorrelated backgound input. It overlays the sensory input each spiny stellate receives in synchrony, and decorrelates their output spikes. Each spiny stellate sends its spike trains onto most pyramidal neurons such that each pyramidal reads the cumulative *population firing rate* $\nu(t)$. B) For the simplified Gauss-Neuron we can analytically derive $\Delta\nu(t)$ following an EPSC, received on top of random recurrent input with a correlation time τ_{corr}. The faster response for smaller τ_{corr} is reflected in a larger bandwidth of the transfer function $\Delta I(t) \rightarrow \Delta\nu(t)$. C) The EPSC-driven excursion $\Delta\nu(t)$ rises above the fluctuating $\nu(t)$ baseline (see A) if the bandwidth is large or if the spike count noise is small, because the number of spiny stellate neurons is large: 2,000 neurons achieve ≈95% detection rate if τ_{corr}=15ms (cyan marker) but only 60% if τ_{corr}=2ms (orange marker).

Our approach also allowed us to unmask pathological impairments that had escaped conventional electrophysiological analyses [8]. In neurons, which survived transient hypoxia and spreading depression, we observed a reduction of encoding bandwidth even though standard measures found the neurons to be surprisingly normal. We also elucidated how hypoxia leads to AIS degeneration and compromised encoding: glutamate-driven depolarization causes massive calcium influx, which activates the enzyme calpain, known to interfere with key AIS proteins.

[1] O. Revah, et al., A. Neef, F. Wolf, *in preparation*
[2] E. Lazarov, et al., F. Wolf and A. Neef. Science Adv. 4:eaau8621 (2018)
[3] E. Katz, et al., F. Wolf, I.A. Fleidervish PNAS 115:E7184–92 (2018).
[4] A. Palmigiano, et al. Nature Neurosci. 13:4700 (2017)
[5] R. Engelken, et al., F. Wolf. F1000Res 5:2043 (2016)
[6] M. Puelma-Touzel, F. Wolf. PLoS Comput Biol 11:e1004636 (2015)
[7] W. Wei, F. Wolf, X-J. Wang. Phys Rev E 92:032726 (2015)
[8] O. Revah, O. Stoler, A. Neef, F. Wolf, et al. *under review*

8.15 BIAS-FREE ESTIMATION FROM IRREGULARLY SAMPLED OR GAPPY DATA

H. Nobach
N. Damaschke, V. Kühn (University of Rostock)

If the measurement system influences the statistical properties of the measured signal compared with the underlying process, classical signal processing will generate systematic errors in the statistics derived from the measured signal only. In these cases, the influence of the measurement system needs to be analysed to develop effective corrections to allow statistical estimation free of systematic errors.

Using the experience with bias-free estimation from stochastically sampled data [1, 2] e.g. in laser Doppler velocimetry, the application of the developed estimators has been extended towards equidistantly sampled data with gaps of arbitrary spectral composition [3].

Fig. 8.32 shows two test cases with irregular sampling, with data gaps, where the occurrence of outliers is correlated and a case of stochastic sampling. The appropriate autocovariance functions (calculated from longer data sets) have obvious deviations from the simulated process for commonly used methods, e.g. interpolation or Lomb-Scargle's method. The consideration of the sampling process instead yields bias-free estimates.

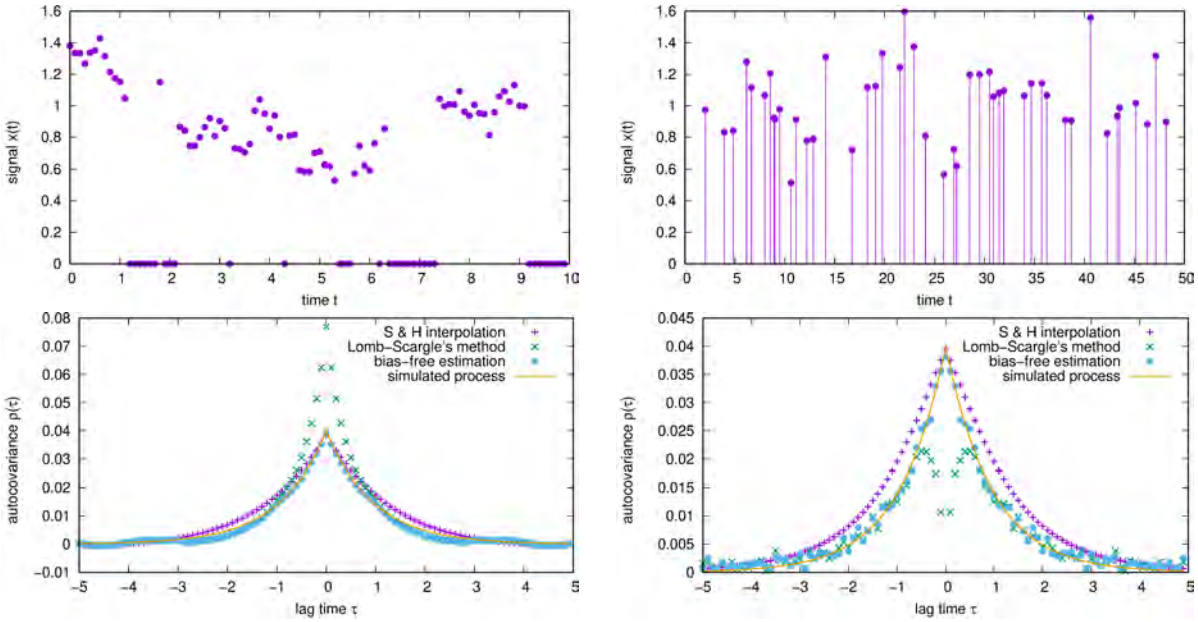

Figure 8.32: Test cases of signals with irregular sampling and autocorrelation function derived hereof, left: equidistant sampling with data gaps, right: stochastic but not entirely random sampling.

[1] H. Nobach, Proc. of the 18th Int. Symp. on the Appl. of Laser and Imaging Techn. to Fluid Mech., July 04–07, 2016, Lisbon, Portugal
[2] N. Damaschke, V. Kühn, H. Nobach, Digital Signal Processing, vol. 76 (2018), 22–33
[3] N. Damaschke, V. Kühn, H. Nobach, Bias-Free Estimation of the Auto- and Cross-Covariance and the Corresponding Power Spectral Densities from Gappy Data (in preparation)

8.16 ADAPTIVE CONTROL IN STOCHASTIC EVOLUTIONARY PROCESSES

C. LaMont, C. Eksin, A. Nourmohammad

Controling an evolving population is a common goal in devising strategies against viral infections, cancer progression or drug resistance in bacteria. Immune-triggered control is often done by vaccination to induce an immune memory against pathogens, so that it acts quicker in future exposures. Currently, the goal of vaccine design against rapidly evolving viruses (like HIV) is to elicit potent broadly neutralizing antibodies to trap the virus by targeting its vulnerable regions. Directing the immune system to utilize a specific antibody is a problem of *adaptive control* to trigger a *rare event* in a non-linear stochastic system.

We are currently approaching the immune control problem from a theoretical perspective. Our goal is to devise adaptive control strategies for stochastic evolving systems with dynamics inferred from molecular data. Designing an optimal control strategy $u^*(t)$ involves minimization of a cost function $C(\mathbf{x}, u, t)$, which depends on the state of the system $\mathbf{x}$ and the control protocol u, over a desired window of time $[t_0 : t_f]$, subject to the underlying evolutionary dynamics,

$$\mathbf{u}^*(\mathbf{x}, t_0, t_f) = \text{argmin}_{u_{t_0 \to t_f}} \int_{t_0}^{t_f} C(\mathbf{x}, u, t) dt. \tag{8.1}$$

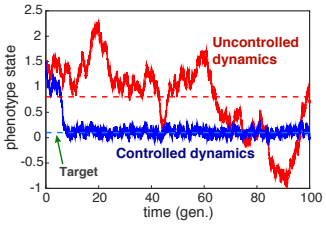

Figure 8.33: Adaptive control to drive a population to a desired state.

Fig. 8.33 shows our preliminary numerical analysis of the control problem in a coevolutionary process to drive the affinity of immune-pathogen interactions to a desired phenotypic state [1].

In the case of vaccination, we want to minimize long-term viral growth by reliably inducing effective antibodies to suppress viral escape. Control optimization in a nonlinear stochastic coevolutionary system is a complex computational problem, which we address by using analytical approximations and numerical methods. Informed by our analysis of the immune response, we will develop an effective theoretical description for BCR co-evolution with viruses, based on the binding affinity and breadth of the repertoire; see ref. [2].

One of the main limitations for control in natural systems is incomplete monitoring of dynamics, e.g., due to restrictions in clinical studies. Our approach is to (i) identify informative observables to monitor and perturb, (ii) to update the belief about the system in response to interventions, and (iii) to optimally perturb and control the system based on accumulated information. We will quantify the cost and limits of control in an evolving system, given the finite monitoring of its complex dynamics and the extent of its evolutionary predictability.

[1] Eksin, C and Nourmohammad, A. Adaptive immune control in chronic infections. (Working Paper)

[2] Nourmohammad A, Otwinowski J, Plotkin JB. Host-pathogen coevolution and the emergence of broadly neutralizing antibodies in chronic infections. PLoS Genet. 2016; 12: e1006171.

8.17 SUBSAMPLING SCALING: A THEORY ABOUT INFERENCE FROM PARTLY OBSERVED SYSTEMS

V. Priesemann
A. Levina (Tübingen)

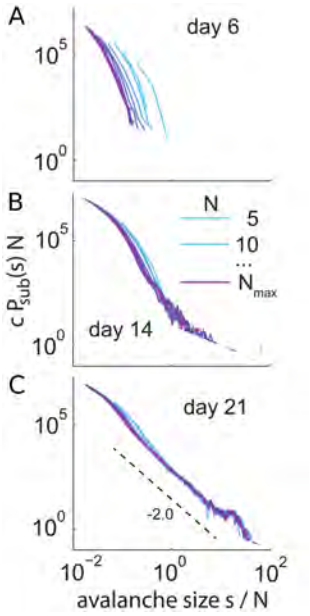

Figure 8.34: Using the subsampling-scaling ansatz, we reapproached the long-debated question of whether avalanche size distributions of neural activity *in vitro* are scale free, indicating a critical state [5]. **A-C.** Avalanche distributions evaluated under further sampling for $N = 5$ to $N_{max} = 60$ neurons in developing networks. The immature network (day 6) does not show a collapse, but with maturation (day 21), the network develops scale free distributions. The avalanche size distributions of the full system would extend over at least five orders of magnitude. (Figure modified from [1]).

In real-world applications, observations are often constrained to a small fraction of a system. Such spatial subsampling can be caused by the inaccessibility or the sheer size of the system, and cannot be overcome by longer sampling. Spatial subsampling can strongly bias inferences about a system's aggregated properties [1, 2, 3, 4] (see Sec. 8.3). To overcome the bias, we derived analytically a subsampling scaling framework that is applicable to different observables, including distributions of neuronal avalanches, of node degrees or of the number of people infected during an epidemic outbreak. We demonstrated how to infer the correct distributions of the underlying full system, how to apply it to distinguish critical from subcritical systems, and how to disentangle subsampling and finite size effects. Lastly, we applied subsampling scaling to neuronal avalanche models and to recordings of developing neural networks. We showed that only mature, but not young networks follow power-law scaling, indicating self-organization to criticality during development.

To illustrate subsampling with the example of node degree distributions, assume a graph with some degree distribution $P(s)$. To implement subsampling, every node of the graph is observed with probability p, and missed otherwise. Only edges (connections) between observed nodes can be observed, and hence every edge of a given node is observed (or missed) with the same probability p (or $1 - p$). The aim is to infer the degree distribution $P(s)$ of the full graph from the subsampled degree distribution $P_{sub}(s)$. The scaling ansatz that can recover the "parent distribution" $P(s)$ from the subsampled one depends on the class of distribution $P(s)$ belongs to. For scale free distributions the *approximate* scaling ansatz is linear in p (or equivalently linear in the number of sampled units N). For exponential distributions, the ansatz is more intricate, but holds exactly (see [1]). Having derived the correct subsampling-scaling ansatz, one can test whether system properties are e.g. scale-free, even under strong subsampling. This generalizes to distributions of other properties, like avalanche sizes or epidemic outbreaks, making this approach applicable to variety of problems. Applying the subsampling scaling ansatz to recordings *in vitro*, where about 60 of 50.000 neurons were sampled, we inferred that neuronal avalanche distributions of the full network are scale-free and span at least five orders of magnitude (Fig. 8.34).

[1] A. Levina, V. Priesemann, Nat. Commun. **8**, 15140 (2017)
[2] M. P. Stumpf et al., Proc. Natl. Acad. Sci. U.S.A. **102**, 4221-4224 (2005)
[3] J. Wilting, V. Priesemann, Nat. Commun. **9**, 2325 (2018)
[4] V. Priesemann, M Munk, M. Wibral, BMC Neurosci. **12**, 119 (2009)
[5] J. Beggs, D. Plenz, J Neurosci. **23**, 35 (2003)

8.18 DATA ASSIMILATION, PARAMETER ESTIMATION, AND MACHINE LEARNING

U. Parlitz, S. Herzog, J. Schumann-Bischoff, A. Schlemmer, H. tom Wörden, D. Hornung, S. Luther
F. Wörgötter (University of Göttingen), P. J. van Leeuwen (University of Reading, UK), C. Masoller (Univ. Politècnica de Catalunya, Spain)

In cardiac dynamics and many other fields of life sciences mathematical models are often semi-empiric and may comprise (many) variables and parameters whose values are difficult to measure. In such cases it is desirable to (cross) estimate variables, which are difficult to assess from those that can be easily measured. In control theory this task is addressed by constructing an observer based on a given mathematical model describing the process of interest. Once all state variables of the model have been estimated, the model (e.g., a PDE) can be used to simulate and forecast the future evolution of the dynamical process. This combination of cross estimation and prediction of dynamical variables is the core of all data assimilation methods [1]. A purely data driven alternative is provided by machine learning methods which can be trained to estimate not directly observed variables, to deblur measurement data, or to forecast the future evolution. To achieve these goals we employed Echo State Networks [2, 3], Convolutional Neural Networks [4] (Figure 8.18), and Nearest Neighbour Prediction using local states [5]. All these different methods turned out to be very efficient for modelling complex spatio-temporal (cardiac) dynamics and are promising tools for evaluating experimental data, for parameter estimation [6], and for enhancing imaging techniques like inverse ECG or ultrasound imaging.

Unsupervised nonlinear dimension reduction for image processing has been devised for ordering anterior chamber optical coherence tomography (OCT) images [7], a machine learning approach that can be used for glaucoma detection.

In order to organize large and complex numeric datasets and connect them to experimental data, analysis results and meta data, our open source research data managment system CaosDB [8] is used and extended.

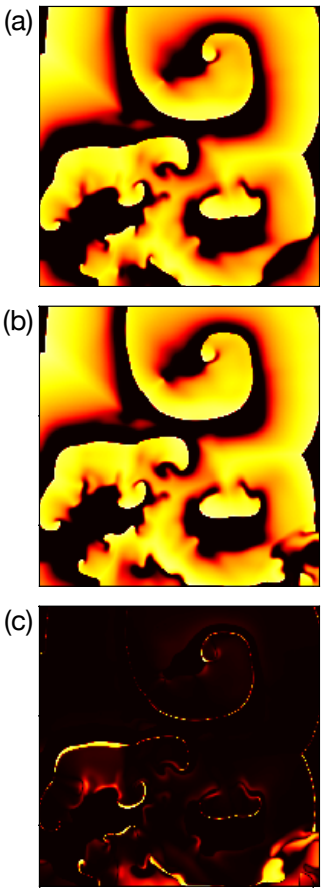

Figure 8.35: Forecast of the temporal evolution of the membrane voltage of the Bueno-Orovio-Cherry-Fenton (BOCF) model using a convolutional neural network combined with conditional random fields [4] at time $t = 1500$, i.e. approximately 4.3 spiral rotation periods after initialising the (iterated) network prediction. Shown are (a) the original BOCF dynamics, (b) the forecast provided by the network, and (c) the difference between original and forecast.

[1] F. R. Pinheiro, P. J. van Leeuwen, U. Parlitz, Q.J.R. Meteorol. Soc. **144**, 305 (2018)
[2] R. S. Zimmermann and U. Parlitz, Chaos **28**, 043118 (2018)
[3] L. A. Thiede and U. Parlitz, Neural Networks (in print) (2019)
[4] S. Herzog, F. Wörgötter, U. Parlitz, Frontiers in Appl. Math. and Stat. **4**, 60 (2018)
[5] J. Isensee, G. Datseris, U. Parlitz, unter review (2019)
[6] J. Schumann-Bischoff, S. Luther, U. Parlitz, Phys. Rev. E **94**, 032221 (2016)
[7] P. Amil, L. González, E. Arrondo, C. Salinas, J.L. Guell, C. Masoller, U. Parlitz, Scientific Reports **9**, 1157 (2019)
[8] T. Fitschen, A. Schlemmer, D. Hornung, U. Parlitz, S. Luther, arXiv preprint arXiv:1801.07653 (2019)

8.19 DATA ANALYTICS FOR MULTI-DIMENSIONAL NONLINEAR DYNAMICS

J. Casadiego, D. Maoutsa, M. Timme
C. Kirst (Rockefeller), H. Hähne (Oldenburg), M. Nitzan (Harvard)

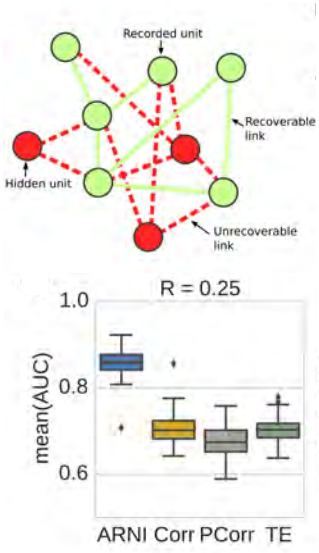

Figure 8.36: Data analytics for collective nonlinear dynamics enables network inference from partially hidden systems (top) and outperform purely information-based methods (bottom) [1].

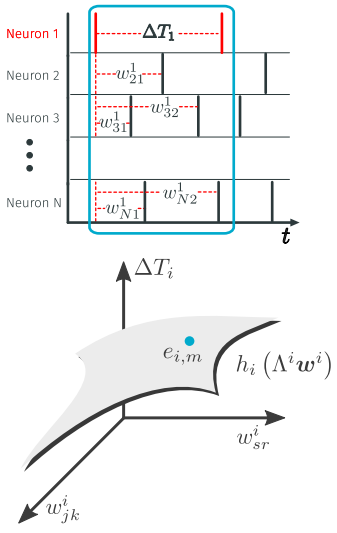

Figure 8.37: Event space representations transform discrete dynamics such as spike trains into suitable data sets for network inference [3].

The complex interaction topologies of many natural and human-made networked systems essentially underlie their collective dynamics. Commonly, forward perspectives are taken to model and analyze such systems: varying the parameters of pre-defined models gives hope to reproduce the collective dynamics observed. Beyond such standard approaches, two avenues of advances enable us to also take inverse perspectives today. First, technological progress yields the dynamics of many individual network units at unprecedented resolution. Second, our capabilities to understand the consequences of such measurements rapidly increase through advancing tools of machine learning and data analytics.

In the Network Dynamics team, we develop novel data-driven approaches to extract knowledge from multi-dimensional data resulting from the nonlinear dynamics of networks and address fundamental problems of inference, design and information processing.

Data analytics for dynamics: from function to structure and back. Combining methods from nonlinear dynamics, statistics and stochastics, we have recently developed a number of data-driven tools for inferring or predicting the structural, not only correlative, interaction topology of networks from the data sampled from their collective dynamics alone [1, 2, 3, 4, 5]. We specifically aim at extracting information from partially hidden data and in a model-free setting. For instance, some network units may be hidden from observation or, instead of a continuous (e.g. membrane potential) dynamics, only discrete events (e.g. spike times) data may be available. Applications include systems with time-continuous (e.g. gene expression levels) [1], time-discrete interactions (e.g. neural spike trains) [3] and dynamically evolving structures in social and biomolecular networks [4, 5].

Distributed information routing. Determining general mechanisms underlying reliable information routing in networks is a key theoretical challenge in many fields of science, ranging from biology to engineering. Recently, we identified a generic mechanism to route information that enables a flexible reorganization of information sharing and routing patterns [6] and may yield "spooky" action-at-a-distance. Furthermore, we established the theoretical foundations for information routing in complex networks. Our approach equally applies to signals communicated on top of collective reference states that oscillatory or otherwise out of equilibrium.

[1] J. Casadiego et al., Nature Comm. **8**, 2192 (2017)
[2] M. Nitzan et al., Science Adv. **3**, e1600396 (2017)
[3] J. Casadiego, et al., Phys. Rev. Lett. **121**, 054101 (2018)
[4] N. Molkenthin and M. Timme, Phys. Rev. Lett. **117**, 168301 (2016)
[5] N. Molkenthin et al., Phys. Rev. Lett. **121**, 138301 (2018)
[6] C. Kirst et al., Nature Comm. **7**, 11061 (2016)

8.20 INTERPLAY OF LINEAR AND NONLINEAR LOCALIZATION

R. Fleischmann, G. Green

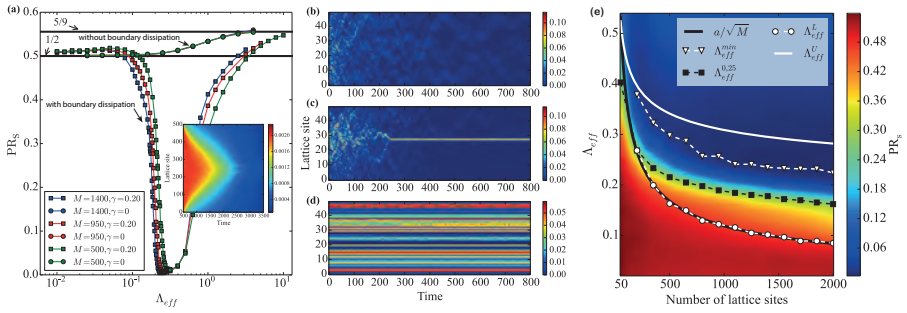

Figure 8.38:
The dynamical phase transition of self-localization. **(a)** Participation ratio PR_s (i.e. the extend of the wave function) vs. nonlinearity Λ_{eff} without ($\gamma = 0$) and with weak boundary dissipation ($\gamma = 0.2$) for several systems sizes M. The inset shows the averaged norm of 500 realizations at the phase transition, $\Lambda_{\text{eff}} = 0.215$. Examples of the time evolution of extended inital conditions ($M = 50$) with boundary dissipation for different nonlinearities (Λ_{eff}): **(b)** decaying state (0.1), **(c)** single breather (0.5) and **(d)** multi-breather state (40). **(e)** The onset of the phase transition occurs at the nonlinearity (Λ^L_{eff}) where the largest localization length in the Anderson approximation becomes smaller than the system size. An upper bound (Λ^U_{eff}) can be derived from the Peierls-Nabarro barrier.

One of the most intriguing features of the dynamics in nonlinear lattices is that excitations can spontaneously localize even in homogeneous lattices. This discrete self-trapping (the formation of *discrete breathers*) is a milestone discovery in nonlinear science. It has been observed experimentally in various systems ranging from nonlinear optical waveguides arrays to Bose Einstein condensates in optical lattices. A very intriguing path to self-trapping, *self-localization*, has been found in extended "leaking" optical lattices with weak boundary dissipation simulated by the discrete nonlinear Schrödinger equation (DNLS): in closed lattices initially extended waves stay extended at all times for all nonlinearities (i.e. interaction strength). If some atoms are allowed to escape at the boundaries, however, the atom cloud can spontaneously localize within the lattice. We previously had shown that a dynamical phase transition occurs with the nonlinearity as control parameter (cf. Fig. 8.38) and that a upper bound for its critical value can be derived from the Peierls-Nabarro energy barrier [1]. We have now shown that the onset of self-localization and the distribution of the breather positions can be understood by studying (linear) Anderson localization in the potential landscape formed by the instantaneous wave functions [2].

We found another fascinating interplay of linear and nonlinear localization in the dynamics of the (continuous) nonlinear Schrödinger equation in weakly diffracting random media, with applications from oceanography to optics and quantum optics [3] (cf. Fig. 8.39).

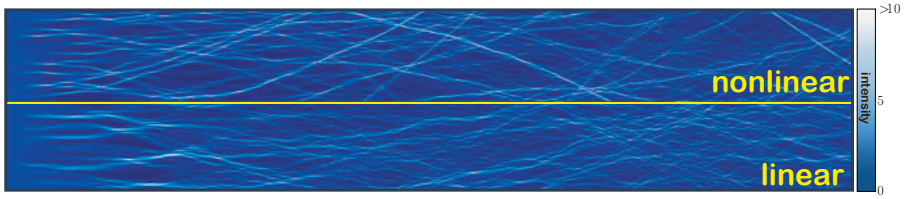

Figure 8.39:
Branched flow in the linear ($g = 0$) and nonlinear ($g < 0$) Schrödinger-equation $i\partial_t\psi = -\frac{\Delta}{2}\psi + V\psi + g|\psi|^2\psi$ in a weak random potential $V(x, y)$. The branch structure formed by random caustics gets enhanced by nonlinear self-focusing, and at an *optimal* ratio of random and nonlinear focusing the strongest intensity fluctuations can be found.

[1] H. Hennig and R. Fleischmann, Phys. Rev. A **87**, 033605 (2013).
[2] J. Kruse and R. Fleischmann, J. Phys. B **50**, 055002 (2017).
[3] G. Green and R. Fleischmann, under review

8.21 RIDE POOLING SYSTEMS: THEORY AND EXPERIMENT

S. Herminghaus, M. Timme, J. Schlüter, T. Baig, M. Patscheke, L. Deutsch, D. Manik, N. Molkenthin

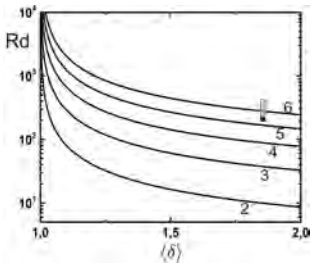

Figure 8.40: Contour curves of the average number of passengers per vehicle, in the plane spanned by the dimensionless request frequency (Rd) and the average tortuosity, δ, of the vehicle routes. The error bar applies to all curves and is partly due to the unknown Riemann curvature of the traffic network (grey) and partly due to the unknown distribution of travel distances (black).

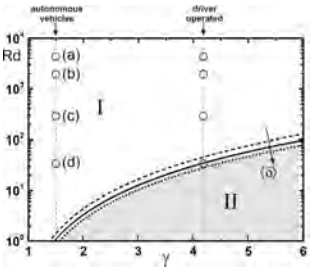

Figure 8.41: If γ is the ratio of the costs for running a minibus (including driver salary) divided by the costs for running a private car, the white area (I) indicates parameters for which the system can be run economically if there are enpugh customers. Open circles correspond to parameters if existing scenarios. (a) New York City; (b) Hamburg; (c) Göttingen; (d) Eichsfeld (rural area near Göttingen).

Traffic is one of the major obstacles on our way to a sustainable management of our planet. As traffic flows can be viewed (and treated) as active fluids, there is a growing research endeavour towards the development of sustainable public transport systems [1]. As a first step, we have investigated the statistical physics of ride pooling systems in a mean-field framework [2]. A particularly interesting aspect of these systems is that traffic space is not Euclidean, but strongly curved, which needs to (and can [2]) be accounted for in the theoretical treatment.

Aside from important general characteristics governing the performance of such systems (Fig. 8.40), it was found that they exhibit a first-order-type phase transition between a niche market (usually found if many transport systems compete with each other) and market dominance of the ride pooling system. It could be shown that whether or not this pahse transition exists mainly depends upon two parameters, one of which is the relative running cost of the deployed vehicles (γ), the other is a non-dimensionalized demand frequency. This is shown in Fig. 8.41. The region where this phase transition exists is denote by **I**. It is separated from region **II** where the niche market is the only possible mode. The exact location of the boundary depends slightly upon the average tortuosity of the routes, δ. One of the main goals of the project is to find ways to establish the phase of market dominance of the ride pooling system under realistic conditions. We are therefore conducting pilot projects in several areas not too far from Göttingen (cf. Fig. 8.42). In these projects, data are collected which hopefully will allow to devise cooperative public transport systems for future mobility in both rural and urban settings.

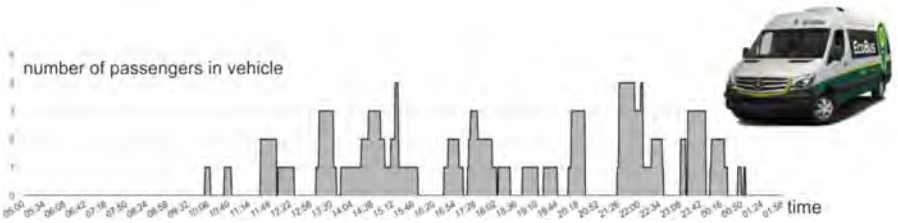

Figure 8.42: Example of occupation of a single vehicle (see top right image) in the course of a day during the pilot project in the Harz mountains. Significant pooling is obviously achieved.

[1] A. Sorge, D. Manik, S. Herminghaus, M. Timme, *Towards a unifying framework for demand-driven transport (D3T)*, Proc. Winter Simul. Conf., 2800-2810 (2015)

[2] S. Herminghaus, *Mean field theory of demand responsive ride pooling systems*, Transportation Research A: Policy and Practice **119** (2019) 15.

8.22 QUANTIZED SELF-ASSEMBLY OF DISCOTIC RINGS IN A LIQUID CRYSTAL CONFINED IN NANOPORES

A. W. Zantop, M. G. Mazza
K. Sentker (TUHH), M. Lippmann (DESY),
T. Hofmann (Helmholtz-Zentrum Berlin), O. H. Seeck (DESY),
A. V. Kityk (Czestochowa), A. Yildirim (BAM), A. Schönhals (BAM),
P. Huber (TUHH)

Disklike molecules stack up in columns, which arrange in a 2D lattice leading to discotic columnar liquid crystals (DLCs). Because of overlapping π electrons of the aromatic cores DLCs exhibit long-range self-assembly and self-healing mechanisms in combination with high one-dimensional charge mobility along the columnar axes.

In this work [1] we present a temperature (T) dependent optical birefringence, x-ray diffraction, and Monte Carlo simulation study on the structure of an archetypical DLC (HAT6) confined in an array of cylindrical pores (17 nm across, 360 μm in length) in a silica membrane. Figure 8.43(b) shows the retardation $R(T)$ of HAT6 imbibed in nanopores with edge-on molecular anchoring at the walls. In contrast to the bulk case, $R(T)$ increases towards positive values upon cooling (0.15 K/min) indicating alignment of the molecular director perpendicular to the pore axis, see the inset in Fig. 1(b). Interestingly, the collective molecular order does not evolve in a monotonic manner. Rather, a sequence of small plateaus, separated by five pronounced changes in $R(T)$, results in a staircaselike transition, both upon cooling and heating. To obtain a microscopic picture, we perform parallel-tempering Monte Carlo simulations. Figure 8.44(a) shows the T dependence of the nematic order parameter. Similarly to the optical experiments, a stepwise increase in the orientational order is clearly visible as T decreases. Typical molecular configurations at different T's are shown in Fig. 8.45. In summary, we have found a quantized phase transition of a liquid crystal confined to nanopores. Optical birefringence, x-ray diffraction experiments, together with MC simulations show that the stepwise transformation originates in the formation of circular concentric rings.

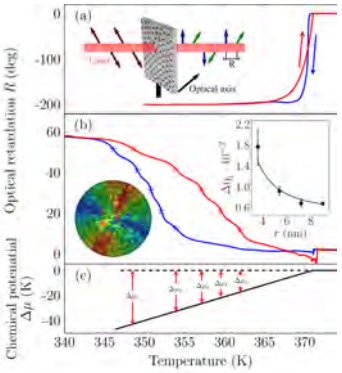

Figure 8.43: Birefringence measurement of the normalized retardation R of HAT6 in the bulk and (b) confined [cooling (blue) and heating (red)]. An MC simulation snapshot of the formation of concentric columnar rings. (c) Chemical potential $\Delta\mu$-T phase diagram of HAT6 in the vicinity of the isotropic-columnar bulk transition.

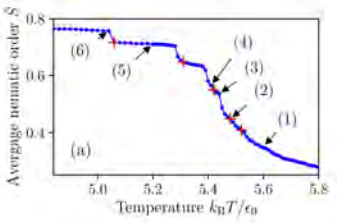

Figure 8.44: The T dependence of the average nematic order parameter (blue circles) shows discontinuous jumps, marked with red crosses. Inset: Cross-sectional view on the molecular arrangement in the nanopore at $k_BT/\epsilon_0 = 4.94$.

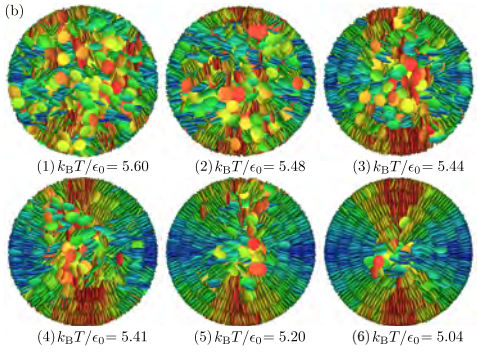

Figure 8.45: Radial snapshots of molecular configurations at the T's marked as (1...6) in Fig. 8.44. A progressive growth of concentric rings is visible

[1] K. Sentker, *et al.*, Phys. Rev. Lett. **120**, 067801 (2018).

8.23 MEMORY FORMED BY VISCOELASTIC RESPONSE

M. Kramar, K. Alim

The concept of memory in biology is traditionally linked to organisms with a nervous system. However, even a very simple organism that survives by foraging for food has to be able to process and store sensory information. We study the mechanism of memory encoding in *Physarum polycephalum*, a model organism on the verge between simple and complex life. Upon receiving a food stimulus, *P. polycephalum* reorganises its network-like body to exploit a food source. Previous location of stimuli are thereby imprinted in the network morphology. As a stepping stone to understand how stimulus location is translated into morphological changes of the network architecture we identified three interrelated mechanisms of information encoding that run on separate timescales: transient short-term memory on the scale of tens of minutes, long-term memory on the scale of hours and finally external memory marking the organisms' previous location [2].

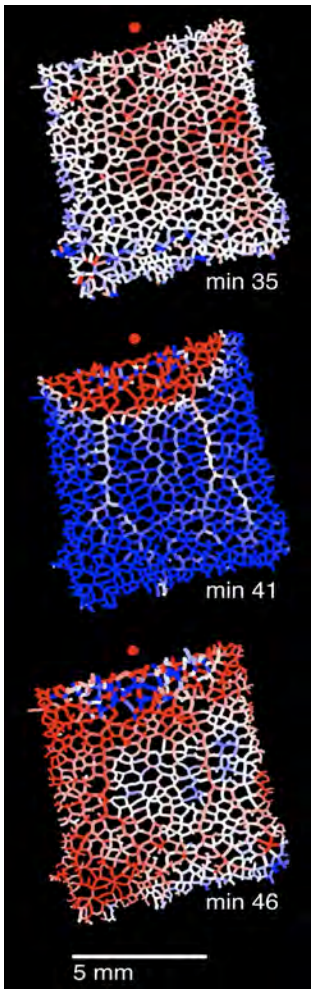

Figure 8.46: *P. polycephalum* network reacting to a stimulus applied in minute 35 (red dot). Tubes undergoing dilation are marked in red, those that undergo contraction in blue, and white denotes no change in tube diameter.

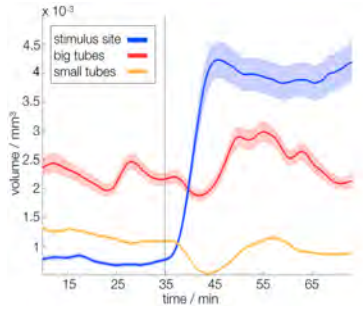

Figure 8.47: Characteristic responses of tubes grouped by travel time from stimulus site show viscoelastic response of tube walls to advected signal, stimulus time in gray.

Focusing on transient memory, we find that the initial response of the network to a food stimulus is tube dilation, which propagates into the network from stimulus site, followed by tube contraction, see Fig. 8.46. Our finding that stimulus information propagates by cytoplasmic flows within the network [1] suggest grouping tube diameter dynamics by travel time from stimulus, see Fig. 8.47. Given the constraint of fixed body mass, tubes outside the immediate stimulus site show the same characteristic response of reversible tube dilation. Tube dilation is later the farther tube location is from stimulus site. These quantitative observation suggest that a food stimulus is translated into a soluble signal that is transported by internal flows and reversible softens tube walls as it propagates into the network.

We identify a novel mechanism of self-organisation of flow networks. The active mechanical response of individual tubes to the transported signal reroutes flows thereby self-organising signal transport - even storing information on stimulus location in the network architecture itself.

[1] K. Alim, N. Andrew, A. Pringle, M.P. Brenner, Proc. Natl. Acad. Sci. U.S.A. **114**, 5136 (2017)

[2] C.R. Reid, T. Latty, A. Dussutour, M. Beekman, Proc. Natl. Acad. Sci. U.S.A. **109**, 17490 (2012)

8.24 OBSERVING BALLISTIC TRANSPORT BEYOND THE MEAN FREE TIME

G. Datseris, T. Geisel, R. Fleischmann

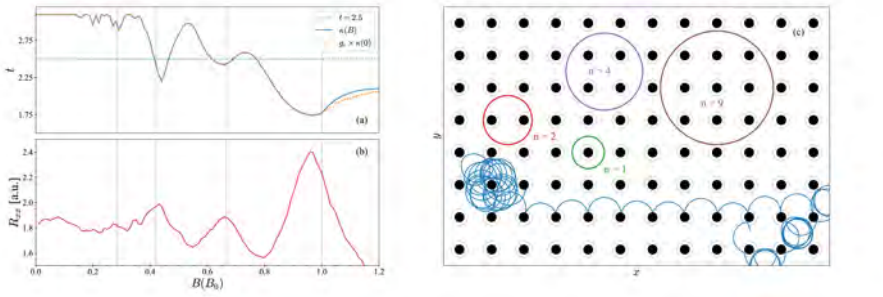

Figure 8.48:
Ballistic transport in a model of an antidot-lattice in graphene. **(a)** Mean time between consecutive collisions with antidots compared to the volume ratio of chaotic orbits $g_c = 1 - g_R$. The time unit is a/v_F, i.e. the ratio of lattice spacing and Fermi-velocity. **(b)** Magnetoresistance of the periodic Sinai billiard in the presence of stochastic impurity scattering (which destroys velocity correlations) with mean free time $\tau_i = 2.5$, which is shorter than the cyclotron periods π/B at the resonances. (c) Orbits at different magnetic field values in the antidot lattice. The closed orbits around 1,2,4, and 9 antidots correspond to the nonlinear resonances. Their magnetic field values are indicated in panels a and b by dotted vertical lines. It is clearly visible that the magnetoresistance peaks in b correspond to the dips in the mean collision time in a.

In electronic transport (as well as in photonics, phononics and other fields of physics) an effect is called ballistic, if the dynamics of the carriers appears to depend only on the superstructure of the device and controlling external forces, i.e. the dynamics is unimpeded by stochastic forces and impurities. Therefore to observe a ballistic effect in experiment the general rule is that the associated time-scales of the dynamics should be (much) shorter than the mean free time, e.g. the impurity scattering time. We have found a very general mechanism that can circumvent this rule in *mixed phase space* systems [1].

In nonlinear Hamiltonian systems chaotic dynamics generically coexists with regular motion in *nonlinear resonances*. They therefore have a mixed phase space structure of *regular islands* embedded in a *chaotic sea.* We have shown that nonlinear resonances can be observed in transport experiments, even when their time-scales are much larger than the mean free time. At the basis of this surprising finding is a general mathematical relation (*Kac's Lemma*) [2] between return times and accessible phase space volumes in Hamiltonian systems.

As an example we have studied magnetotransport in *antidot superlattices* in graphene, which are nanoscale realizations of a periodic Sinai billiard, i.e. circular repulsive scatterers periodically arranged in the two-dimensional substrate. At zero magnetic field the dynamics is purely chaotic, but at certain higher fields nonlinear resonances corresponding to cyclotron like motion occur. They are observable as peaks in the magnetoresistance of such samples (Fig. 8.48), even for impurity scattering times smaller than the periods of the resonances. This happens because the chaotic orbits change their dynamics due to the mere existence of the resonances. The mean time κ between collisions of the chaotic orbits with antidots, which dominates their contribution to the resistance, turns out to be directly proportional to the phase space volume fraction g_R occupied by nonlinear resonances. As a function of the magnetic field B we derived $\kappa(B) = [1 - g_R(B)]\,\kappa(0)$, reproduced with astounding accuracy by our simulations in Fig. 8.49.

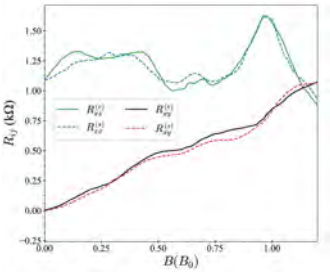

Figure 8.49: Simulations in an extended antidot model with smooth instead of hard potential walls (as in the Sinai billiard). Comparison of our numerical magneto- and Hall-resistances curves (dashed lines) for $\tau_i = 2.5$ with the experiments on graphene antidot-lattice of Ref. [3] (solid line).

[1] G. Datseris, T. Geisel, and R. Fleischmann, under review
[2] J. D. Meiss, Chaos **7**, 139–147 (1997)
[3] A. Sandner et al., Nano Letters **15**, 8402 (2015).

8.25 IMPACT OF DISORDER ON FLOWS AND TRANSPORT IN POROUS MEDIA

P. Fantinel, S. Biswas, L. Goehring, K. Alim
T. Dawent (Nottingham Trent University), R. Holtzman (Jerusalem),
D.A. Weitz, M.P. Brenner (Harvard)

Porous media underlie broad applications in materials design and architecture, the geosciences, food sciences, and more emergent areas of increasing societal concern, such as energy conversion in fuel cells and batteries. Efficient mass transfer in their tubular pore space network is crucial for function. How does structural disorder affect flows and transport through porous media?

We develop a statistical theory for flows in porous media starting from the insight that flow in a given tube of the tubular pore space is only specified by the tube upstream and the splitting ratio of the upstream flow among different tubes at a network node point, following Kirchhoff's law. Comparing numerical simulations, experiments and the analytical predictions of this statistical theory we find that the flow distribution of an entire porous medium is entirely specified by the distribution of splitting ratio [1]. The key insight here is that not pore specific parameters like for example the pore size distribution but solely the pore space disorder specified by the splitting ratio is governing the flow distribution, see Fig. 8.50.

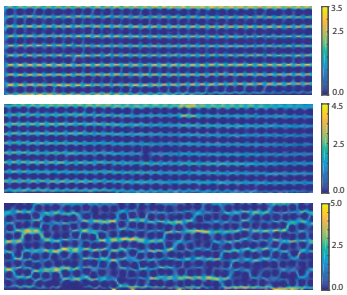

Figure 8.50: Flow velocity field broadens as disorder increases (top to bottom). Experimentally tracked flow velocities normalized by average flow velocities.

Our findings pave the way to optimise porous media function by predicting their optimal morphology and build the foundation for active porous media built of responsive material. To this end we have demonstrated how local structure can modify the patterns and mean-field response of flows in porous media, again by a powerful mixture of fully customisable micro-fluidic experiments with simulations and theory, see Fig. 8.51. We show that the introduction of even weak local correlations in pore size significantly alters the physics of fundamental processes like drying [2, 3], or fluid-fluid displacement [4]. These new behaviours can be related to changes in very generic models, such as the universality and critical exponents of of invasion percolation [5]. This collaborative and interdisciplinary programme of work is now turning to the investigation and development of materials which respond to multi-phase flows, for example by chemical changes, or elastic deformation.

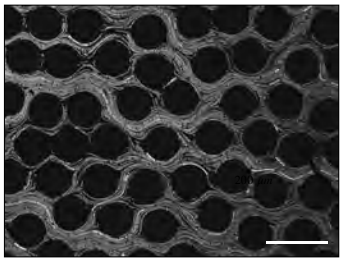

Figure 8.51: Tracks of particles flowing through a disordered mircopattern. Scale bar 200μm.

[1] K. Alim, S. Parsa, D.A. Weitz, M.P. Brenner, Phys. Rev. Lett., **119**, 144501 (2017)
[2] O. Borgman, P. Fantinel, W. Lühder, L. Goehring, R. Holtzman, Water Resour. Res., **53**, 5645 (2017)
[3] P. Fantinel, O. Borgman, R. Holtzman, L. Goehring, Sci. Rep. **7**, 15572 (2017)
[4] O. Borgman, E. Segre, T. Darwent, L. Goehring, R. Holtzman, arXiv:1901.00835 (2019)
[5] S. Biswas, P. Fantinel, O. Borgman, R. Holtzman, L. Goehring, Phys. Rev. Fluids 3, 124307 (2018)

8.26 MECHANICS AND OSCILLATORY INSTABILITIES OF CELL ADHESION AND MIGRATION

N. Kamprad, C. Schich, H. Witt, M. Schröder, C. Westendorf, C. Kreis, O. Bäumchen, A. Krekhov, A. Pumir (ENS Lyon), **C. Beta, E. Bodenschatz, M. Tarantola**
T. Lampert, P. Devreotes (Johns Hopkins University), W.-J. Rappel (UCSD), H. Hsu, J. Negrete Jr. (University Lausanne), A. Bae (Rochester University), J. Faix (MH Hannover), A. Chizhik, B. Geil, A. Janshoff, J. Enderlein, T. Salditt (University of Göttingen)

Biological adhesion is essential for a plethora of cell types and thus cell locomotion relies on substrates displaying a compatible surface chemistry. *Dictyostelium discoideum* (*D.d.*), a soil-living slime mould, faces the challenge of overcoming variable chemistry by employing fundamental forces of colloid science. To understand the origin of *D.d.* adhesion, we realized and modified a variety of conditions comprising specific as well as dato unknown adhesion proteins [1], glycolytic degradation, ionic strength, surface hydrophobicity and van der Waals interactions. Employing AFM-based single cell force spectroscopy we show that experimental force curves upon retraction exhibit two regimes, a continuum and a stochastic part, relying on unbinding of individual binding partners and bond clusters (see Fig. 8.52A and B). This versatile mechanism allows *D.d.* to adhere to a large variety of natural surfaces [2], while monolayer forming, stratifying cell cultures show an expanded set of adhesion mechanisms including spatiotemporal, three-dimensional patterns of cortical tension modulation [3].

Cell movement towards an external source of chemoattractant is crucial to a variety of biological processes. In a further focus, we address how chemoattractant binding induces changes in the dynamical state of the actin cytoskeleton. We investigate the transient response to a short pulse of cAMP of *D.d.* cells shown to have noisy and oscillatory actin polymerization [4]. We found that stimulation causes a transient and biphasic response and furthermore, by comparing with cells lacking the motor protein myosin II (see Fig. 8.52C to E), we quantified the degree of coupling between myosin II and actin contraction dynamics (Fig. 8.52F). We model the observed behavior by differential delay kinetics with inhibitory variables and Hill-kinetics, taking into account the intrinsic cell to cell variability [5] and thus are able to reproduce the most important kinetic features of the amoeboid chemotactic dynamics.

[1] T. J. Lampert, N. Kamprad, M. Edwards, J. Borleis, A. J. Watson, M. Tarantola, P. N. Devreotes, *PNAS*, 114, E7727, 2017
[2] N. Kamprad, H. Witt, M. Schröder, C.T. Kreis, O. Bäumchen, A. Janshoff, M. Tarantola, *RSC Nanoscale*, 10, 22504, 2018
[3] Y. A. Miroshnikova, H. Q. Le, D. Schneider, T. Thalheim, M. Rübsam, N. Bremicker, J. Polleux, N. Kamprad, M. Tarantola, I. Wang, M. Balland, C. M. Niessen, J. Galle, S. A.Wickström, *Nat. Cell Biol.*, 20, 69, 2018
[4] J. Negrete, A. Pumir, H.-F. Hsu, C. Westendorf, M. Tarantola, C. Beta, E. Bodenschatz, *Phys. Rev. Lett.*, 117, 148102, 2016
[5] H.-F. Hsu, E. Bodenschatz, C. Westendorf, A. Gholami, A. Pumir, M. Tarantola, C. Beta, *Phys. Rev. Lett.*, 119, 148101, 2017

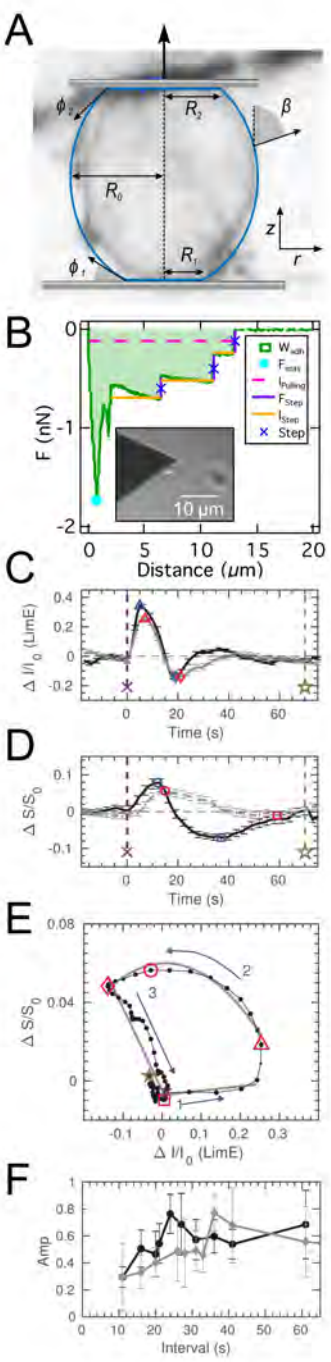

Figure 8.52: A) Parameterization of *D.d.* cell adhering to AFM cantilever B) Exemplary force curve, inlet: cellular AFM probe C) LimE-GFP actin fluorescence intensity time course upon cAMP pulse (x) w/o myosin (black/grey) and corresponding projected area change (D). E) Poincare plot of actin and corresponding area changes with markers as above E) Resonance curves of periodic cAMP-based forcing of *D.d.* w/o myosin.

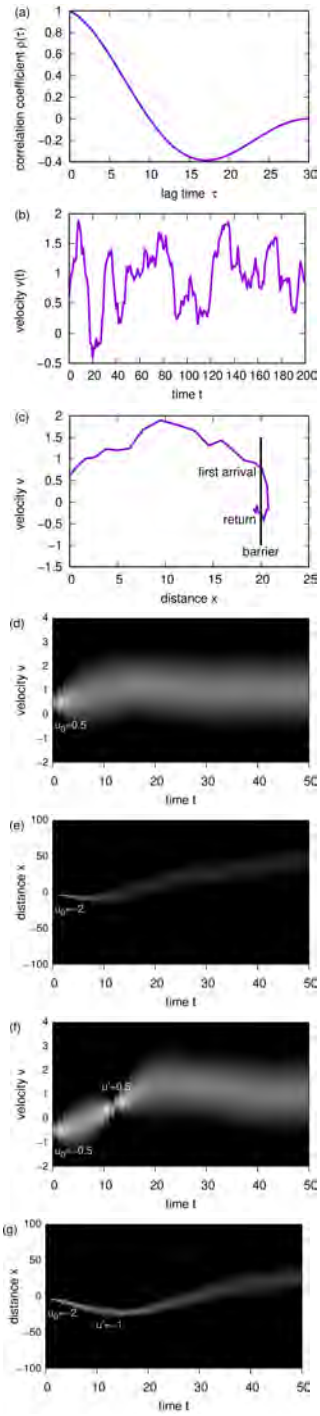

Figure 8.54: Functions of the simulated stochastic process: (a) arbitrary correlation coefficient function, (b) exemplary velocity time signal, (c) trajectory of a particle with return, (d) probability density of $u(t)$ after one observation u_0, (e) probability density of traveled distance $x(t)$ after one observation u_0, (f) probability density of $u(t)$ between and after two observations u_0 and u', (g) probability density of traveled distance $x(t)$ between and after two observations u_0 and u'

8.27 TIME-OF-FLIGHT STATISTICS IN RANDOM WALKS WITH DRIFT AND ARBITRARY CORRELATION

S. Eule, H. Nobach

First passage properties underlie a wide range of random processes, such as the triggering of chemical reactions or the extinction of a population. While the first passage problem of an over-damped Brownian particle is a classical problem of stochastic analysis, little is known about the first passage properties of particles, where inertia cannot be neglected. We investigate the first passage problem of particles immersed in a random velocity field that is characterized by a given distribution and decaying velocity correlation function and focus on the simplest case of a Gaussian velocity field. This model provides a simple showcase to study first passage problems of turbulent diffusions on intermediate scales, where large and small scales exchange energy and material — a problem highly relevant for technical applications due to the efficient mixing properties of turbulent flows.

As a first step, the first-passage time distribution and absolute current of particles is studied in a one-dimensional setup with a mean velocity $\langle v \rangle$ and a Lagrangian velocity correlation function $\rho(\tau) = \langle v(t)v(t+\tau)\rangle / \langle v^2(t)\rangle$[1]. The particles are released at time zero from the origin and the time θ is measured until the particles reach a certain distance x from the origin. In random flows multiple passages are possible that give rise to an absolute current of particles through x. In Fig. 8.53 our analytical prediction for the absolute current of arrivals is plotted, which is compared to numerical simulations of the process. Since our theory imposes no restrictions on the particular form of $\rho(\tau)$ arbitrary Lagrangian correlation functions can be processed (Fig. 8.54a).

To predict the first arrival distribution, the probability of particles returning to the barrier is required. For this, in addition to the various probability density functions shown in Fig. 8.54, also the joint probability density of distances traveled around two observations of velocities is needed, which is not available yet and which is under investigation at the present.

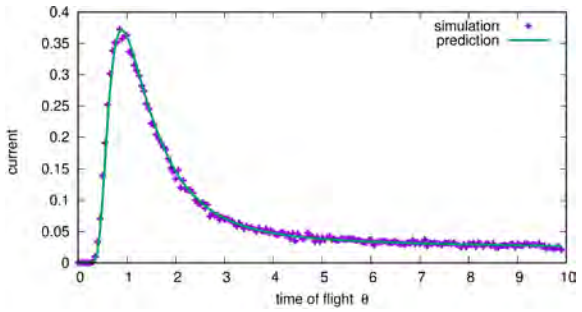

Figure 8.53: Probability distributions of the absolute current at a distance x. Numerical simulation against analytical prediction for $\langle v(t)\rangle = 1$, $\langle v^2(t)\rangle = 4$, $x = 3$.

[1] H. Nobach, S. Eule, First Passage Time Distributions and Absolute Currents of Particles in Gaussian Velocity Fields (in preparation)

8.28 ADSORPTION-INDUCED SLIP INHIBITION OF COMPLEX FLUIDS AT INTERFACES

M. Rivetti, P.D. Fowler, O. Bäumchen
M. Ilton (University of Massachusetts, USA), K. Dalnoki-Veress (McMaster University, Canada), T. Salez (Univ. Bordeaux, France), J.D. McGraw, M. Benzaquen, E. Raphaël (ESPCI Paris Tech, France)

The motion of a liquid along a solid surface, called interfacial slip, represents a fundamental phenomenon in fluid dynamics. For sufficiently high solid/liquid friction, the fluid velocity parallel to the interface goes to zero at the boundary. This no-slip boundary condition represents a standard approximation for describing fluid flow at macroscopic length scales. At microscopic scales, however, deviations from the no-slip boundary conditions have been observed [1, 2]. At such small scales, slip governs liquid transport and, thus, plays a major role in a variety of micro- and nanofluidic scenarios.

We use surface tension driven flow of thin liquid films, together with lubrication models, to extract the slip length of polymeric liquids on ultra-smooth surfaces. Already in the late 1970s, De Gennes predicted extraordinarily large slip for polymeric liquids, which originates from the ability of long polymer chains to form entanglements. We compare the results of two complementary experimental approaches, the capillary levelling of a stepped liquid film (see Fig. 8.55) and the dewetting of a liquid front. For an initially stepped film, the surface profile evolves in a self-similar fashion, i.e. flow causes the profile to broaden, but the characteristic shape remains fixed and the broadening is determined by a power law in time (see Fig. 8.56). By monitoring the self-similar profile and fitting it to a lubrication model, nanorheological information can be obtained. In order to extract the slip length b from capillary levelling, height profiles were recorded on a slippery substrate and compared to measurements on a no-slip surface (see Fig. 8.56) [3].

While dewetting experiments confirmed the theoretical scalings put forward by de Gennes, i.e. $b \propto M_w^3$ for high molecular weights M_w, we find that slip is inhibited for entangled polymer chains at low shear rates [3]. The levelling data saturates at high M_w (see Fig. 8.57), which is consistent with a model that includes physical adsorption of polymer chains at the solid/liquid interface. These findings contrast drastically with the ideal conditions for slip without chain adsorption at higher shear rates as seen in dewetting studies. Recently, we extended our capillary levelling studies towards elastocapillary phenomena [4].

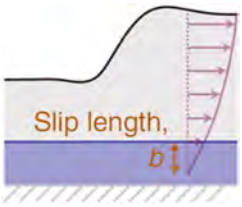

Figure 8.55: Flow field in a liquid film driven by levelling.

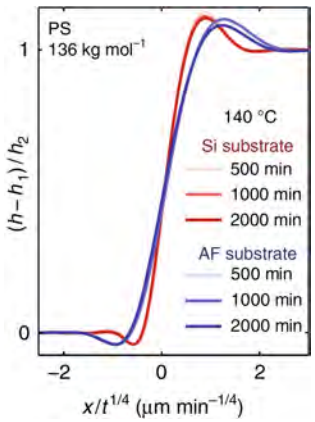

Figure 8.56: Levelling profiles on a no-slip surface (Si) and on a slippery substrate (AF).

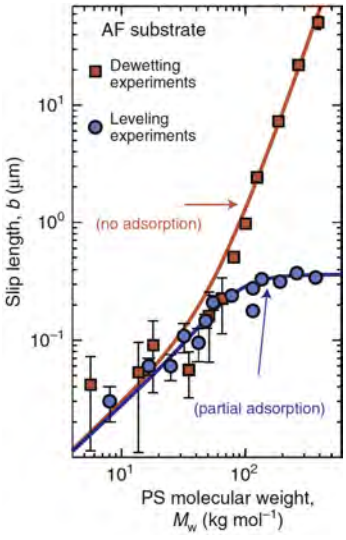

Figure 8.57: Measurements of the slip length b: dewetting (orange) and levelling (blue).

[1] S. Haefner, M. Benzaquen, O. Bäumchen, T. Salez, R. Peters, J.D. McGraw, K. Jacobs, E. Raphaël, and K. Dalnoki-Veress, *Nature Communications* **6**, 7409 (2015).
[2] M. Ilton, O. Bäumchen, and K. Dalnoki-Veress, *Phys. Rev. Lett.* **115**, 046103 (2015).
[3] M. Ilton, T. Salez, P.D. Fowler, M. Rivetti, M. Benzaquen, J.D. McGraw, E. Raphaël, K. Dalnoki-Veress, and O. Bäumchen, *Nature Communications* **9**, 1172 (2018).
[4] M. Rivetti, V. Bertin, T. Salez, C.Y. Hui, C. Linne, M. Arutkin, H. Wu, E. Raphaël, and O. Bäumchen, *Phys. Rev. Fluids* **2**, 094001 (2017).

8.29 INTERACTIVE DROPLETS ON SOFT, LIQUID, AND RIGID SURFACES

S. Karpitschka
J. H. Snoeijer (Twente), H. Wijshoff (Eindhoven), B. Andreotti (Paris)

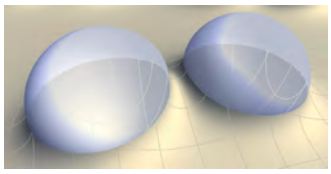

Figure 8.58: Drops on elastic surfaces interact through elastocapillary deformations.

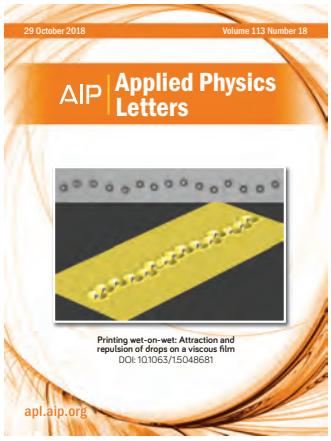

Figure 8.59: Droplets on immiscible liquid films interact through capillary waves (APL journal cover October 29, 2018).

Figure 8.60: Coalescence of spreading surfactant solution drops. Depending on geometry and composition, noncoalescence (a), fingering (b), or chasing (c) is observed.

Droplets on soft surfaces interact due to the elastocapillary deformation that surrounds them (Fig. 8.58). On an elastic half-space, droplets always attract, whereas on thin elastic layers, repulsion is observed in the far-field. This model system correctly predicts the length scales of integrin clustering in focal cell adhesion [1]. Droplet interaction results in an overdamped motion, governed by viscoelastic dissipation in the substrate. Force and dissipation balances in soft wetting have not yet been fully resolved and remain under active investigation [2, 3].

Similarly, micron-sized drops interact by a capillary mechanism when deposited on films of immiscible liquids. This scenario is highly relevant in modern ink-jet printing, where the print substrate is typically coated with a primer liquid, e.g. to promote precipitation of color pigments. Each deposited droplet emits a capillary wave and interacts with the waves of its neighbors (see Fig. 8.59). In contrast to the elastic case, here the interaction is mediated by a spreading surface oscillation instead of a quasi-static deformation. Consequentially the interaction forces not only depend on geometry, but also on time [4].

Equally relevant for color printing is the interaction of droplets from different, miscible liquids that are deposited on a rigid high energy surface. A surface tension contrast between two droplets of small mutual surface activity can suppress their coalescence by a Marangoni-driven hydrodynamic mechanism [5]. Similar holds for aqueous surfactant solutions: drops with different surface coverages show manifold interaction behaviors (see Fig. 8.60), depending on the droplet geometry and composition [6]. Intriguingly, nanoscopic precursor films may strongly impact macroscopic drop dynamics (Fig. 8.60 c & d).

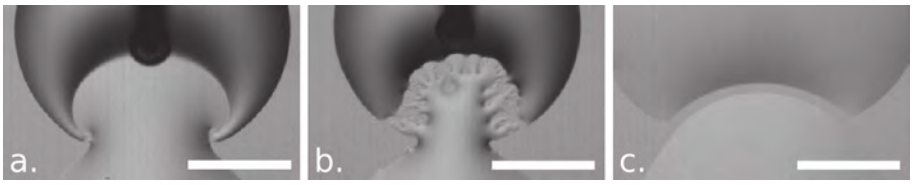

[1] S. Karpitschka, A. Pandey, L. A. Lubbers, J. H. Weijs, L. Botto, S. Das, B. Andreotti, J.H. Snoeijer, Proc. Natl. Acad. Sci. U.S.A. **113**, 7403 (2016)
[2] M. van Gorcum, B. Andreotti, J. H. Snoeijer, S. Karpitschka, Phys. Rev. Lett. **121**, 208003 (2018)
[3] S. Karpitschka, S. Das, M. van Gorcum, H. Perrin, B. Andreotti, J.H. Snoeijer, Proc. Natl. Acad. Sci. U.S.A. **115**, E7233 (2018)
[4] M. A. Hack, M. Costalonga, T. Segers, S. Karpitschka, H. Wijshoff, J. H. Snoeijer, Appl. Phys. Lett. **113**, 183701 (2018)
[5] S. Karpitschka, H. Riegler, Phys. Rev. Lett. **109**, 066103 (2012)
[6] M. A. Bruning, M. Costalonga, S. Karpitschka, J. H. Snoeijer, Phys. Rev. Fluids **3**, 073605 (2018)

8.30 EVOLUTION OF EXPRESSION LEVELS, FROM GENES TO NETWORKS

A. Nourmohammad

An organism's physical traits and fitness are largely determined by the regulation of expression of a large number of genes and their amount of protein production. Differences in gene expression within a population and across related species may be due to adaptive (i.e., advantageous) evolutionary changes in response to the environment fluctuations during evolution. The gene expression phenotype is encoded by many interacting genetic loci (large degrees of freedom) with a highly degenerate genotype-to-phenotype map, which is often at least partially unknown. This has made it difficult to characterize a system-wide modes of evolution for gene expression.

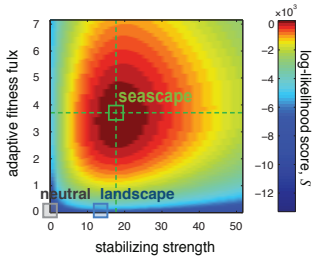

Figure 8.61: Evolution of gene expression follows two distinct molecular clocks [1]. On short timescales, expression level is constrained by strong stabilizing selection (x-axis), and it is adaptive to environmental fluctuations on longer timescales (model of fitness seascape), yielding a significant fitness flux (y-axis).

Using concepts from statistical physics, I have developed a probabilistic inference framework to partition the divergence of a phenotype over an evolutionary period into an adaptive component in response to changes in the environment, and stochastic fluctuations from random mutations and reproduction. I showed that time-dependent statistical observables of a phenotype can distinguish between various evolutionary modes, including equilibration and conservation in static environments (or fitness landscape), or non-equilibrium adaptation to a time-dependent environment (or fitness seascape). Using this new inference method, I showed that 64% of the observed gene expression divergence across 7 Drosophila species are adaptive changes driven by directional selection (Fig. 8.61), and identified specific functional classes with strong adaptive evolution [1]. In a recent collaborative work, we have used this approach to demonstrate the evolutionary significance of gene expression variation among cells for the functionality of the innate immune system in primates and in rodents [2].

Within each organisms, a large number of genes interact and determine the output of a biological pathway, e.g., a metabolic or a regulatory response to inputs from the environment. In collaboration with Peter Andolfatto at Columbia University, we have recently generated high-throughput measurements of gene expression levels in various Drosophila species. Expression level of a gene is a proxy for the amount of protein production and its activity in a given tissue. I am currently developing methods to infer interactions between genes within known biological pathways, infer modes of evolution (e.g., adaptation or conservation) of pathway response, and infer novel pathways based on covariation of expression levels within individuals and across species of Drosophila.

[1] Nourmohammad, A., Rambeau, J., Held, T., Kovacova, V., Berg, J., Lässig, M. Adaptive evolution of gene expression in Drosophila. Cell Reports 2017; 20(6) 1385-1395.

[2] Hagai, T., *[...]*, Nourmohammad, A., Lässig, M., and Teichmann S.A. Gene expression variability across cells and species shapes innate immunity, Nature 2018; 563, 197-202.

8.31 THE OPEN-SIR-MODEL: DISEASE CONTROL IN REFUGEE TRANSIT CAMPS AND OTHER OPEN POPULATIONS

W. Reimann, S. Eule, T. Geisel

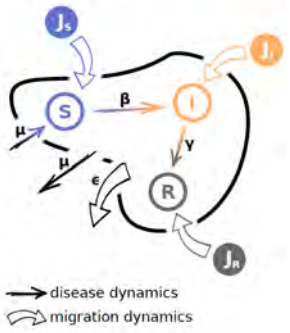

Figure 8.62: Sketch of the Open-SIR-model (OSIR).

In disease control a problem of topical importance is posed by a single open population subject to migration, where the endemic disease level needs to be projected and controlled. Refugee transit camps where new refugees constantly arrive while others leave them are a typical example for such an open population, others are nursing homes and livestock farms. The design and implementation of effective disease containment measures are priority objectives to relieve the humanitarian condition in refugee camps.

We forecast the effects of migration on the longterm endemic level of a population by evaluating a new analytically solvable model, the Open-SIR-model (OSIR). We obtain exact solutions that allow (i.) to predict the change of the endemic level under varying migration and ii.) to devise intervention strategies based on vaccination of incoming individuals only and to determine the relevant vaccination coverage thresholds. We find that immigration often changes the endemic state in an unexpected and counterintuitive way. For example, it is possible that on the one hand the inflow of healthy individuals worsens the situation of the population. On the other hand the health situation of the population can amazingly improve, even when the fraction of infected in the inflow is higher than the proportion of infected in an isolated population. We obtain concrete results predicting how the endemic state changes depending on variations in the migration strength and composition and use these results to devise state-dependent interventions. In particular, for susceptible immigrating individuals we determine the necessary vaccination coverage upon which immigration always improves the health situation of the population and the immigration rate dependent critical vaccination rate that leads to complete eradication of the disease from the population.

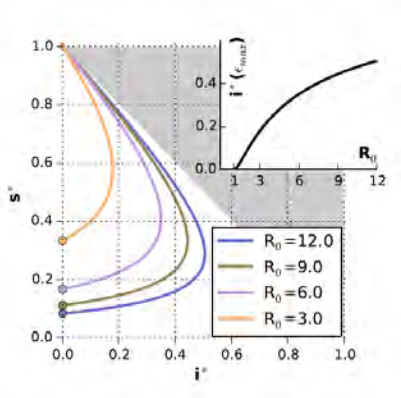

Figure 8.63: Immigration of healthy individuals ($s_{\text{ext}} = 1$, $i_{\text{ext}} = 0$) of strength E has a non-monotonic impact on the number of infected $i^*(E)$ and the endemic state $(s^*(E), i^*(E))$ within the population. The parameters correspond to a typical infectious disease in humans. This figure and its inset demonstrate the counterintuitive effect that a moderate inflow of only healthy individuals can raise the endemic disease level by orders of magnitude to a significant fraction of the population.

[1] W. Reimann, S. Eule, and T. Geisel, to be publ.

8.32 LEVERAGING FUNCTIONAL ASSAYS TO BIOPHYSICALLY MODEL PROTEIN INTERACTIONS

J. Otwinowski, G. Isacchini, A. Nourmohammad

Proteins functions are defined largely by their three-dimensional structures, which are in turn determined by their genetic sequence. Recently developed functional assays, called deep mutational scanning (DMS), allow for high-throughput quantification of mutated molecular variants. These studies have greatly expanded our view of functional landscapes of biomolecules, and have brought insights that were not accessible from structure alone.

A recent DMS experiment has produced high quality information on how a small bacterial protein (protein G) folds and binds to a antibody fragment for half a million mutated protein variants [1]. We have developed a biophysical model of how mutations affect fold stability and the stability of the protein-protein interface [2]. Predicted changes in fold stability are in physical units and match independent measurements. The inferred energy landscape shows how each position is sensitive to folding and binding independently and shows the distribution of mutants in the phase space (Fig. 8.64).

We are extending this model to predict the physical contacts within the protein, which involves estimating a sparse set of pairwise interactions in folding energy. Furthermore, we are adding physico-chemical information and structural information to reduce the dimensionality of the model and add predictive power. The ultimate goal is to produce a model that can take structural data and reliably predict the mutations on function on new proteins without any functional measurements.

Simultaneously we are developing machine learning models for more limited single mutant sequence-function data from HIV [4] and influenza proteins [3] and their interactions with antibodies. Our understanding of the impact of mutations on these viruses guides research on vaccine development and viral evolution. Viral proteins mutate to escape binding to immune molecules, but there are costs to intrinsic growth for mutating in regions critical for viral function. Our goal is to infer sequence-structure-function relationships to understand viral function and immune escape with a predictive model using DMS data and structural and evolutionary features. Such work may be critical in understanding how to stimulate broadly neutralizing antibodies, which is the focus of current vaccine research in HIV and influenza.

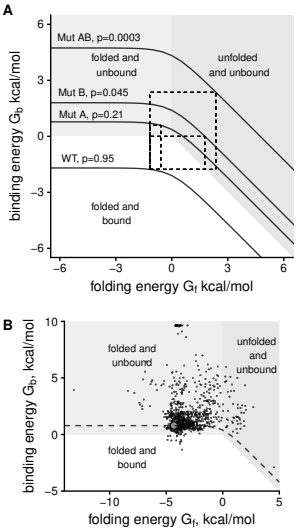

Figure 8.64: Biophysical model inferred from half a million mutated protein G variants and associated measures of binding. Model consists of a three state Boltzmann distribution with folding and marginal binding energies. (A) Measured binding fractions p for hypothetical single and double mutants in phase space. Constraints from all observed double mutants and additivity in energy makes inference feasible. (B) Projection of inferred single mutant energies onto phase space.

[1] Olson CA, Wu NC, Sun R. A Comprehensive Biophysical Description of Pairwise Epistasis throughout an Entire Protein Domain. Current Biology. 2014; 24(22):2643-51

[2] Otwinowski J. Biophysical Inference of Epistasis and the Effects of Mutations on Protein Stability and Function. Mol Biol Evol. 2018;35(10): 2345-2354.

[3] Doud MB, Hensley SE, Bloom JD. Complete mapping of viral escape from neutralizing antibodies. PLOS Pathogens. 2017 Mar 13;13(3):e1006271.

[4] Dingens AS, Haddox HK, Overbaugh J, Bloom JD. Comprehensive Mapping of HIV-1 Escape from a Broadly Neutralizing Antibody. Cell Host & Microbe. 2017; 21(6):777-787.e4.

PART III

SUPPORT

FACILITIES

9

Contents

9.1 MICROSCOPY FACILITY

C. Westendorf

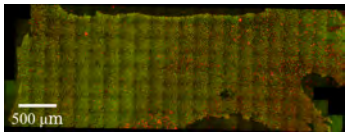

Figure 9.1: Stitched image after sequential imaging of the fixated and stained mammalian brain ventricle surface. The corresponding 184 z-stacks were recorded by spinning disk microscopy (60x, Olympus BX63 / Yokogawa). Image origin: Kapoor/Westendorf.

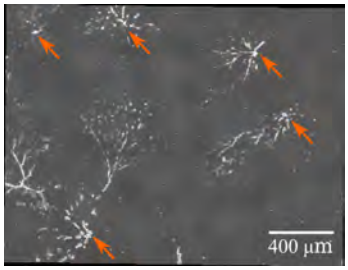

Figure 9.2: Stitched image of a fast sequential 5x5 frame recording of aggregating *D. discoideum* (10x, Olympus IX81).The arrows indicate the multiple aggregation centers visible within the enlarged region of interest. Image origin: Tirado/Westendorf.

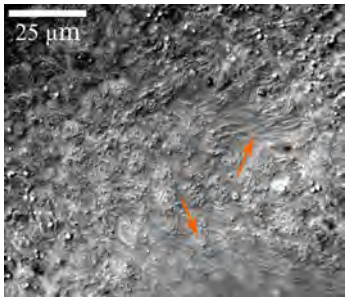

Figure 9.4: Ciliated surface of the mouse brain ventricular system. Images were recorded with 100 fps to time resolve the cilia beating (DIC, 60x, Olympus BX51). Arrows indicate beating cilia. Image origin: Kapoor/Westendorf.

The microscopy facility of the MPIDS combines a set of advanced light- and laser based microscopes. It is operated by the LFPB department (Bodenschatz), but is open to users from the other departments as well as external users from the neighboring MPIBPC. The current focus of the biophysical subgroups within the LFPB department are single cell biophysics, quantitative and synthetic biology. Therefore, the selection of the microscopes applies techniques of life cell imaging aided by sensitive cameras/detectors (fig. 9.3). The backbone of the facility are the confocal laser scanning microscopes (Olympus FV1000) and a confocal spinning disk microscope (Olympus), which serve for a broad range of experiments, such as single cell stimulation and fast 3D imaging of migrating *Dictyostelium discoideum*. These are complemented by a high precision light microscopy set-up (Deltavision), which achieves its z-resolution by deconvolution of epifluorescence z-stacks.

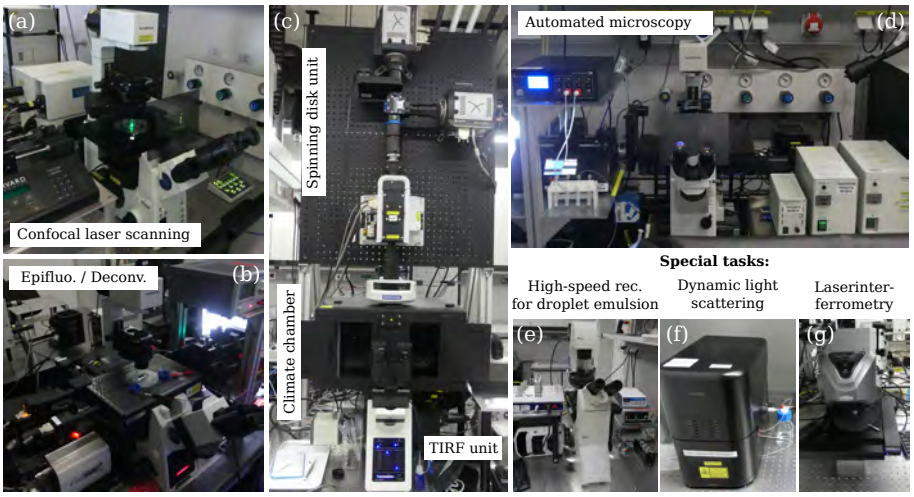

Figure 9.3: Selection of the currently operated microscopes. (a) Confocal laser scanning microscope (Olympus FV1000). (b) High precision epifluorescence (deconvolution enhanced) microscopy (Deltavision). (c) Dual set-up consisting of a spinning disk unit and a Fluorescence/TIRF unit (Olympus BX63/IX83). (d) Fully automated microscopy with large scale recording and additional control of auxiliary devices. (e-g) Set-ups designed for special tasks.

Within the past 3 years we have substantially enhanced our facility to fulfill the raised demand by experiments in quantitative and synthetic biology. First, we upgraded several inverted and upright light microscopes by automating these, allowing for long time and large scale unsupervised recording / experiments (see figures 9.1, 9.2, and 9.4 for examples). Second, we purchased set-ups for specialized tasks, such as high speed recording of droplet formation and dynamic light scattering to measure the size distribution of liposomes or even isolated exosomes. Finally, the microscopy facility takes part in the scientific education. Every new user of the facility is taught a short course to be appropriately trained to use the respective microscope and apprentices are taught basics of microscopy as part of their education at the MPIDS.

9.2 THE MAX PLANCK TURBULENCE FACILITY

C. Küchler, S. Weiss, M. F. Wedi,
G. G. Nunnari, F. Nordsiek, E. Bodenschatz
G. P. Bewley (Cornell U.)

To understand turbulence in a fundamental sense and to make predictions useful in real-world applications, one needs not only to observe turbulence at high Reynolds numbers, but also to realize flows with various spatial and temporal large scale properties. These well defined flows must go hand in hand with precise measurements. In addition one must have the ability to adjust the conditions in various ways, so that dependencies can be uncovered. The facilities at the MPIDS make it possible not only to generate turbulence with the highest Reynolds numbers yet possible under laboratory conditions, but to do so with unprecedented control. To match our achievements in controlling turbulent flows, we have advanced measurement technologies, and have even adapted these to field experiments of natural flows.

The Variable Density Turbulence Tunnel (VDTT) [1] is a recirculating pressurised wind tunnel that consists of two measurement sections with cross-sectional areas of $1.9\,\mathrm{m}^2$ and lengths of 9 m and 7 m. The maximum flow speed is approximately 5.5 m/s. The chief merits of the VDTT are that it produces high Reynolds number flows and stable operating conditions. Furthermore, the Reynolds number is finely adjustable by changing the pressure of the gas in the tunnel, usually sulphur hexafluoride (SF_6) up to a pressure of 15 bar. Further, an active grid consisting of 111 individually controllable flaps creates turbulent wakes of variable size and intensity [7] and can be used to systematically change the Reynolds number as well as the structure of the turbulent fluctuations. Injecting turbulent kinetic energy into the flow through the active grid allows us to reach Reynolds numbers up to 6000 (compared to 1700 when a classical grid of crossed bars is used), which is unmatched by any other wind tunnel flow in the world. The wind tunnel is currently equipped with hot-wire anemometers and the implementation of a stationary particle tracking system is scheduled.

The Prandtl tunnel is an open-circuit wind tunnel dating to the 1930's. The wind tunnel is 11 meter long with a measurement section of 1.2m x 1.5m and maximum wind speed of 12 m/s. It can be equipped with hotwire anemometers and thanks to the large measurement section it is suitable for a large variety of experiments. It is also often used to test prototypes and equipment that will later be installed in the VDTT.

The High Pressure Convection Facility (HPCF) [2] utilizes a general-purpose pressure vessel called the "U-Boot", which is 5.3 m long and has a diameter of 2.5 m and can be filled with SF_6 up to a pressure of 19 bar. We precisely control both the temperature and the pressure in the vessel. Within the vessel are two cylindrical Rayleigh-Bénard (RB) experiments (diameter 1.1 m, heights 2.2 m and 1.1 m) that reach Rayleigh numbers as high as 10^{15}. Recently, we installed a rotating table for the RB cells inside the U-Boot, which allows for the study of turbulent heat convection under the influence of rotation.

Figure 9.5: The Variable Density Turbulence Tunnel (VDTT)

Figure 9.6: The Prandtl Tunnel

Figure 9.7: The "U-Boot", a general-purpose pressure vessel, housing the High-Pressure Convection Facility (HPCF)

Figure 9.8: The "Cigar", a general-purpose pressure vessel

Figure 9.9: The von Kármán mixer

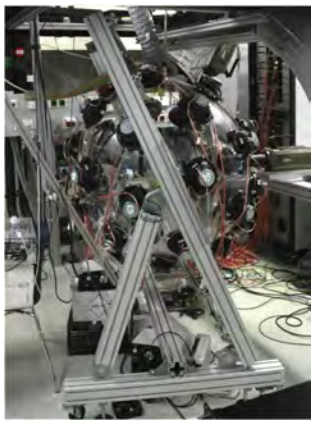

Figure 9.10: A "soccer ball"

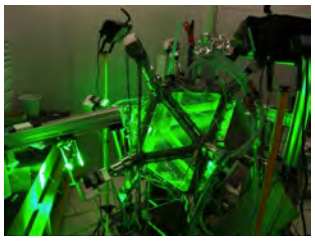

Figure 9.11: The Lagrangian Exploration Module

The "Cigar" is a general-purpose pressure vessel with a length of 4 m and an inner diameter of 1.5 m. It can be filled with SF_6 up to a pressure of 19 bar to perform smaller convection or turbulence experiments or to test equipment for the other pressurized facilities.

Two von Kármán mixers generate high Reynolds number turbulent water flows between two counter-rotating baffled disks. Because the average displacement of fluid particles near the middle of the mixers is close to zero, their motions can be followed for a long time. The mixers are about a half-meter in diameter, and R_λ can be as high as 1200. Large glass windows provide optical access for imaging techniques. The apparatus can be pumped down to reduced-pressure for the study of bubble dynamics. A frequency doubled high-power (50 W), high-repetition-rate Nd:YAG laser is devoted to measurements in this apparatus.

Theoretical knowledge is most developed for turbulence that is stationary and isotropic. But real flows are neither. Three novel apparatuses [3, 4], make it possible for the first time to control the degree to which a turbulent flow is anisotropic both, in gases and in water. We produce cloud-like conditions in one soccer ball.

The facilities make use of state-of-the-art three-dimensional Lagrangian particle tracking (LPT) technologies that we have developed in-house. The technology relies on multiple ultra high-speed cameras viewing the same particles from different angles, with megapixel resolution and kilohertz frame rates. Recently we have developed a techniques that enables us to measure the 3D vorticity in water flow. We also employ a Dantec hot-wire system in conjunction with nano-fabricated hot-wires from Princeton University, a LaVision tomographic particle image velocimetry system, and a TSI laser Doppler velocimetry and particle sizing system. All of this equipment is compatible with pressures up to 15 bar. Some of these techniques require substantial light, which is typically produced by Nd:YAG lasers or argon-ion lasers. The systems produce data at rates that necessitate high-performance computing and storage clusters.

The Max Planck Turbulence Facilities (MPTF) are open to visiting researchers. For example it has been used in the European High-Performance Infrastructures in Turbulence (EuHIT) project[1]. It aims to integrate cutting-edge European facilities for turbulence research across national boundaries [5, 6].

[1] E. Bodenschatz, G. P. Bewley, H. Nobach, M. Sinhuber, H. Xu, Rev. Sci. Instrum. **85** (2014) 093908
[2] G. Ahlers, D. Fünfschilling, E. Bodenschatz, New J. Phys. **11** (1009) 123001
[3] K. Chang, G. P. Bewley, E. Bodenschatz, Journal of Fluid Mechanics **692** (2012), 464-481
[4] R. Zimmermann, H. Xu, Y. Gasteuil, M. Bourgoin, R. Volk, J.-F. Pinton, E. Bodenschatz, Rev. Sci. Instrum. **81** (2010), 055112
[5] http://www.euhit.org
[6] http://www.euhit.org/media/EuHIT_EN.480p.mp4
[7] K. P. Griffin, N. J. Wei, E. Bodenschatz, G. P. Bewley, Exp. Fluids **60** (2019) 55

[1]The European Commission supported the project European High-Performance Infrastructures in Turbulence (EuHIT, Grant Agreement Number 312778)

9.3 SCIENTIFIC MECHANICAL ENGINEERING FACILITY

U. Schminke

The requirements for experimental work at the Max Planck Institute for Dynamics and Self-Organization are versatile and very demanding. They require the highest quality in mechanical engineering from design and verification/certification to construction. The sizes of mechanical parts employed in the scientific experiments range from micrometers to many meters. They are used in various environments from the laboratory, to mount Zugspitze, and on research vessels like the Maria S. Merian. Parts are uniquely designed and manufactured for highly specialized experiments. Designs are conducted by the mechanical engineer, who heads the facility, in tight collaboration with the scientists. CAD 3D construction software is used not only to construct and develop the parts but also to conduct Finite Element Structural Analysis. The components created in the designs are then processed quickly, flexibly, and with high quality in the mechanical workshop according to the drawings or directly from the CAD design data with the help of a CAM interface. With a simulation integrated in the CAM software, potential errors occurring during the production process can be detected and eliminated before the actual part is machined. In addition, the 3D-CAD output can be used in scientific presentations and publications.

Many of the unique experiments employ automated, integrated, computer-controlled systems. Very often, actuators, sensors, etc. with the associated control and testing devices are integrated into the mechanical components. In close cooperation with the Scientific Electronics Facility, the mechanical constructions are finetuned with the electronics.

Figure 9.12: The team of the scientific mechanical engineering facility.

Mechanical production is accomplished with computerized turning, milling, grinding, 3D printing, and other machines which cover the full area of precision mechanics. In order to produce precision parts with geometrically complex shapes, we have 5D-milling machines and 3D-printers.

The training of apprentices has also been an important part of the work of the facility from the very beginning. In the last ten years, our trainees have passed these examinations with distinction.

9.4 RESEARCH ELECTRONICS FACILITY

L. Diaz, A. Barthel, O. Kurre, H. Nobach

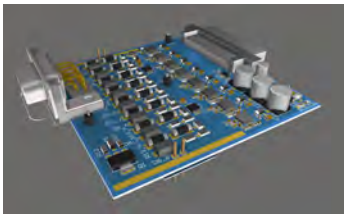

Figure 9.13: 3D Representation of a Multi-Channel Electrocardiography Board

Figure 9.14: Programmable Defibrillator for customized Shock Sequences

Figure 9.15: Gold microelectrodes on a glas substrate realized with laser ablation for life sciences

Figure 9.16: Transparent electronics made possible on ITO coated glas. The fabrication was done in the Research Electronics's Printed circuit Board Lab

The diverse, outstanding projects at the frontier of MPIDS research require professional planning, development, manufacturing, installation, programming and maintenance of highly specialized electronic components and devices. In order to be able to better meet these challenges, we have a new research infrastructure at the institute since February 2018, which makes its expertise in electronics available to the entire institute. The Research Electronics facility bundles the institute's human and material resources in order to be able to offer them more efficiently and more broadly.

The staff of the Research Electronics facility develops and builds highly specialized, unique electronic circuits for measuring and control tasks incl. the electronic interfaces between computer and measurement technology for scientific apparatuses that cannot be commercially obtained. The circuits are designed with CAD engines and then build in house.

To do this, recently, the equipment pool has been expanded by a circuit board plotter, an electroplating machine, a stencil printer, a vapor phase reflow soldering machine, a laser structuring system and by an SMD placement machine. This opens the possibility to build practice-oriented printed circuit boards and ready-for-use devices from the developed circuit designs for the use in the experimental environment all in house.

At the present, two engineers and two technicians work in the Research Electronics facility. In the long-term perspective, we want to broaden our horizons in order to cope with new and interesting tasks. According to our ideas, in the future three engineers and three electronics technicians will work full-time in the group. In addition, we will continue to train electronics technicians for equipment and systems in the future.

With the installation of this new infrastructure for Research Electronics, we are meeting the strongly increased demand for individual experimental and scientific devices, which are unique and therefore have to be specially developed and built. Many of these tasks are performed by the Research Electronics facility. The staff closely collaborates with the scientists providing valuable advice and expertise in all stages of the construction process from the first idea to the finished component and the experimental application. In doing so, we also comply with the urgent recommendation of the advisory board, which has repeatedly pointed out the need for a powerful infrastructure for Research Electronics in the past.

9.5 MICROFABRICATION FACILITY

L. Turco

The Microfabrication Facility provides space, equipment, and assistance to design and manufacture devices for several groups within the institute and for other research institutions. The clean room (35 m2-Class 1000) is used to develop silicon masters via photo-lithography and it is equipped with a spin coater for deposing thin layers of SU-8 photoresist, hotplates for baking the resist and two mask aligners (EVG-620, UV-KUB 3) for exposing the wafers to UV illumination. Structures with features of 7-10 micrometers can be fabricated and a white light interferometer (Wyko NT1100) is used to accurately measure film thickness, surface roughness and surface features.

Figure 9.17: Clean room.

Microfluidic devices are assembled outside of the clean room environment after replica molding of the fabricated silicon master.

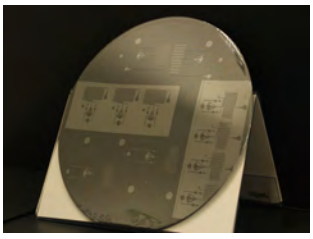

Figure 9.18: SU-8 wafer used for replica molding.

The facility is also equipped with a 3D laser lithography system (Photonic Professional GT) used to build unique 3D structures and devices with submicron resolution. Starting from the CAD model of the structure, using embedded software it is possible to rapidly print the structures with high degree of complexity via two photon polymerization of a UV curable photoresist. Beside lithography, a high precision milling machine (DMU 50, DMG Mori Seiki) is used to pattern microchannels in hard plastic and metals for fabricating structures from 150 microns up to 10 cm.

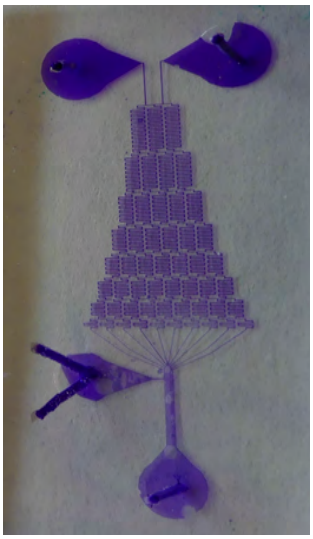

Figure 9.19: Microfluidic device fabricated by replica molding of PDMS.

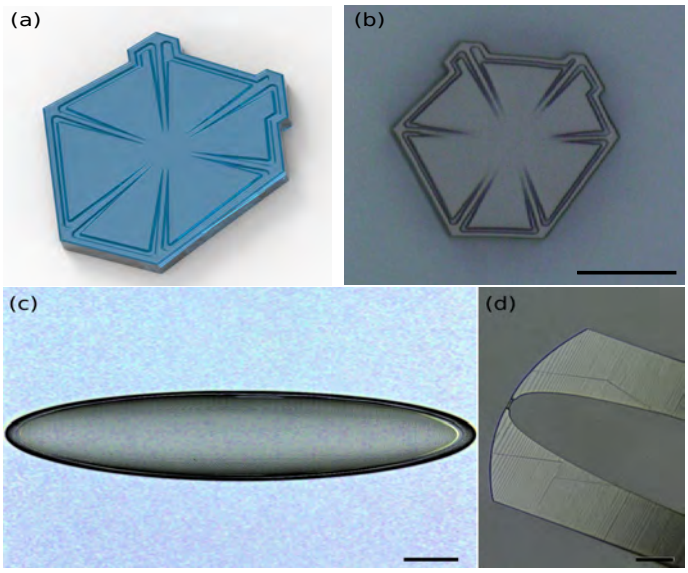

Figure 9.20: CAD Model of a snow crystal with hexagonal prism shape (a) and the fabricated 3D printing (b). Scale bar 70 microns. 3D printed elliptic particles (c) and hot wire probe (30 microns long and 4 microns thick) from measuring small-scale turbulence. Scale bar 100 microns.

The facility plays a pivotal role in developing microfluidic platforms for generating compartments that mimic cellular systems within the Max Plank Network on Synthetic Biology (MaxSynBio/cors), a joint Max Plank- BMBF initiative. Training and assistance in microfabrication at all levels, from design to the use of microfluidic devices, is provided by the facility.

9.6 UFS SCHNEEFERNERHAUS

J. Moláček, G. Bagheri, G. Bertens, E. Bodenschatz

The field measurement laboratory is a facility operated by MPIDS at the research station Schneefernerhaus near the peak of Zugspitze mountain at an altitude of 2650 m. Location of the laboratory provides easy access to the two topmost outside platforms of the station, which are best suited for study of atmospheric turbulence and cloud dynamics. On the top platform, we have installed a mast with a set of 3D sonic anemometers to conduct long-term year-round measurements of the wind and turbulence conditions at the UFS. Also situated on the top platform is a Lagrangian particle tracking apparatus dubbed the "Seesaw", consisting of a 6.5 m-long set of rails along which a vibration-damped box housing a set of high-speed cameras can be driven at speeds of up to 7.5 m/s by two electromagnetic motors. Precise control of the translation velocity and tilt of the rail with respect to the horizontal makes it possible to match the west-east and vertical components of the mean flow and follow cloud particles over time intervals longer than those achievable with a stationary setup. Illumination is provided by a 300 W green laser housed in the laboratory.

Figure 9.21: Mast with sonic anemometers at the UFS.

Figure 9.22: A dual phase-Doppler interferometry probe.

A dual phase-Doppler interferometry probe allows measurement of cloud droplet size distribution and individual velocities. The set of tools and equipment stored at the laboratory, together with the in-house machine shop, allows rapid development of new field experiments.

9.7 MOBILE CLOUD LABORATORY

O. Schlenczek, G. Bagheri, P. Höhne,
F. Nordsiek, M. Schröder, E. Bodenschatz

Each Cloudkite carries a suite of instruments to measure fluid properties and particle properties in clouds. But to interpret the time series of wind speed and other quantitites measured by the Cloudkite as well as evaluating flight safety, we need additional instruments on the ground to get the big picture in terms of cloud and boundary layer dynamics. Additionally, we need to transport the Cloudkite to the field, have a location to repair instruments, and bring some computing power to do data analysis in the field. To accomplish this, we are building the Mobile Cloud Laboratory (MCL), an instrumented van to transport the Cloudkite and function as a mobile weather station. A CAD visualization is shown in Figure 9.23. The quantities measured on the

Figure 9.23: CAD visualization of the customized MCL van.

ground are basic meteorology (temperature, pressure, relative humidity, wind speed and direction), dewpoint via chilled mirror, precipitation rate, hydrometeor size distribution, cloud ceiling and backscatter, and the atmospheric electric field via field mill. Specifically, the wind and electric field measurements are important to evaluate the risk of high winds and potential lightning.

9.8 HIGH-PERFORMANCE COMPUTING FACILITY

D. Fliegner, H. Degering

The demand of computing power and storage space is constantly increasing throughout all scientific groups of the MPIDS as simulations go into higher detail, tackle more complex problems, and experiments use measurement equipment with higher resolution in time and space. The HPC group of the MPIDS provides high capacity storage in blocks of 300TB with mirrors in separate sections of the building and high bandwidth access to them as well as compute clusters for parallel computing, GPU accelerated codes, and fast, big local storage, as well as mirrored and backed-up personal directories. The necessary infrastructure scales way over single workstations and below traditional large computing centers, but has to allow for interactive use, e.g. for developing large-scale parallel applications or directed parameter space exploration.

Figure 9.24: Cooling cabinets with HPC clusters in the new server room of the MPIDS. Open racks for infrastructure servers in the front. The cabinets have a dedicated control and monitoring unit, are built in a modular fashion so that they can easily be moved, and can be customized to cool up to 36 kW.

The HPC group makes sure that the landscape of HPC clusters is as homogenous as possible minimizing maintenance workload and maximizing interoperability. Currently, the HPC hardware at MPIDS is in transition from DELL to Lenovo machines and Mellanox Infiniband to Intel Omnipath network interconnects for the parallel clusters. Scientists at the MPIDS have direct access to HPC clusters with a total of about 1000 HPC systems with 23,000 CPU cores, approximately 125 TB RAM, and 16 PB of storage capacity.

Hosting computing facilities of that size requires a very dense packing of servers which is provided by using multicore machines and efficient designs like blade server enclosures. Power densities of 24kW per square meter cannot be cooled by traditional open air flow cooling with false floors. An efficient cooling system is required from an environmental perspective, but also is mandatory from a financial point of view as in traditional cooling systems electricity costs of the cooling can be as high as 30% of the electricity costs for the computers themselves. MPIDS was among the first institutes to solve this issue by using optimized water cooled cabinets with a heat exchanger and redundant fans each to cool only the necessary parts of the server rooms, as shown in the photo above.

To improve service reliability as well as data security, the institute moved about 250kW of the institute's compute servers to a new site in the former 'Fernmeldezentrale' of Göttingen University, where the university computing center GWDG runs a large server room. Restructuring the first floor of the main building of the MPIDS brought the necessity to establish a new server room for the main clusters of the institute in the foundation of the new building of the MPIDS.

In order to manage such a complex facility a monitoring system based on open source software was set up, which collects important health data of both the HPC hardware and the cooling facilities on a frequent basis. This data is summarized on a comprehensive overview, its history can be assessed for diagnostics and the system is able to perform emergency shutdowns autonomously in case of cooling failure to prevent machine damage by high temperatures.

INFRASTRUCTURE

10

Contents

The Max Planck Institute for Dynamics and Self-Organization (MPIDS) has an efficient and powerful infrastructure to support its scientific activities. It is lead by the Chief Operation Officer. It is divided into the two core areas Administrative Services and Scientific Technical Services. The Administrative Services are Human Resources, Budget and Finance, Facility Services and Information Technologies. The Scientific Technical Services comprise the following facilities: High Performance Computing , Scientific Electronics, and Scientific Mechanical Engineering (please see the chapter facilities). In addition, Quality Management, Press and Public Relations, and General Service are part of the office of the Chief Operation Officer. Support tasks for the entire infrastructure are carried by the General Services. The institute's own transportation service ensures that tight schedules and timetables can be implemented between the institute's locations, the numerous cooperation partners and the Scientific Meeting Center. The infrastructure, based on flat hierarchies, not only ensures an optimal research environment, but also frees the institute directors and scientists from numerous everyday tasks.

10.1 ADMINISTRATIVE SERVICES

The Institute's Administrative Services covers a wide range of responsibilities and tasks and are subdivided into Human Resources, Budget and Finance, Facility Services and Information Technologies. On the basis of various legal regulations and norms, funding regulations and guidelines of the Federal Government, it is the task of the administration to ensure a comprehensive, legally secure, science-promoting and sustainable organization of all administrative processes. The administration acts as consultant and service provider for science as well as for all fields of the infrastructure. In all its activities, MPIDS is supported in internal and external communication by the Press and Public Relations Office. Through the creation of an internal monthly newsletter "MPI News" and the implementation of a series of lectures entitled "Science before the Weekend", as well as through professional press releases, press conferences, the maintenance of the websites and the organization of events for specific target groups, the staff unit makes a valuable and most important contribution to the public image of MPIDS and to the identification and motivation of the institute's staff. As an important anchor for a sustainable institute organization, MPIDS has created a Quality Management Unit. Starting from the moderation of numerous meetings to create a common vision, the staff unit accompanies and manages all institute processes. By analyzing individual processes, their interfaces and their respective outputs, processes can be clearly defined and optimized in accordance with current legal provisions and standards. The uniform documentation finally ensures a legally compliant institute organization and covers scientific, non-scientific as well as overarching areas such as occupational safety or environmental protection. This is supplemented by the risk management system introduced in 2018, which identifies risks for all areas of the institute,

draws attention to them and ultimately promotes the development of suitable preventive and emergency measures. The General Services and Transportation assists in all specialist areas of the infrastructure and supports catering within the framework of events, and also assumes newly created tasks, such as staffing the reception.

Human Resources

HR advises and supports in all issues relating to the employment of scientists at all stages of their careers as well as infrastructure employees. This includes all personnel, legal and organizational issues including work permits, health insurance, and tax and social benefits. In 2017 an on-line employee application system was established that significantly improved the application and selection process of new employees. HR installed highly successful exchange platforms that meet multiple times per year with the office assistants to discuss new developments and requirements. Through the joint development and formulation of an institute wide vision, an easy and general understanding of the aims of the institute was successfully established. By these and additional measures, like management training, the creation of flat hierarchies, and the promotion of internal communications, a clear convergence of the scientific and non-scientific areas was established. The desire for joint activities arose in response to the very positive working atmosphere. Within this framework, HR successfully manages team-building measures, company retreats, health events, and the annual, highly popular, Christmas party.

Budget and Finance

Budget and Finance includes accounting, budgeting and taxation, asset management and annual accounts, all purchasing and customs procedures, export control, and manages third-party funds, the scientific meeting center, the vehicle fleet, the guest catering, the event organization and all travels. eProcurement, the electronic ordering system of the Max Planck Society, was introduced in 2017. It enables orders to be placed by catalogue or free text, thus optimizing work flow. The scientists of the MPIDS continue to be very successful in attracting third-party funding for cutting edge science. Financed by the overhead of the acquired projects, the third-party funding group plays an important role in the application and multi-faceted administration of third-party funding projects. The experienced staff members support and advise on the application and administration of raised funds according to the different requirements of the respective funding agencies including the application for funds from the EU. The transformation of the guesthouses into a scientific meeting center is also remarkable. Through the redesign of common rooms and the creation of quiet rooms for concentrated work, the environment for the promotion of scientific cooperation could be further optimized.

10.2 FACILITY MANAGEMENT

The service area "Building Services and Industrial Engineering" is divided into electrical engineering and industrial engineering. The building and operating technology department is responsible for the maintenance and servicing of the entire technical infrastructure of the institute, including heating, cooling, sanitation and ventilation, electrical engineering, fire alarm technology, telecommunications, gas warning systems and emergency call systems. While small and medium-sized repairs and maintenance are carried out by team members, larger tasks are outsourced and coordinated by the Facility Management. The service unit also takes care of all janitorial and cleaning work.

10.3 INFORMATION TECHNOLOGY

The IT service (ITS) group is tasked with operating the computer network and the servers needed for running central infrastructure applications of the MPIDS. The ITS group also provides desktop support for the infrastructure departments and consulting services for the scientists.

In addition to maintenance and development of the existing IT infrastructure the ITS group has to deal with issues resulting from the huge amount of data produced and processed at the MPIDS. Since there are usually no off-the-shelf solutions that meet the requirements of the scientific users, the ITS group has to participate actively in the development of customized solutions geared towards contributing to a versatile and useful IT ecosystem. This includes topics like searchable web access for Terabytes of data, long term archival and supporting the development of processing and analysis pipelines for data generated by experiments.

In close cooperation with the local data center (GWDG) and the University of Applied Science in Göttingen, masters theses on those topics are offered and supervised by the ITS group. An apprenticeship program has been initiated that contributes to the IT education of young people and an apprentice will begin working at the MPIDS in September 2019.

OUTREACH

11

Contents

11.1 PUBLIC RELATIONS

Carolin Hoffrogge, press officer

Public outreach and media relations are recognized as an important part of the Institute's responsibility. This is shown not only by the increasing number of press releases, but also by the Institute's ongoing participation in public events and exhibitions. All outreach and media activities are coordinated in the Institute's press office.

Press releases

Press releases continue to be an important means of communicating with the local, national, and international media. These releases deal with scientific results from all Departments and Max Planck Research Groups, inform the media about important prizes awarded to MPIDS scientists, and advertise special events the Institute organizes or takes part in. Most press releases are published in German and English. In recent years, the number of press releases issued per year has continued to be high, but could even be increased. In addition, these press releases frequently spark the interest of industrial partners or direct other colleagues from science and research to our work.

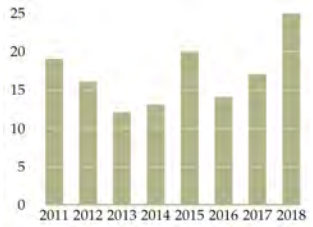

The number of MPIDS press releases over the last years

Guided Tours

The MPIDS offers school and student groups regular tours of the Institute. Young participants learn about science, either in the Institute's own experimental hall, in the computer cluster or in laboratories: the public relations office and the scientists involve explain the scientific content in a clear and attractive manner.

The 'Jugend forscht' prize winners visited the MPIDS

Future Day

Once a year in spring, 30 students from Göttingen and the surrounding area visit us for our future day. It is lively and turbulent for the 5th to 10th graders. They get the impression of a working day in a basic research institute. During their visit, girls and boys experienced research on dynamics and self-organization up close: currents such as those found on a small scale in the brain or heart, or currents on a large scale such as those found in clouds. The Future Day is always a major success for both the young visitors, but also for the scientists involved.

EcoBus – from basic research to the streets and into the media

Start of the EcoBus pilot project in Bad Gandersheim

The starting shot has been fired on June 10, 2018 - the first five EcoBuses ran during the 60th Gandersheim Cathedral Festival in and around Bad Gandersheim and in the neighbouring community of Kalefeld. After just five days' break, the second pilot project started on August 10, 2018 with ten busses in the Harz mountains between Goslar, Clausthal-Zellerfeld and Osterode am Harz. With the EcoBus the MPIDS wants to promote low-cost, environmentally friendly mobility in rural areas. In the long term, the EcoBus aims to become established as a rural mobility system and to connect existing transport options with

Impressions from the Future Day 2018

one another. Therefore, it will complement the already existing, well-frequented public transport corridors, and will reinforce classical transit and cab services. EcoBus has teamed up with regional public transport organizations (Zweckverbände) and a transport company (Regionalbus Braunschweig) to operate the ten busses. To promote EcoBus, the EcoBus team at the MPIDS, together with Southern Lower Saxony Programme (SNP) Headquarter, has been developing in the past years a network involving heads of municipal authorities, further regional public transport managers and Göttingen University researchers. Over 40 public institutions have signed up as Ambassadors for EcoBus. In sum, the EcoBus is very well recognized in Lawer Saxony, in Germany and even in places like Amarvati in India. Furthermore, EcoBus has a wide public recognition throughout Germany due to a broad media coverage. In addition, EcoBus has its own webpage: www.ecobus.jetzt.

New films

In 2018, two new image films about individual research projects were produced at the Institute. The four-minute film "Kammerflimmern - Mit Ultraschall dem Ursprung auf der Spur" (Ventricular fibrillation - On the trail with ultrasound) shows part of the research carried out by Professor Dr. Stefan Luther's Biomedical Physics Research Group. The film can be seen not only in the film gallery on our homepage, but is also regularly shown at medical fairs in Germany.

The five-minute film "EcoBus – Der Pilotstart" shows the first field study of the EcoBus ride pooling system in the southern Lower Saxony region of Bad Gandersheim and Kalefeld in the district of Northeim. The film is particularly suitable as an explanatory film for the EcoBus team led by Director Professor Herminghaus and is prominently featured on the first page of the www.EcoBus.jetzt homepage, as well as

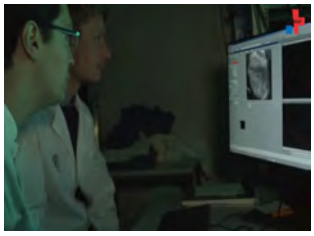

The new film about our heart research projects

The new film about the EcoBus project start

in the Institute's film gallery.

Max Planck Day in Göttingen - school, stage and pub

On September 14, 2018, the Göttingen Max Planck Institutes celebrated the Max Planck Day at unusual locations and with many interested guests. With more than 40 researchers in the schools, a moving Max Planck on stage and a fun pub evening combining science with humour and live music - the Max Planck Day offered a full and varied program from early in the morning until late in the evening. In this way, the five Göttingen Max Planck Institutes - together with many other institutions of the Max Planck Society throughout Germany - celebrated three anniversaries: the 70th anniversary of the founding of the Max Planck Society, the 160th birthday of Max Planck and the 100th anniversary of the award of his Nobel Prize.

Stage performance during the Max Planck Day: Albert Einstein (left) talks to Max Planck

Stefan Luther and Ranga Yogeshwar at the 'Highlights Show' in Dortmund

Highlights of Physics

The highlights of physics were presented in Dortmund's city center over one week in September 2018 with the participation of the Biomedical Physics Research Group of Professor Dr. Stefan Luther. On the first evening, the well-known German moderator Ranga Yogeshwar opened the Science Festival with a big show in the Westfalenhalle. Among many visitors (>6000), there were also prominent guests: Federal Research Minister Anja Karliczek, novelist Frank Schätzing and medical professor Dietrich Grönemeyer. First, moderator Yogeshwar called Professor Stefan Luther, head of the research group "Biomedical Physics", on stage. Luther and his group work on the theme of the show "Heart racing". Physicist Luther impressively demonstrated how ventricular fibrillation develops, and how he and his team plan to use a gentler method to prevent fibrillation in the future. The audience in the Westfalenhalle was able to follow this process for themselves in a La-Ola wave using their mobile phones.

Night of Science 2019

Göttingen hosted a major science festival for the fourth time; the MPIDS contributed to the "Night of Science" (January 26, 2019) organized by the University of Göttingen, the Max-Planck-Institutes and other Campus partners. At the festival the MPIDS contributed lectures like "How heavy rain emerges". In addition, MPIDS scientists offered hands-on activities and information stands, introducing the guests to the world of turbulent flows and complex fluids. Highlights of the "4th Night of Science" was a spectacular laser experiment demonstrating the turbulent flows in clouds and the intelligence of slime moulds.

Stefan Luther at the Science Night 2019

Background information about animal testing and crisis communication

On 10 August 2017, a team consisting of chairman, animal welfare officer and press spokeswoman provided information on aspects of animal experiments at the Institute. In addition, the staff was informed about possible scenarios for crisis communication.

Summer festival

Each summer we celebrate our annual summer festival, together with our neighbor institute MPIBPC. Informal discussions, sporting activities, a "Brain Match Quiz" and musical highlights turned the summer day into a happy event.

Göttinger Literaturherbst

As in previous years, the MPIDS took part in the annual literary festival in Göttingen, the "Göttinger Literaturherbst". This festival features

The organization team of the 'brain match quiz' during the science summer party 2017

a scientific lecture series where internationally renowned scientists present their latest books in the unique atmosphere of the historic Paulinerkirche in Göttingen. These lectures are introduced and chaired by scientists from the local Max Planck Institutes, with the aim of stimulating a vigorous exchange of ideas. In 2018, a highlight was the lecture, which was awarded this year's Science Communication Medal. The prize is awarded as part of the scientific series of talks during the Göttinger Literaturherbst and distinguishes individuals who have shown strong commitment to communicate current scientific results to the general public. In 2017 the award winner was the American cognitive scientist Douglas Hofstadter, in year 2018 the British materials scientist Mark Miodownik received the Science Communication Medal.

Theo Geisel with Douglas R. Hofstadter at the Göttinger Literaturherbst 2017

Future press/public relations work

In future, the Institute's press and public relations work will be enriched by a newInstitute brochure. In addition, scientists will be portrayed in the form of audio podcasts accompanied by photo galleries. The website will also follow the relaunch of the Max Planck Society. In the same way, we want to provide long-term social media channels, such as Facebook and Twitter with research content.

11.2 INTERNAL COMMUNICATION

Science before the weekend

As of February 2015, we have restarted the series "Science before the weekend". In understandable, attractive and entertaining lectures, scientists of MPIDS explain their work to the institute's staff in German language. This greatly contributes to internal communication within the Institute and is regularly attended by up to 50 listeners.

Internal Newsletter MPI Aktuell

For efficient, quick, and straightforward internal communication an email newsletter has been initiated. It is distributed to all employees once a month and contains brief information about news items, new appointments, important dates, and publications. In addition, each month a special topic (such as new research co-operations, public events or scientific results) is highlighted in more detail. In this way, the newsletter offers both quick and in depth information.

11.3 THE GÖTTINGEN CAMPUS

The Göttingen Campus Council (GCC) was established by the university in 2006 in order to coordinate campus wide activities with the non-university institutes. The main task of the GCC is the consultation between the executive committees of the University (Presidential Board, University Medical Centre Board, Senate) and the non-university institutes. Our institute is one of the eight non-university members of the GCC and is represented by Professor Dr. Eberhard Bodenschatz. Topics range from joint teaching and research activities, towards the identification of research foci for the development of the Göttingen Campus.

The Campus Marketing Group exists since 2016 and exchanges information once a quarter about joint activities such as the Night of Science, the Göttingen Literaturherbst, joint advertising products, the Campus Göttingen website, the Campus Göttingen Calendar or activities such as the " Belebten Schaufenster" (lively shop windows).

11.4 MAX PLANCK CAMPUS

Together with the neighbor Max Planck Institute for Biophysical Chemistry (MPIBPC) and the Gesellschaft für wissenschaftliche Datenverarbeitung mbH Göttingen (GWDG) the MPIDS forms the Göttingen Max Planck Campus. Several infrastructures, such as the Otto-Hahn-Library and the canteen, are available to all partners of the Max Planck Campus and help cultivate an atmosphere of exchange and participation. In the past years, further efforts have been made to increase the cooperation between Max Planck Institutes and create synergistic projects.

Board of Trustees

Since January 2013, the MPIDS and the MPIBPC have a joint Board of Trustees. The board supports exchange between the institutes and the general public and advises the institutes on social and scientific policy. Members of the Board of Trustees include representatives from politics, economy, science, and media.

Meetings of the Scientific Members of MPIDS and MPIBPC

The meetings of the scientific Members of the MPIDS and the MPIBPC consolidate the close collaboration of both institutes on a scientific level. In these meetings the directors of both institutes convene regularly to discuss not only scientific issues, but also organizational and infrastructural topics concerning the Max Planck Campus as a whole.

Further Max Planck Campus Activities

In recent years, several tools have been established to foster the scientific exchange between researchers from both Max Planck Institutes. Most prominently, this is the Campus Seminar, a regular series of lectures held weekly. In these lectures, scientists from both institutes present their projects and results to their colleagues thus allowing for a preliminary exchange of ideas with the aim of triggering scientific cooperation. A more unofficial framework for getting to know colleagues from the MPIBPC and their research is offered by mutual activities such as the summer festival.

HOW TO REACH US AT THE MAX PLANCK INSTITUTE FOR DYNAMICS AND SELF-ORGANIZATION

Fassberg site (main building)

Address:
Am Fassberg 17
D-37077 Göttingen
Germany

Departments:	Fluid Physics, Pattern Formation, and Biocomplexity (Prof. Eberhard Bodenschatz) Dynamics of Complex Fluids (Prof. Stephan Herminghaus) Living Matter Physics (Prof. Ramin Golestanian)
Max Planck Research Groups:	Biological Physics and Morphogenesis (Dr. Karen Alim) Biomedical Physics (Prof. Stefan Luther) Statistical physics of evolving systems (Dr. Armita Nourmohammad) Neural Systems Theory (Dr. Viola Priesemann) Turbulence, Complex Flows and Active Matter (Dr. Michael Wilczek) Theory of Biological Fluids (Dr. David Zwicker)
Independent Research Units:	Dynamics in mesoscopic systems (Dr. Ragnar Fleischmann) Theory of Turbulent Convection (PD Dr. Olga Shishkina)
Emeritus Group:	Nonlinear Dynamics (Prof. Theo Geisel)
Services:	Institute Management, Administration, Facility Management, Electronics and Mechanics Workshops, IT-Services, Library, Outreach Office, Stock Rooms, Lecture Hall, Göttingen Turbulence Facility, Clean Room, and Cell Biology Laboratories

By plane
From Frankfurt am Main Airport (FRA): Use one of the railway stations at the airport. Trains to Göttingen (direct or via Frankfurt main station) leave twice an hour during daytime (travel time: 2 hours). From Hanover Airport (HAJ): Take the suburban railway (S-Bahn) to the Central Station (»Hannover Hauptbahnhof«). From here direct ICE trains to Göttingen depart every 1/2 hour.

By train
Göttingen Station is served by the following ICE routes: Hamburg-Göttingen-Munich, Hamburg-Göttingen-Frankfurt am Main, and Berlin-Göttingen-Frankfurt. From Göttingen railway station: On arrival at Göttingen station take a taxi (15 minutes) or the bus (20 minutes). At platform D take the bus No. 21 (direction: »Nikolausberg«) or No. 23 (direction: »Faßberg« or »Universität Nord«). After about 20 minutes get off at the »Faßberg« stop, which is directly in front of the entrance of the Max Planck Campus (MPIDS and MPI for Biophysical Chemistry). Ask at the gate to get directions.

By car
Leave the freeway A7 (Hanover-Kassel) at the exit »Göttingen-Nord«, which is the northern of two exits. Follow the direction for Braunlage (B 27). Leave town – after about 1.5 km at the traffic light (Chinese restaurant on your right) turn left and follow the sign »Nikolausberg«. The third junction on the left is the entrance to the Max Planck Campus (MPIDS and MPI for Biophysical Chemistry). Ask at the gate to get directions.

Bunsenstraße site (Scientific Meeting Center)

Independent Research Unit:	Cluster Dynamics (Prof. Udo Buck)
Emeritus Group:	Molecular Interactions (Prof. Jan Peter Toennies)
Services:	Scientific Meeting Center

Address:
Bunsenstraße 10
D-37073 Göttingen
Germany

By plane
From Frankfurt am Main Airport (FRA): Use one of the railway stations at the airport. Trains to Göttingen (direct or via Frankfurt main station) leave twice an hour during daytime (travel time: 2 hours). From Hanover Airport (HAJ): Take the suburban railway (S-Bahn) to the Central Station (»Hannover Hauptbahnhof«). From here direct ICE trains to Göttingen depart every 1/2 hour.

By train
Göttingen Station is served by the following ICE routes: Hamburg-Göttingen-Munich, Hamburg-Göttingen-Frankfurt, and Berlin-Göttingen-Frankfurt. From Göttingen railway station: From the Göttingen station you can take a taxi (5 minutes) or walk (20 minutes). If you walk, you need to leave the main exit of the station and turn to the right. Follow the main street, which after the traffic lights turns into Bürgerstraße. Keep walking until you come to the Bunsenstraße. Turn right – you will reach the entrance gate of the MPIDS after about 300 m.

By car
Leave the freeway A7 (Hanover–Kassel) at the exit »Göttingen«, which is the southern exit. Follow the direction »Göttingen Zentrum« (B3). After about 4 km you will pass through a tunnel. At the next traffic light, turn right (direction »Eschwege« B27) and follow the »Bürgerstraße« for about 600 m. The fourth junction to the right is the »Bunsenstraße«. You will reach the institute's gate after about 300 m.